DOE/PC/91057--T9

DEVELOPMENT OF A STABLE COBALT-RUTHENIUM FISHER-TROPSCH CATALYST

FINAL REPORT

prepared for
The U. S. Department of Energy
Pittsburgh Energy Technology Center

under
Contract No. DE-AC22-91PC91057

prepared by

Robert R. Frame and Hemant B. Gala

UOP
Des Plaines, Illinois

February 1995

MASTER

Patent cleared by Chicago
OPC on May 26, 1994.

BS

DISCLAIMER

Portions of this document may be illegible in electronic image products. Images are produced from the best available original document.

TABLE OF CONTENTS

ABSTRACT

The reverse micelle catalyst preparation method has been used to prepare catalysts on four supports: magnesium oxide, carbon, alumina-titania and steamed Y zeolite. These catalysts were not as active as a reference catalyst prepared during previous contracts to Union Carbide Corp. This catalyst was supported on steamed Y zeolite support and was impregnated by a pore-filling method using a nonaqueous solvent.

Additional catalysts were prepared via pore-filling impregnation of steamed Y zeolites. These catalysts had levels of cobalt two to three and a half times as high as the original Union Carbide catalyst. On a catalyst volume basis they were much more active than the previous catalyst; on an atom by atom basis the cobalt was about of the same activity, i. e., the high cobalt catalysts' cobalt atoms were not extensively covered over and deactivated by other cobalt atoms.

The new, high activity, Y zeolite catalysts were not as stable as the earlier Union Carbide catalyst. However, stability enhancement of these catalysts should be possible, for instance, through adjustment of the quantity and/or type of trace metals present.

STEM (Scanning Transmission Electronic Microscopy) analysis was a very useful tool during this work. It allowed determination of the size and atomic composition of cobalt crystallites. During the work with high cobalt Y zeolite catalysts STEM analysis showed that some (large) crystallites were present outside of the zeolite matrix in addition to the expected smaller ones present within

the zeolite pores. Furthermore, STEM analysis showed that the trace component zirconium was not evenly distributed across the variously-sized cobalt crystallites. Specifically, it was more likely to be found within the small crystallites in the zeolite pores than in the large ones extraneous to the pores. Since zirconium is added to stabilize the catalyst, solving the stability problem above might, therefore, be as simple as achieving a better zirconium distribution throughout the crystallites.

A primary objective of this work was determination whether small amounts of ruthenium could enhance the activity of the cobalt F-T catalyst. The reverse micelle catalysts were not activated by ruthenium, indeed STEM analysis provided some evidence that ruthenium was not present in the cobalt crystallites. Ruthenium did not seem to activate the high cobalt Y zeolite catalyst either, but additional experiments with Y zeolite-supported catalysts are required. Specifically, cobalt and cobalt/ruthenium catalysts should be re-made in stable versions to allow good assessment of initial catalyst activity. Such catalysts should be evaluated at high space velocities so that only moderate initial conversions result. Under the standard screening test used in this work initial conversions with the high cobalt catalysts were very high with or without ruthenium. The initial deactivation rates also appeared to be high. Thus accurate initial activities could not be determined. It is possible that cobalt-ruthenium catalysts were most active but appeared less active than cobalt-only catalysts during a run because they exhibited a faster deactivation rate.

Should ruthenium prove not to be an effective promoter under the simple catalyst activation procedure used in this work, more complex activation procedures have been reported which are claimed to enhance the cobalt/ruthenium interaction and result in activity promotion by ruthenium.

ACKNOWLEDGEMENT

The authors express their gratitude to Dr. Jule Rabo and Prof. Dr. Hans Schulz for helpful discussions. Furthermore, Prof. Schulz generously furnished us with a copy of the three volume Schering report on the Fischer-Tropsch process.

Dr. Hayim Abrevaya was the principal investigator during the early stages of this contract and was available as a consultant throughout.

Tony Polak, then of UOP, wrote an in-house review of Fischer-Tropsch related surface science studies in 1982. This has been useful throughout this contract and particularly so as background in writing the final report.

In addition to the undersigned, the Fischer-Tropsch team at UOP included at various times the following individuals: Dr. Hayim Abrevaya, Dr. Michael Quick, Dr. Alan van Til, Dr. Susan Lambert, Dr. Steven Bradley, Dr. Michelle Cohn, Frank Dobbs, William Targos, Elaine Schumacher, Sheila Adami, Robert Wasberg, Mark Heynis, Steve Bass and Kevin Kocis.

Finally, we acknowledge the team at DOE, both from the PETC and Washington, D.C. offices for their helpful support during this work.

Robert R. Frame Hemant B. Gala

1. OBJECTIVE

1.1 OBJECTIVE

Develop a supported cobalt-ruthenium catalyst for Fischer-Tropsch (F-T) processing of synthesis gas.

1.2 OVERVIEW

The eventual goal of this research is a high activity cobalt-based catalyst for use in slurry bubble reactors. A potential catalyst of this type has been developed using a modified Y zeolite and a pore-filling impregnation method. This approach was used when it was found that high activity catalysts could not be prepared by the original, reverse micelle, approach.

The experimental sections of this report describe preparation and evaluation of both the reverse micelle and Y zeolite-supported catalysts. Reverse micelle catalysts were prepared on a number of different supports. The Y zeolite catalysts were prepared on a support resulting from steaming and acid-washing Y zeolite. The resulting material is essentially crystalline with Y zeolite type channels but large (50-100 Å) amorphous "cages". The current high activity catalysts resulted from impregnation of higher levels of cobalt onto the modified Y zeolite than were used in an earlier similar catalyst developed by Union Carbide during previous DOE contracts.

Ruthenium is known to produce a very high activity F-T catalyst alone, however, it is too expensive for such a use. Thus it has been suggested to use it in small amounts in cobalt-based catalysts as an activity promoter. During the reverse micelle work no strong evidence for ruthenium promotion was found; this work indicated that the reverse micelle method results in poor dispersion of ruthenium into cobalt crystallites. Because the Y zeolite approach was only started midway through the contract, time was not available to fully explore the effect of small amounts of ruthenium on catalyst performance.

Most catalysts were only screened in a pilot plant which contained a tube reactor to quickly assess activity and selectivity. However, an evaluation was made of the high activity Y zeolite-type catalyst in a slurry autoclave plant, a type of test that results in a longer run.

2. INTRODUCTION

This section is a brief summary of cobalt-catalyzed Fischer-Tropsch (F-T) processing. It was written as a forward to the work done under this contract and was not meant to be a complete summary of all the work done in this area. Since Fischer and Tropsch discovered this process approximately sixty years ago hundreds of papers and patents have been written; a comprehensive summary of this area would require more space than is available in this report.

2.1 FISCHER-TROPSCH BACKGROUND

The Fischer-Tropsch (F-T) process is one of several which use synthesis gas (H_2 + CO) as feed. A complex product is formed. F-T usually employs either an iron or cobalt catalyst although ruthenium and nickel have also been used. In addition, multimetallic catalysts such as cobalt-ruthenium have been described. Currently synthesis gas is available from methane or coal; in either case it is an expensive feed, largely due to the high capital cost of a synthesis gas plant. Fifty to seventy percent of the total cost of a F-T complex will be due to the synthesis gas plant. Since F-T catalysts require very pure feed, feed pretreatment is an additional expense. To stand these expenses F-T can only compete with high, rather than the current low, priced petroleum.

F-T processing was used in Germany during World War II to convert coal-derived synthesis gas into transportation fuels when the Allies cut off their supply of petroleum. Following the war only the South Africans who faced the continual threat of a petroleum embargo continued to develop F-T

processing. They possess a coal resource and historically cheap labor to mine it. As a result, several generations of F-T reactors have been built there to process coal-derived synthesis gas. Although much of this work has not been published, Dry, among others, have been active in the literature.

F-T research gained momentum in the mid-1970's after the Arab oil embargo. Projects were then started at many academic, industrial and government laboratories as part of the worldwide synthetic fuels effort; there are reviews which cover this recent work.[1, 2, 3, 4, 5] Although much of this effort was scaled back by the late 1980's some interest remains, particularly in the area of methane-derived synthesis gas conversion, since part of the world's methane resource is in remote areas where there is no market for it. One large-scale F-T plant has been built to convert synthesis gas from such methane into transportation fuel, namely Shell's Indonesian plant. It uses tube reactors of narrow dimension to aid heat removal from the very exothermic F-T reactions. Over seventy thousand tubes divided between three reactor assemblies are used!

The Shell plant is an example of F-T by fixed bed processing which is also the type of processing used in the initial German plant of 1935. Fluidized catalyst beds (liquid and gas phase) have also been used. In liquid phase (slurry) processing part of the heavy products produced during F-T processing (wax) is retained in the reactor as a liquid to fluidize the catalyst under the influence of the feed gas bubbles and to provide a heat transfer agent for the exothermic F-T reactions. This type of processing is called liquid phase Fischer-Tropsch (LPFT) processing.

2.2 COMPARISON OF IRON AND COBALT FISCHER-TROPSCH CATALYSTS

In this contract novel cobalt-based F-T catalysts were the goal, specifically ones containing cobalt and minor amounts of ruthenium. Cobalt and iron catalysts are different in many respects. The former are usually supported whereas the latter are usually derived from bulk iron oxide. Small amounts of other metals are used in both catalysts but the ones used are not the same for both catalysts. Both catalyst types are reduced prior to use, however, the cobalt catalyst requires higher temperatures (300° C or higher vs. 260-280° C). The working cobalt catalyst is entirely in the zerovalent state, while iron works in at least a partially oxidized state. The cobalt catalyst operates about 200° C compared to about 270° C for the iron catalyst. This is an important difference, it means that the iron catalyst can be reduced in the F-T reactor whereas the cobalt catalyst usually has to be reduced in a separate vessel capable of withstanding the higher reduction temperature.

Iron catalyzes the shift reaction (carbon monoxide with water to produce hydrogen and carbon dioxide); cobalt doesn't. Some workers believe this reaction is catalyzed by iron oxide sites on the iron catalyst.

The equation below illustrates the stoichiometry of the preponderant F-T reactions (alkane formation):

$$CO + 2H_2 \longrightarrow -CH_2- + H_2O$$

According to this stoichiometry a 2 : 1 molar ratio of hydrogen to carbon monoxide is required; this is the ratio resulting from partial oxidation of methane:

$$2CH_4 + O_2 \longrightarrow 2CO + 4H_2$$

Cobalt is the catalyst of choice for such-derived synthesis gas. Iron, however, is used for hydrogen-poor synthesis gas, most especially that from coal ($\approx$ 0.7 molar ratio of hydrogen to carbon monoxide), since the shift reaction has the effect of producing hydrogen from product water. (At the expense of some of the carbon!)

2.3 CALCULATIONS

The conversions and selectivities calculation method used in this work (Appendix 1) requires argon internal standard in the feed. The data required to calculate conversions and $C_1 -> C_4$ hydrocarbon and carbon dioxide selectivities were obtained throughout the runs with an on line gas chromatograph. A second on line gas chromatograph, which performed a different analysis method, was used to obtain the data needed to calculate $C_2 -> C_4$ alcohol selectivities.

2.4 REACTION MECHANISM

The F-T products are mostly alkanes, alkenes and oxygenates of wide molecular weight range. The mechanism describing their formation is complicated. Apparently relatively large metal crystallites are needed, small ones can produce high levels of methane. The cobalt catalyst is usually supported and formation of sufficiently large crystallites (50-100 Å) can be a problem. The initial work during this contract was directed toward forming 50-100 Å cobalt aggregates via impregnation of cobalt-containing reverse micelles. Subsequent work was also directed toward forming these sorts of aggregates but by using a support with 50-100 Å pores. The support used was steamed and acid-

washed Y-zeolite.

The currently favored F-T mechanism is the original one of Fischer and Tropsch.[6] It involves cleavage of carbon monoxide as the first step. This cleavage occurs at surface cobalt sites and results in surface carbon and oxygen. Most of the oxygen ends up as water although some oxygenate molecules also result. The carbon builds up to the main products of the F-T process which are alkanes and alkenes by the steps of hydrogenation and insertion. Surface-bound methyl and methylene radicals may thus be formed from carbon by hydrogenation. Chains may be formed by insertion of methylene radicals into the surface-bound methyl and alkyl radicals.

A non-dissociative mechanism was in vogue until the late 1970's when fresh theories and evidence supporting the dissociative mechanism were advanced by Rabo and co-workers,[7, 8] and later by many others as well. Araki and Ponec[9] and Wentrcek and co-workers[10] supported a dissociative mechanism for methane formation over nickel surfaces at about the same time. Rapid dissociation of carbon monoxide on the catalyst surface in the presence of hydrogen is a key aspect of the theory proposed by Biloen, Helle and Sachtler to explain how hydrocarbons are formed by F-T catalysts.[11] Their acceptance of this theory was based on work they did with metals containing surface coverages of ^{13}C formed by disproportionation of ^{13}CO to ^{13}C and $^{13}CO_2$ at 523° C and 0.5 bar. They prepared carbidic materials with measured amounts of ^{13}C that were active when reacted with successive pulses of $^{12}CO/H_2$ each sufficient to consume 20% of the ^{13}C. They found hydrocarbon products which contained ^{13}C under conditions where the carbidic carbon had been demonstrated not to equilibrate back to carbon monoxide. Thus it appears that the surface ^{13}C reacted with hydrogen, putatively forming $^{13}CH_2$ and $^{13}CH_3$, the latter of which can form $^{13}CH_4$ via reaction with hydrogen and higher ^{13}C hydrocarbons via insertion of $^{13}CH_2$. Others invoked the dissociative

mechanism at about the same time as Biloen, et. al.[12, 13, 14] The small amounts of oxygenates found in F-T products could arise according to this mechanism by insertion of carbon monoxide into a growing chain, presumably this would be a chain termination step.[5]

Petit and Brady and later Bock have explored the dissociative mechanism by generating carbenes on the surface of F-T metals.[15, 16, 17] Petit and Brady showed that decomposition of diazomethane in the absence of hydrogen on F-T metals or in the presence of hydrogen on metals that cannot adsorb it dissociatively results in ethylene as the only product. However, decomposition of diazomethane on F-T metals in the presence of hydrogen leads to a normal F-T product slate.

The dissociative mechanism has been criticized by Henrici-Olive and Olive, particularly with regard to the relevance of the Petit experiment.[18, 19] However, Smutek has defended it while emphasizing this experiment.[20]

Hoffmann and co-workers have reviewed the mechanistic work done up to the mid-1980's and provided an extended Huckel model for F-T catalysis based on the dissociative mechanism.[21] This model covers all of the steps in this mechanism not just the initial carbon monoxide cleavage. They discuss, for instance, the mobility of carbon intermediates on the surface and how that can relate to the F-T products. In their logic surface mobility is related to d-band filling. The chain propagation step can be visualized as migration of an alkyl group and/or methylene into close proximity allowing facile coupling (chain growth). Hoffmann, et. al. have made strides toward understanding the theoretical underpinning of F-T catalysis with a theory that is predictive, for instance, the differences in product distribution between Co (shorter chains) and Fe (longer chains) is due to different carbon fragment mobility as predicted by the different d-band filling in these two

metals. This theory is also interesting since all F-T catalysts result from paramagnetic or ferromagnetic materials, and metal d-band electrons also determine a material's magnetic properties (Figure 1). Understanding why some materials are magnetic but not F-T catalysts should be a goal of future experiments.

Iron exists under F-T conditions with both iron-carbon and iron-oxygen bonds on the surface. It is an F-T catalyst as well as a shift catalyst. Cobalt is one element to the right of iron in the periodic chart. Under T-T conditions its surface contains no detectable cobalt-oxygen bonds. Cobalt is an F-T catalyst but not a shift catalyst perhaps because it is not partially oxidized to cobalt oxide. It is apparently in the metallic state during F-T catalysis, possibly with a surface covering of carbon. Furthermore, it is intrinsically more selective to methane and other light hydrocarbons than iron. Nickel is one element to the right of cobalt; it also is in the metallic state under F-T conditions, under F-T conditions its surface also possibly contains a carbon layer. Nickel can catalyze the formation of hydrocarbons, but only forms ones heavier than methane with difficulty. It is also not a shift catalyst. One strength of Hoffmann's theory is that it provides an explanation for the difference in carbon number selectivities resulting from catalysts across the row: iron-->cobalt-->nickel. Presumably this theory can also be extended to explain why stable surface carbon-oxygen bonds are favored going from right to left across this row.

In summary, the dissociative mechanism now seems to be the accepted one for F-T processing. In addition, the Hoffmann theory is available which attempts to understand the factors controlling all of the mechanistic steps including the polymerization steps. This is, so far, a theory based on simple assumptions. For instance, the theory uses a metal slab model which assumes a flat surface with atom spacing characteristic of a crystal face. The slab is free of surface bonds other than the

surface carbon ones required to build up F-T products. The actual iron F-T catalyst is known to contain metal-oxygen and metal-carbon bonds on the surface. Furthermore, an actual F-T catalyst, iron or cobalt, almost certainly has an irregular surface with "steps" and "kinks" which will probably strongly effect the catalyst performance. However, Hoffmann's theory is comprehensive in that it attempts to cover all steps of the F-T process not just the first, "dissociation", step. Furthermore, it provides an explanation for the difference in carbon number selectivities across the row: iron-->cobalt-->nickel.

2.5 CARBON NUMBER SELECTIVITY

The wide range of carbon number products in F-T processing can be understood in terms of the mathematics first used by Schulz[22] and Flory[23] for condensation polymerization. Thus if a complete product work-up is performed during F-T processing and if a plot is made of log selectivity to each carbon number vs. carbon number, a straight line (single alpha case) or a hyperbolic curve appearing to result from two straight lines (so-called double alpha case) results. Plots of the above type are customarily called Schulz-Flory or Anderson-Schulz-Flory plots. Alpha (α) is the slope of the straight line(s); in Schulz-Flory kinetics it is the probability of a carbon chain of n atoms growing to one of n + 1 carbon atoms. Until recently most F-T data was presented as being of the single α type, however, it now appears that most, if not all, F-T catalysts produce the double α type of product distribution, certainly in LPFT double α appears to be the norm. It is possible that early workers reported single α behavior because the breakpoint was at a high carbon number, requiring a complete product analysis to "see" the breakpoint. Such product analyses are facilitated by modern analytical techniques that were not available when the early F-T work was done. Catalysts which are very selective to methane and other light products, such as cobalt catalysts, can produce

a product distribution which at least gives the appearance of being single α in nature since undetectable amounts of heavy materials may be formed.

Yates[24] presented a review containing a discussion of the experimental evidence for double α behavior. For instance, the first note of it appears to have been at a German pilot plant in 1943 during the "Schwarzheide tests". However, this data was not widely circulated and explanations for the double alpha product distribution first started to appear years later. Thus, in 1983 Koenig and Gaube[25] theorized it to be due to two different catalyst sites, one promoted by potassium and one not. Later, however, Dictor and Bell[26] and Satterfield[27] observed the double alpha phenomenon with potassium-free catalysts.

Novak and co-workers[28, 29] have also presented a two active site mechanism, one a condensation site and the other a cracking site. However, Yates points out that Schulz[30] and Pichler and Schulz[31] had earlier determined that cracking does not occur significantly on iron or cobalt F-T catalysts.

There is an alternate explanation for the double α effect. Satterfield's group[24] and Iglesia, et. al. at Exxon[32] propose that this effect is due to two chain growth processes. One of them is the historic one which involves one carbon atom insertion into a growing chain. The other is growth by readsorption of product alkenes followed by their incorporation into chains. Although alkenes are primarily hydrogenated upon readsorption there was ample evidence prior to the mechanistic ideas of Satterfield's and Iglesia's groups that alkenes, particularly ethylene and to a lesser extent propylene and 1-butene can initiate and terminate chain growth.[30, 33-35] There was also some evidence[30] that ethylene but not propylene can propagate growing chains as well. The basic concept addressed by Satterfield's and Iglesia's groups is the same, but Iglesia theorizes that alkene

participation is related to fugacity implying more participation by higher molecular weight alkenes than Satterfield's and the historic experiments above might imply. It is known that most of the heavy F-T products are alkanes not alkenes, implying that the heavy products are the most strongly readsorbed and are reactive in, at least, the hydrogenation reaction.

Satterfield and his students have developed a mathematical model for the double α case.[36, 24] It is not dependent on a given double α mechanism. Included is a nonlinear regression method to assign values called α_1 and α_2 to the hyperbolic curve. These two constants roughly correspond to the values α_1 and α_2 that result from simple linear regression analysis of the apparently straight-line parts of the hyperbola.

No catalyst or set of operational conditions have been discovered that allow good control of carbon number selectivity during F-T processing with iron or cobalt catalysts. Except for methane, it is not possible to make a single carbon number product such as only C_4's or even a fairly narrow carbon range product such as only $C_4 -> C_6$. To date changing carbon number selectivity during F-T processing only means changing the magnitude of α, for instance, a change in catalyst composition can shift the product distribution from one that is biased toward low molecular weight products to one that is biased toward higher molecular weight ones or vice versa. However, regardless of the catalyst both high and low molecular weight products will be formed.

Conversion of synthesis gas to C_1 products with other metal catalysts is also possible. For instance, very high methane selectivities can be obtained using a nickel catalyst and very high methanol selectivities can be obtained, for instance, with a palladium catalyst.[7]

2.6 OTHER FISCHER-TROPSCH SELECTIVITIES

F-T processing is highly selective in one respect: the carbon chains are primarily unbranched. This is consistent with chain growth via sequential carbon atom insertions into a metal-carbon bond, with only a small number of insertions by $>C_1$ species. Only low levels of cyclic and aromatic products are formed, although in special cases aromatics yield can be as high as 18%.[37]

Most of the heavier F-T products are saturated molecules; alkenes can be prominent among the low molecular ones. Of the two most studied F-T catalysts (Fe and Co), iron is more prone to form alkenes than Co.

2.7 COBALT CATALYST DESCRIPTION

The cobalt catalyst is usually supported and results from reduction of supported cobalt salt(s). Manganese and zirconium are commonly-used promoter metals for cobalt. Anderson has reviewed the cobalt catalyst up to the early 1980's.[38] He gives the composition of key cobalt catalysts and cites earlier reviews of this type of catalyst. According to Anderson, Fischer's cobalt/thoria/ magnesia catalyst is the forerunner of all supported, cobalt-containing F-T catalysts. Much early work was devoted to removing thoria from this composition culminating in catalysts supported on zirconia-magnesia and titania-magnesia. Kieselguhr was also a support component for some of the earliest cobalt catalysts.

By the time of the Anderson review, there were many other cobalt catalysts including ones on

supports such as silica and alumina as well as others supported on the historic materials above. There had also been extensive studies of the performance of such catalysts under a multiplicity of conditions.

Much of the recent F-T work has, in fact, been concentrated on cobalt- rather than iron-based catalysts. This is due to the current abundance of cheap methane and the utility of the cobalt catalyst for conversion of methane-derived synthesis gas.

Exxon, for instance, have done extensive research on this type of catalysis since at least the early 1980's. Some of their more recent patents describe cobalt-manganese spinels which can be promoted by copper.[39, 40] Copper apparently promotes conversion, manganese also promotes conversion and also causes a lowering in the selectivity to methane. These catalysts apparently exhibit the low selectivity to carbon dioxide expected from cobalt-based catalysts. However, the carbon dioxide selectivity appears to be somewhat higher than typically obtained with cobalt catalysts. Presumably a spinel (Co_2MnO_4/1% Cu) will allow more cobalt to be loaded into the reactor per unit volume of catalyst than a supported catalyst. Interestingly, copper-promoted iron-manganese spinels have also been patented as low methane and carbon dioxide selective catalysts.[41]

Exxon have also done a considerable amount of work on cobalt and cobalt-ruthenium catalysts supported on titania. Their cobalt-ruthenium work follows earlier work by Kobylinski (Gulf-Chevron) who also investigated cobalt and cobalt-ruthenium catalysts but used other supports.[42-45] This type of catalyst often has other metals such as zirconium present as adducts.[46] Both sets of workers found that a small amount of ruthenium can promote catalyst activity and selectivity to C_5+ products. They believe these effects are due to small amounts of ruthenium lodged in cobalt

crystallites. Special efforts were, therefore, made during catalyst preparations to insure that cobalt and ruthenium were in intimate contact. Exxon believes ruthenium has the ability to keep the catalyst surface free of deactivating molecules, perhaps through reaction of them with hydrogen. Exxon have also found that ruthenium-containing catalysts are more easily regenerable; they believe the explanation is the same as above. Exxon have provided a recent review of their work and that of earlier workers.[47]

Many other supports have been used for the cobalt catalyst. For instance, alumina has been used by Exxon as a second stage catalyst in a two stage F-T process.[46] In this scheme the first stage is operated at a lower pressure than the second stage. The use of alumina in this example is based on Exxon's finding that alumina-supported catalysts are more active at relatively low pressures than other supported cobalt catalysts.

Lapidus and co-workers have also recently investigated alumina-supported catalysts[48] and compared them to ones supported on silica. They found that the extent of calcination affected the ultimate selectivity of the catalyst. Extensive calcination decreased the liquid product selectivity of a silica-supported catalyst, whereas it increased that of an alumina-supported one.

Shell have also been active recently in the area of cobalt-catalyzed F-T processing. This has led to the F-T plant in Sintulu, Malaysia which is the only commercial F-T plant outside of South Africa. It processes methane-derived synthesis gas with an unknown catalyst which, however, is likely supported and cobalt-based.

A recent Shell patent describes a catalyst activation procedure.[49] This procedure is for activation

of fresh catalysts and reactivation of spent ones as well. It incorporates treatment with hydrogen at pressures in excess of those previously used for such catalyst treatments. It is written to cover simple one stage activations but also the multistage one of Kobylinski, it. al. which is called ROR (reduction/oxidation/reduction).[50]

Additional recent work on silica-supported catalysts is due to Ishihara and co-workers.[51] The particular catalysts studied were ones containing cobalt and nickel, with the extreme examples being either all cobalt or all nickel. Activity was maximal for the 50 : 50 cobalt : nickel catalyst. Surprisingly the methane selectivity was not a linear function of the amount of nickel, rather it was a minimum for the 50 : 50 catalyst. However, even at a minimum it was still a high 30%. The selectivity minimum might, in part at least, be do to the high conversion obtained with the 50 : 50 catalyst, since methane selectivity during cobalt catalysis is known to decrease as conversion increases.

2.8 REACTORS

Commercial F-T plants have traditionally used packed or fluidized bed reactors. In both cases the product liquids and gases are removed from the reactor as fast as they are formed. Provisions such as narrow tube reactor geometry must be provided to remove heat from the very exothermic F-T reactions. Slurry liquid phase processing is a newer concept although Koebel did seminal work on it in the 1940's and early 1950's at the Rheinprussen Corporation plant at Hamburg Niederrhein, Germany. The driving force behind its development is the ability of the liquid phase to act as a heat transfer agent to remove heat from the reactor, since F-T processing is very exothermic.

The first F-T plant was built in Germany in the 1930's. It had a fixed-bed reactor full of catalyst pellets and was operated between 200 and 270° C.[52] Due to the high exothermicity of the F-T reactions, precise catalyst temperature control was impossible. This resulted in shortened catalyst life. The product liquids were approximately a 50 : 50 mix of naphtha and higher boiling fractions. The most recent fixed-bed plants are in South Africa; they employ Arge reactors which use high catalyst loadings and high space velocities. The product liquids are about 40% naphtha with the balance heavier.

The M.W. Kellogg Co. has developed a type of fluidized-bed reactor called an entrained-bed reactor. It is used in the South African Synthol process. In it the catalyst and synthesis gas contact at the bottom of the reactor and proceed up together at 300-335° C. Cyclones separate products and catalyst; boilers are used to remove heat. The South Africans have developed two generations of Synthol reactors, Synthol I and II. Synthol II resulted from a cooperative effort with Badger Engineers Inc. to rectify problems associated with Synthol I.[53] The Synthol reactors are operated to produce a light product which is about 78% naphtha, 7% heavies and the balance gases and oxygenates. The high gasoline yield from this processing implies a high methane yield as well. This is apparently not a problem in South Africa which is short of natural gas. However, in most other places this would be a problem since natural gas is currently in over supply.

South Africa operates its F-T plants to make fuel, but also sells specialty chemicals after separating them from the diverse F-T product. For instance, they sell wax and purified oxygenates. Total product sales coupled with very low priced coal and essentially paid off plants allow them to break even against petroleum at a fairly low price. However, even they admit that they do not break even when petroleum is below about twenty dollars a barrel. Furthermore, some of the markets they sell

F-T products into are probably nearly saturated even with the relatively small amount of product produced in South Africa.

Koebel's LPFT work continued for a while after the Second World War.[54] The plant he and co-workers used contained a 1.55 meter diameter by 8.6 meters tall bubble reactor with internal cooling coils. The slurry of wax and catalyst moved upflow with co-current synthesis gas which contained hydrogen and carbon monoxide in the molar ratio of 0.7. The gas bubbles cause ebullition of the catalyst particles resulting in a well-mixed slurry. There was a recycle loop which allowed removal of wax product and spent catalyst. Fresh catalyst was also added on this loop to maintain catalyst loading at 10-20 wt% of the slurry. At a feed gas linear velocity of 9.5 cm/sec and operating conditions of 268° C and 12 atm. Koebel reported a temperature gradient of only 1° C and a catalyst concentration gradient of 0.2 to 0.6 wt% at 10 wt% average catalyst loading. Carbon monoxide conversion was 91% with 34.5 wt% of the hydrocarbon product in the range C_1---> C_4.

Koebel reported conditions for operating the slurry bubble reactor which produced extraordinary hydrocarbon distributions. For instance, he observed no methane product with 50-500 g of catalyst per liter of suspension, catalyst particle size 0.002---> 1 nm, gas flow rate 10-30 times the percent weight of catalyst base metal in the suspension (gas flow expressed as NL/hr/liter of catalyst suspension) and plant operating pressures of 3---> 150 atmospheres.[55] However, in the review of LPFT which he wrote with Ralek[54] it is said that about 4% of the total product from the 1952-1953 campaign with the demonstration plant was methane + ethane. Even this is quite low, particularly in light of the fact that the plant was being operated under conditions favoring production of gasoline not diesel fuel, and the carbon monoxide conversion was 90%. High conversions favor high methane + ethane selectivity.

LPFT processing was continued in the U.S. after the Second World War by the U.S.Bureau of Mines.[56] After the Bureau of Mines work until the mid 1980's additional liquid phase processing research was continued at various laboratories; a review was published in 1983.[36] Liquid phase processing was aggressively pursued in the 1980's, for instance, Mobil finished an LPFT contract in 1985.[57] Performance results from this and Koebel's earlier work are compared in Figure 2.

Currently research and development on liquid phase reactors and F-T catalysts to use in them is being done in many laboratories. The hydrodynamics of such reactors as well as kinetic rates of the various processes which have been performed in them have been studied and summarized by Deckwer[58] and Fan.[59-62] Catalyst development is currently being sponsored by the DOE at the University of Kentucky and Texas A & M University.

The DOE is also sponsoring an international consortium of private companies for operation of a 0.572 m diameter slurry bubble reactor at LaPorte, Texas. One of the consortium members, Air Products Co., provides site support. An LPFT reactor of this type is purported to be operational in South Africa, possibly about 1 meter in diameter. In addition, Exxon, Statoil and Rentech have respectable internal projects for LPFT development. Rentech have constructed a plant near Denver, Colorado to convert synthesis gas from biogenetic methane formed at a garbage site. Finally, Air Products Co. have made a major effort to commercialize the slurry bubble concept for alcohol synthesis before their involvement in the DOE LaPorte consortium.

A slurry autoclave reactor (stirred tank) is usually used to certify LPFT catalysts, however, this is a time-consuming way to screen new catalysts. Although the eventual goal of the research done under the current contract is a catalyst for LPFT use, the actual state of development of the reverse

micelle and zeolite-supported catalysts at the outset was not very far advanced and extensive catalyst screening was anticipated. In fact, most of the catalyst evaluations in this report were screening in nature and were performed by a quick fixed-bed catalyst evaluation procedure. However, a few of the zeolite-supported catalysts were sufficiently developed by the end of this contract to warrant evaluation in the slurry autoclave plant.

One problem contemplated with LPFT processing is separation of the catalyst from the liquid phase. This separation is necessary because the F-T product can contain wax reaction products that cannot be removed from the catalyst by distillation. Probably the easiest way to minimize this problem would be to use a catalyst with an α which favors high light ends selectivities (low wax). However, this is a limited solution since a low wax catalyst invariably is excessively selective to methane and ethane. Furthermore, LPFT kinetics favor double α behavior which insures some wax product even from high light end's selective catalysts. The Mobil work of the mid-1980's (iron catalyst) showed that a relatively iron-free wax could be produced by known solid-liquid separation technology. However, the wax still contained several hundred parts per million of iron and even this is sufficient to require a separate iron removal step to protect, for instance, the hydrocracking catalyst used to crack the wax to diesel boiling range material.

Separation of catalyst from wax will have to be addressed with a supported LPFT catalyst as well as non-supported catalysts such as Mobil's iron catalyst. There might be some advantages due to a supported cobalt catalyst. First of all, cobalt catalysts do not produce as much wax as iron catalysts due to their bias toward low molecular weight products. Secondly, cobalt tends to be more active per atom than iron so less catalyst will have to be loaded to achieve a given conversion target. Lastly, one might be able to choose a support that is more stable to attrition than bulk phase iron

catalysts resulting in fewer fines in the wax.

Catalyst particle integrity in the F-T reactor is important for LPFT. Particle attrition will magnify the separation problem. However, determining catalyst particle stability is a difficult experimental problem. Determining particle/particle attrition alone might not be enough. Particles could also attrit due to build up of stress from pressure within catalyst pores resulting from formation of long carbon chains. This would be similar to the spalling that the chromium on silica polyethylene catalyst is known to undergo. Direct measure of the rate of attrition of the catalyst particles in the stirred autoclave might also prove erroneous since the particle/particle attrition might be far different than in the slurry bubble reactor. During the cobalt catalyst research no work was done on catalyst particle integrity since only a few slurry autoclave runs were performed.

3. EXPERIMENTAL SUMMARY

3.1 INTRODUCTION

The catalysts prepared during this work were screened in a fixed-bed pilot plant. Their performance was compared to a reference catalyst which resulted from two earlier DOE contracts to Union Carbide Corporation. A drawing of this plant is in Figure 3. Most of these screening runs were performed according to the conditions outlined in Figure 4. These conditions were adopted early in this work when it was found that the initial catalysts were not very active at the condition used to evaluate the reference catalyst (Condition 1). The second two conditions are more strenuous than the first insuring some high conversion data to allow assessing methane and ethane selectivity at reasonable conversions.

In the fixed bed runs 13 g of catalyst were loaded with 160 g of quartz sand diluent. The large mass of diluent was needed to facilitate heat removal from the reactor since the F-T reactions are very exothermic. During the fixed-bed runs reactor bed temperatures were measured by means of an internal sliding thermocouple.

A few of the most promising catalysts were evaluated in a slurry autoclave pilot plant (drawing: Figure 5, simplified schematic: Figure 6). The benefits of such testing are several-fold. First of all a heavy oil is added to the autoclave reactor at startup to aid maintenance of a constant reaction temperature which promotes catalyst stability. Secondly, the run length is longer than in the fixed bed screening tests which allowed determination of catalyst stability.

Regardless of the test method, the feed was always a blend of hydrogen, carbon monoxide and argon with a hydrogen to carbon monoxide molar ratio of two. A typical feed composition (mole percent) was: hydrogen = 64, carbon monoxide = 31, argon = 5. Although the feeds were quite pure, they were pretreated through molecular sieves and hot alumina to remove any remaining impurities.

3.2 REVERSE MICELLE CATALYSTS

The reverse micelle method was shown in a previous DOE contract to UOP to be capable of forming 50-100 Å ruthenium aggregates on a support. In the current work this method was used to prepare cobalt and cobalt-ruthenium catalysts on a variety of supports. Preparation and evaluation of these catalysts are discussed in Section 4; they were not very active and were only screened in the fixed-bed pilot plant.

3.3 Y-ZEOLITE SUPPORTED CATALYSTS

Catalysts were prepared on two different samples of steamed Y-zeolite. The preparation methodology was similar to that used during two previous DOE contracts to Union Carbide (prior to the Union Carbide/UOP joint venture). Some changes to the original catalyst preparation method were investigated. A few of these catalysts were more active than the reference catalyst, these were evaluated in the autoclave pilot plant as well as the fixed-bed plant. Most of these catalysts were only evaluated in the fixed-bed pilot plant, their preparation and evaluation are covered in Section 5.

During both the screening and autoclave runs light gas analyses were performed by an on line gas chromatograph. These on line analyses were used to calculate conversions and selectivities (CO_2 and $C_1 -> C_4$) via the calculation method in the Appendix which is based on the feed internal standard (argon).

4. DEVELOPMENT OF REVERSE MICELLE CATALYSTS

This section contains a brief summary of the UOP-developed reverse micelle method for preparing catalysts with uniformly-sized ruthenium aggregates. Also summarized is the work done during the current contract toward development of reverse micelle type cobalt and cobalt/ruthenium catalysts.

The cobalt and cobalt/ruthenium catalysts were screened in the fixed-bed pilot plant. None were active enough at the first of the three test conditions to warrant further testing in the slurry autoclave pilot plant. All catalysts were at least evaluated at the first condition of the three condition test described in Section 3 (Figure 4). Most were evaluated at all three conditions.

4.1 BACKGROUND

Depositing uniformly-sized aggregates of metal onto supports via reverse micelles and subsequently using such composites as catalysts for F-T synthesis was first demonstrated by H. Abrevaya at UOP during the previous DOE Contract DE-AC22-84PC70023. This impregnation method was based on previous work by Stenius, et. al.[63] who developed a way to prepare small, regularly-sized (30-50 Å), metal aggregates using surfactant molecules. In this methodology, the aqueous core (Figure 7) of a reverse micelle is used to carry metal salt(s) to the catalyst surface. The catalyst preparation method developed by Abrevaya uses metal-containing reverse micelles for support impregnation followed by the steps of calcination and reduction with hydrogen.

The ruthenium-only catalysts from the above contract were very active but would be costly to

produce. The original objective of the current contract was preparation of reverse micelle catalysts containing mainly cobalt, but with a small amount of ruthenium as, hopefully, an activity promoter.

4.2 CATALYST PREPARATIONS

All reverse micelle catalysts were impregnated in the same way. First a mixture was made of n-hexane and Berol 050, a surfactant from Berol Kemi, Stenungsund, Sweden. After standing overnight the mixture was filtered and an aqueous solution of salts of the metals to be impregnated was added. This admixture was shaken and added to a set of vials. Enough metal salts were present in each vial to impregnate two grams of support. After addition of support the vials were intermittently swirled for four minutes. After the support settled the liquids were pipetted out and the impregnated support was allowed to dry overnight at room temperature. The dried samples were separately analyzed for metals, those with similar metals levels were combined. STEM analyses were performed on some of the combined samples. Catalysts were calcined at 300° C then reduced at 380° C for four hours under hydrogen before they were evaluated in the fixed-bed pilot plant.

Control catalysts were prepared on the supports via simple evaporative impregnation of aqueous solutions of metal salts.

The reference catalyst was one prepared during a previous DOE contract to Union Carbide Corp. via a pore-filling method which uses a solution of metal salts in an organic solvent and a modified Y zeolite support.

4.3 CATALYST SUPPORTS

Examples of reverse micelle and aqueous impregnated catalysts were prepared on each of these supports: magnesium oxide, carbon and alumina-titania.

4.4 CATALYST PERFORMANCE

Screening test results from the various catalysts are summarized below. None of the experimental catalysts were promising enough vs. the reference catalyst to warrant further testing.

4.4.1 REFERENCE CATALYST PERFORMANCE

The reference catalyst was supported on a sample of steamed and acid-washed Y zeolite. Steaming causes large (50-100 Å diameter) amorphous pores to form within the crystalline framework of the Y zeolite crystallites. After the acid wash which removes residual, steaming-derived, amorphous alumina from the crystalline channels, the new large pores are accessible via the crystalline channels of the remaining Y zeolite. The large pores can support cobalt crystallites of the size required for effective F-T catalysis, namely 50-100 Å. Catalysts with cobalt crystallites much below 50 Å become quite selective for methane. During the previous development it was found that small amounts of manganese and zirconium are beneficial for lowering light ends selectivities and stabilizing catalyst activity.

The reference catalyst was evaluated in Run 65, plots of conversions and selectivities vs. hours on

stream from this run are attached as Figures 8 to 14. It was a longer run than the screening runs with experimental catalysts below. This catalyst appeared to reach a line out in activity and selectivity by fifty hours on stream. In comparing its performance to that of the experimental catalysts below, the fifty hour conversions and selectivities will be used. After extended use at other feed rates, the catalyst was returned to the starting conditions at three hundred and fifty hours on stream. The activity had diminished during the time at the other conditions, for instance, the carbon monoxide conversion between fifty and one hundred hours on stream was forty percent whereas after return to the initial conditions it was twenty percent.

4.4.2 PERFORMANCE OF CATALYSTS SUPPORTED ON MAGNESIUM OXIDE

The first reverse micelle catalysts made under this contract were inactive. The first active ones were supported on a very pure sample of magnesium oxide which was particularly noteworthy in containing very little sulfur. Previous magnesium oxide samples had failed to produce active catalysts.

Three catalysts from this pure magnesium oxide support were evaluated. Two resulted from aqueous impregnation and one from reverse micelle impregnation. The metals content of these catalysts and a brief overview of their performance appear in Figure 15. The reverse micelle impregnated catalyst seemed to be slightly more active and less selective to methane than the two catalysts resulting from aqueous impregnation. However, all three were less active than the reference catalyst of Run 65.

Plots of conversions and selectivities vs. hours on stream for the three runs with magnesium oxide-

supported catalysts are attached as Figures 16 to 32. Run 63 used a reverse micelle catalyst. This run was performed before the three condition test was being used, however, the start up conditions were the same as condition 1 of the three condition test. The carbon monoxide conversion seemed to be stabilizing at or slightly above seventeen percent by fifty-five hours on stream at which time the temperature was increased. A carbon monoxide conversion of about twenty percent resulted when the temperature was increased to 224° C. The methane selectivity was about ten percent at 211° C and twelve percent at 234° C; this selectivity is known to increase as temperature increases. Problems with the on line gas chromatograph caused most of the ethane and ethylene selectivity data to be lost. The propane and propylene selectivities are in Figure 17.

The two catalysts prepared via aqueous impregnation were evaluated by the three condition screening test in Runs 69 and 72. The catalyst of Run 69 was less active (Figure 20) than that of Run 72 (Figure 25). Furthermore, the Run 69 catalyst lost activity during the entire one hundred hour run whereas that of Run 72 appeared to approach an activity line out; by one hundred hours on stream it was much more active than the Run 69 catalyst. One difference between the two catalysts was the lack of manganese in the Run 69 catalyst. Both catalysts produced the lowest level of methane at the last condition. The Run 72 catalyst achieved 80% carbon monoxide conversion at the last condition but exhibited a high methane selectivity of 27 mole %.

Composition-wise the Run 72 catalyst was the one most similar to the Run 63 reverse micelle catalyst, however, at condition one it was less active (6 vs. 17% carbon monoxide conversion and produced much more methane than the Run 63 catalyst (24 vs. 10 mole %). Thus with magnesium oxide support the reverse micelle method did produce a more active/less methane selective catalyst, however, the activity and selectivity were not as good as the previously developed zeolite catalyst.

4.4.3 PERFORMANCE OF CATALYSTS SUPPORTED ON CARBON

Two catalysts were prepared on Carbotrap B carbon, one via reverse micelle impregnation and one by aqueous impregnation. These two catalysts only contained cobalt and ruthenium. They are compared to the reference Y zeolite catalyst in summary fashion in Figure 33. Neither of these catalysts was as active as the reference. Of the two, the one resulting from aqueous impregnation was more active. Both of these catalysts were more selective to methane than the reference catalyst.

Plots of conversions and selectivities vs. hours on stream for the two runs with carbon-supported catalysts are in figures 34 to 44. Both catalysts lost activity throughout the two short runs. The aqueous impregnated catalyst became more selective for methane as the run progressed (Figure 40) whereas the reverse micelle impregnated one produced less methane and was more stable with regard to methane production. Both catalysts were similar in ethane selectivity (Figures 36 and 41). The Run 67 catalyst was slightly more selective to propane + propylene than the run 77 catalyst, (Figures 37 and 42).

Although the reverse micelle catalyst did seem to be more promising than the aqueous catalyst for low methane selectivity, the fact that the reference catalyst was so much more active caused the work on carbon-supported catalysts to be stopped.

4.4.4 PERFORMANCE OF CATALYSTS SUPPORTED ON ALUMINA-TITANIA

Metals content and performance overview of the two catalysts prepared on alumina-titania support are in Figure 45. More detailed performance data from the two screening runs with these two catalysts are in the conversion and selectivity plots vs. hours on stream in Figures 46 to 57. The Run 68 catalyst was prepared via the reverse micelle route whereas the Run 73 catalyst was prepared via aqueous impregnation. Both of these catalysts contained only cobalt and ruthenium. Neither was as active as the reference catalyst, of the two the aqueous impregnated one was most active.

The reverse micelle impregnated catalyst was less selective to methane than the aqueous impregnated one, although it was still much more selective to methane than the reference catalyst.

4.5 STEM ANALYSES

STEM analyses were performed on pre-reduced samples of reverse micelle and aqueous impregnated catalysts. Six catalysts were so studied, one of each impregnation type on each of the three supports. Additionally, a STEM analysis was performed on the reference catalyst.

REFERENCE CATALYST. STEM analysis of this material was done with difficulty. The zeolite particles were not very transparent, however, the crystallites that could be observed were in the 50-100 Å range, elemental analyses were performed on eleven crystallites and are reported in Figure 58.

MAGNESIA-SUPPORTED CATALYSTS. Fresh samples of pre-reduced catalysts used in Runs 63 and 69 were analyzed. Elemental analyses of individual crystallites from each of these catalysts are attached as Figures 59 and 60. The Run 63 (reverse micelle) crystallites contained, on the whole, less ruthenium than those of the Run 69 crystallites (aqueous), suggesting that ruthenium was more likely to exit as small, undetectable, crystallites in the reverse micelle catalysts..

The Run 63 sample had detectable crystallites ranging in size from 60 to 300 Å whereas the Run 69 material exhibited crystallites in the range 50 to 350 Å with most being 100 to 200 Å. Thus the crystallite size ranges from reverse micelle and aqueous impregnation were about the same.

The amounts of manganese and zirconium in the crystallites of the Run 63 catalyst are summarized in Figure 59. The levels of these two metals in the crystallites were very irregular compared to their levels in the reference catalyst (Figure 58).

CARBON-SUPPORTED CATALYSTS. The two carbon-supported materials exhibited different crystallite size ranges. The Run 67 material (reverse micelle) exhibited mainly 20-40 Å crystallites, however, some as large as 60 Å were observed. The Run 77 catalyst (aqueous), on the other hand, had many in the 300 to 500 Å range with most in the 100-300 Å range. With this support the reverse micelle method did seem to produce a narrow crystallite size range close to that desired. However, once again the reverse micelle cobalt crystallites contained less ruthenium than those from aqueous impregnation (Figures 61 and 62).

ALUMINA-TITANIA-SUPPORTED CATALYSTS. The two catalysts on this support were reasonably active but highly selective for methane. Crystallites were hard to locate on these

materials, the cobalt was probably, therefore, highly dispersed with most crystallites below the limit of detection by STEM. Small crystallites are known to be selective for methane. Individual crystallites that could be discerned were analyzed for cobalt and ruthenium. Once again it was the crystallites from the aqueous impregnation which contained ruthenium whereas the ones from reverse micelle impregnation usually contained little or no ruthenium (Figures 63 and 64).

4.6 SUMMARY

None of the reverse micelle-impregnated catalysts were active enough to satisfy the goals of this work. .

All seven of the experimental catalysts contained ruthenium, and were, in fact, less active than the reference catalyst resulting from previous DOE contracts to the Union Carbide Corporation for development of a ruthenium-free, Y-zeolite supported, cobalt-based F-T catalyst. In some cases it appeared to have been well incorporated into the cobalt crystallites (aqueous impregnations), in other cases it wasn't (reverse micelle impregnations). Since all of these catalysts were of low activity compared to the ruthenium-free reference catalyst no cobalt-free catalysts were prepared. Rather, the focus of this work was shifted to the previously-developed method of catalyst preparation utilizing a Y-zeolite support. This work is summarized in the following section.

5. DEVELOPMENT OF HIGH ACTIVITY Y-ZEOLITE SUPPORTED CATALYST

This section summarizes further development of a Y zeolite-supported catalyst.

5.1 BACKGROUND

As originally developed under DOE contracts to Union Carbide Corp. this catalyst contained 8 wt % cobalt. In the current work much more active catalysts were prepared which contained as much as 28 wt% cobalt. The activity per mole of contained cobalt was about the same as the earlier catalyst indicating that even at very high levels the individual atoms of cobalt were still accessible as catalyst, i. e., little cobalt, at best, was deactivated by being covered over with other cobalt atoms. The new catalysts were more active on a total catalyst volume basis, such activity is very critical for use in a LPFT reactor. In such a reactor the liquid (wax) phase is the major phase, for efficient operation the catalyst should comprise 20 % or less of the total reactor volume.

In the original Union Carbide catalyst of the mid 1980's manganese and zirconium were found to be useful adducts for control of, respectively, selectivity and stability. In the current work ruthenium was also added to some catalyst formulations to determine whether it could be useful for enhancing catalyst activity.

The original Union Carbide catalyst was supported on an unbound zeolite powder. This catalyst resulted from a pore-filling type of impregnation utilizing an ethylene glycol solution of salts of cobalt, manganese and zirconium. Pre-steaming of the support resulted in formation of roughly

50-100 Å amorphous pores within the crystalline structure of the Y-zeolite. X-Ray analysis after steaming showed that the crystalline nature of the remaining Y-zeolite was largely intact. The acid wash serves the purpose removing extraneous amorphous alumina from the crystalline channels of the Y-zeolite framework. This alumina originates during the steaming process and its loss from the crystalline zeolite structure is what causes formation of the large pores. Removal of the amorphous alumina increases the rate of diffusion of reactant and product molecules during catalysis and also facilitates introduction of metals into the large pores during catalyst preparation. Acid-washing is accomplished with little loss in crystallinity.

The large pores were desired in the support to dimensionally stabilize the cobalt as 50- 100 Å crystallites, i. e., the crystallites would be resistant to agglomeration. This size crystallite is considered optimal for F-T catalysis, small crystallites are very selective for methane and, in addition, are prone to form volatile ruthenium carbonyls which can exit the catalysis zone with the gas effluent. In the current work with very high cobalt loadings at least some of the cobalt is present external to the zeolite as >100 Å crystallites.

In the present work, except for the catalysts in Sections 5.2.1 and 5.2.2 below, the Y-zeolite supported catalysts were prepared according to the preparation method outlined in Figure 65. In the exceptional cases water replaced ethylene glycol as impregnation solvent. The new catalysts are discussed below in terms of how they compare to each other and to the reference catalyst from the previous Union Carbide DOE contracts.

5.2 PREPARATION AND EVALUATION OF CATALYSTS

5.2.1 AQUEOUS IMPREGNATIONS, STEAMED BUT NOT ACID-WASHED Y-ZEOLITE SUPPORT

Four catalysts were prepared on a sample of steamed, but not acid-washed Y-zeolite. This material was later used as a support for other catalysts after acid-washing. Metals were impregnated from aqueous solutions of their salts, unlike the reference catalyst which used an ethylene glycol solution. All four catalysts were evaluated in the fixed-bed pilot plant according to the three condition test. The amounts of metals present on these catalysts and an overview of catalyst performance compared to the reference catalyst are in Figures 66 to 68. The amount of cobalt on each of these catalysts was about the same as on the reference catalyst. The new catalysts were all of about the same activity. However, this activity was lower than that of the reference catalyst.

Of the four new catalysts, the one which incorporated a small amount of ruthenium was the most selective to methane + ethane. Since this catalyst did not evince superior activity, the presence of ruthenium was in no way beneficial and was, in fact, a detriment to the desired catalyst performance.

The manganese and zirconium adducts did not facilitate superior catalyst performance compared to the Run 80 catalyst which only contained cobalt.

5.2.2 AQUEOUS AND REVERSE MICELLE IMPREGNATED CATALYSTS, STEAMED AND ACID-WASHED Y-ZEOLITE SUPPORT

Five catalysts were prepared on three samples of steamed and acid-washed Y-zeolite. Each acid washing was under a separate set of conditions, each used a separate aliquot of the steamed Y-zeolite used for the catalysts in Section 5.2.1. The washing conditions are in Figure 69 along with properties of the washed material and amounts of metals impregnated onto the support.

Nitric acid was used for all of the washes. The first sample resulted from a thirty-six hour wash with 2M nitric acid. Two catalysts were prepared from this support. The second wash also lasted thirty-six hours but used 3M nitric acid. One catalyst was prepared from this support. The final wash again used 3M nitric acid but the length of the wash was seventy-two hours. Two catalysts were prepared from this support.

One of the two catalysts prepared on the seventy-two hour washed material was prepared via reverse micelle impregnation. The other four catalysts were prepared by aqueous impregnation.

These catalysts were <u>not</u> all of the same activity. Catalyst activity increased as the severity of the washes increased. Activities and selectivities are summarized in Figures 70 and 71.

The surface area, as determined by nitrogen porosimetry, did not change much as the washes became more severe. The washes did seem to eventually cause a slight increase in the pore volume (Figure 69). Plots of fractional pore volume vs. pore radius from nitrogen porosimetry are attached

as Figure 72; there was at best a slight change in the pore distribution as the washes became more severe. However, the amount of aluminum did decrease continually as the severity of the washes increased. It is possible that channels open to nitrogen when the aluminum content was high were not yet open to the metal salts used in the impregnation step, and/or were not yet fully capable of allowing product molecules to diffuse out.

The most active catalyst was the one evaluated in Run 87. It was prepared on a support that had been acid-washed for seventy-two hours. It was initially more active than the reference catalyst but lost activity throughout the time it was operated at Condition 1. The methane and ethane selectivities were low compared to the other four new catalysts but slightly higher than obtained with the reference catalyst. Run 87 was continued past the normal shut down time for the screening runs to allow a return to the original conditions (Figures 73 to 78). The activity loss observed at Condition 1 had continued throughout the run; the conversions upon return to Condition 1 were lower. This activity loss was no doubt accelerated by Conditions 2 and 3 at 231° C. The methane and ethane selectivities were also slightly higher at the end of the run. This could have been due in part to the lower conversions since with cobalt catalysts methane and ethane are known to be conversion dependent with higher selectivities resulting at lower conversions. One question not resolved is whether zirconium would have stabilized the catalyst. The above work illustrates that the most extensively nitric acid-washed supports provided the most active catalyst.

The reverse micelle catalyst evaluated in Run 86 was less active than the aqueous catalyst prepared from the same support (Run 87). It also did not exhibit the low methane + ethane selectivity of the Run 87 catalyst. this was the last reverse micelle catalyst evaluated in this work.

5.2.3 ETHYLENE GLYCOL IMPREGNATIONS, STEAMED AND ACID-WASHED Y-ZEOLITE SUPPORT

Solutions of metals in ethylene glycol were used to impregnate supports in the original Union Carbide work. A "pore filling" approach was used, namely enough ethylene glycol solution was added to the support powder to barely wet it. There are no residual impregnation liquors; the impregnated support is dried and calcined.

The first ethylene glycol impregnated catalyst was evaluated in Run 95. The support was from the second batch of seventy-two hour washed Y-zeolite. The properties of this material were slightly different than those of the initial batch (Figure 79). The catalyst prepared from this material contained minor amounts of manganese, zirconium and rhenium, the amounts of which are also in Figure 79. After reduction this catalyst was screened in the fixed-bed pilot plant. It was maintained at Condition 1 until the rate of loss of activity from the initially high activity had slowed appreciable (Figures 80 to 85). The carbon monoxide conversion decreased from 100% to 61% during this period. The methane selectivity increased from 9 to 12 mole %. The conversions at the apparent line out were similar to those of the reference catalyst but the methane selectivity was higher. For this run since the catalyst was quite active, the first condition change was a feed rate reduction to allow assessment of selectivities at higher conversion. The feed rate was halved resulting in a carbon monoxide conversion of 85% and a lowered methane selectivity (11 mole %). The final condition change was a temperature increase to 221° C. This resulted in an initial carbon monoxide conversion of 98%, but strong indication of a faster rate of catalyst deactivation. The temperature increase also resulted in an increase in methane selectivity, even though the catalyst

was operating at a much higher conversion. This was probably due to the higher temperature since a conversion increase alone should result in lower methane selectivity.

Bench experiments indicated that the extensively washed Y-zeolites could adsorb greater quantities of metals than present on the reference catalyst. Furthermore, it was shown that short washes with hydrochloric acid could replace the long nitric acid washes, a considerable savings in time and, ultimately, cost. Long hydrochloric acid washes result in destruction of the Y-zeolite crystallinity resulting in formation of amorphous silica.

A high cobalt catalyst was prepared on a support resulting from three hours of wash with 3.87 M hydrochloric acid. The properties of the earlier seventy-two hour nitric acid-washed zeolites and the three hour hydrochloric acid-washed one are compared in Figure 86. The surface area after hydrochloric acid wash was 582 m^2/g, a strong indication that no loss in crystallinity resulted from the acid wash since the prewashed steamed Y-zeolite had a similar high surface area (591 m^2/g). The three hour hydrochloric acid wash removed more aluminum than the seventy-two hour nitric acid washes.

The high cobalt catalyst contained 17.6 wt% cobalt, double the amount on the earlier catalysts including the reference catalyst. The surface area and pore volume of the material after impregnation of metals and calcination were 313 m^2/g and 0.33 cc/g compared to 329 m^2/g and 0.36 cc/g for the Run 95 material. After reduction this catalyst was evaluated in Run 97 and was so active that the evaluation was only at Condition 1. Plots of conversions and selectivities vs. hours on stream are attached as Figures 87 to 93. At the end of the one hundred and thirty hour run the catalyst appeared to be reaching a carbon monoxide conversion line out of about 73%. This is

about 10% higher than the conversion at a comparable time during Run 95. The selectivities, however, were the same in these two runs with the exception that in Run 97 the butene selectivity was slightly lower than in Run 95. The methane selectivity started at 10 mole % and appeared to be lining out between 12 and 13 mole % at the end of the run.

With the lower activity catalysts the inlet temperature was very close to the catalyst bed maximum temperature, however, with the high activity catalyst the catalyst bed maximum temperature was initially about 20° C above the inlet temperature. This is illustrated by the temperature profiles in Figure 94. This means that the catalyst was operating *de facto* at a much higher temperature than desired, and, therefore, that the large amount of quartz sand diluent was not enough to remove all the heat generated at the top of the catalyst bed. The slurry autoclave reactor operates with more diluent (290 g of wax) and since it is stirred there are no appreciable differences between the temperatures at different points within the reactor. The very active high cobalt catalyst was thus evaluated in the slurry autoclave reactor.

5.2.4 BOUND CATALYST: FIXED-BED AND SLURRY AUTOCLAVE EVALUATIONS

The overall objective of this work was development of a cobalt-ruthenium catalyst for LPFT. The activity and selectivity of the high cobalt catalyst was promising enough to warrant a determination of its potential as such a catalyst. For a commercial application binding will be necessary to furnish catalyst shapes large enough to be separated from the F-T product wax by mechanical means since the zeolite alone is a very fine mesh powder.

Binding was accomplished by making a mull with Ludox followed by drying, calcination and crushing of the large pieces. Ludox is an aqueous solution of a silica precursor which reverts to silica when heated. It is a common material for binding catalyst powders. The zeolite to silica weight ratio in the bound catalyst was 75:25. The metals analyses before and after binding are in Figure 95.

The bound catalyst was first evaluated in the fixed-bed pilot plant as Run 99. Enough was loaded so that the amount of zeolite in the reactor was the same as in Run 97. The feed rate per gram of cobalt in the reactor was the same in Runs 95 and 97.

Plots of conversions and selectivities vs. hours on stream are attached as Figures 96 to 102. Once again the entire run was performed at one test condition, Condition 1 of the three conditions of the screening test. As in Runs 95 and 97, the initial conversions were very high followed by a period of activity loss. By run's end the carbon monoxide conversion appeared to be near line out at about 55%. This is less than resulted from the unbound version of this catalyst. It is not unexpected to find some loss in conversion due to binding, since the binder can block access to some of the catalyst active sites.

The selectivities also appeared to approach line out by the end of the run. The near line out conversions and methane, ethane and ethylene selectivities from Runs 97 and 99 are compared in Figure 103. The C_1 and C_2 selectivities were quite close as were the propane and butane selectivities. However, the bound catalyst was less selective to propylene and butylene:

ALKENE	SELECTIVITIES, MOLE %	
	RUN 97	RUN 99
PROPYLENE	2.1	4.1
BUTYLENE	1.7	3.1

Temperature profiles for Run 99 are included in Figure 104. In spite of the somewhat lower activity than Run 97, there was still a noticeable exotherm in the catalyst bed.

A fresh sample of the run 99 catalyst was evaluated in the slurry autoclave pilot plant (Run 61). The catalyst was reduced at 350° C in flowing hydrogen in a tube reactor before being loaded into the slurry autoclave reactor. The initial conditions during this run were 211° C and feed rate = 4.9 NL/hr • g cobalt. Plots of conversions and selectivities vs. hours on stream for Run 61 are attached as Figures 105 to 112.

Since this was the first slurry autoclave run with a cobalt catalyst from this contract, several conditions were studied. Catalyst activity loss had slowed appreciably by 80 hours on stream when the first condition change was made. At this time the carbon monoxide conversion also appeared to be approaching line out at 10 mole %. The other light gas selectivities were also approaching line out at this time.

The first condition change at 80 hours on stream was made so that the catalyst would operate at

a temperature closer to the that of Run 99 which utilized a 211° C inlet but had a noticeable exotherm meaning the actual operating temperature was higher than the inlet temperature. Thus the temperature was increased to 221° C, after which it was apparent that the catalyst deactivation was still occurring, although slowly. Deactivation rates generally increase as the temperature increases. Performance at this set of conditions is compared to that during Run 99 in Figure 103. The conversions in the two runs were about the same among the selectivities only that of methane is noteworthy, it being slightly lower in Run 61.

By the end of the run the temperature had been increased to 241° C. Additional catalyst deactivation had occurred by then and, as might have been expected, the catalyst was very selective for methane (20 mole %) at this high temperature.

Near the end of the run potassium was added to the reactor as a solution of potassium laurate in isopropanol/heptane. During work being done simultaneously on a DOE contract for development of an iron-based LPFT catalyst it had been found that so-added potassium can increase conversion and decrease the selectivities to light gases. In this case no change in the light hydrocarbon selectivities was noted. At best a small decrease in conversions and a small increase in carbon dioxide selectivity occurred.

5.2.5 EFFECT OF CHANGING THE CATALYST REDUCTION TEMPERATURE

Two runs were performed with catalysts that were reduced at 325° C and 375° C instead of the normal 350° C. The catalysts for these two runs resulted from separate fresh samples of catalysts containing 18.5 wt% of cobalt. These resulted from impregnation of the washed Y-zeolite resulting

from the second three hour hydrochloric acid wash which earlier provided the support for the Run 101 catalyst. Properties of the support and final metals levels are in Figure 86. Run 102 utilized catalyst from a 375° C reduction whereas Run 104 utilized one from a 325° C reduction. Both of these runs were performed under conditions identical to those of the earlier Run 97. In each the initial fast rate of change of conversions and selectivities had slowed appreciably by run's end. Both of the runs were approximately 100 hours long, a tabular summary of catalyst performance during them and the earlier Run 97 is in Figure 113. The 375° C reduction temperature resulted in the least active catalyst, the 325° C and 350° C reductions produced catalysts of about the same activity. The selectivities during all three runs were nearly the same. The 325° C reduced catalyst was a little less selective to methane and a little more selective to carbon dioxide than the other two. Based on this an even lower activation temperature was investigated.

A 27 wt % cobalt catalyst was reduced at 300° C for two hours, it resulted from work outlined in the following section of this report. It was evaluated in a similar fashion to the Run 110 catalyst (350° C reduction) including use of a 6.5 rather than 13 G loading of catalyst. This run is not summarized because except for somewhat lower conversions (carbon monoxide + hydrogen = 80%, carbon monoxide = 75%) the performance was the same as the Run 110 catalyst. So far the low temperature reductions produce slightly inferior catalysts. Additional 300° C reductions might be warranted, perhaps a longer reduction period is needed.

Low reduction temperatures are of interest because the LPFT reactor will almost certainly not allow an *in- situ* reduction at temperatures much above the F-T processing temperature (<300° C). Thus for a high temperature reduction costly equipment will be required for an *ex-situ* reduction.

5.2.6 STEM ANALYSIS: HIGH COBALT CATALYST PRECURSOR

A sample of the pre-reduced material used in Runs 102 and 104 was analyzed by STEM. Metal oxide crystallites ranging from 30 (the smallest the STEM instrument can see) to 2000 Å were found, the average being 500 Å. Some of the crystallites were associated with the zeolite, some were not. Crystallite composition varied. There was a tendency for the zirconium and ruthenium not to be found together. Ruthenium was rarely seen in crystallites smaller than 100 Å, whereas zirconium was mostly noted in crystallites smaller than 200 Å. Manganese content varied among the crystallites examined but seemed to increase in the smaller crystallites. Representative STEM photographs are attached as Figures 114 and 115. Additionally, tables containing representative STEM elemental analyses of various-sized crystallites are attached as Figure 116.

The pre-reduction precursor of the catalysts used in Runs 110 and 121 had similar 30 to 2000 Å crystallites by STEM. There were, however, more crystallites. Crystallites were again observed which were free of the zeolite. Zirconium was again associated with the smaller particles and again tended to be associated with the zeolite.

The STEM work indicates that this high cobalt level catalyst contained at least some metals exterior to the 50-100 Å pores of the steamed zeolite. In fact some of the metal crystallites existed entirely free of the zeolites. Others appeared to have grown attached to the zeolite such as those in the bottom left of Figure 115. The performance data indicates that the external cobalt is active for F-T synthesis, and, since the lowest methane selectivities were found for the highest cobalt-level catalysts, the external cobalt must not have been extremely selective for methane.

The STEM work indicates, additionally, that further work must be done to understand the affect of the trace metals. They do not seem to be evenly distributed throughout the crystallites!

5.2.7 VERY HIGH COBALT CATALYSTS

Catalysts containing approximately 27 wt% cobalt were prepared. The first of these was evaluated in Run 101; it was prepared on the second lot of 3 hour hydrochloric acid-washed support (Figure 86). A fresh sample of the steamed Y-zeolite used for the first hydrochloric acid wash was used for the second washing. Performance during Run 102 is summarized as a series of plots of conversions and selectivities vs. hours on stream (Figures 117 to 122). The high activity of the catalyst can be further illustrated by the temperature profiles in Figure 123.

A second catalyst with a cobalt level similar to that of the Run 101 catalyst was prepared. This catalyst was supported on material resulting from the third three hour hydrochloric acid wash of the original steamed Y-zeolite sample (Figure 86). It was also screened in the fixed-bed pilot plant (Run 110) but less catalyst and more diluent were used to decrease the intensity of the catalyst bed exotherm. Performance during this run is summarized as a series of plots of conversions and selectivities vs. hours on stream in Figures 124 to 129. The feed rate per gram of cobalt was the same as in Run 101; this resulted in less heat being generated on the catalyst bed as evidenced by the temperature profiles in Figure 130.

The conversions after the usual initial high rate of catalyst deactivation were still quite high (carbon monoxide conversion = 82% at 100 hours on stream). Therefore, the earlier high conversions with this very high cobalt-type catalyst were not just due to the high temperature of operation resulting

from the intense exotherm. The maximum temperature on the catalyst bed during Run 110 was, in fact, very close to that on the bed during Run 97 (compare Figures 130 and 131).

At 100 hours on stream the feed rate was reduced by half. This initially resulted in an increase in conversion some of which was rapidly lost, in part at least, due to continued loss in catalyst activity. However, it is also likely that the system required some time to equilibrate at the new feed rate. The conversions did appear to approach line out after the feed rate change (carbon monoxide conversion = 85% at 140 hours on stream). The catalyst bed maximum temperature before and after the feed rate change was the same. Although less feed was going into the plant, the higher conversion no doubt resulted in approximately the same amount of heat being produced.

Operating the 27% cobalt catalyst with less catalyst and more diluent produced the desired effect, namely high conversions at 211° C inlet temperature with a low exotherm on the catalyst bed. A tabular summary of the performance during Runs 97, 101 and 110 is attached as Figure 132. The lowest methane selectivity of any of the catalysts developed under this contract resulted during Run 110

5.2.8 ADDITIONAL VERY HIGH COBALT CATALYSTS

The initial sample of commercial steamed Y-zeolite was consumed prior to these experiments. A second sample was obtained, but it was from a different commercial lot. An aliquot of it was washed for three hours with hydrochloric acid before being used as a support for the catalysts below.

Two catalysts were prepared from this support, each contained slightly more than 28 wt% of cobalt. Support and catalyst analyses for these two catalysts are summarized in Figure 133. Each catalyst was reduced for two hours at 350° C with hydrogen prior to use in fixed-bed pilot plant Runs 122 and 123. The ruthenium-containing catalyst (Run 122) was inferior to the earlier similar composition catalyst evaluated in fixed-bed pilot plant Run 110. The performance difference between the two catalysts can be illustrated through comparison of the temperature profiles during the two runs (Figures 130 and 134). In Run 110 the initial catalyst bed maximum temperature was slightly over 220° C; at 132 hours on stream the profile had hardly changed. During Run 122, however, the maximum temperature decayed from slightly over 220° C to about 217° C at 138 hours on stream. The temperature decay continued throughout the run. Loss of catalyst activity witnessed by decay of temperature in this fashion is characteristic of deactivation mechanisms such as covering over the reactive sites with reaction by-products such as coke (in this case perhaps wax) or destruction of these sites, for instance, by a thermal mechanism such as sintering. Loss of activity due to feed impurities, on the other hand, causes loss of active sites from the inlet of the reactor where feed impurities first adsorb. In such cases the temperature maximum usually is constant but moves further and further away from the inlet.

The difference between the two ruthenium-containing catalysts is also apparent in the plots of conversion and selectivity vs. hours on stream in Figures 135 to 139. The rate of loss of activity during Run 122 was severe and never slowed, whereas in Run 110 the rate of activity loss slowed and the catalyst appeared to be approaching activity line out by run's end.

The least stable ruthenium catalyst was prepared on the second support. However, a ruthenium-free catalyst was also prepared on this support. It was activated and tested in a similar fashion to

the two ruthenium-containing catalysts (Run 123). It was more active and more stable than either of these catalysts. It is possible that something, as yet not understood, went wrong during preparation of the Run 122 catalyst. It is also possible that the initial activity of the Run 122 catalyst was very high but that it suffered a very rapid deactivation.

The ruthenium-free catalyst was evaluated in Run 123. Temperature profiles during this run are summarized in Figure 140. The initial catalyst activity was so high that the catalyst bed maximum temperature was at the inlet with heat being transferred back to the incoming feed. A little deactivation occurred at the beginning of the run causing the maximum temperature to move a bit down from the inlet. A slight increase in the catalyst bed maximum temperature was noted, perhaps due to slight upward adjustments in the reactor heaters to maintain the target inlet temperature which previously had been maintained, in part, by the reaction heat. However, after the slight change at the beginning of the run the catalyst bed maximum was stable. It was higher and more stable than the corresponding temperature during the two runs with the ruthenium-containing catalysts; it was 232° C at 210 hours on stream.

The two best runs (110 and 123) are compared in summary fashion in Figure 141. The conversion and methane selectivity were higher in Run 123. Normally with cobalt catalysts the methane selectivity decreases at higher conversion. That the opposite is true in the present comparison is probably at least in part due to the higher effective temperature during Run 123; methane selectivity increases with increasing temperature. The higher temperature during Run 123 also partially accounts for the higher conversions noted during this run. Conversions and selectivities as a function of hours on stream are summarized in Figures 142 to 145.

The Run 122 and 123 catalysts were evaluated in slurry autoclave tests. In both cases the catalysts were activated at 350° C in a fixed-bed reactor prior to loading into the autoclave reactor. Catalysts were moved to the autoclave under a nitrogen atmosphere. The Run 123 catalyst was activated by a somewhat different procedure than was used for any of the other catalysts. During its activation there was a calcination and second reduction with hydrogen after the first hydrogen reduction. However, in both cases the catalysts were used without being bound. In the earlier slurry autoclave evaluation of a lower cobalt catalyst, the catalyst was bound with silica before being evaluated. Both of the autoclave runs with the very high cobalt catalysts were disappointing. In both cases very low conversions were obtained, although the ruthenium-free catalyst seemed to line out at a better conversion than the ruthenium-containing one. Conversions, selectivities and operational conditions vs. hours on stream for these two runs are summarized in Figures 146 to 155.

The second slurry autoclave evaluation (Run 74) provided information that was unexpected but enlightening from the standpoint of further catalyst development. The catalyst was very active initially at 200° C operating temperature. The initial high conversions decayed rapidly over a ten hour period. At twenty-five hours on stream the operating temperature was increased to 210° C. Normally such a temperature increase would provide an increase in conversion. In this case it didn't, probably due to the continuing high rate of activity loss. It is possible that binding would have provided a more activity stable catalysts under the conditions of liquid phase processing. For instance, the powdery catalyst could have been splashed to the sides of the autoclave during use. Obviously, the high initial activity of the Run 74 catalyst was close to that expected.

5.2.9 STEM ANALYSIS OF A REDUCED VERY HIGH COBALT CATALYST

STEM-wise, reduced and pre-reduced catalysts were similar. For instance, STEM analysis of a reduced high cobalt catalyst similar to the ruthenium-free catalyst of Run 123 showed the same wide range of crystallite sizes as earlier such analyses of pre-reduced catalysts. The reduced catalyst contained small crystallites within a zeolite matrix (dark spots in light gray, zeolite, particle mid-center of Figure 156) and large amorphous cobalt particles (entire Figure 157). The latter particles were extraneous to the zeolite. Both types of cobalt were also present in pre-reduced (high) cobalt catalysts.

Atomic analysis of the crystallites by STEM showed most of the zirconium associated with the large rather than small cobalt crystallites (Figure 158). This was also observed with pre-reduced catalysts analyzed by STEM earlier in this work. Zirconium is added to the catalyst composition to promote activity stability, therefore, it is possible that the activity loss noted with high cobalt catalysts is due to deactivation of the large crystallites.

6. CONCLUSIONS

Cobalt-based F-T catalysts from a reverse micelle impregnation route have, so far, exhibited low activity and excessive methane selectivities. Various compositions of metals have been tried, some with cobalt and others with cobalt and ruthenium. Three supports have been used. The reverse micelle approach was abandoned when it appeared that nothing attempted had promise of producing a catalyst superior to the one which resulted from two previous contracts to the Union Carbide Corporation. This catalyst was prepared on a modified Y zeolite support.

The Union Carbide catalyst resulted from impregnation of about 8 wt% cobalt on a steamed, acid-washed Y zeolite. This support is unique in a way that makes it a good fit as a F-T catalyst support. Steaming produces 50-100 Å amorphous pores or "cages" linked by crystalline channels. Metal crystallites, 50-100 Å in diameter and stable to agglomeration, may formed in these pores.

It has now been found that catalysts more active than the reference catalyst may be formed by the simple expedient of impregnating more cobalt. Catalysts with cobalt levels as high as 27 wt% have been prepared. Activity gains going from 8 wt% to 16 wt% and from 16 wt% to 27 wt% have been documented.

Although more active, the high cobalt catalysts were not as stable as the Union Carbide one. This is possibly due to a maldistribution of zirconium which was added to the original composition as a stabilizing agent. STEM analysis indicates that the zirconium tends to remain associated with cobalt

that is actually within the pores of the zeolite. Some of the cobalt in the high cobalt catalysts is external to the zeolite pores.

Small amounts of ruthenium have been added to the high activity compositions. However, the ruthenium rate enhancement expected from earlier work by Gulf/Chevron and Exxon could not be documented. Additional experiments are warranted because Gulf/Chevron and Exxon have employed special activation procedures to insure good ruthenium distribution and these techniques have not yet been evaluated.

Quite a bit of characterization work has been done. STEM has proven to be a particularly useful method of analysis. For instance, with the high cobalt, zeolite-supported, catalysts it has shown that some of the cobalt is present external to the pores of the zeolite as fairly large crystallites with a porous or "Raney" type of structure.

7. FUTURE DIRECTIONS

Experimental evidence that a small amount of ruthenium can promote Y-zeolite-supported cobalt F-T catalysts is lacking. For instance, the catalysts for Runs 122 and 123 were similar in composition except the Run 122 catalyst contained a low level of ruthenium. The Run 122 catalyst lost activity fastest. Because of the very high initial activity of these catalysts it was not possible to tell which was initially more active. Additional work with ruthenium-promoted catalysts is warranted.

STEM analysis of a reduced high cobalt catalyst similar to the ruthenium-free Run 123 catalyst above showed a wide range of crystallite sizes (Figures 164 and 165). Earlier STEM analyses before reduction had given same result. This is a different observation than expected from the previously-developed low cobalt level catalyst of Union Carbide. In this catalyst the cobalt exists mainly as 50-100 Å crystallites within the pores of the steamed Y-zeolite support. The high cobalt catalyst had particles that were definitely too big to be within the pores of the steamed zeolite.

Atomic analysis of the crystallites (by STEM) showed that most of the zirconium was associated with the small rather than large cobalt crystallites (Figure 166). This was also observed with pre-reduced catalysts analyzed by STEM earlier in this work. Zirconium is added to the catalyst composition to promote activity stability, therefore, it is possible that the activity loss noted with high cobalt catalysts was due to deactivation of the large crystallites. Future work should be directed toward obtaining a better zirconium distribution, perhaps by simply adding more zirconium to the composition. Interestingly, STEM analysis showed that the other trace metal, manganese, was more

evenly distributed through the small and large particles.

Once the stability issue has been addressed, the ruthenium vs. ruthenium-free problem should be settled. Initially high space velocity data will be required in order to reduce initial conversions and allow an assessment of whether or not the ruthenium catalyst is more active. If not, methodology similar to that described by Gulf/Chevron[42-45] and Exxon[46, 47] should be used, i.e. multiple oxidation/reduction cycles to enhance ruthenium distribution.

Additional attempts should be made to develop a method for low temperature catalyst reductions. Reasonable approaches would be longer reduction times at the lower temperatures and/or incorporation of a reduction promoting metal into the catalyst composition.

Finally, additional experiments with surfactant salts are warranted. The initial experiment reported herein was similar to ones performed during development of a precipitated iron catalyst under Contract No. DE-AC22-90PC90055 (final report pending). In such experiments potassium surfactant was added during slurry processing and startling changes in the activity and selectivity of the iron catalyst were noted. Similar changes were not noted with a similar addition to a cobalt catalyst (above experiment). However, potassium is known to be a better promoter for iron than cobalt whereas manganese, ruthenium and zirconium are among those useful for cobalt, perhaps surfactant salts of these metals would promote the cobalt catalyst.

It is also possible that suitable surfactants, perhaps even metal-free ones, might be useful to accelerate the rate of the Fischer-Tropsch reactions during slurry processing by accelerating the rate of mass transfer from the gas bubbles to the wax/catalyst surface.

REFERENCES

1. V.Rao, G.Stiegel, G.Cinquegrane and R.Srivastava, Fuel Processing Technology, 1992, 30, 83-107.

2. M.Dry, *Catalysis: Science and Technology* (J.Anderson and M. Boudart, eds.) Vol. 1, Chapter 4. Springer Verlag, Berlin and New York, 1981.

3. The three volume BMFT-Research Report on Fischer-Tropsch Synthesis prepared by Schering A.G. in cooperation with the Technical University in Munich and the Engler-Bunte Institute at the University of Karlsruhe, 1983.

4. C.Rofer-DePoorter, Chem. Rev., 1981, 81, 447.

5. P.Biloen and W.Sachtler in *Advances in Catalysis* (D.Eley, H.Pines and P.Weisz, eds.), Vol. 30, Academic Press, 1981, 165.

6. F.Fischer and H.Tropsch, Brennst.-Chem., 1926, 7, 97.

7. M.Poutsma, L.Elek, P.Ibarbia, A.Risch and J.Rabo, J. Catal., 1978, 52, 157.

8. J.Rabo, A.Risch and M.Poutsma, J. Catal., 1978, 53, 295.

9. M.Araki and V.Ponec, J. Catal., 1976, 44, 439.

10. P.Wentrcek, B.Wood and H.Wise, J. Catal., 1976, 43, 3363.

11. P.Biloen, J.Helle and W.Sachtler, J. Catal., 1979, 58, 95.

12. G.Low and A.Bell, J. Catal., 1979, 57, 397.

13. J.Ekerdt and A.Bell, J. Catal.,1979, 58, 170.

14. J.McCarty, P.Wentrcek and H.Wise, personal communication cited in ref. 20.

15. R.Brady III, R.Petit, J. Am. Chem. Soc. 1980, 102, 6181.

16. R.Brady III, R.Petit, J. Am. Chem. Soc. 1981, 103, 287.

17. H.Bock, G.Tschmutova and H.Wolf, J. Chem. Soc. Chem. Commun., 1986, 1068.

18. G.Henrici-Olive and S.Olive, J. Mol. Catal., 1982, 16, 111.

19. G.Henrici-Olive and S.Olive, J. Mol. Catal., 1983, 18, 367.

20. M.Smutek, J. Mol. Catal., 1984, 24, 257.

21. C.Zheng, Y.Apeloig and R.Hoffmann, J. Am. Chem. Soc., 1988, 110, 749.

22. G.Schulz, Z. Physikal. Chem., 1935, B30, 379.

23. P.Flory, J. Am. Chem. Soc., 1936, 58, 1877.

24. I.Yates, Ph.D. Thesis, Massachusetts Institute of Technology, 1990.

25. L.Koenig and J.Gaube, Chem.-Ing. Tech., 1983, 55, 14.

26. R.Dictor and A.Bell, J. Catal., 1986, 97, 121.

27. C.Satterfield, R.Hanlon, S.Tung, Z.-M.Zou and G.Papaefthymiou, Ind. Eng. Chem. Prod. Des. Dev., 1986, 25, 401.

28. S.Novak, R.Madon and H.Suhl, J. Chem. Phys., 1981, 74(11), 6083.

29. S.Novak and R.Madon, Ind. Eng. Chem. Fund., 1984, 23, 274.

30. H.Schulz, B.Rao and M.Elstner, Erdol and Kohle, 1970, 23, 651.

31. H.Pichler and H.Schulz, Chem.-Ing. Tech., 1970, 42, 1162.

32. E.Iglesia, S.Reyes and R.Madon, 1991, 12th North American Meeting of the Catalysis Society, Lexington, KY.

33. E.Gibson and R.Clarke, J. Appl. Chem., 1961, 11, 293.

34. C.Kibby, R.Pannell and T.Kobylinski, ACS Pet. Chem. Preprints, 1984, 29(4), 1113.

35. R.Summerhayes, S.Thesis, Massachusetts Institute of Technology, 1982.

36. J.Donnelly, I.Yates and C.Satterfield, Energy and Fuels, 1988, 2, 734.

37. A.Lapidus, M.Savel'yev and M.Tsapkina, Petrol. Chem., 1991, 31, 502.

38. R.Anderson, *The Fischer-Tropsch Synthesis*, Academic Press, Inc., New York, 1984, 140.

39. R.Fiato, E.Iglesia and S.Soled, U.S. Patent 5,248,701, 1993.

40. R.Fiato, E.Iglesia and S.Soled, U.S. Patent 5,162,284, 1992.

41. G.Ansell, R.Fiato, E.Iglesia and S.Soled, U.S. Patent 5,169,821, 1992.

42. H.Beuther, T.Kobylinski, C.Kibby and R.Pannell, U.S. Patent 4,585,798, 1986.

43. H.Beuther, C.Kibby, T.Kobylinski and R.Pannell, U.S. Patent 4,413,064, 1983.

44. H.Beuther, C.Kibby, T.Kobylinski and R.Pannell, U.S. Patent 4,493,905, 1985.

45. T.Kobylinski, C.Kibby, R.Pannell and E.Eddy, U.S. Patent 4,605,676, 1986.

46. R.Fiato, European Patent Application Publication No., 0 414 555 A1, filing date 8/23/90.

47. E.Iglisia, S.Soled, R.Fiato and G.Via, J. Catal., 1993, 143, 345.

48. A.Lapidus, A.Krylova, J.Rathousky, A.Zukal and M.Jancalkova, Applied Catal. A: General, 1992, 80, 1.

49. M.Hu, European Patent Application Publication No. 0 533 228 A1, filing date 8/17/92.

50. T.Kobylinski, C.Kibby, R.Pannell and E.Eddy, U.S.Patent 4,670,414, 1967.

51. T.Ishihara, N.Horiuchi, T.Inoue, K.Eguchi, Y.Takita and H.Arai, J. Catal., 1992, 136, 232.

52. J.Haggin, Chem. and Eng. News, Oct 26, 1981.

53. D.Jones, AIChE Spring National Meeting, Houston, Texas, April, 1991.

54. H.Koebel and M.Ralek, Catalysis Reviews Science and Engineering, 1980, 21(2), 225.

55. H.Koebel, German Patent 1,060,854.

56. U.S. Bureau of Mines, Report of Investigation 5043, 1954, 56-62.

57. J.Kuo, "Two-Stage Process for Conversion of Synthesis Gas to High Quality Transportation Fuels", Final report prepared by Mobil Research and Development Co. under U. S. DOE Contract No. DE-AC22-83PC60019, October, 1985. Report No. DOE/PC/60019-9.

58. W.Deckwer, *Reaktionstechnik in Blasensaulen,* Salle + Sauerlander, Frankfurt/Main(D), Germany (1985). English Translation: *Bubble Column Reactors,* Wiley, Chichester, England (1992).

59. H.Bi and L.-S.Fan, A.I.Ch.E.Journal, 1992, 38, 297.

60. S.Kumar, K.Kusakabe, K.Raghunathan, and L.-S. Fan, A.I.Ch.E.Journal, 1992, 38, 733.

61. J.-W.Tzeng, R.Chen and L.-S.Fan, A.I.Ch.E.Journal, 1993, 39, 733.

62. S.Kumar, K.Kusakabe, and L.-S.Fan, A.I.Ch.E.Journal, 1993, 39, 1399.

63. P.Stenius, International Patent Application, PLT/SE81/0091, 1981.

FIGURE 1

MAGNETIC PROPERTIES:

GROUP VIII METALS AND CARBIDES

MATERIAL	CURIE TEMP, °C	FISCHER-TROPSCH ACTIVITY
α-Fe	770	EXCELLENT
α-Co	1115	EXCELLENT
ß-Co	1115	EXCELLENT
Ni	353	SOME, CH_4 GOOD
Ru	PARAMAGNETIC	EXCELLENT
Rh	PARAMAGNETIC	POOR
Pd	PARAMAGNETIC	POOR
Os	PARAMAGNETIC	POOR
Ir	PARAMAGNETIC	POOR
Pt	PARAMAGNETIC	POOR
Fe_3C	210	EXCELLENT
ε-Fe_3C	380	EXCELLENT
X-Fe_3C	247	EXCELLENT
FeC	250	EXCELLENT
Ni_3C (hcp)	PARAMAGNETIC	INERT
Ni_4C	220	SOME

FIGURE 2

Slurry Bubble Demonstrations

Plants	Rheinprussen Plant	Mobil (Low Wax)	Mobil (High Wax)
Temp., °C	268	260	258
Pressure, psig	176	221	221
SV, NL/kgFe/hr	3,400	2,600	2,400
$CO+H_2$ Conv., %	89.0	86.8	82.2
Product Yield, gHC/gFe/hr	0.57	0.37	0.41

JCFA 11/84

CATALYST EVALUATION
PILOT PLANT
BW 12/12/90
MODIFIED 11/6/92
TO SHOW
ACTUAL FLOW 2/24/93 JCFA
THRU FEED
TREATERS

PLANT 700
"ISO-SYNTHESIS" CATALYST EVALUATION

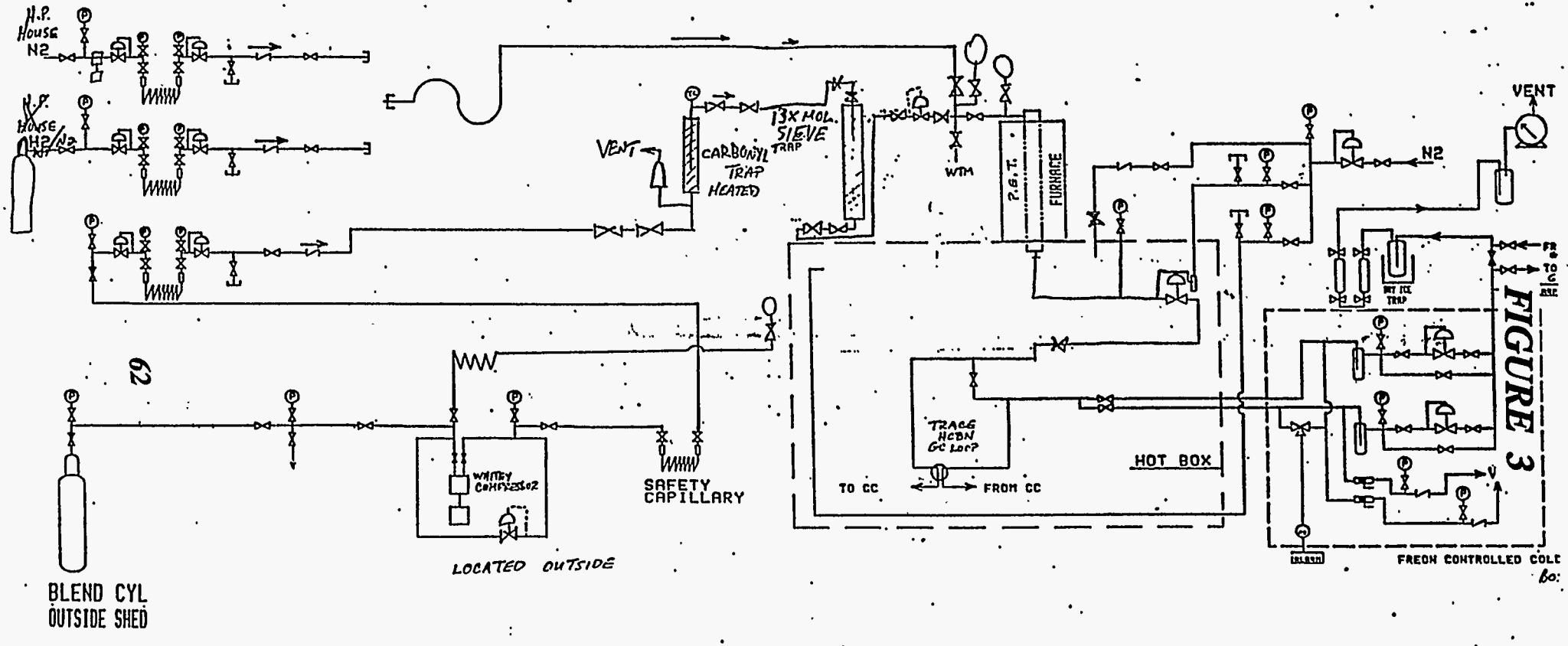

62

FIGURE 3

THREE CONDITION TEST

KEY VARIABLES	CONDITION 1	CONDITION 2	CONDITION 3
PRESSURE, PSIG	287	287	287
TEMP, °C	211	231	231
FEED RATE, (NL/HR G Co)	4.9	4.9	2.5

FIGURE 4

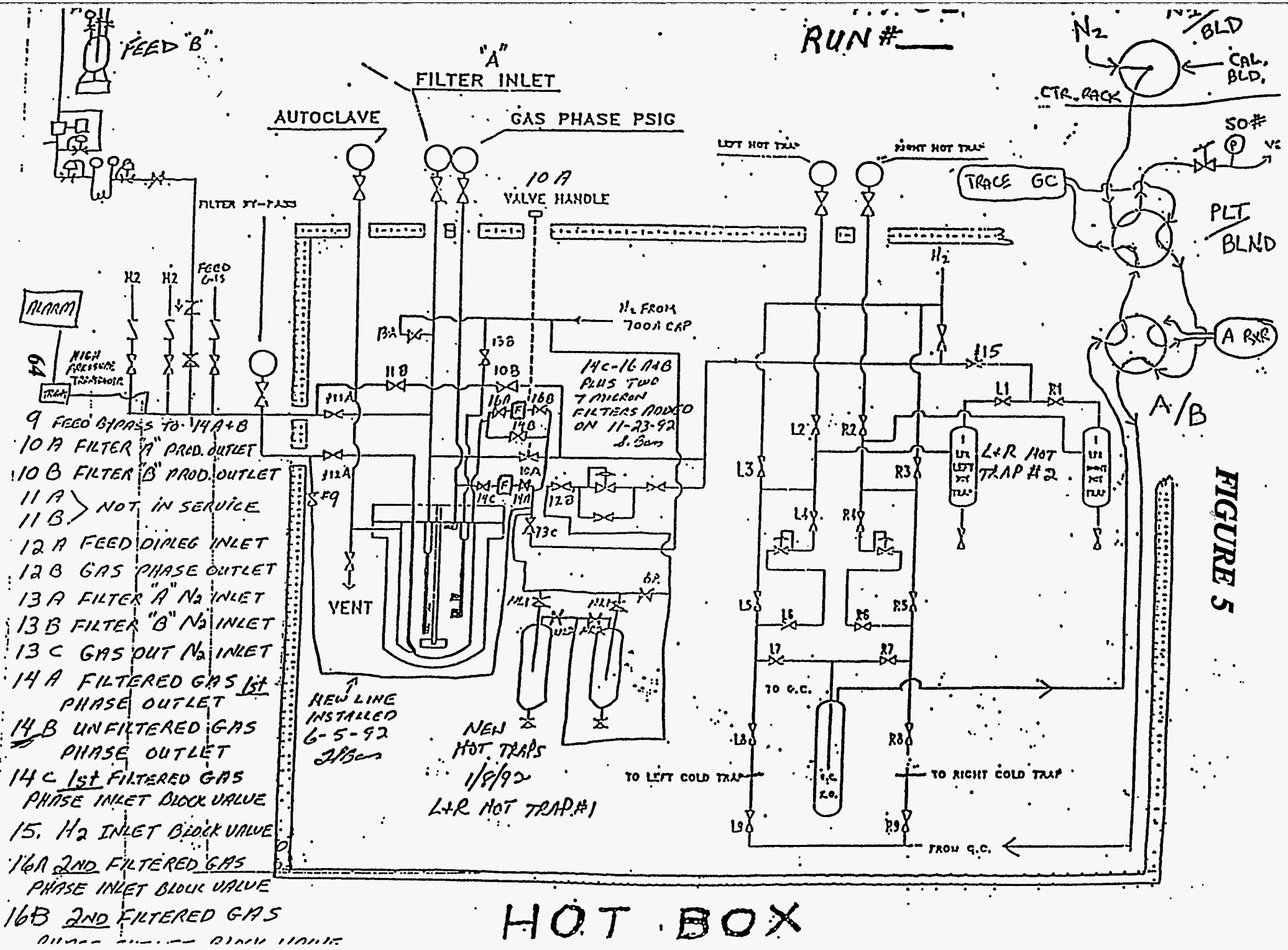
RUN #
FEED "B"
"A" FILTER INLET
AUTOCLAVE
GAS PHASE PSIG
10 A VALVE HANDLE
FILTER BY-PASS
ALARM
HIGH PRESSURE TRANSDUCER
TRAP
H2
H2
FEED GAS
H2 FROM TOOR CAP
14C-16 14B PLUS TWO 7 MICRON FILTERS ADDED ON 11-23-92 S. Barr
VENT
NEW LINE INSTALLED 6-5-92 SBarr
NEW HOT TRAPS 1/8/92
L+R HOT TRAP #1
LEFT HOT TRAP
RIGHT HOT TRAP
L+R HOT TRAP #2
TRACE GC
N2
CAL. BLD.
CTR. RACK
SO#
PLT BLND
A RXR
A/B
TO LEFT COLD TRAP
TO RIGHT COLD TRAP
TO G.C.
FROM G.C.
9 FEED BYPASS TO 14A+B
10 A FILTER "A" PROD. OUTLET
10 B FILTER "B" PROD. OUTLET
11 A
11 B. > NOT IN SERVICE
12 A FEED DIPLEG INLET
12 B GAS PHASE OUTLET
13 A FILTER "A" N2 INLET
13 B FILTER "B" N2 INLET
13 C GAS OUT N2 INLET
14 A FILTERED GAS 1st PHASE OUTLET
14 B UNFILTERED GAS PHASE OUTLET
14 C 1st FILTERED GAS PHASE INLET BLOCK VALVE
15. H2 INLET BLOCK VALVE
16A 2ND FILTERED GAS PHASE INLET BLOCK VALVE
16B 2ND FILTERED GAS
HOT BOX
FIGURE 5

Schematic of Slurry Autoclave Plant

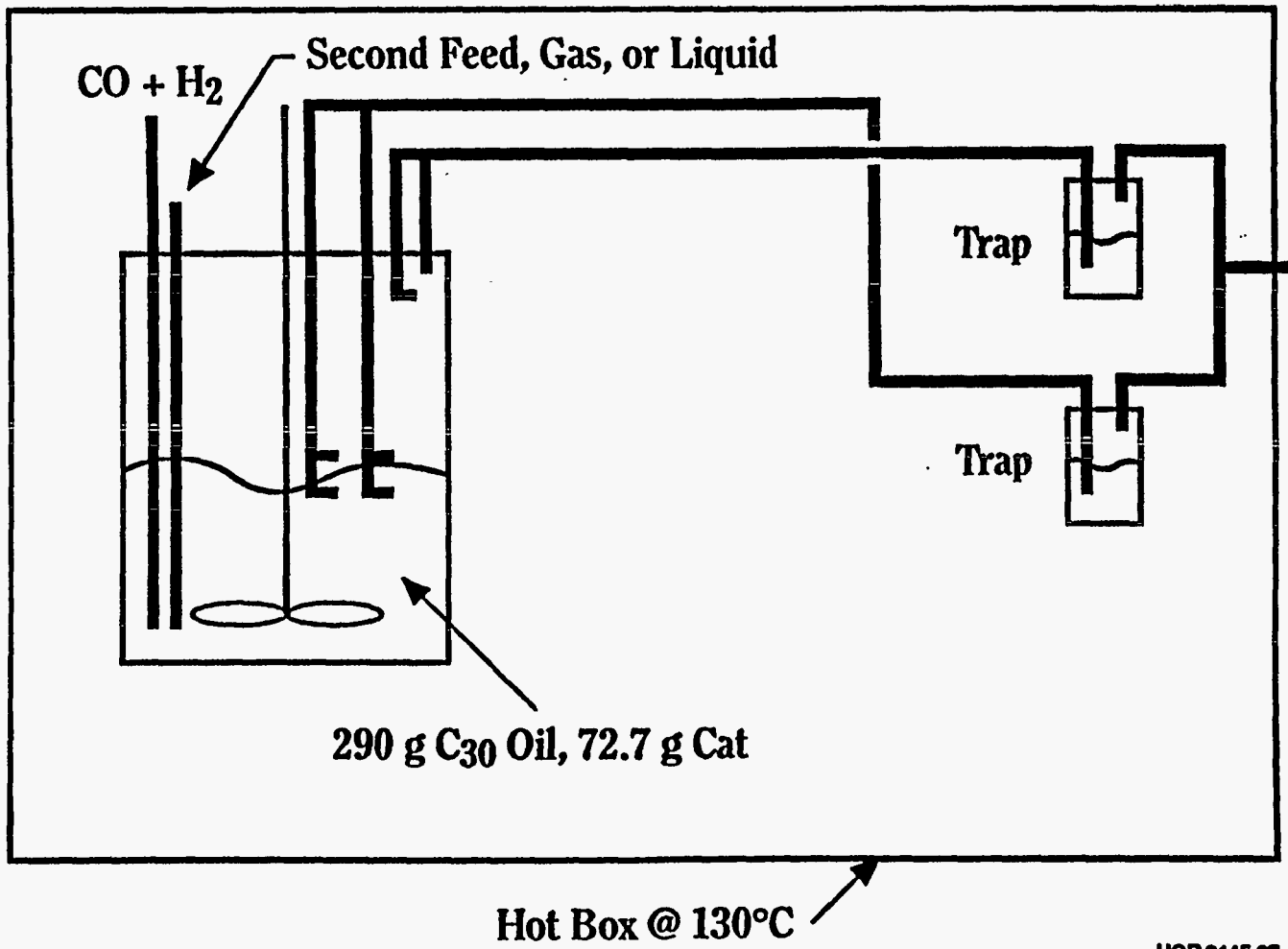

FIGURE 6

FIGURE 7

REVERSE MICELLE PROCEDURE FOR PREPARING SMALL METAL PARTICLES WITH A NARROW SIZE DISTRIBUTION

(P. Stenius et al., International Patent Application PLT/SE81/0091, 1981)

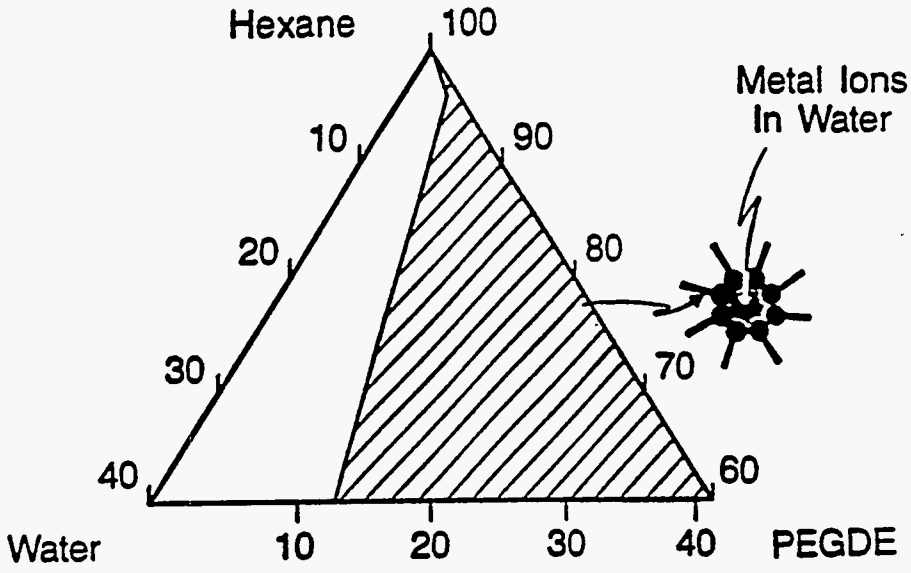

PEGDE: PENTAETHYLENE GLYCOL DODECYL ETHER

FIGURE 8

PLT 700A RUN 65 Tarrytown reference catalyst TC-211

Co,Mn,Zr on acid washed Y 2:1 H_2:CO in feed

13g active in 155g quartz sand

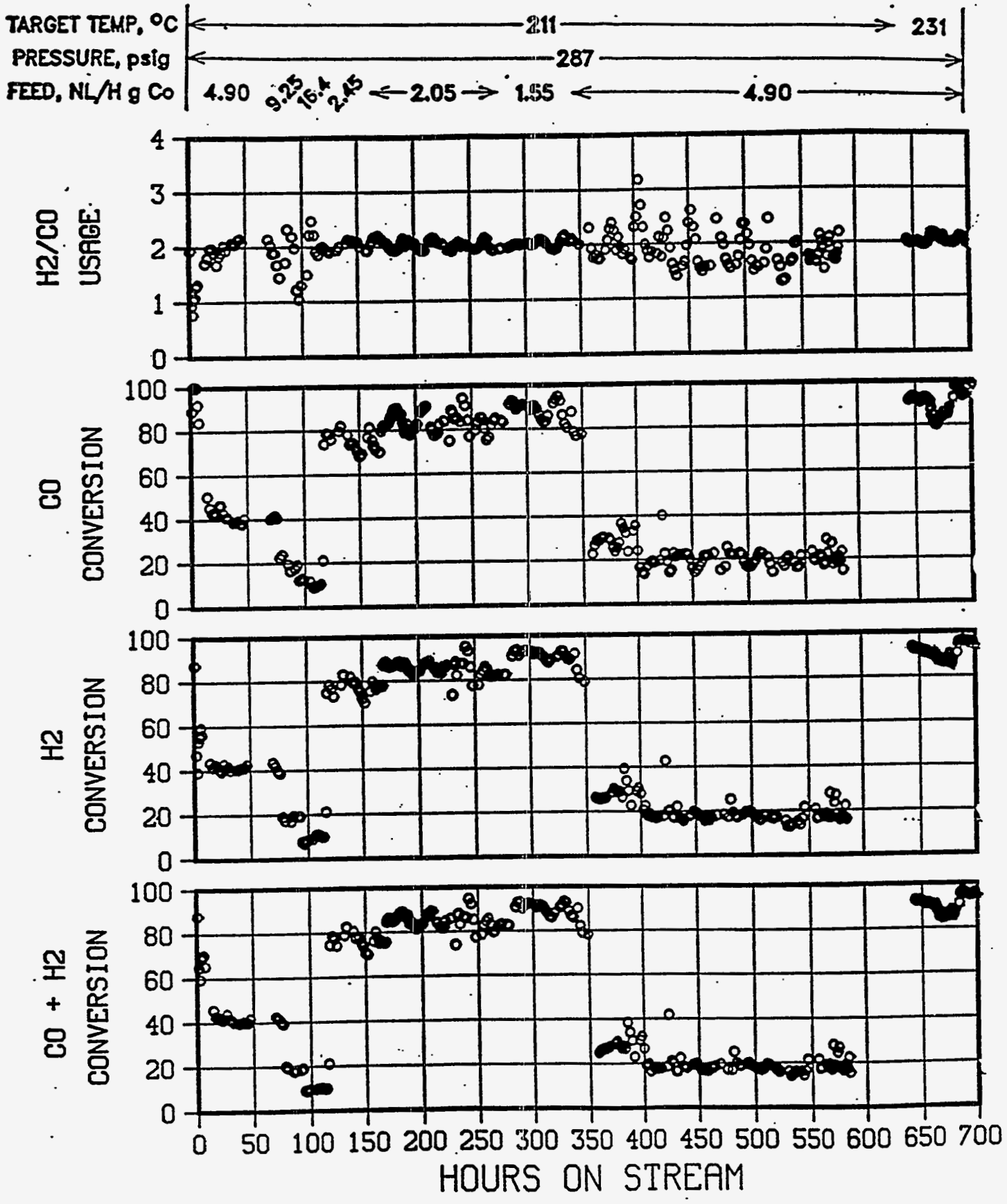

FIGURE 9

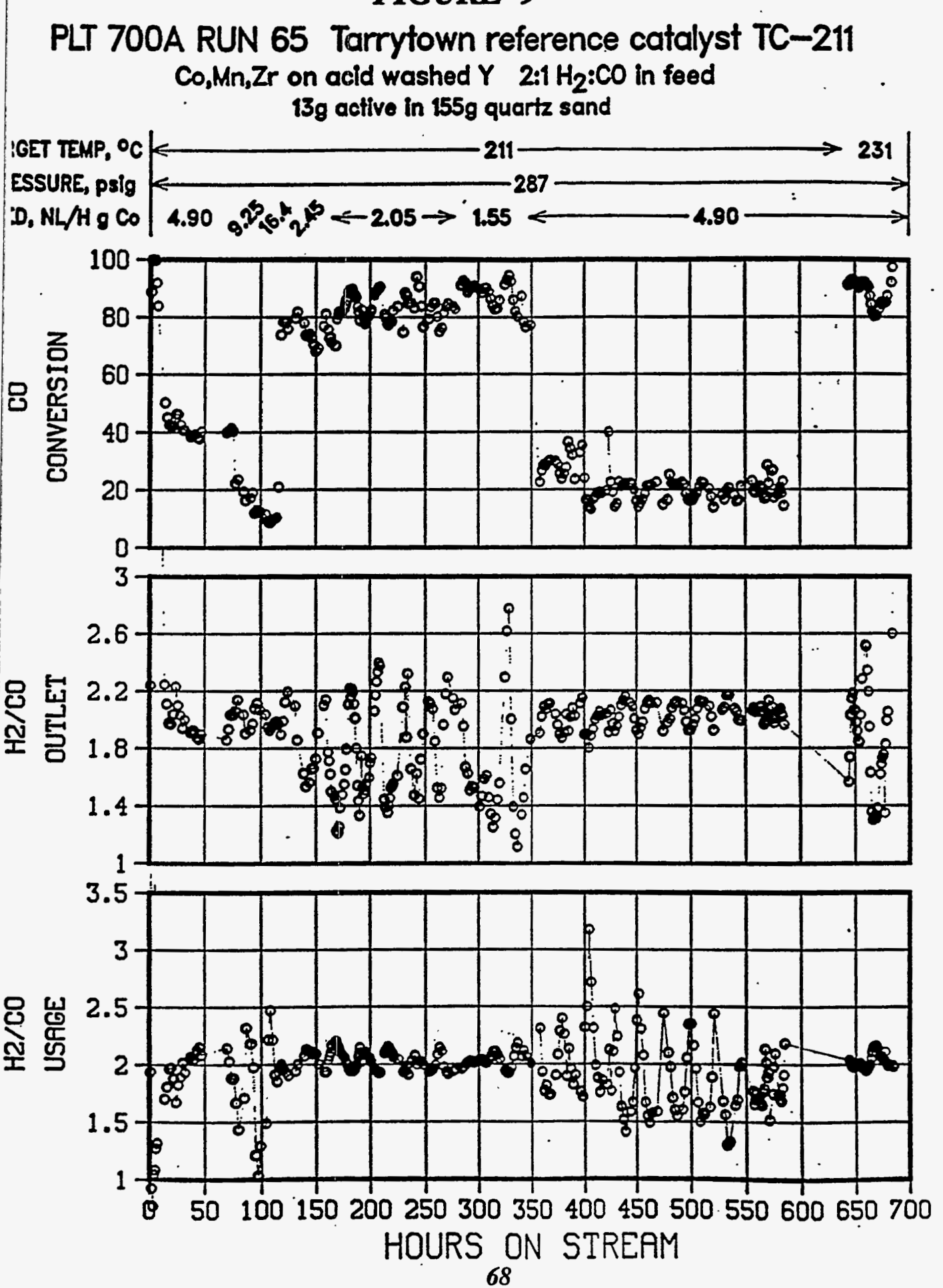
PLT 700A RUN 65 Tarrytown reference catalyst TC-211
Co,Mn,Zr on acid washed Y 2:1 H2:CO in feed
13g active in 155g quartz sand
GET TEMP, °C
211
231
ESSURE, psig
287
D, NL/H g Co
4.90
9.25
16.4
2.45
2.05
1.55
4.90
CO CONVERSION
100
80
60
40
20
0
H2/CO OUTLET
3
2.6
2.2
1.8
1.4
1
H2/CO USAGE
3.5
3
2.5
2
1.5
1
0
50
100
150
200
250
300
350
400
450
500
550
600
650
700
HOURS ON STREAM

FIGURE 10

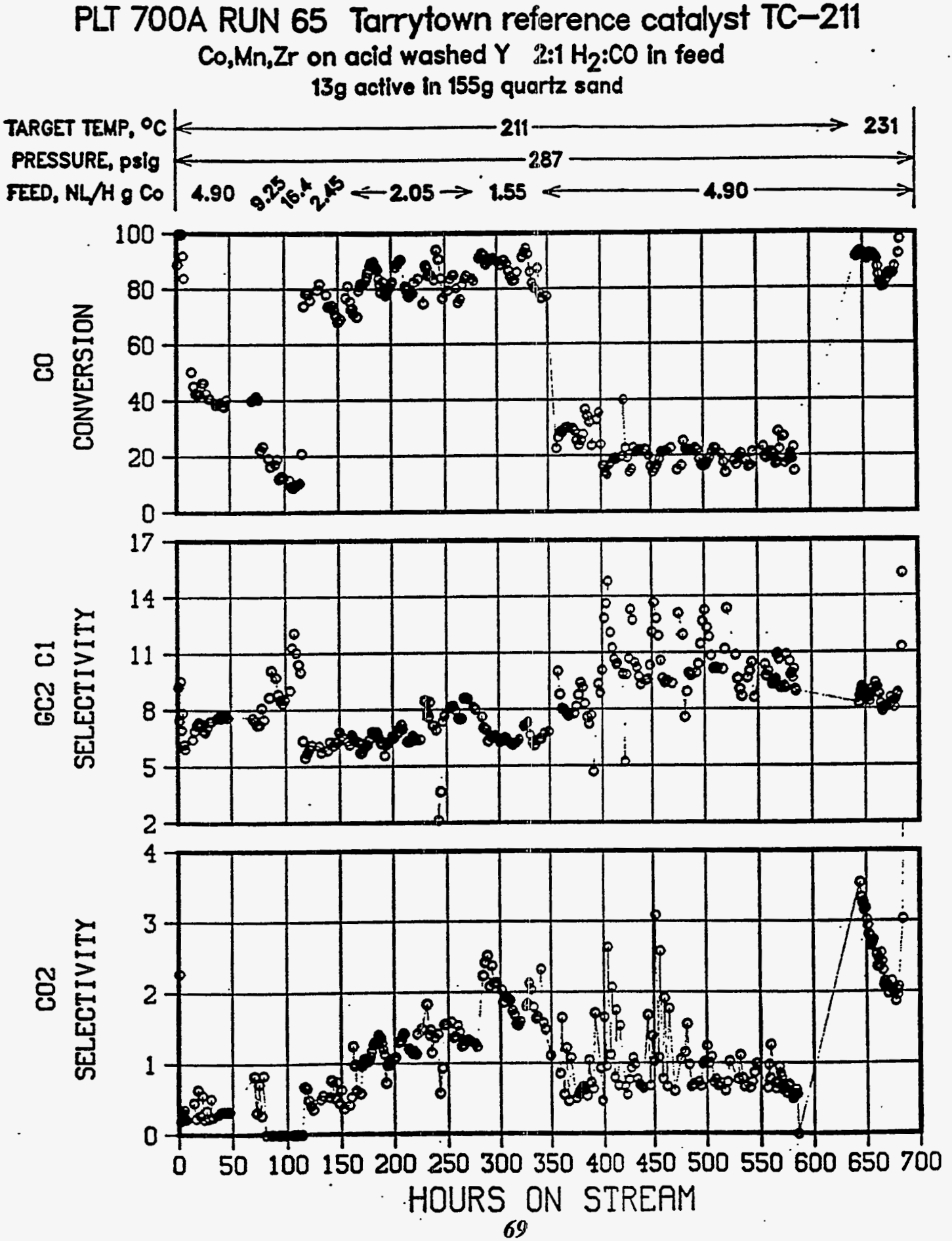
PLT 700A RUN 65 Tarrytown reference catalyst TC-211
Co,Mn,Zr on acid washed Y 2:1 H_2:CO in feed
13g active in 155g quartz sand
TARGET TEMP, °C
211
231
PRESSURE, psig
287
FEED, NL/H g Co
4.90
9.25
16.4
2.45
2.05
1.55
4.90
CO CONVERSION
GC2 C1 SELECTIVITY
CO2 SELECTIVITY
HOURS ON STREAM

FIGURE 11

PLT 700A RUN 65 Tarrytown reference catalyst TC–211

Co,Mn,Zr on acid washed Y 2:1 H_2:CO in feed

13g active in 155g quartz sand

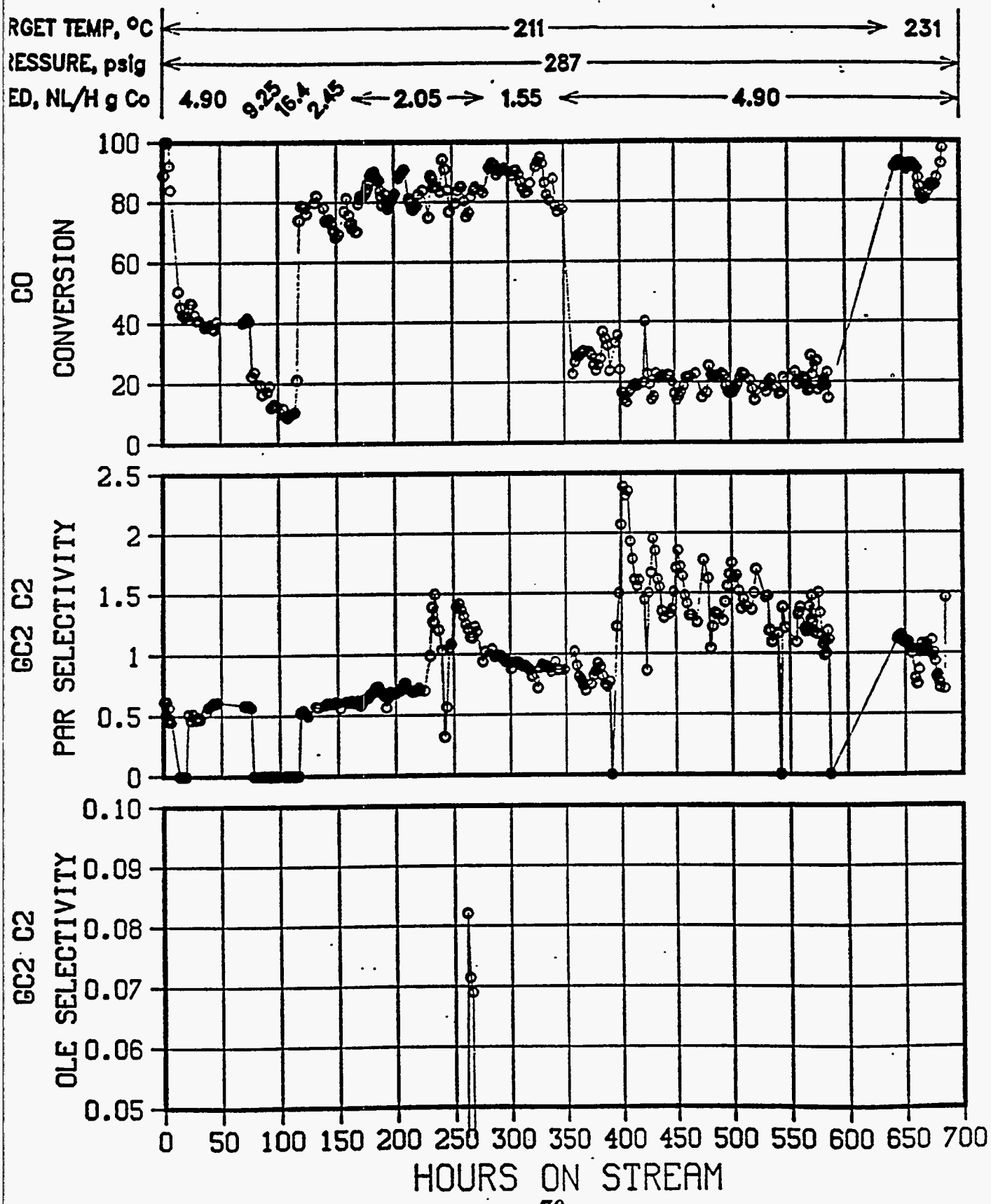

FIGURE 12

PLT 700A RUN 65 Tarrytown reference catalyst TC–211

Co,Mn,Zr on acid washed Y 2:1 H_2:CO in feed

13g active in 155g quartz sand

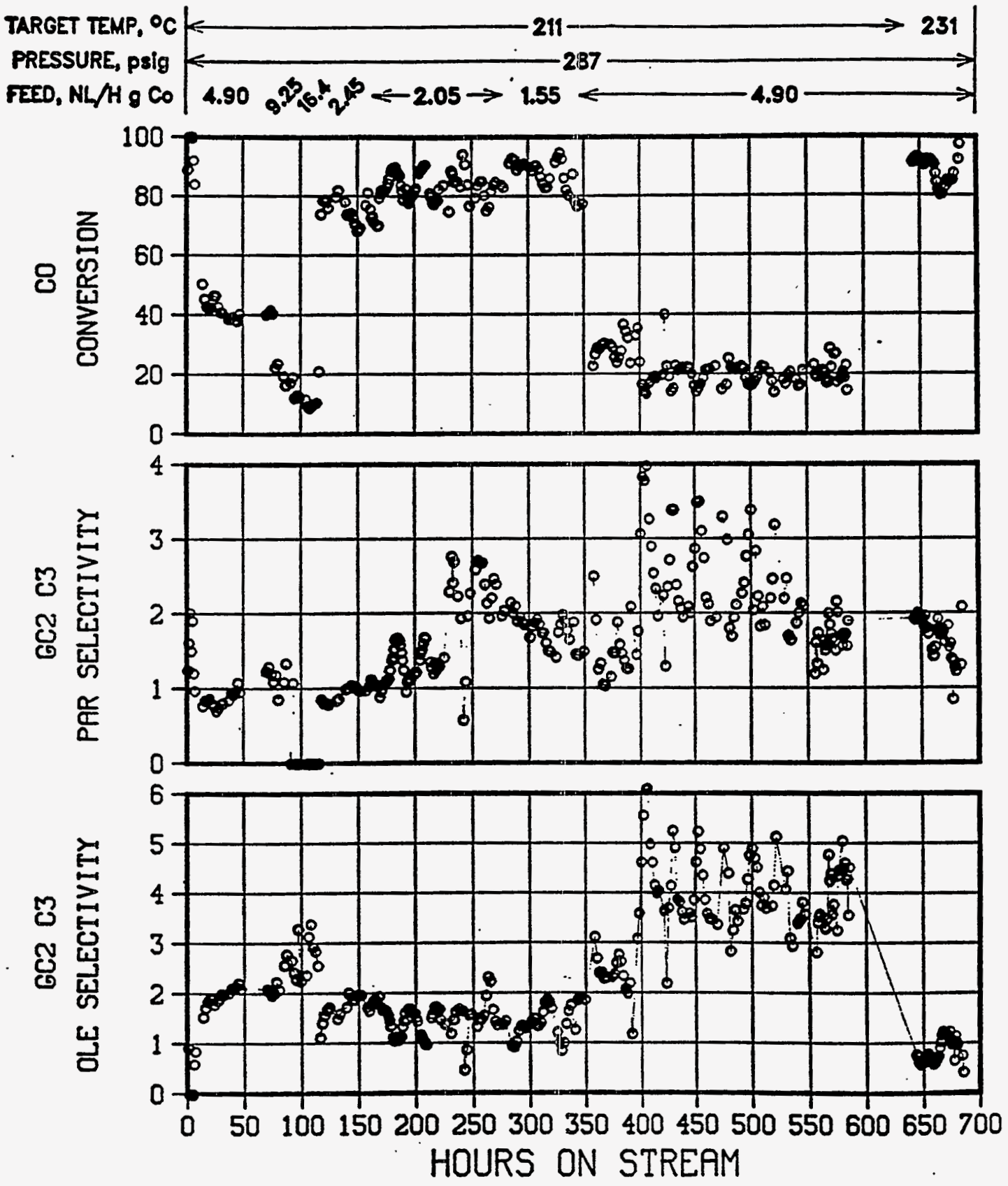

FIGURE 13

PLT 700A RUN 65 Tarrytown reference catalyst TC–211

Co,Mn,Zr on acid washed Y 2:1 H_2:CO in feed

13g active in 155g quartz sand

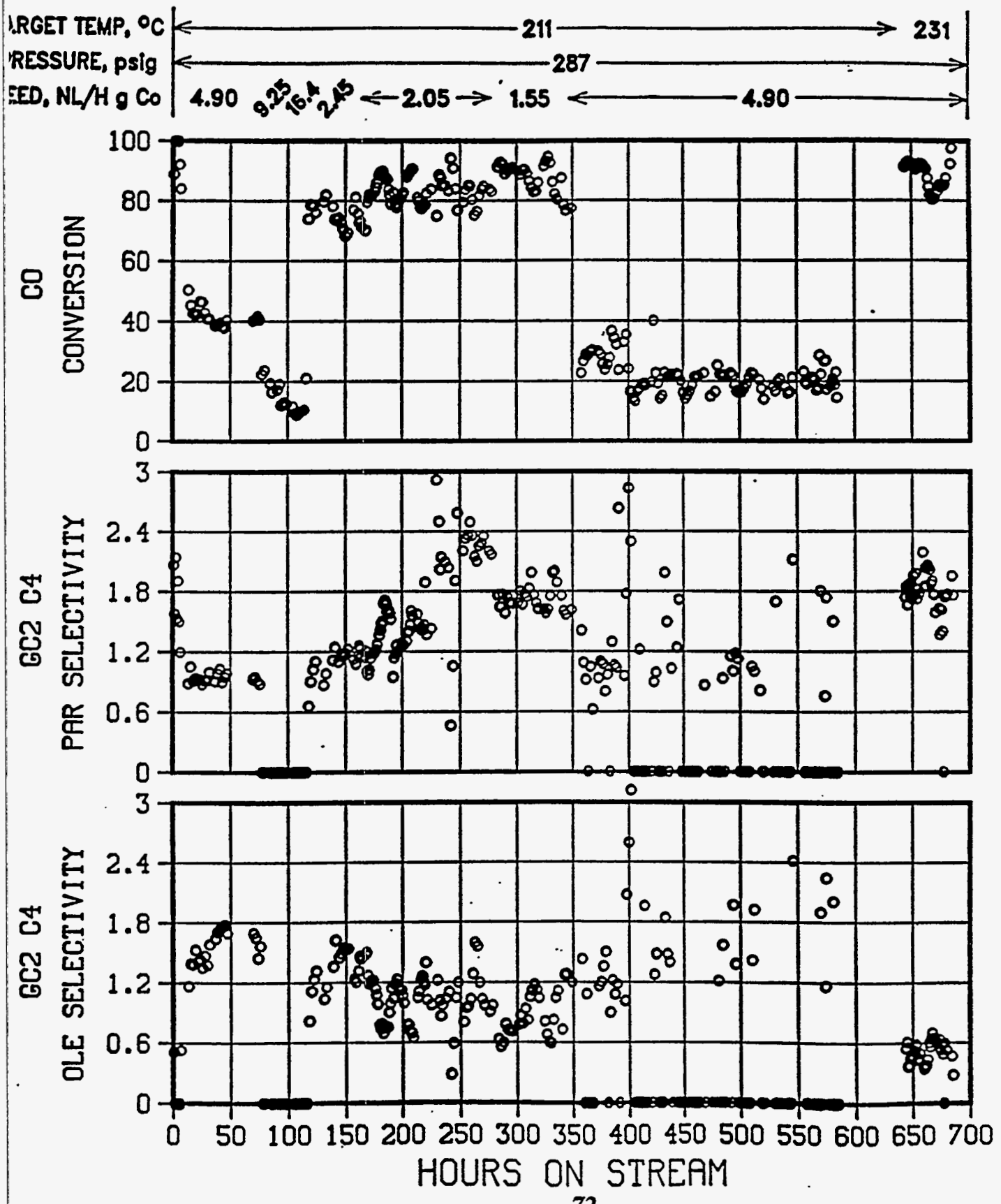

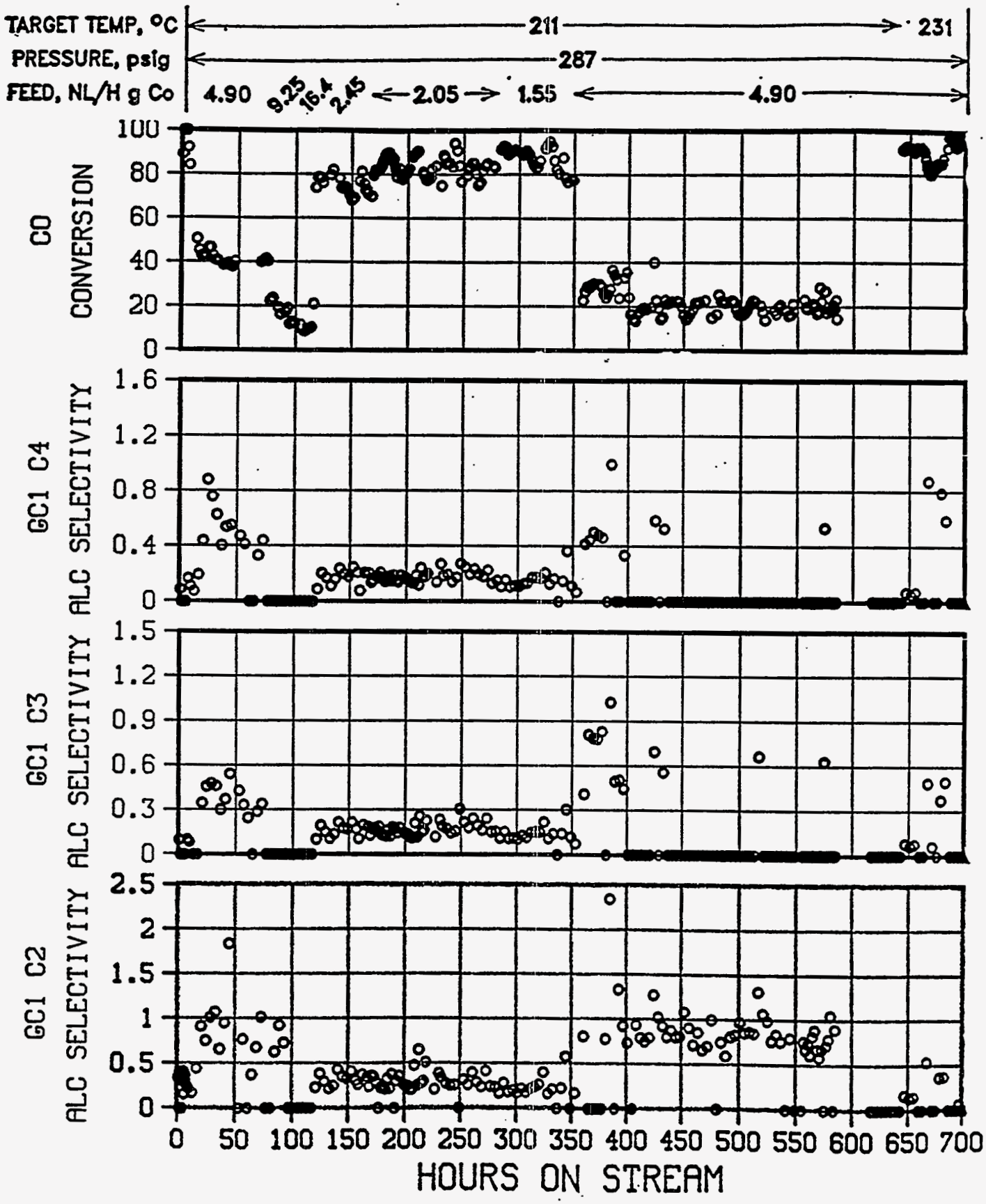
PLT 700A RUN 65 Tarrytown reference catalyst TC-211
Co,Mn,Zr on acid washed Y 2:1 H2:CO in feed
13g active in 155g quartz sand
TARGET TEMP, °C
211
231
PRESSURE, psig
287
FEED, NL/H g Co
4.90
9.25
16.4
2.45
2.05
1.55
4.90
CO CONVERSION
GC1 C4 ALC SELECTIVITY
GC1 C3 ALC SELECTIVITY
GC1 C2 ALC SELECTIVITY
HOURS ON STREAM

COMPARISON OF MAGNESIA-SUPPORTED CATALYSTS TO REFERENCE CATALYST

THREE-CONDITION SCREENING TEST SUMMARY

CATALYST SOURCE	SUPPORT	METALS, WT %	% CO CONV/% C-1 SELEC CONDITION 1	2	3
UNION CARBIDE	STEAMED, ACID WASHED Y ZEOL	Co, 8.3; Mn, 1.3 Zr, 1.0	58/6.0		
DES PLAINES (Run 63)[1]	ULTRA PURE MgO	Co, 7.3; Mn, 0.61 Zr, 0.93; Ru, 1.2	15/10		
DES PLAINES (Run 69)[2]	ULTRA PURE MgO	Co, 8.0; Ru, 0.84 Zr, 0.99	10/13	30/13	50/11
DES PLAINES (Run 72)[2]	ULTRA PURE MgO	Co, 7.5; Mn, 0.60 Ru, 0.60; Zr, 0.90	10/24	65/30	80/27

1. REVERSE MICELLE IMPREGNATION
2. AQUEOUS IMPREGNATION

FIGURE 15

FIGURE 16

PLT 700A RUN 63 Co,Ru,Mn,Zr on MgO

6531-100 w/7.3% Co via Reverse Micelle impregnation 2:1 H_2:CO in feed
13g Active in 160g Alumina

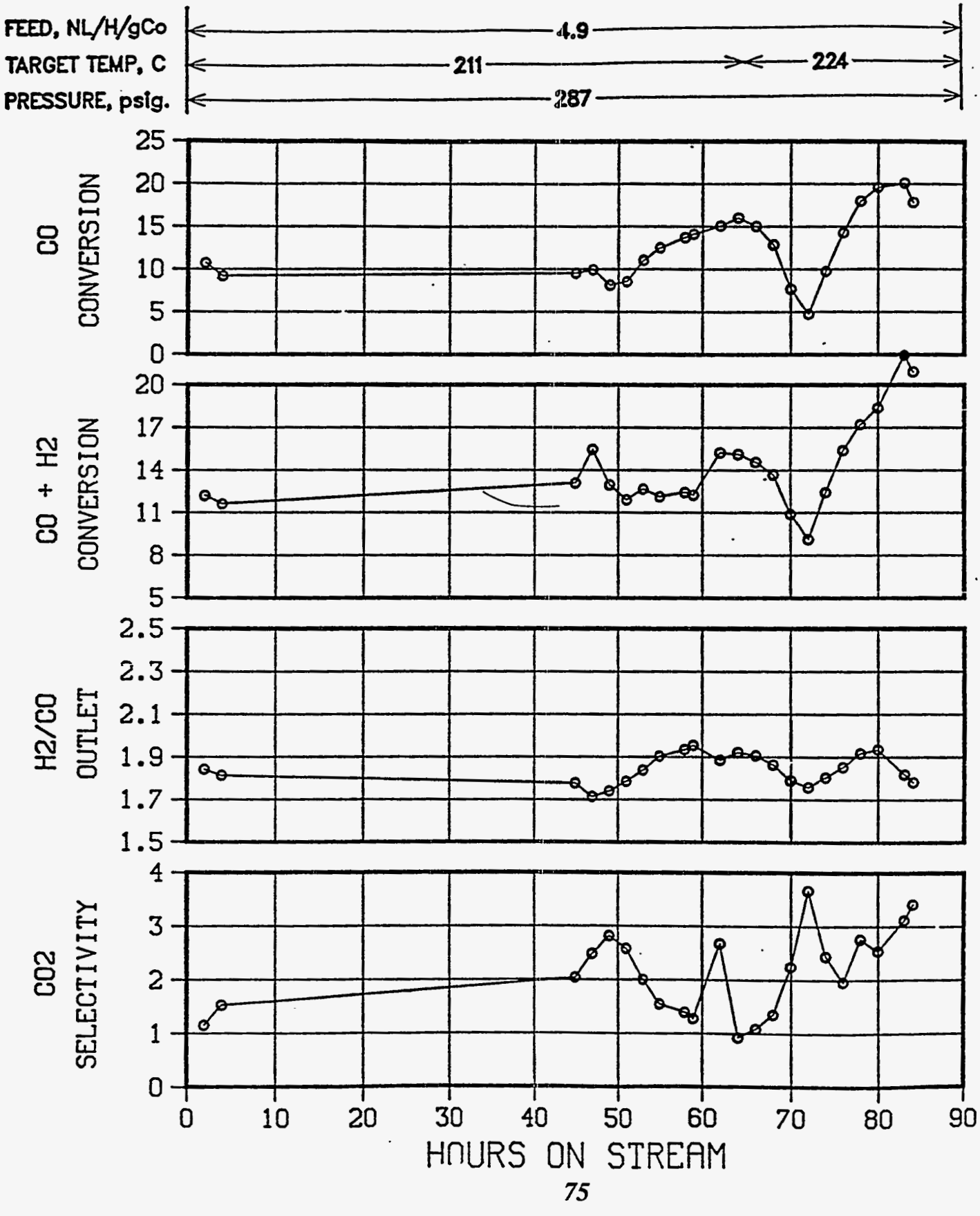

FIGURE 17

PLT 700A RUN 63 Co,Ru,Mn,Zr on MgO

6531-100 w/7.3% Co via Reverse Micelle Impregnation 2:1 H_2:CO in feed
13g Active in 160g Alumina

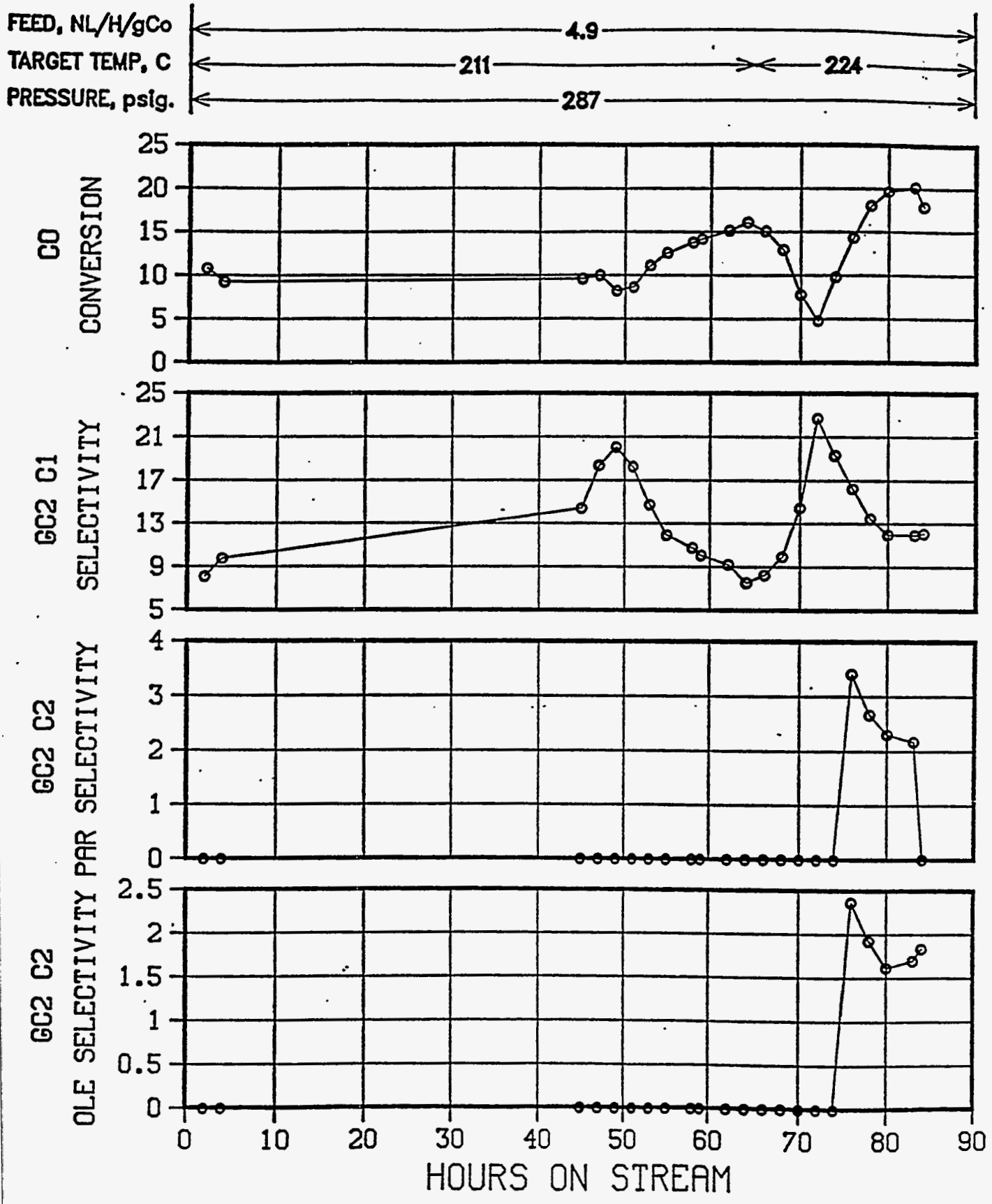

FIGURE 18

PLT 700A RUN 63 Co,Ru,Mn,Zr on MgO

6531-100 w/7.3% Co via Reverse Micelle Impregnation 2:1 H_2:CO in feed

13g Active in 160g Alumina

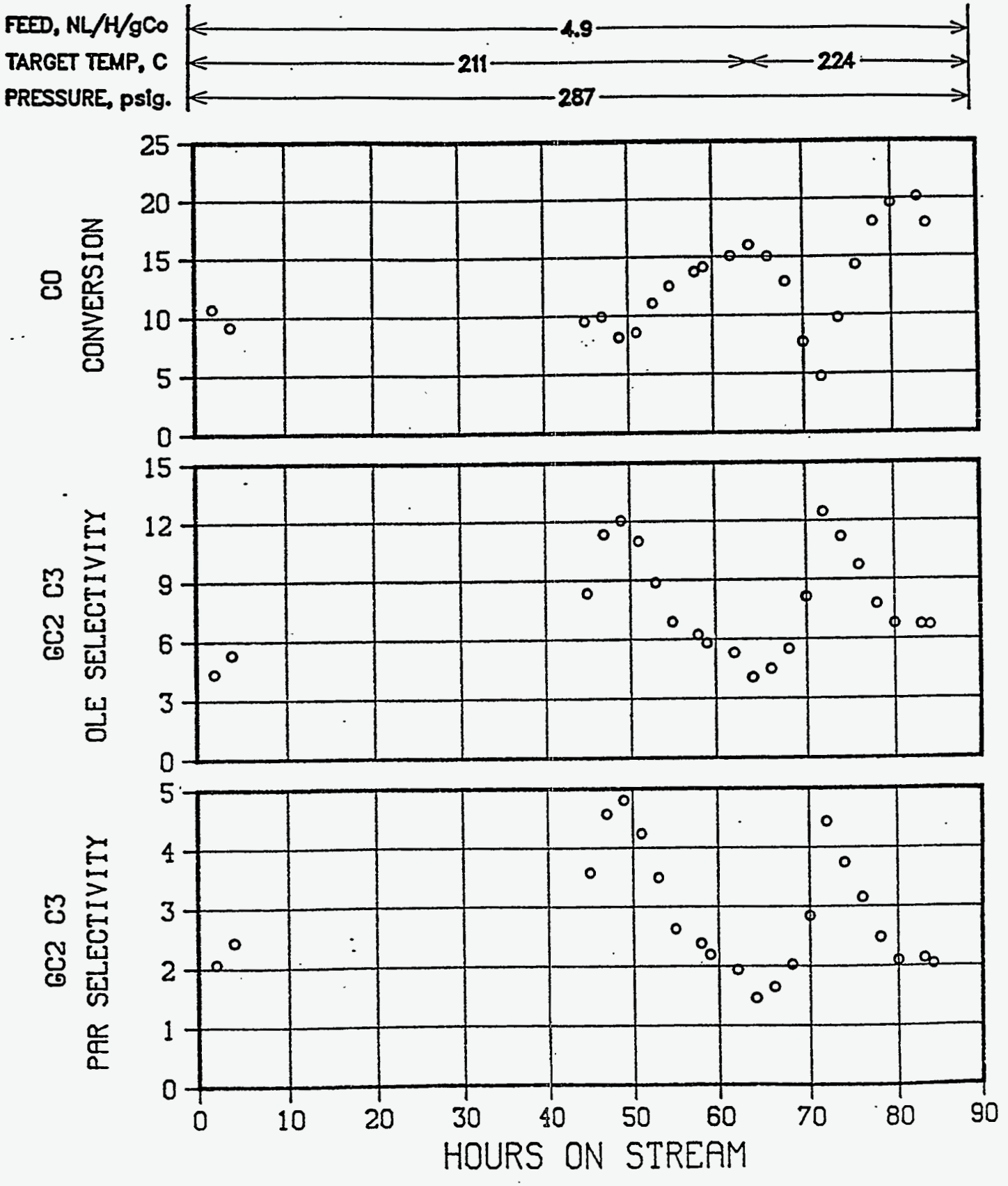

FIGURE 19

PLT 700A RUN 63 Co,Ru,Mn,Zr on MgO

6531-100 w/7.3% Co via Reverse Micelle Impregnation 2:1 H_2:CO in feed
13g Active in 160g Alumina

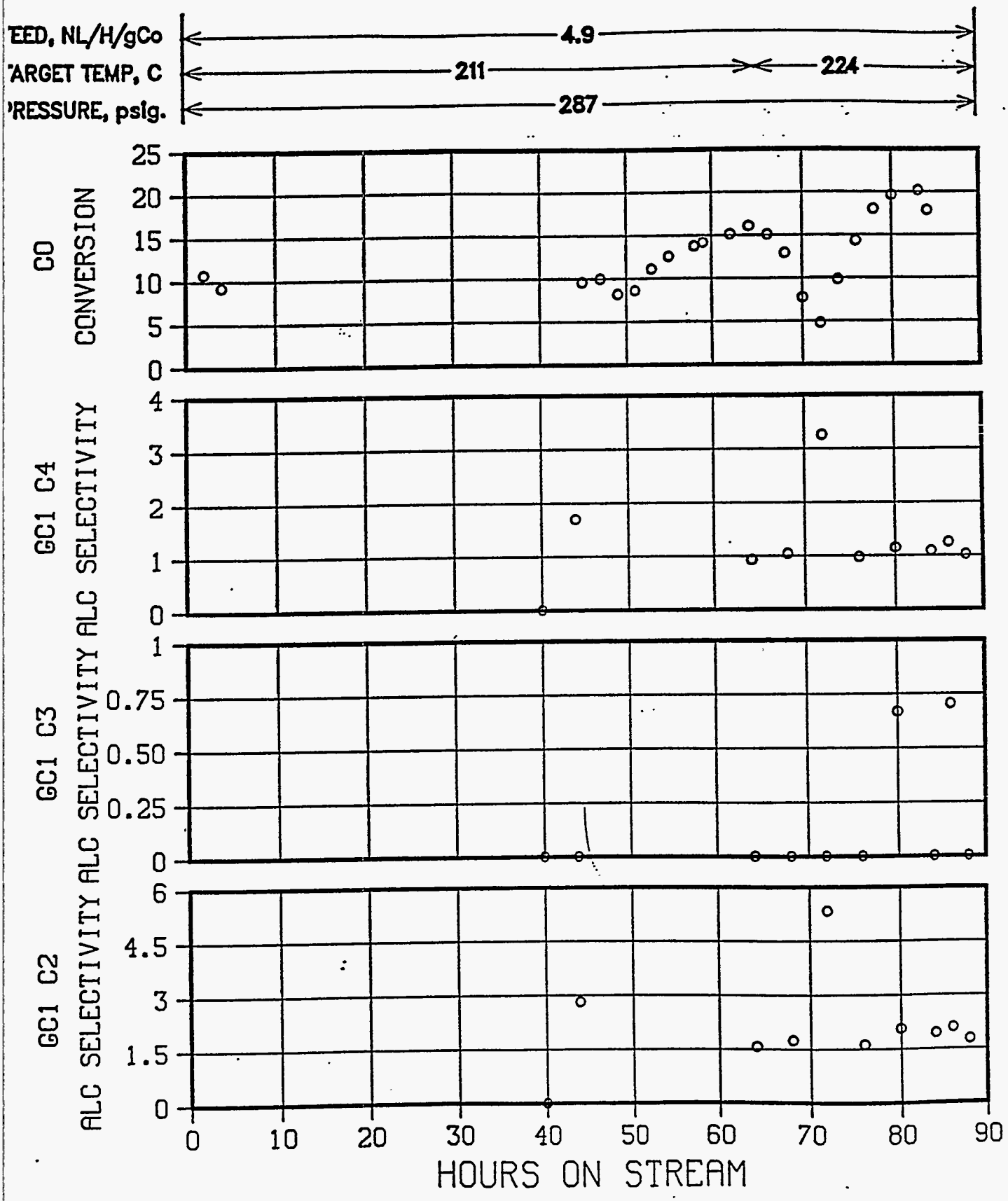

FIGURE 20

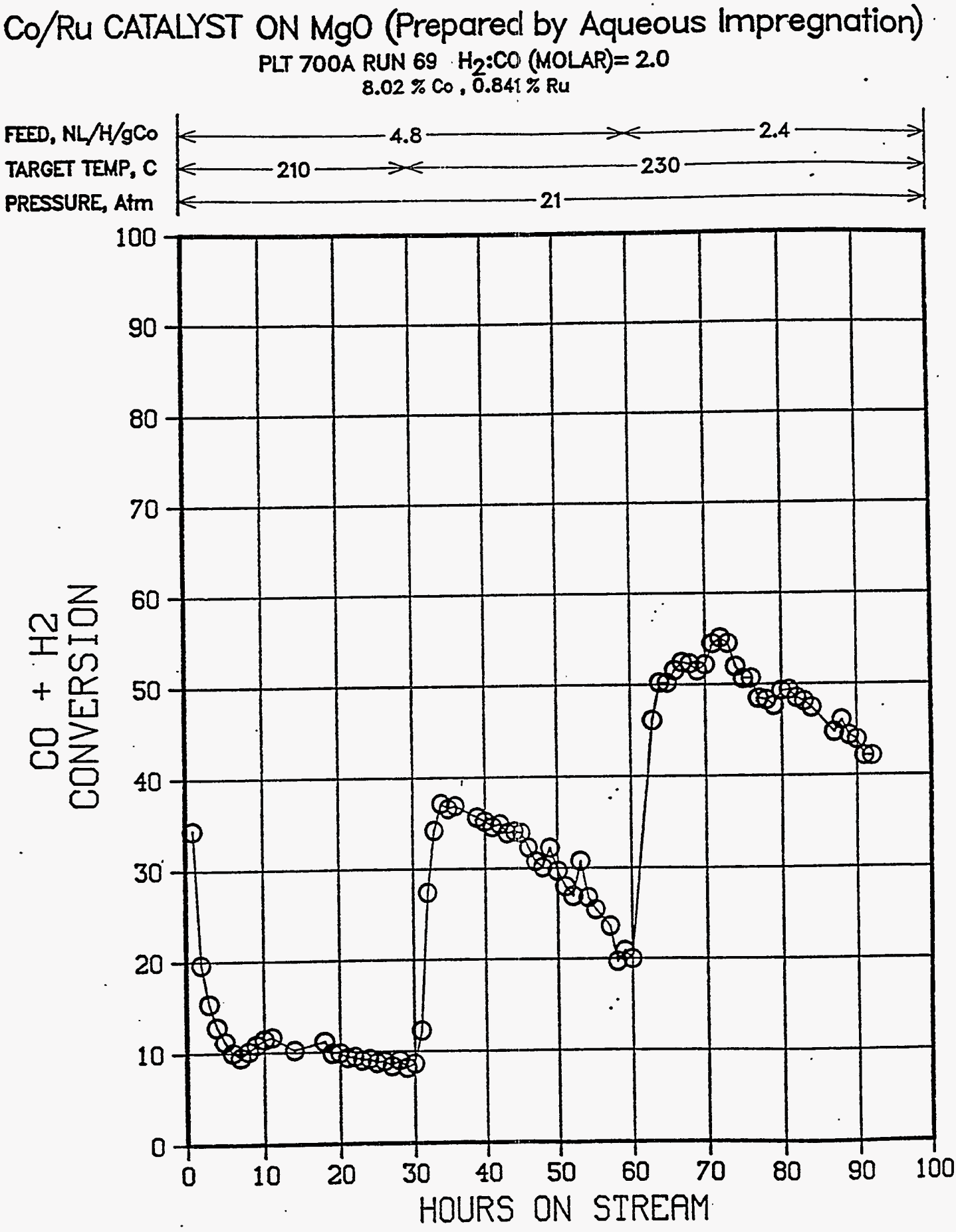
Co/Ru CATALYST ON MgO (Prepared by Aqueous Impregnation)
PLT 700A RUN 69 H2:CO (MOLAR)= 2.0
8.02 % Co , 0.841 % Ru
FEED, NL/H/gCo
TARGET TEMP, C
PRESSURE, Atm
4.8
2.4
210
230
21
CO + H2 CONVERSION
HOURS ON STREAM
0
10
20
30
40
50
60
70
80
90
100

FIGURE 21

:o/Ru CATALYST ON MgO (Prepared by Aqueous Impregnation)

PLT 700A RUN 69 H_2:CO (MOLAR)= 2.0

8.02 % Co , 0.841 % Ru

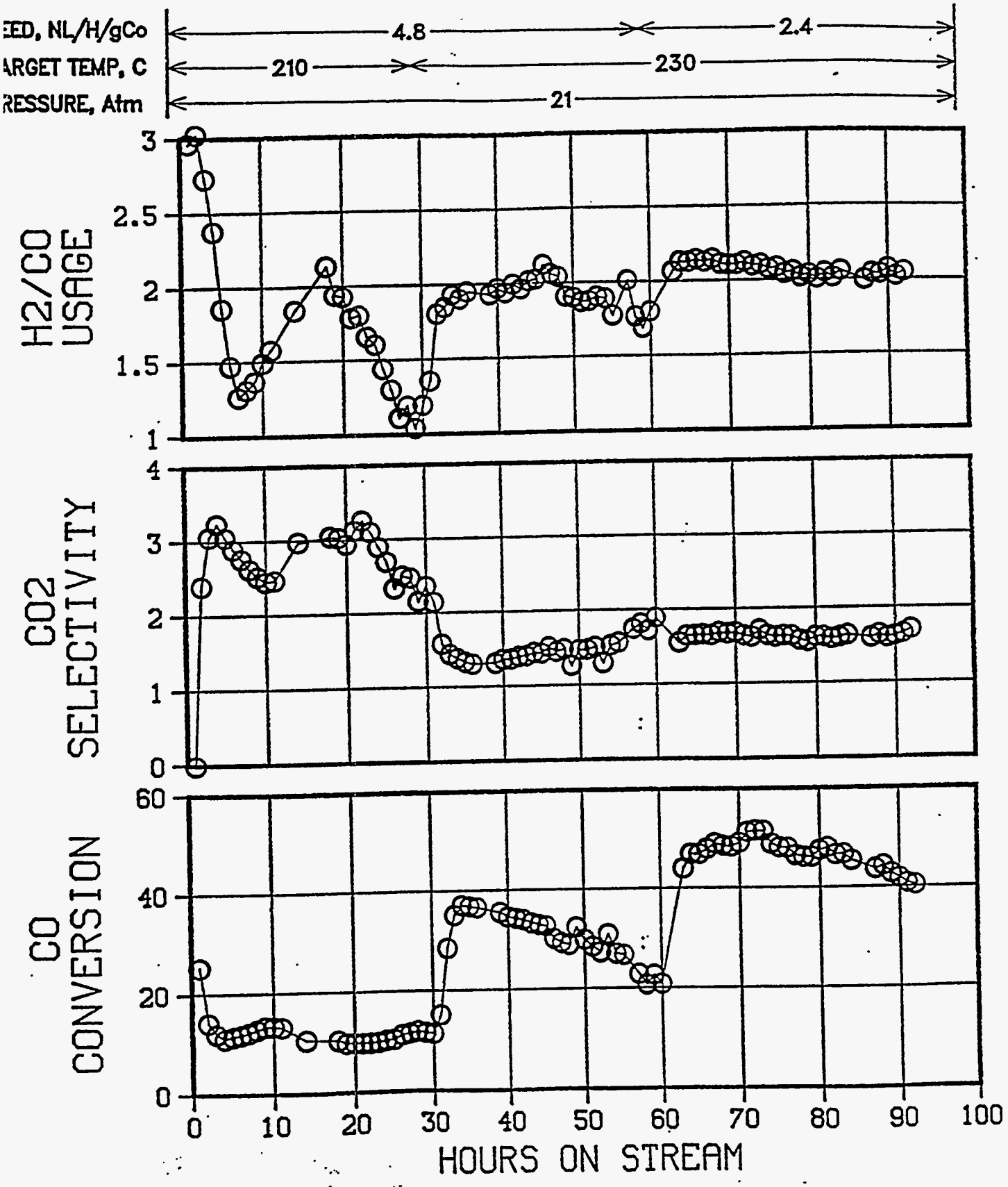

FIGURE 22

Co/Ru CATALYST ON MgO (Prepared by Aqueous Impregnation)

PLT 700A RUN 69 H_2:CO (MOLAR)= 2.0

8.02 % Co , 0.841 % Ru

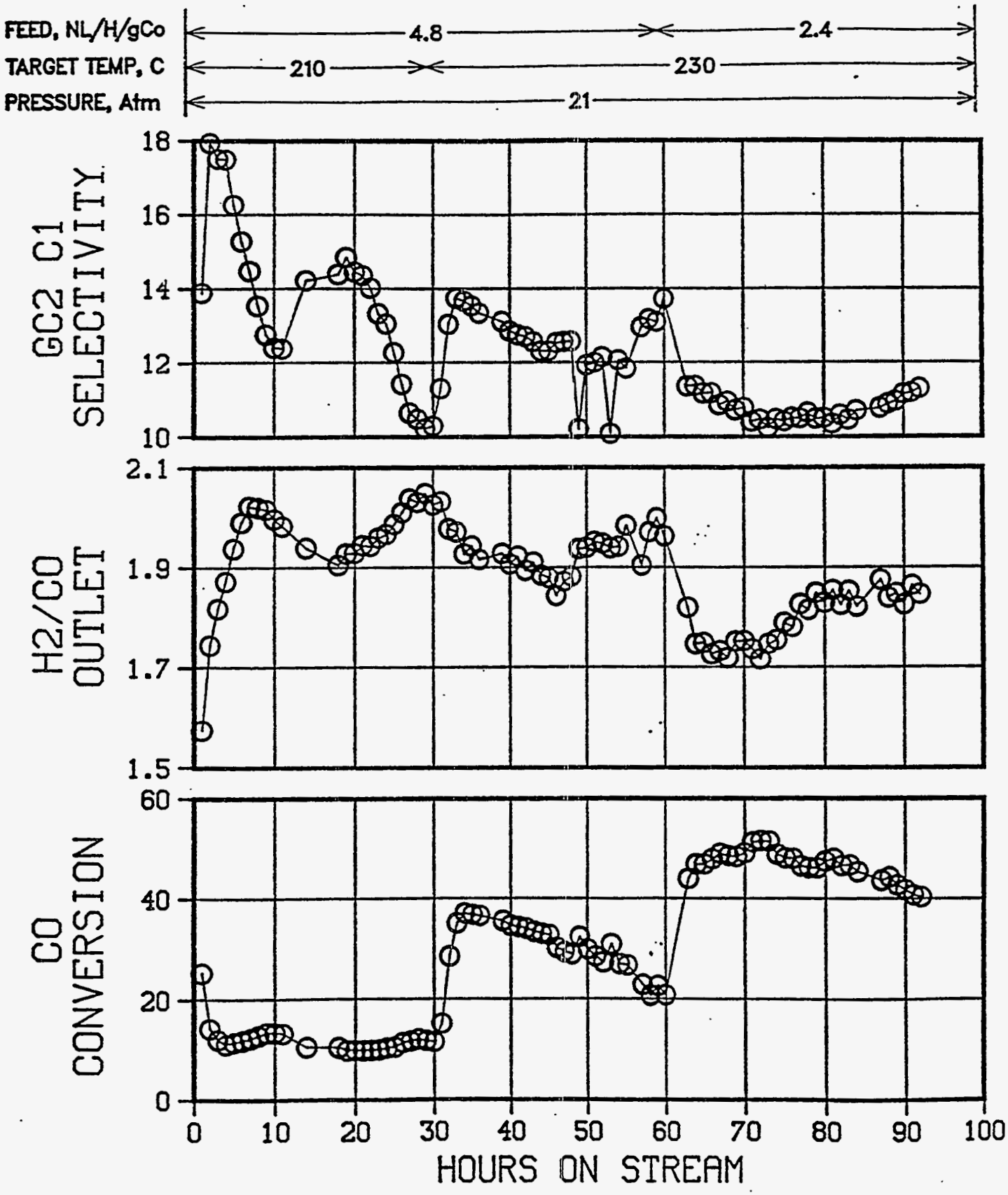

FIGURE 23

c/Ru CATALYST ON MgO (Prepared by Aqueous Impregnation)

PLT 700A RUN 69 H_2:CO (MOLAR)= 2.0

8.02 % Co , 0.841 % Ru

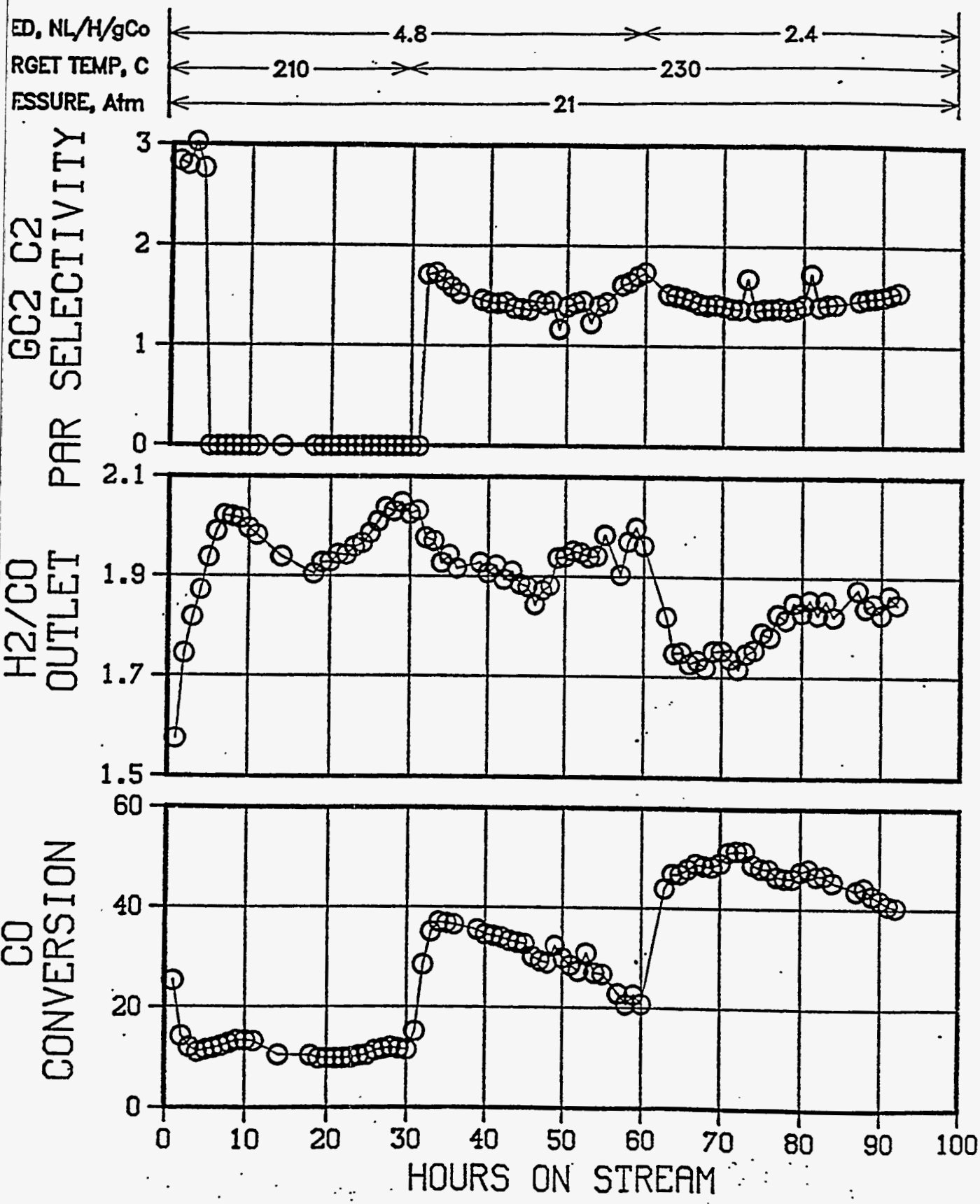

FIGURE 24

Co/Ru CATALYST ON MgO (Prepared by Aqueous Impragnation)

PLT 700A RUN 69 H_2:CO (MOLAR)= 2.0

8.02 % Co , 0.841 % Ru

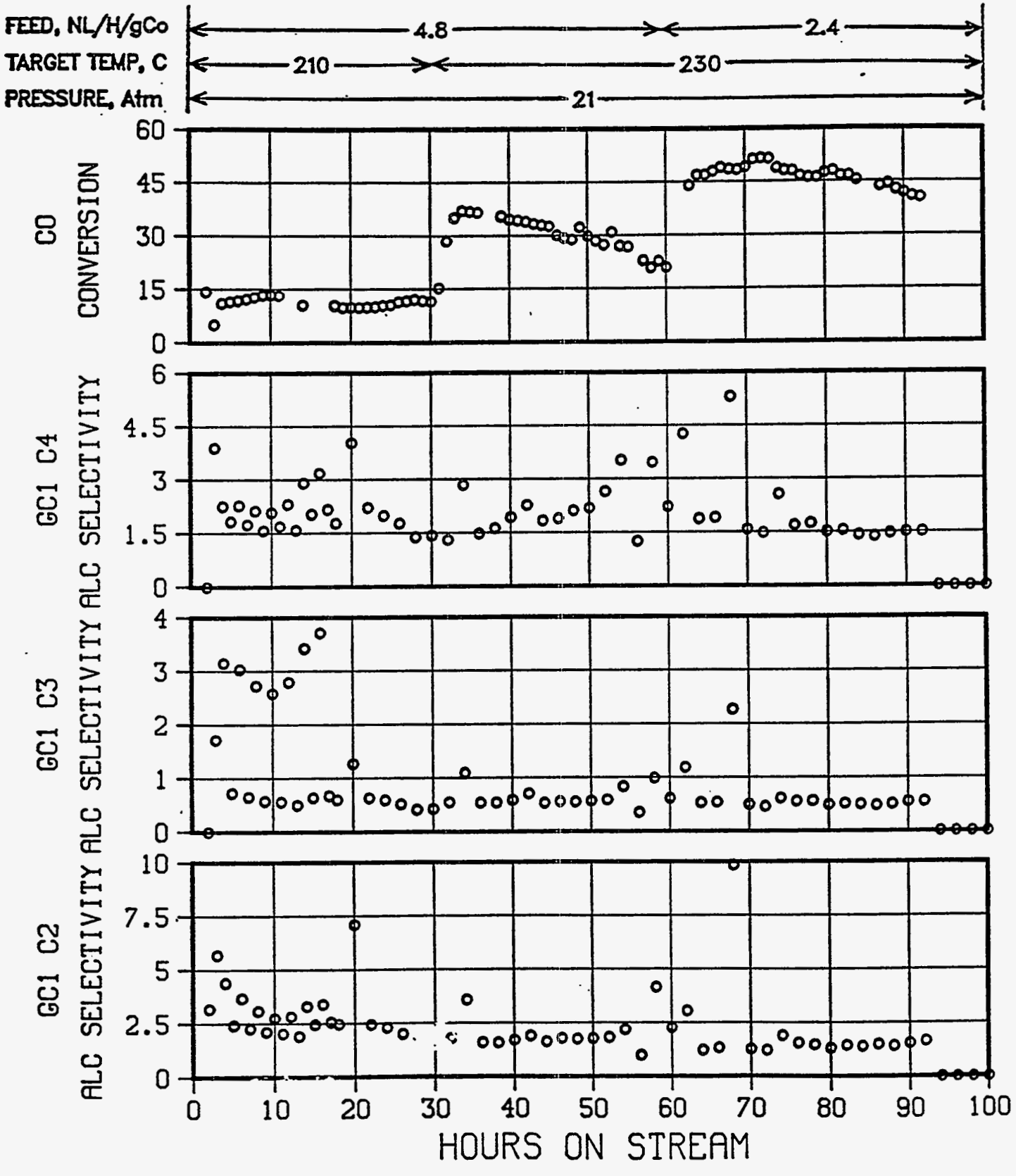

FIGURE 25

PLT 700A RUN 72 · Co,Ru,Mn,Zr on MgO

6531–134 w/7.45% Co via aq. impreg 2:1 H_2:CO in feed

13g Active in 160g SiO_2 sand

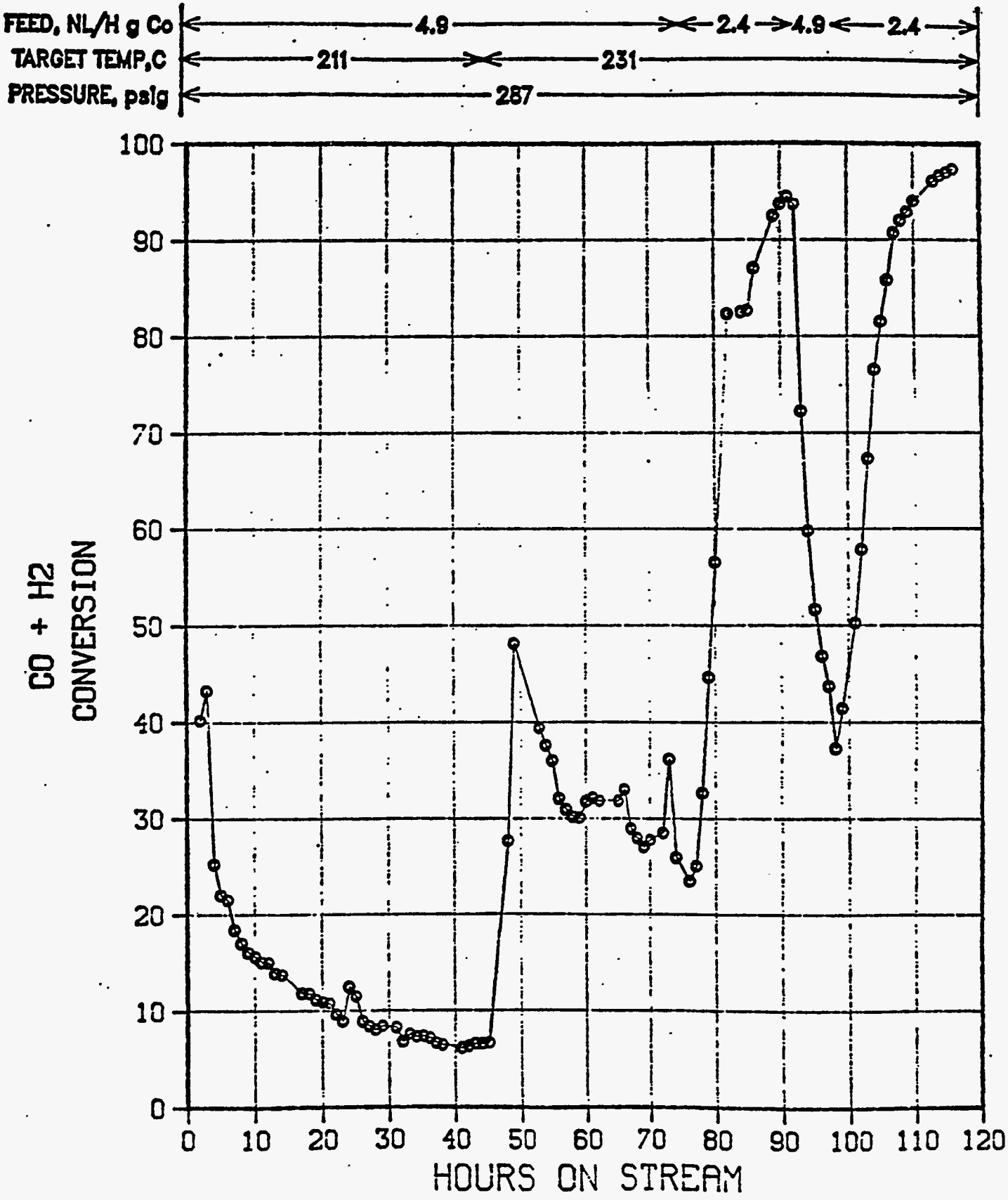

FIGURE 26

PLT 700A RUN 72 Co,Ru,Mn,Zr on MgO

6531-134 w/7.45% Co via aq. Impreg 2:1 H_2:CO in feed

13g Active in 160g SiO_2 sand

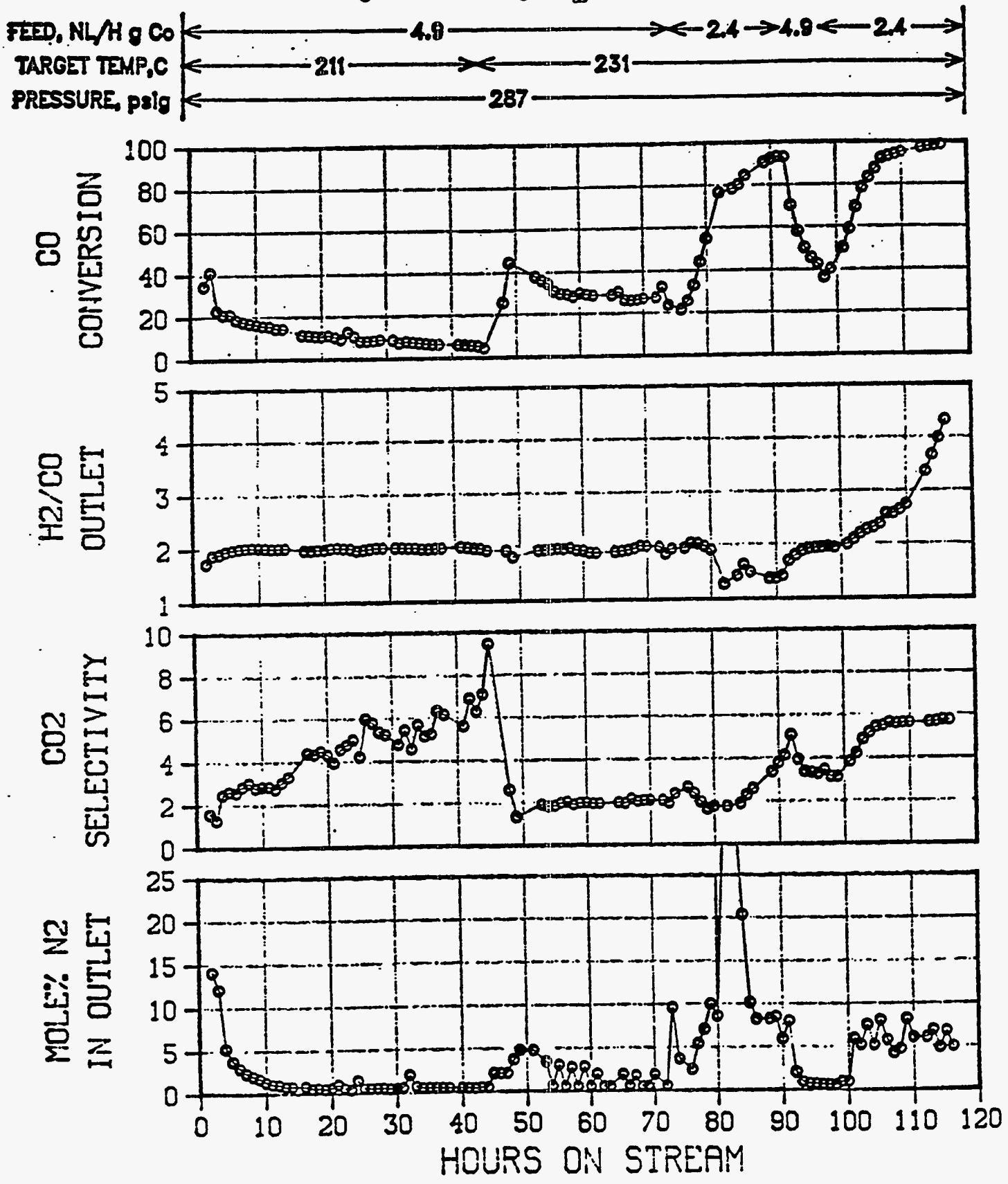

FIGURE 27

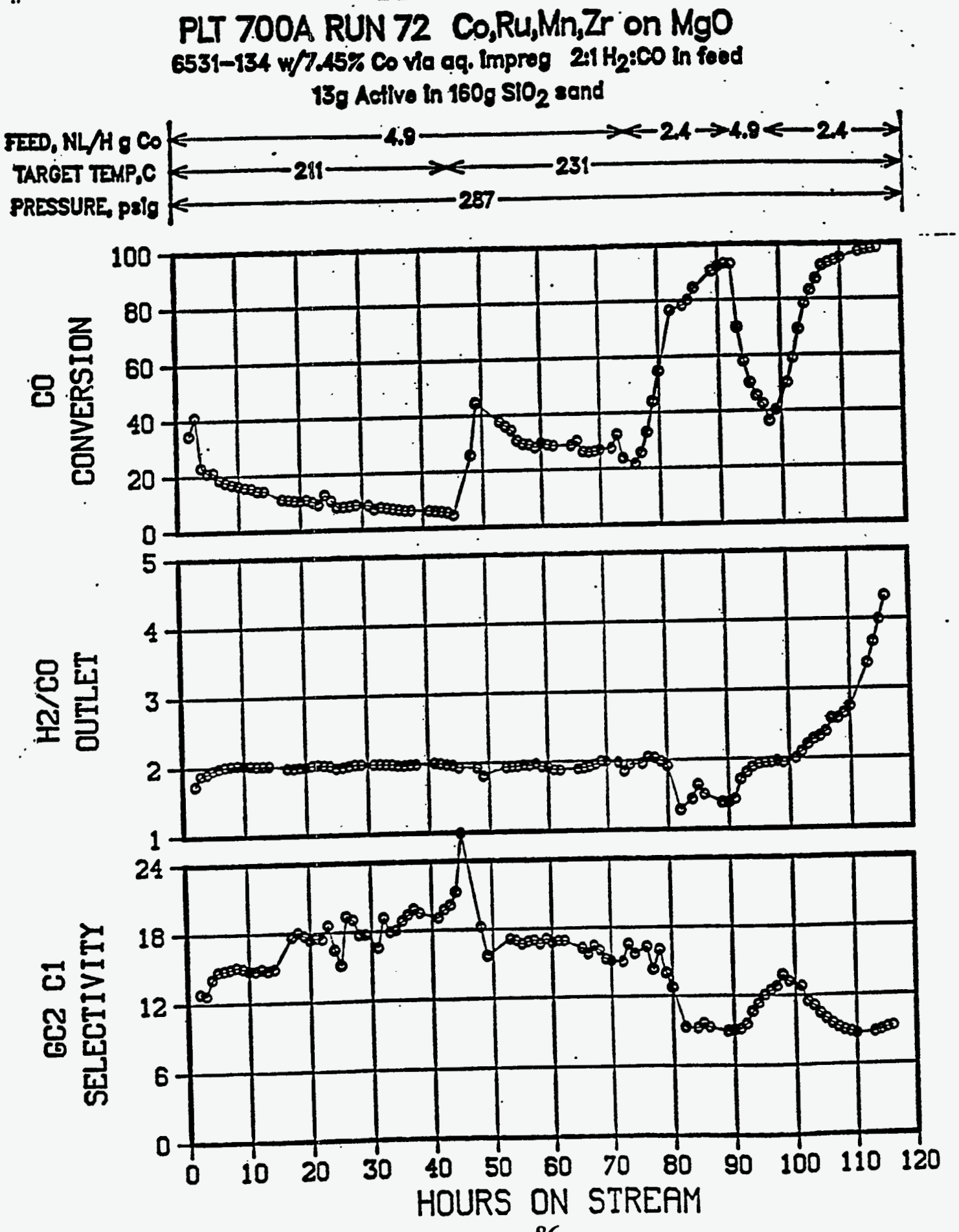
PLT 700A RUN 72 Co,Ru,Mn,Zr on MgO
6531-134 w/7.45% Co via aq. Impreg 2:1 H2:CO in feed
13g Active in 160g SiO2 sand
FEED, NL/H g Co
TARGET TEMP,C
PRESSURE, psig
4.9
2.4
4.9
2.4
211
231
287
CO CONVERSION
H2/CO OUTLET
GC2 C1 SELECTIVITY
HOURS ON STREAM

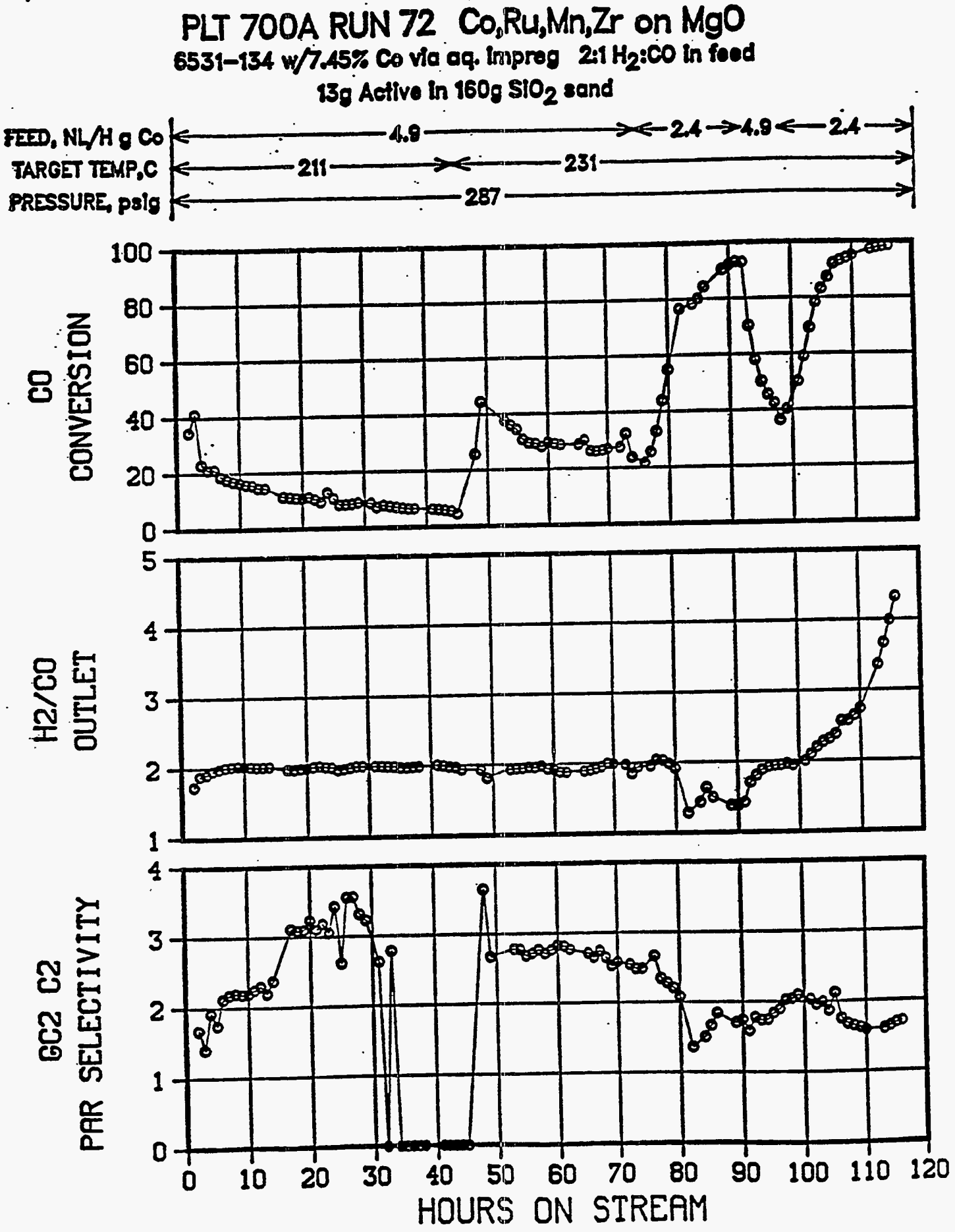
PLT 700A RUN 72 Co,Ru,Mn,Zr on MgO
6531-134 w/7.45% Co via aq. Impreg 2:1 H2:CO in feed
13g Active in 160g SiO2 sand
FEED, NL/H g Co
TARGET TEMP,C
PRESSURE, psig
4.9
2.4
4.9
2.4
211
231
287
CO CONVERSION
H2/CO OUTLET
GC2 C2 PAR SELECTIVITY
HOURS ON STREAM

FIGURE 29

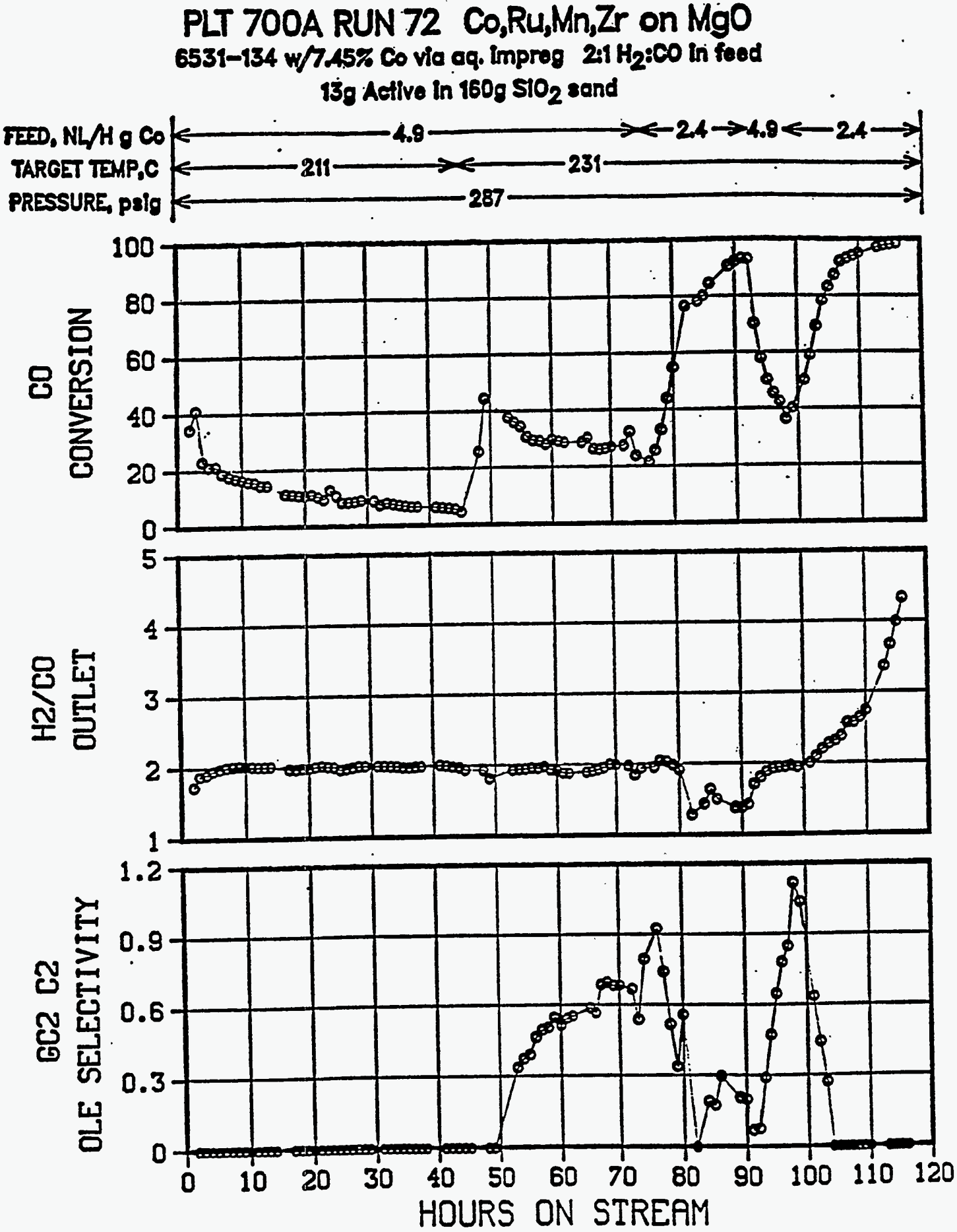
PLT 700A RUN 72 Co,Ru,Mn,Zr on MgO
6531-134 w/7.45% Co via aq. Impreg 2:1 H2:CO in feed
13g Active in 160g SiO2 sand
FEED, NL/H g Co
4.9
2.4
4.9
2.4
TARGET TEMP,C
211
231
PRESSURE, psig
287
CO CONVERSION
100
80
60
40
20
0
H2/CO OUTLET
5
4
3
2
1
GC2 C2 OLE SELECTIVITY
1.2
0.9
0.6
0.3
0
0
10
20
30
40
50
60
70
80
90
100
110
120
HOURS ON STREAM

FIGURE 30

PLT 700A RUN 72 Co,Ru,Mn,Zr on MgO

6531–134 w/7.45% Co via aq. Impreg 2:1 H_2:CO in feed

13g Active in 160g SiO_2 sand

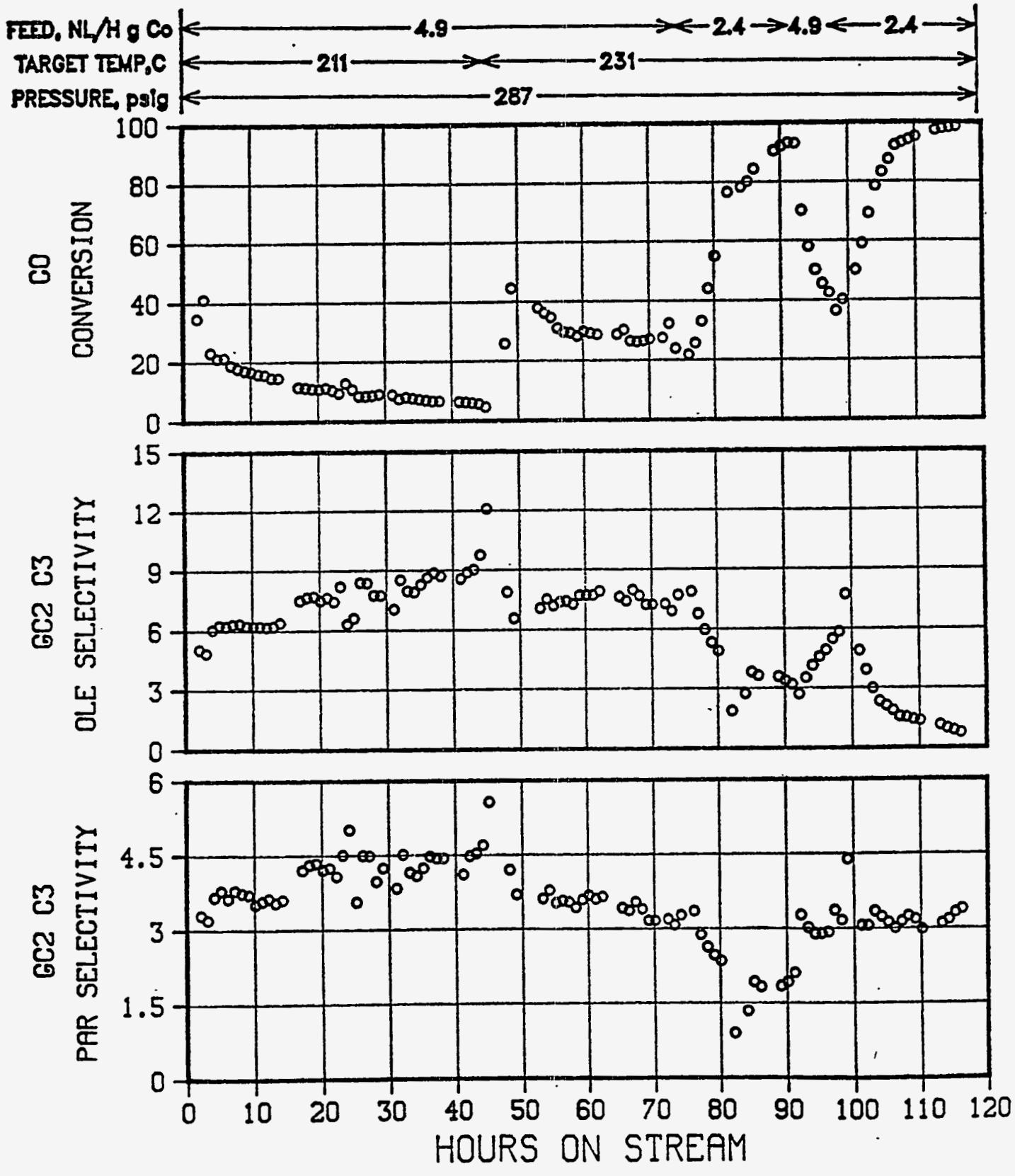

FIGURE 31

PLT 700A RUN 72 Co,Ru,Mn,Zr on MgO

6531–134 w/7.45% Co via aq. impreg 2:1 H_2:CO in feed

13g Active in 160g SiO_2 sand

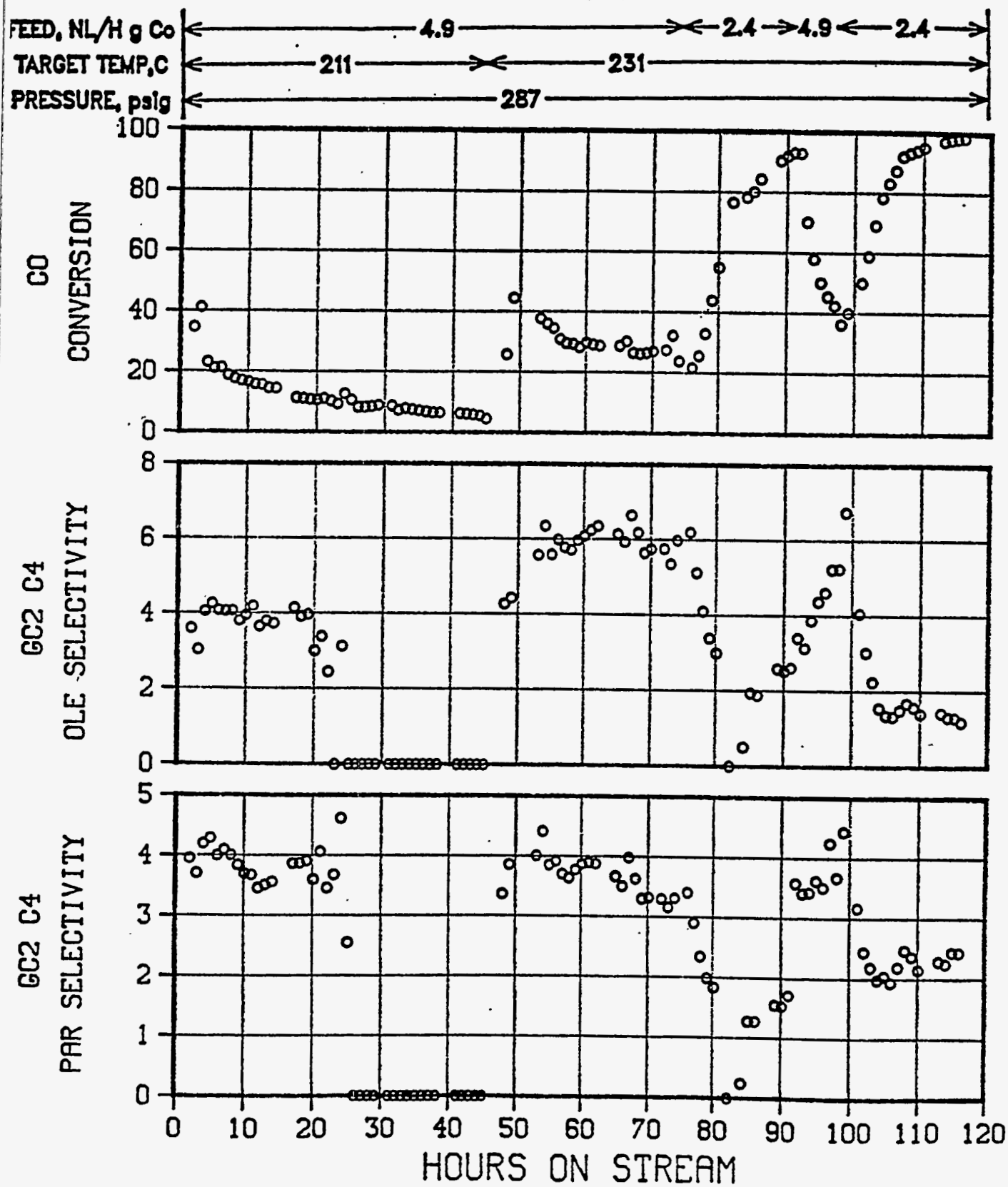

FIGURE 32

PLT 700A RUN 72 Co,Ru,Mn,Zr on MgO

6531-134 w/7.45% Co via aq. Impreg 2:1 H_2:CO in feed

13g Active in 160g SiO_2 sand

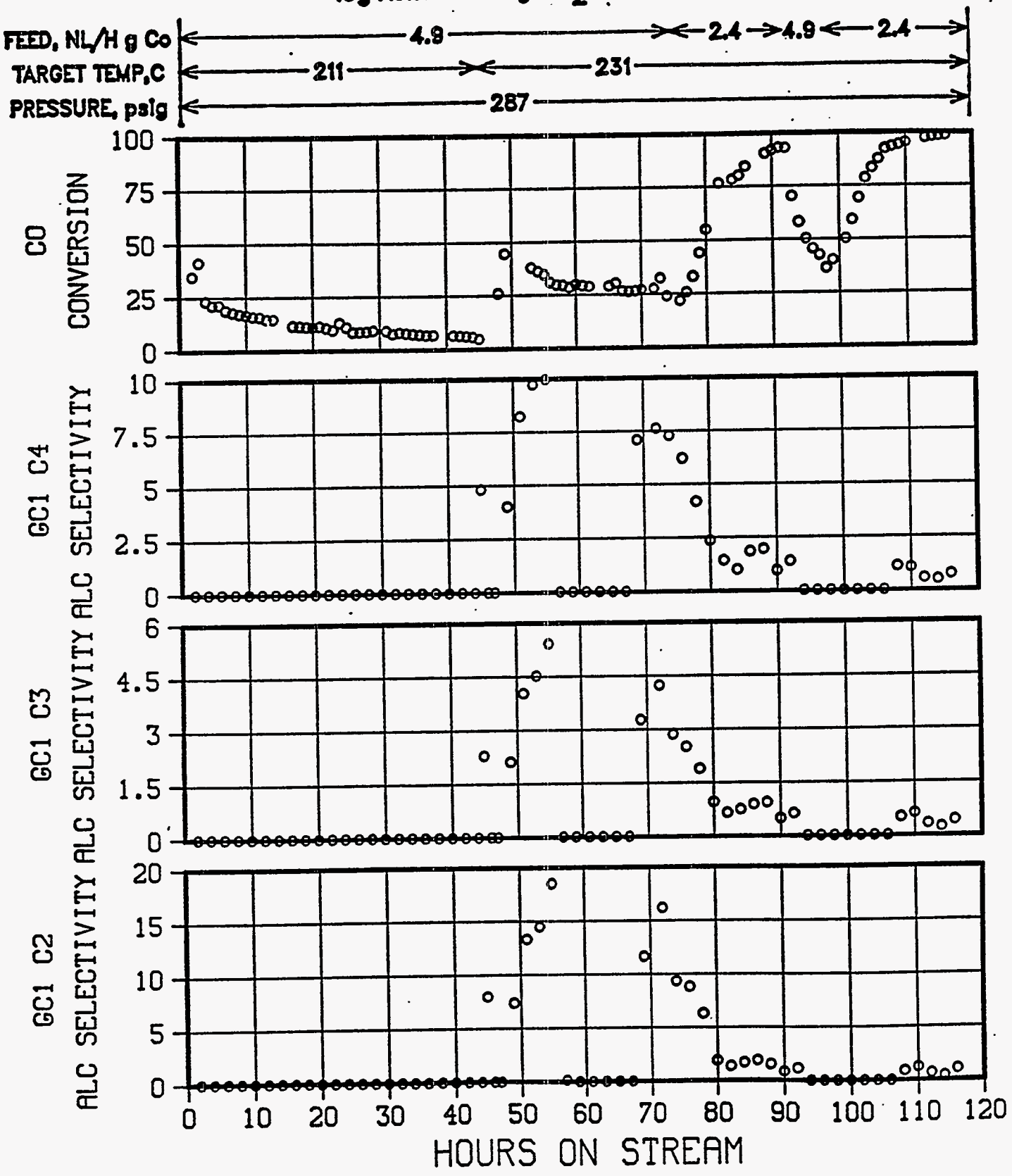

COMPARISON OF CARBON-SUPPORTED CATALYSTS TO REFERENCE CATALYST

THREE-CONDITION SCREENING TEST SUMMARY

CATALYST SOURCE	SUPPORT	METALS, WT %	% CO CONV/% C-1 SELEC CONDITION 1	2	3
UNION CARBIDE	STEAMED, ACID-WASHED Y ZEOL.	Co, 8.3; Mn, 1.3 Zr, 1.0	58/6.0		
DES PLAINES (RUN 67)[1]	CARBOTRAP B	Co,5.8; Ru,1.0	25/22	50/20	60/18
DES PLAINES (RUN 77)[2]	CARBOTRAP B	Co,5.8; Ru,1.0	40/15	75/20	90/24

1. REVERSE MICELLE IMPREGNATION
2. AQUEOUS IMPREGNATION

FIGURE 33

FIGURE 34

BIMETALLIC Co/Ru CATALYST ON C SUPPORT

PLT 700A RUN 67 H_2:CO (MOLAR)= 2.0

5.8 Co : 1.0 Ru : 100 C (BY WT.)

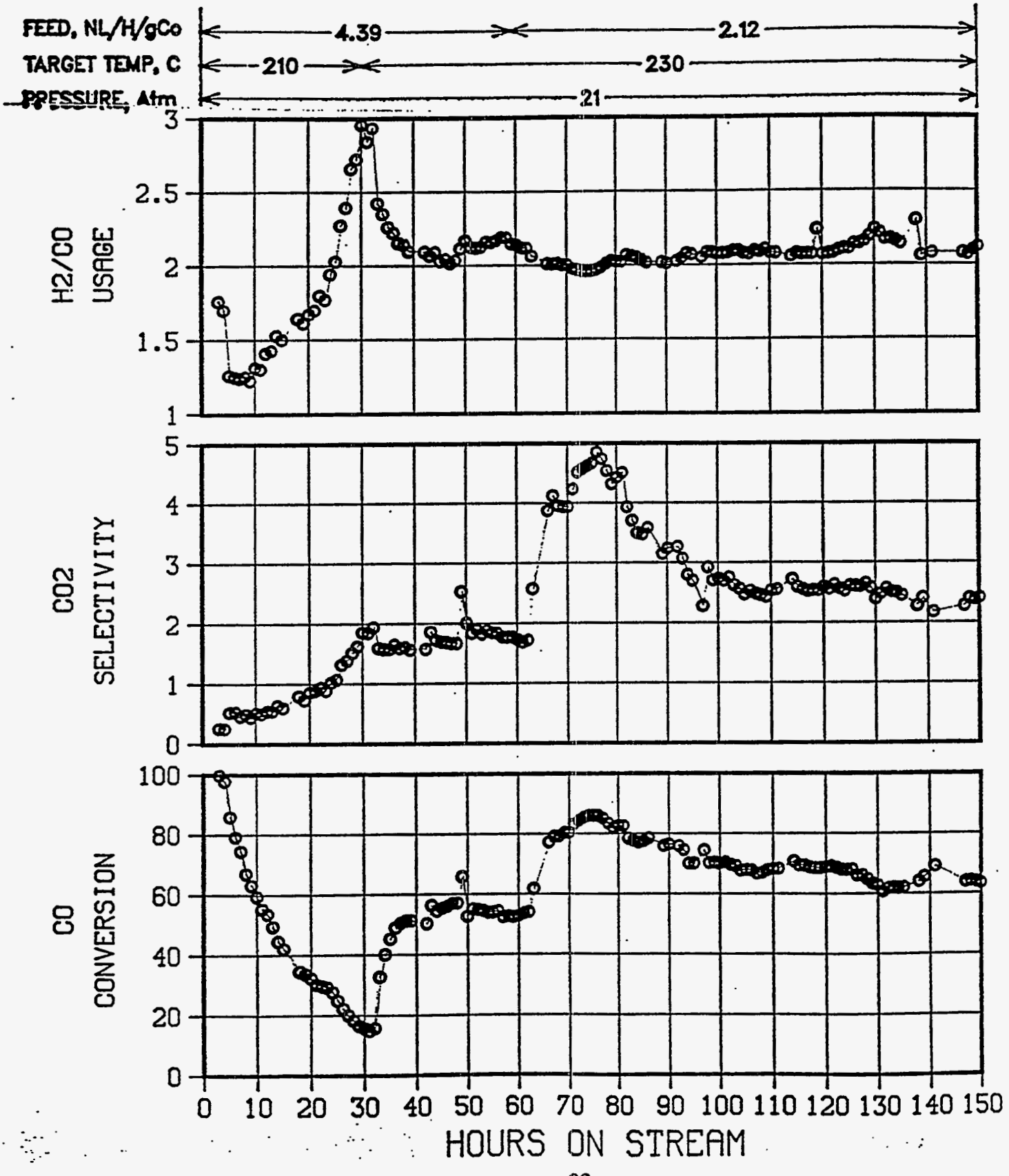

FIGURE 35

BIMETALLIC Co/Ru CATALYST ON C SUPPORT

PLT 700A RUN 67 H_2:CO (MOLAR)= 2.0

5.8 Co : 1.0 Ru : 100 C (BY WT.)

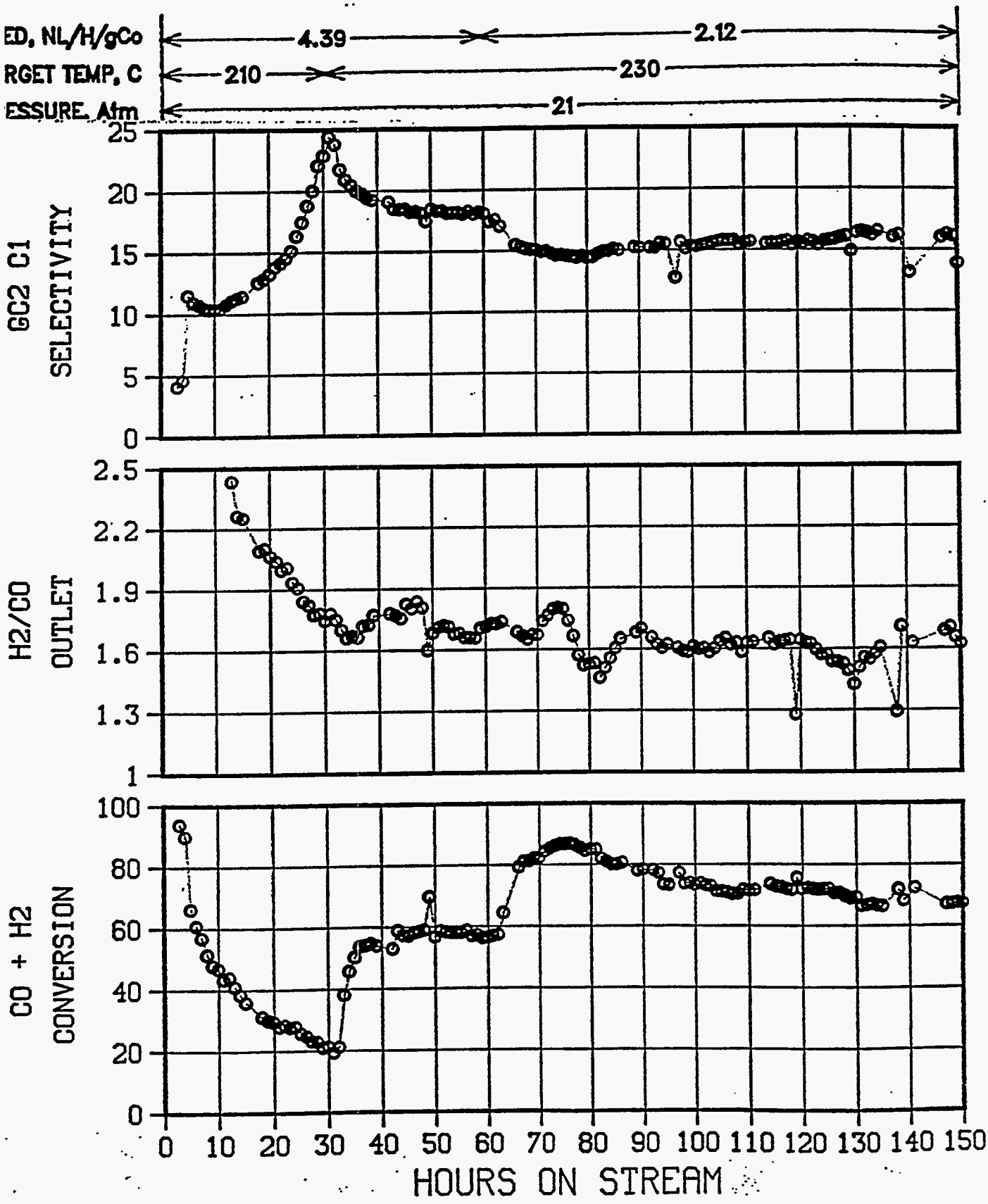

FIGURE 36

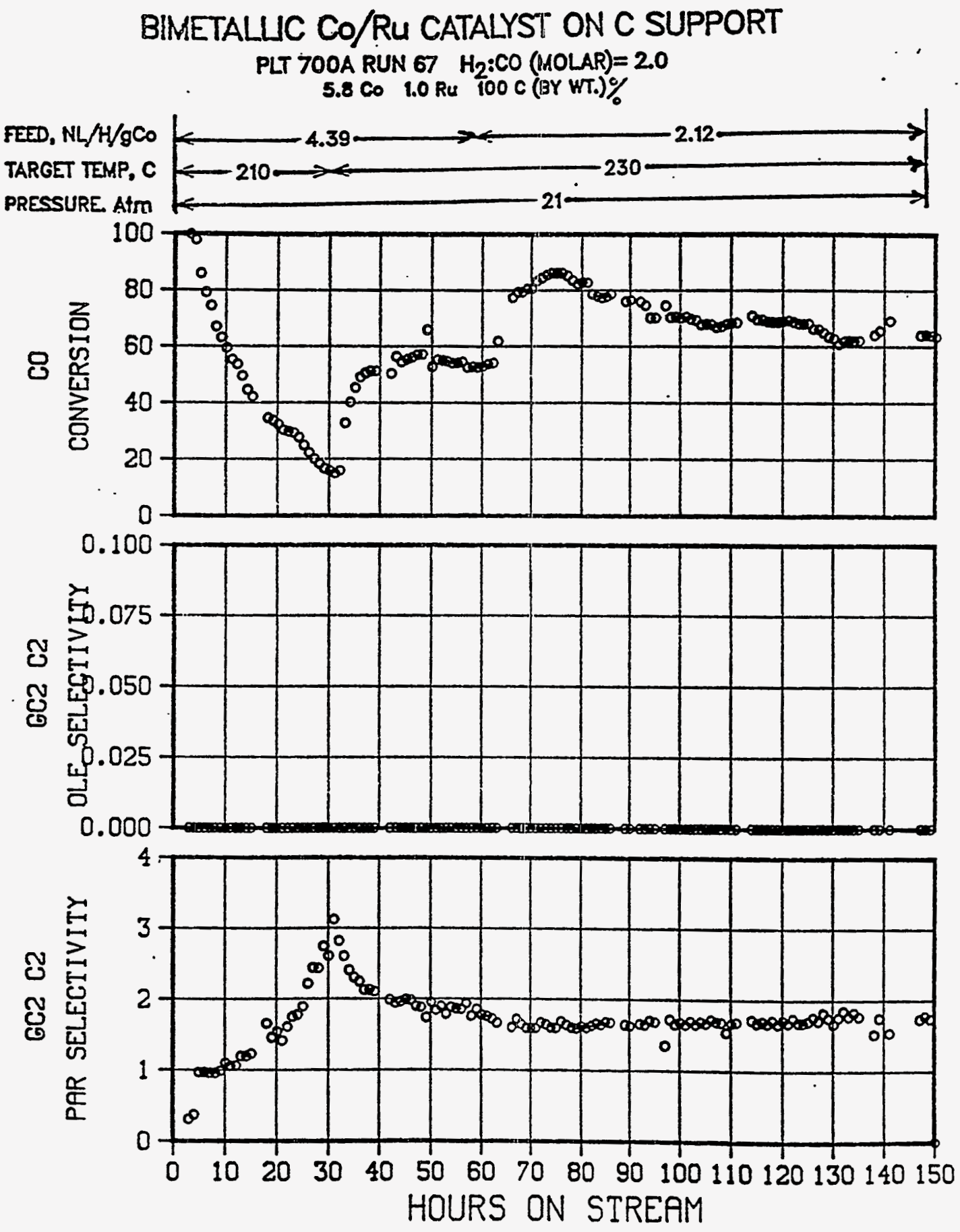
BIMETALLIC Co/Ru CATALYST ON C SUPPORT
PLT 700A RUN 67 H_2:CO (MOLAR)= 2.0
5.8 Co 1.0 Ru 100 C (BY WT.)%
FEED, NL/H/gCo
4.39
2.12
TARGET TEMP, C
210
230
PRESSURE. Atm
21
CO CONVERSION
100
80
60
40
20
0
GC2 C2 OLE SELECTIVITY
0.100
0.075
0.050
0.025
0.000
GC2 C2 PAR SELECTIVITY
4
3
2
1
0
0 10 20 30 40 50 60 70 80 90 100 110 120 130 140 150
HOURS ON STREAM

FIGURE 37

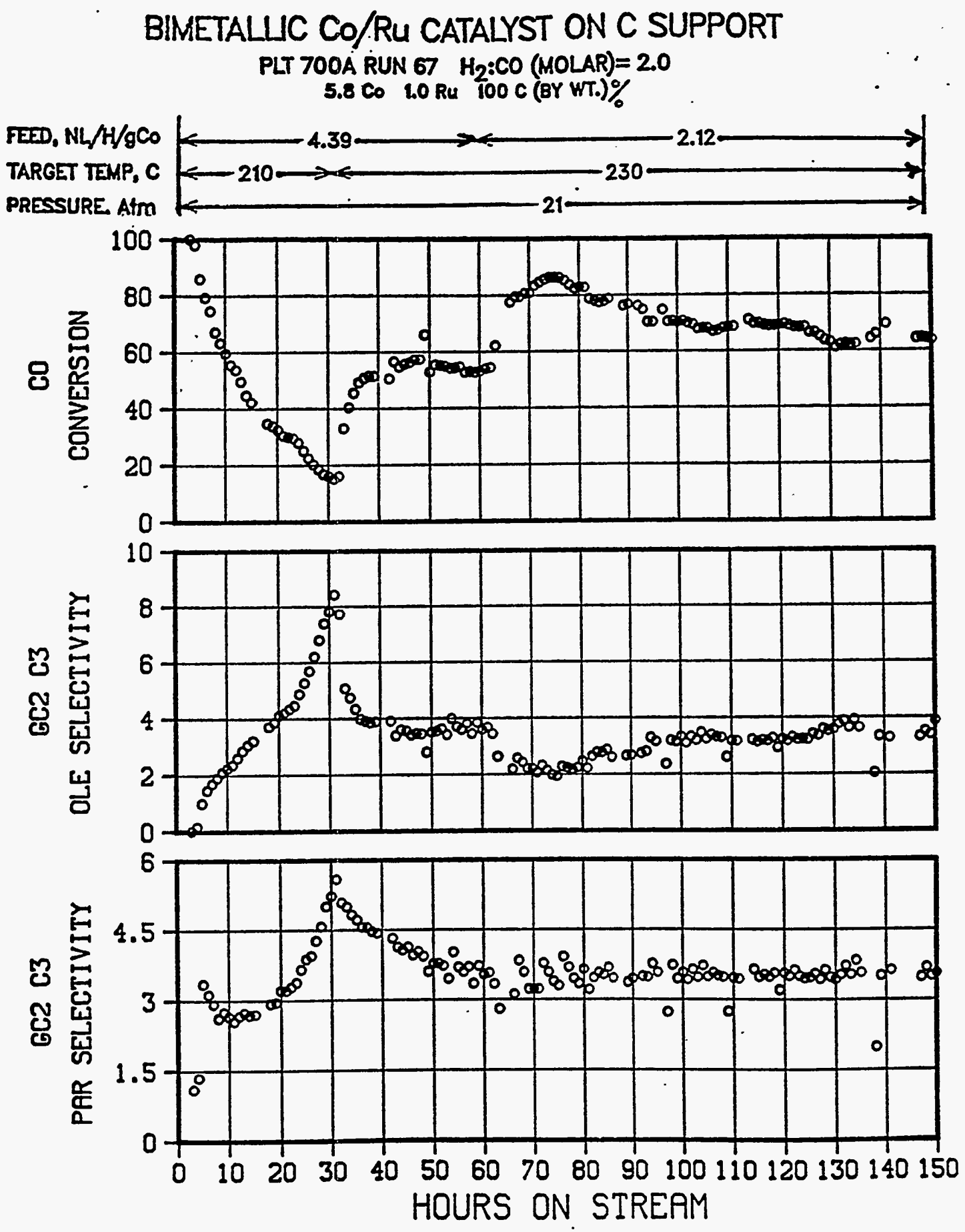
BIMETALLIC Co/Ru CATALYST ON C SUPPORT
PLT 700A RUN 67 H2:CO (MOLAR)= 2.0
5.8 Co 1.0 Ru 100 C (BY WT.)%
FEED, NL/H/gCo
4.39
2.12
TARGET TEMP, C
210
230
PRESSURE. Atm
21
CO CONVERSION
GC2 C3 OLE SELECTIVITY
GC2 C3 PAR SELECTIVITY
HOURS ON STREAM

FIGURE 38

BIMETALLIC Co/Ru CATALYST ON C SUPPORT

PLT 700A RUN 67 H_2:CO (MOLAR)= 2.0

5.8 Co 1.0 Ru 100 C (BY WT.)%

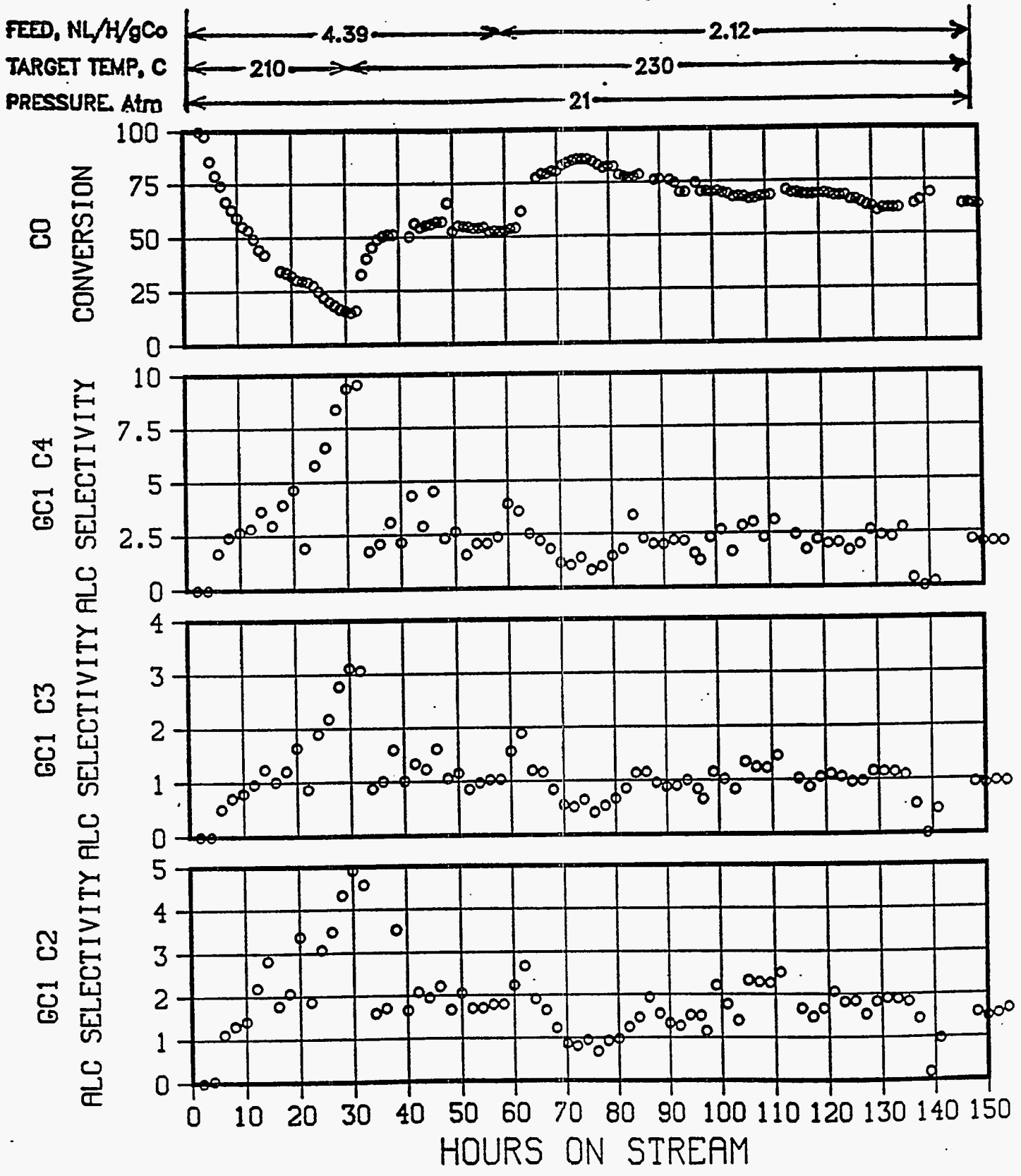

FIGURE 39

PLT 700A RUN 77 Co,Ru on Carbotrap B

6531–160 w/13.6 % Co via aq. impreg 2:1 H_2:CO in feed

13g active in 160g quartz sand

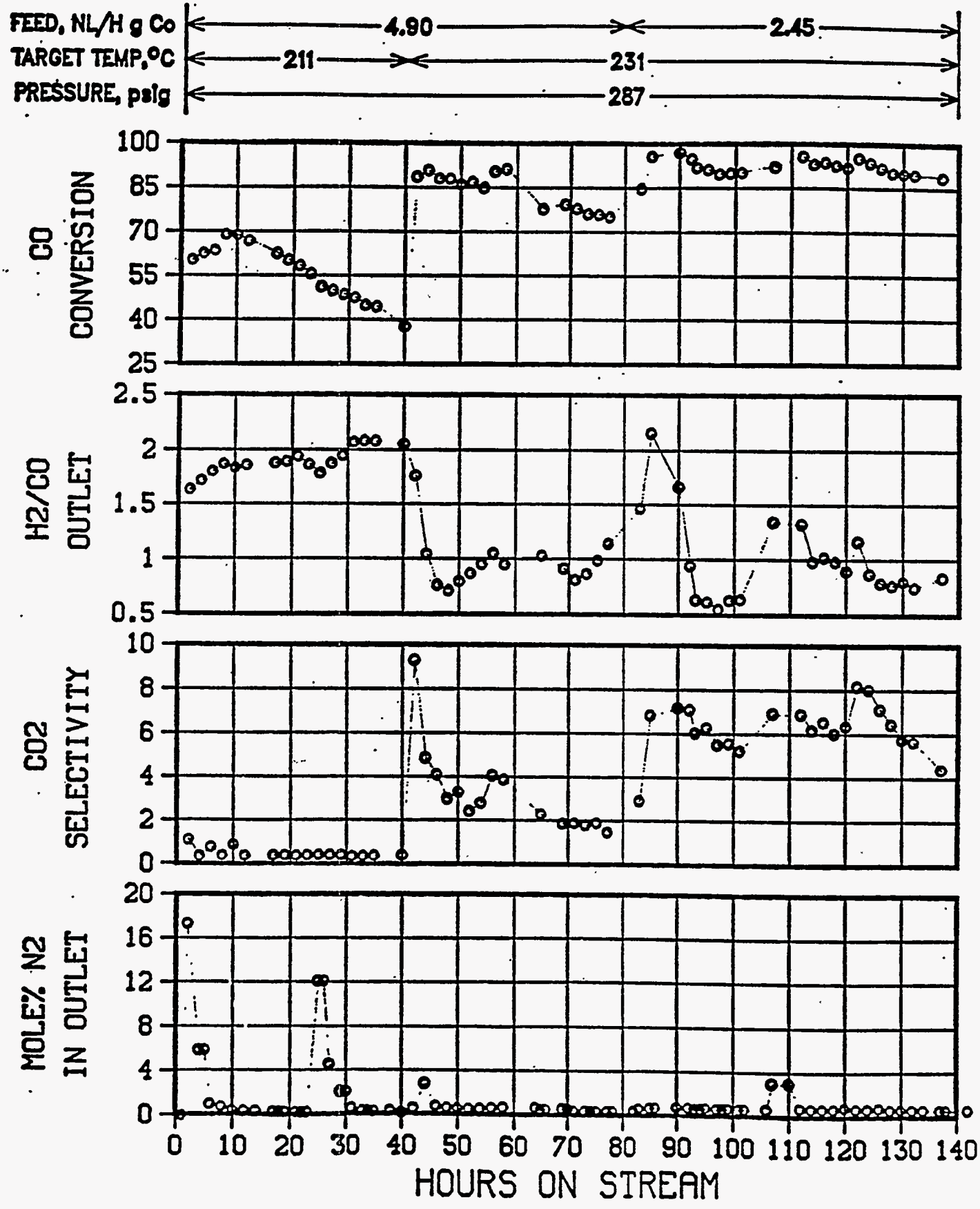

FIGURE 40

PLT 700A RUN 77 Co,Ru on Carbotrap B

6531–160 w/13.6 % Co via aq. impreg 2:1 H_2:CO in feed

13g active in 160g quartz sand

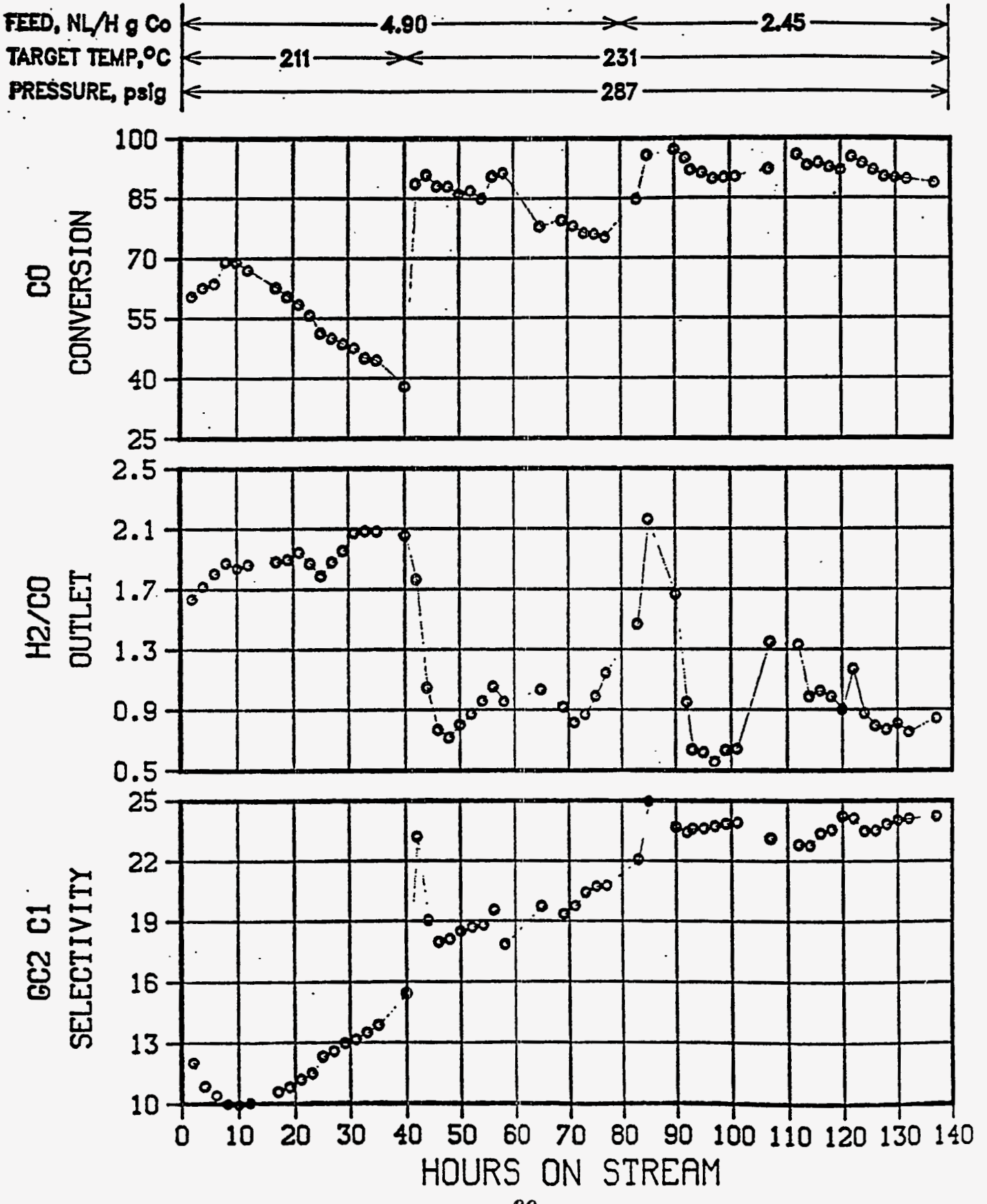

FIGURE 41

PLT 700A RUN 77 Co,Ru on Carbotrap B

6531–160 w/13.6 % Co via aq. impreg 2:1 H_2:CO in feed

13g active in 160g quartz sand

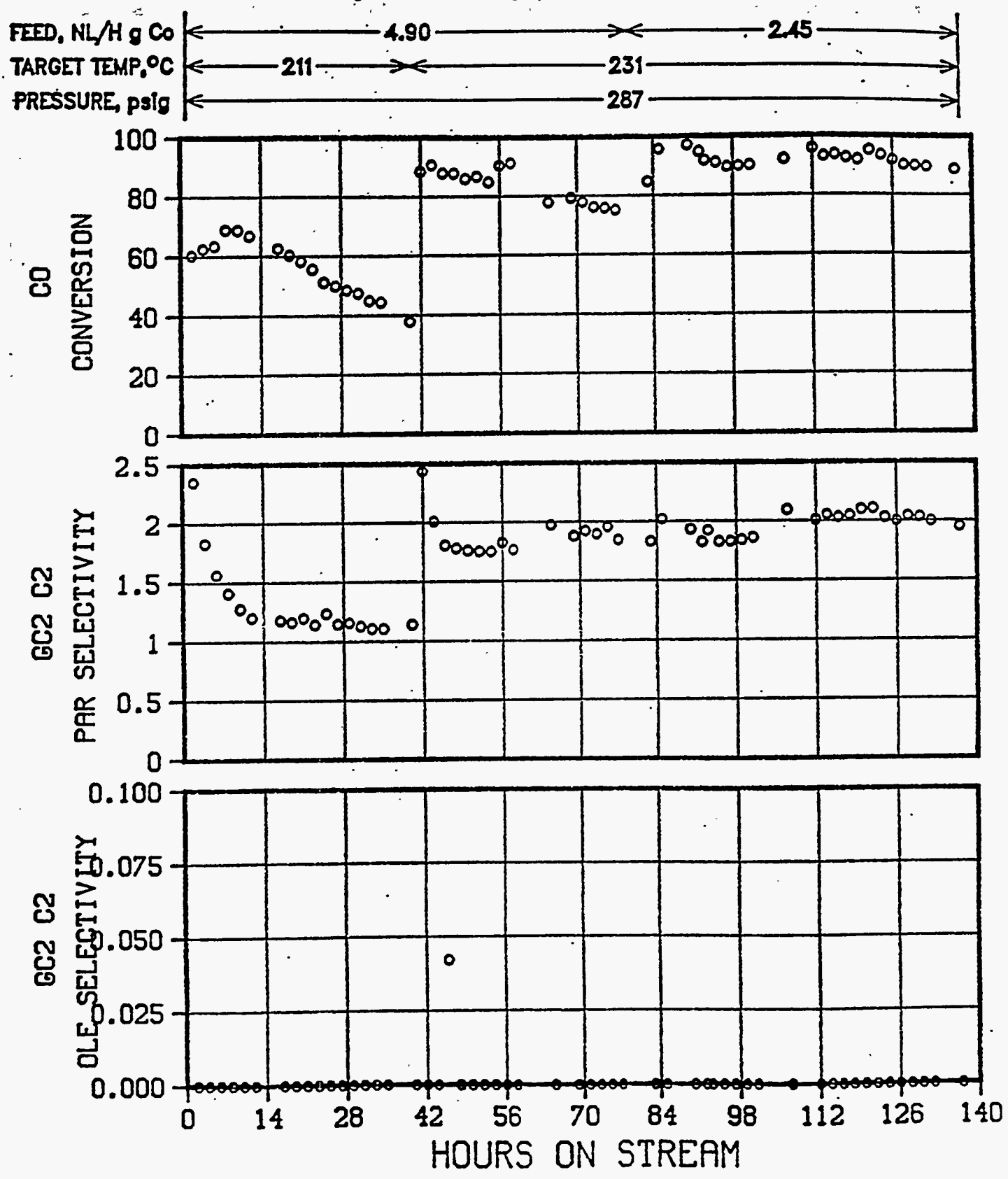

FIGURE 42

PLT 700A RUN 77 Co,Ru on Carbotrap B

6531–160 w/13.6 % Co via aq. Impreg 2:1 H_2:CO in feed

13g active in 160g quartz sand

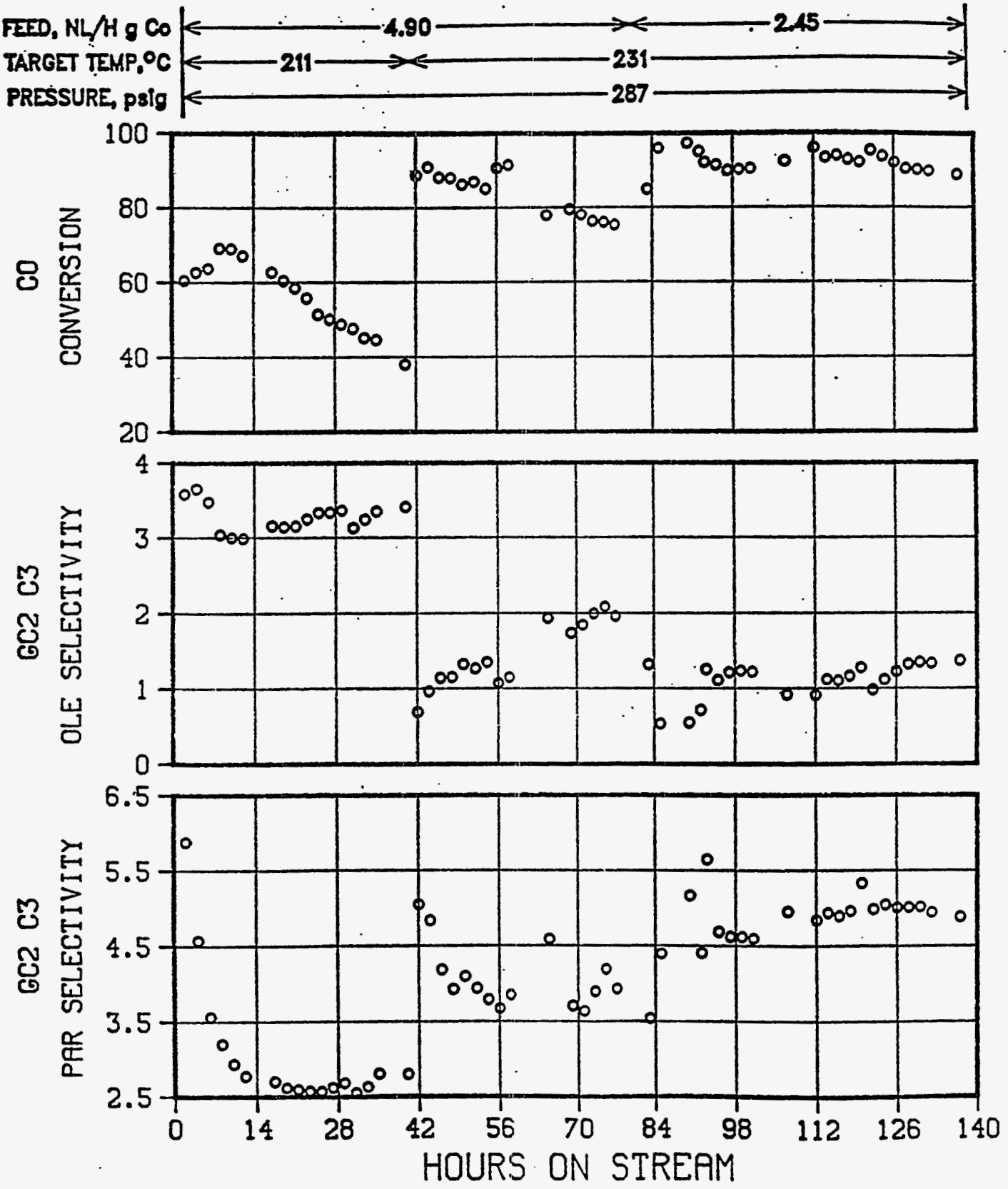

FIGURE 43

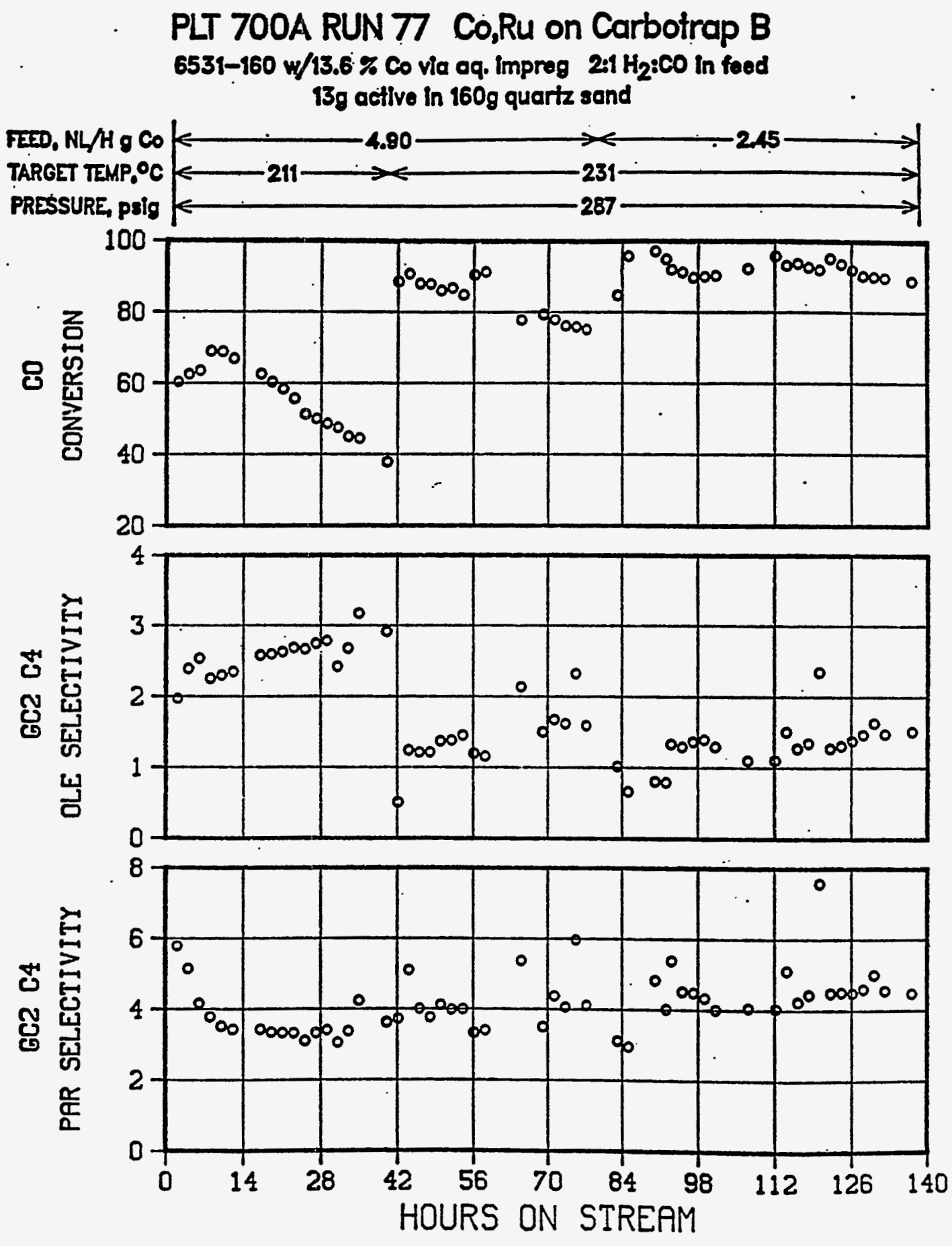
PLT 700A RUN 77 Co,Ru on Carbotrap B
6531-160 w/13.6 % Co via aq. impreg 2:1 H2:CO in feed
13g active in 160g quartz sand
FEED, NL/H g Co
4.90
2.45
TARGET TEMP,°C
211
231
PRESSURE, psig
287
CO CONVERSION
100
80
60
40
20
GC2 C4 OLE SELECTIVITY
4
3
2
1
0
GC2 C4 PAR SELECTIVITY
8
6
4
2
0
0
14
28
42
56
70
84
98
112
126
140
HOURS ON STREAM

FIGURE 44

PLT 700A RUN 77 Co,Ru on Carbotrap B

6531-160 w/13.6 % Co via aq. impreg 2:1 H_2:CO in feed

13g active in 160g quartz sand

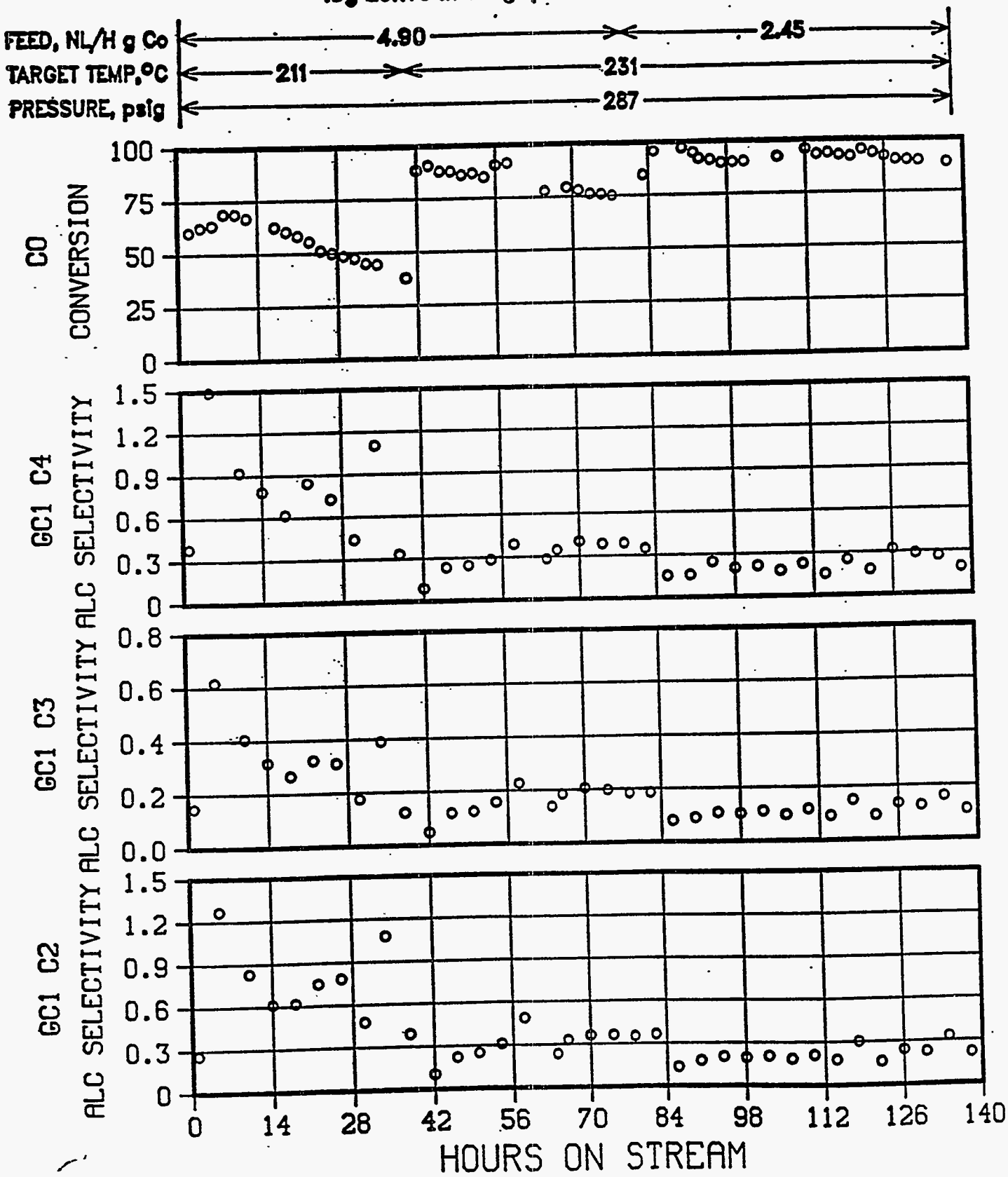

COMPARISON OF ALUMINA-TITANIA CATALYSTS TO REFERENCE CATALYST

THREE-CONDITION SCREENING TEST SUMMARY

CATALYST SOURCE	SUPPORT	METALS, WT %	% CO CONV/% C-1 SELEC CONDITION 1	2	3
UNION CARBIDE	STEAMED, ACID-WASHED Y ZEOL	Co, 8.3; Mn, 1.3 Zr, 1.0	58/6.0		
DES PLAINES (Run 68)[1]	50/50 Al_2O_3/TiO_3	Co, 2.7; Ru, 0.49	20/21	40/25	
DES PLAINES (Run 73)[2]	50/50 Al_2O_3/TiO_2	Co, 7.5; Ru, 0.29	25/45	50/75	100/37

1. REVERSE MICELLE IMPREGNATION
2. AQUEOUS IMPREGNATION

104

FIGURE 45

FIGURE 46

BIMETALLIC Co/Ru CATALYST ON Al_2O_3–TiO_2 SUPPORT

PLT 700A RUN 68 H_2:CO (MOLAR)= 2.0

2.65 % Co , 0.49 % Ru , 50:50 Al_2O_3–TiO_2

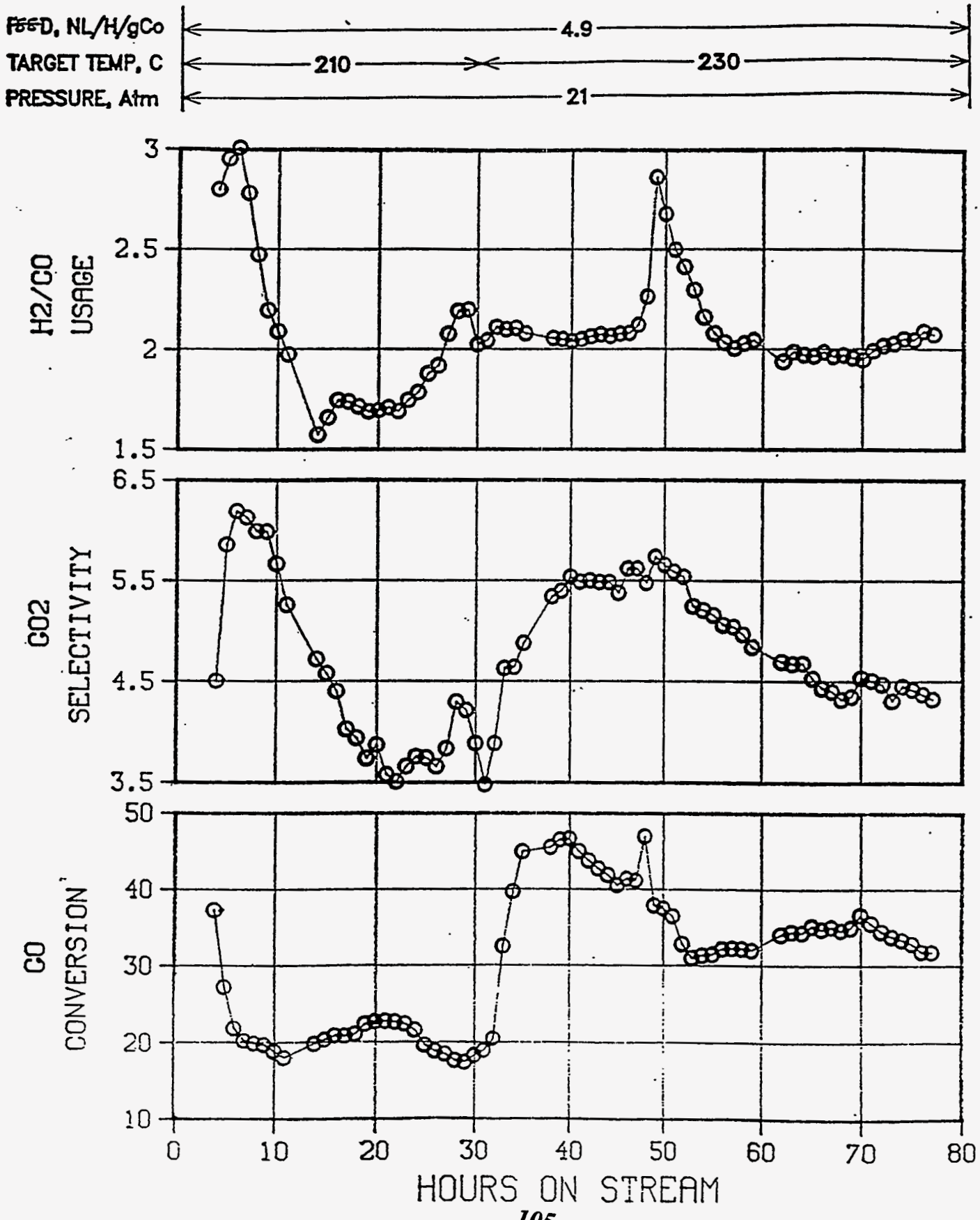

FIGURE 47

BIMETALLIC Co/Ru CATALYST ON Al_2O_3–TiO_2 SUPPORT

PLT 700A RUN 68 H_2:CO (MOLAR)= 2.0

2.65 % Co , 0.49 % Ru , 50:50 Al_2O_3–TiO_2

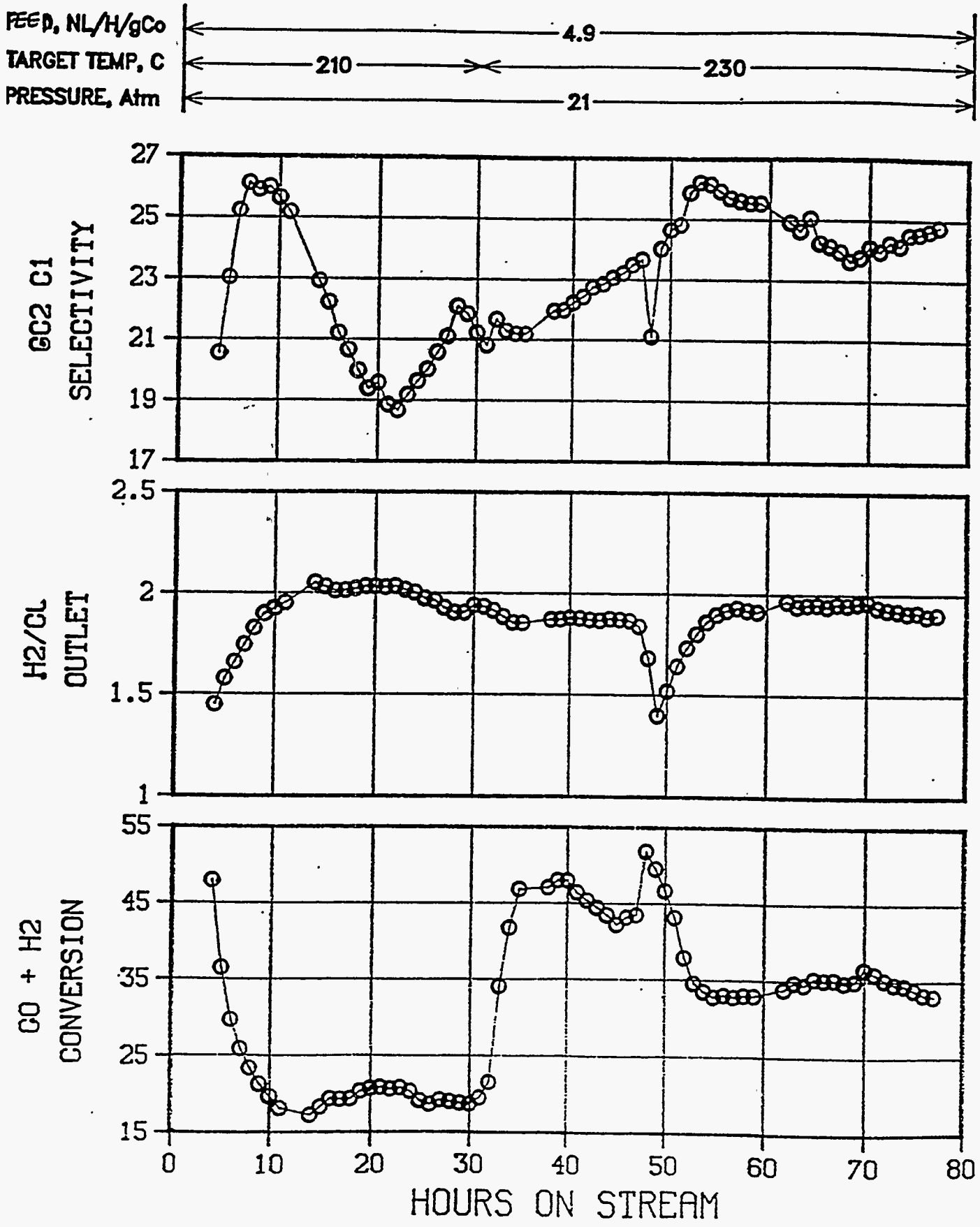

FIGURE 48

BIMETALLIC Co/Ru CATALYST ON Al_2O_3–TiO_2 SUPPORT

PLT 700A RUN 68 H_2:CO (MOLAR)= 2.0

2.65 % Co , 0.49 % Ru , 50:50 Al_2O_3–TiO_2

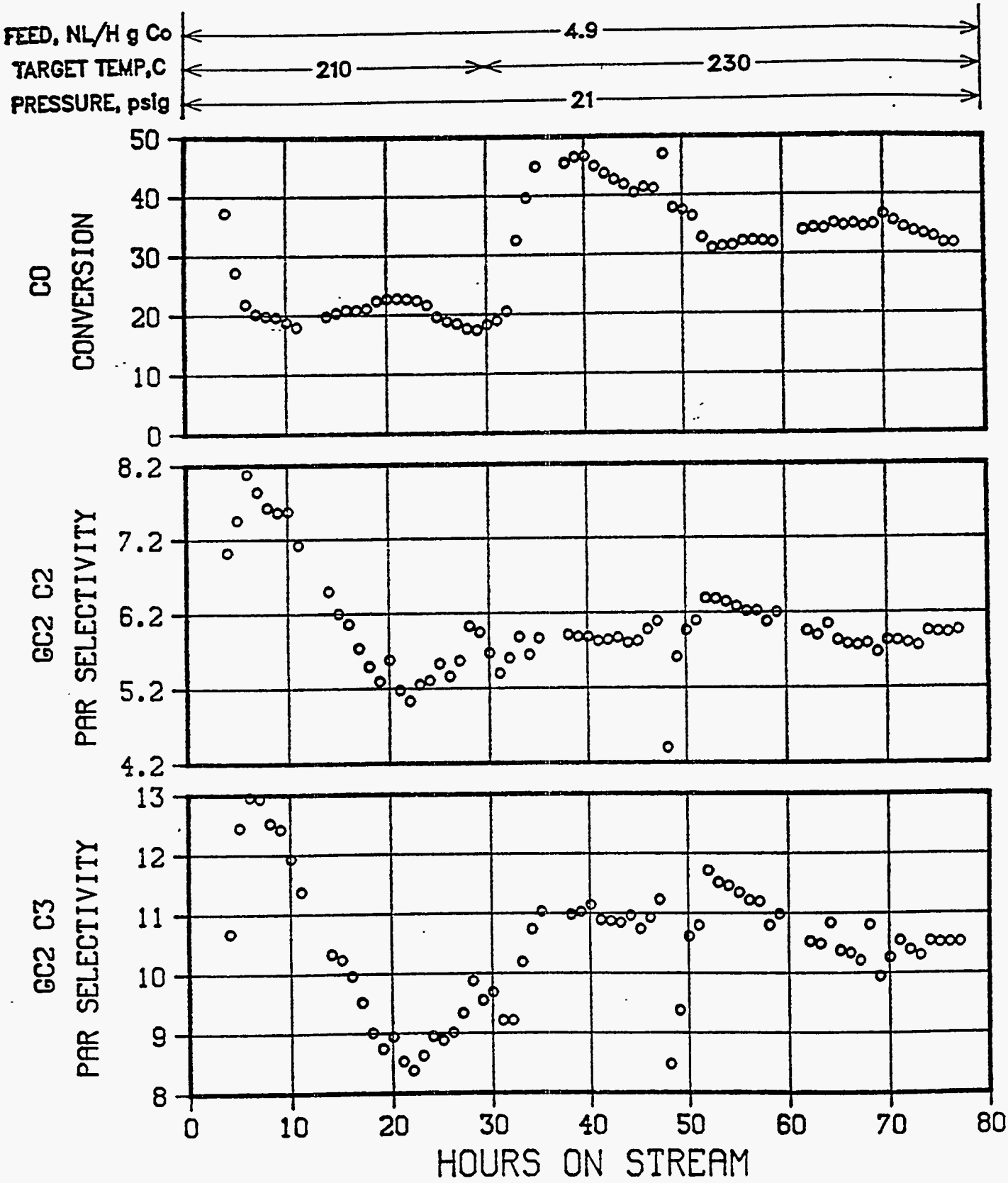

FIGURE 49

BIMETALLIC Co/Ru CATALYST ON Al_2O_3–TiO_2 SUPPORT

PLT 700A RUN 68 H_2:CO (MOLAR)= 2.0

2.65 % Co , 0.49 % Ru , 50:50 Al_2O_3–TiO_2

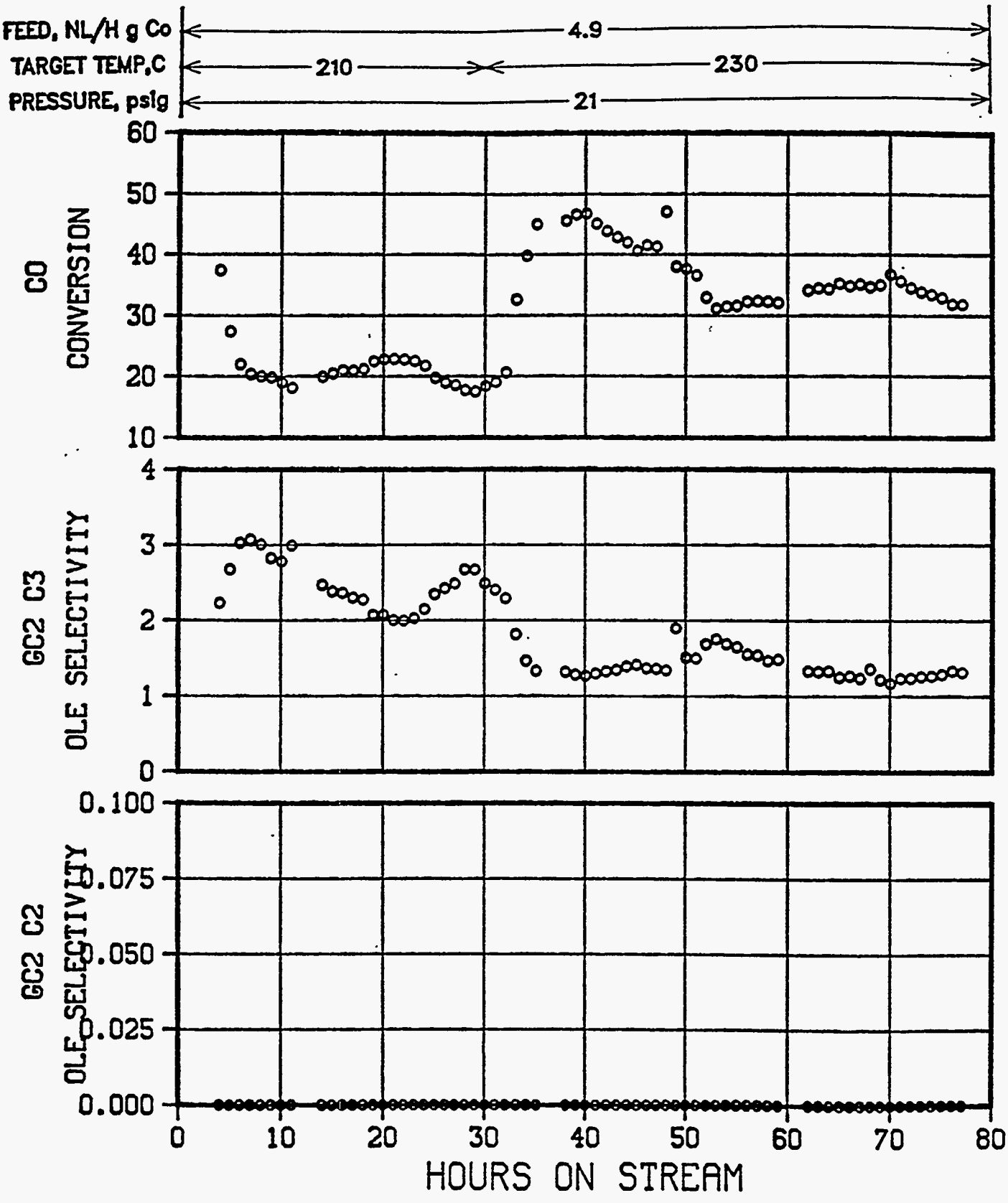

FIGURE 50

BIMETALLIC Co/Ru CATALYST ON Al_2O_3–TiO_2 SUPPORT

PLT 700A RUN 68 H_2:CO (MOLAR)= 2.0

2.65 % Co , 0.49 % Ru , 50:50 Al_2O_3–TiO_2

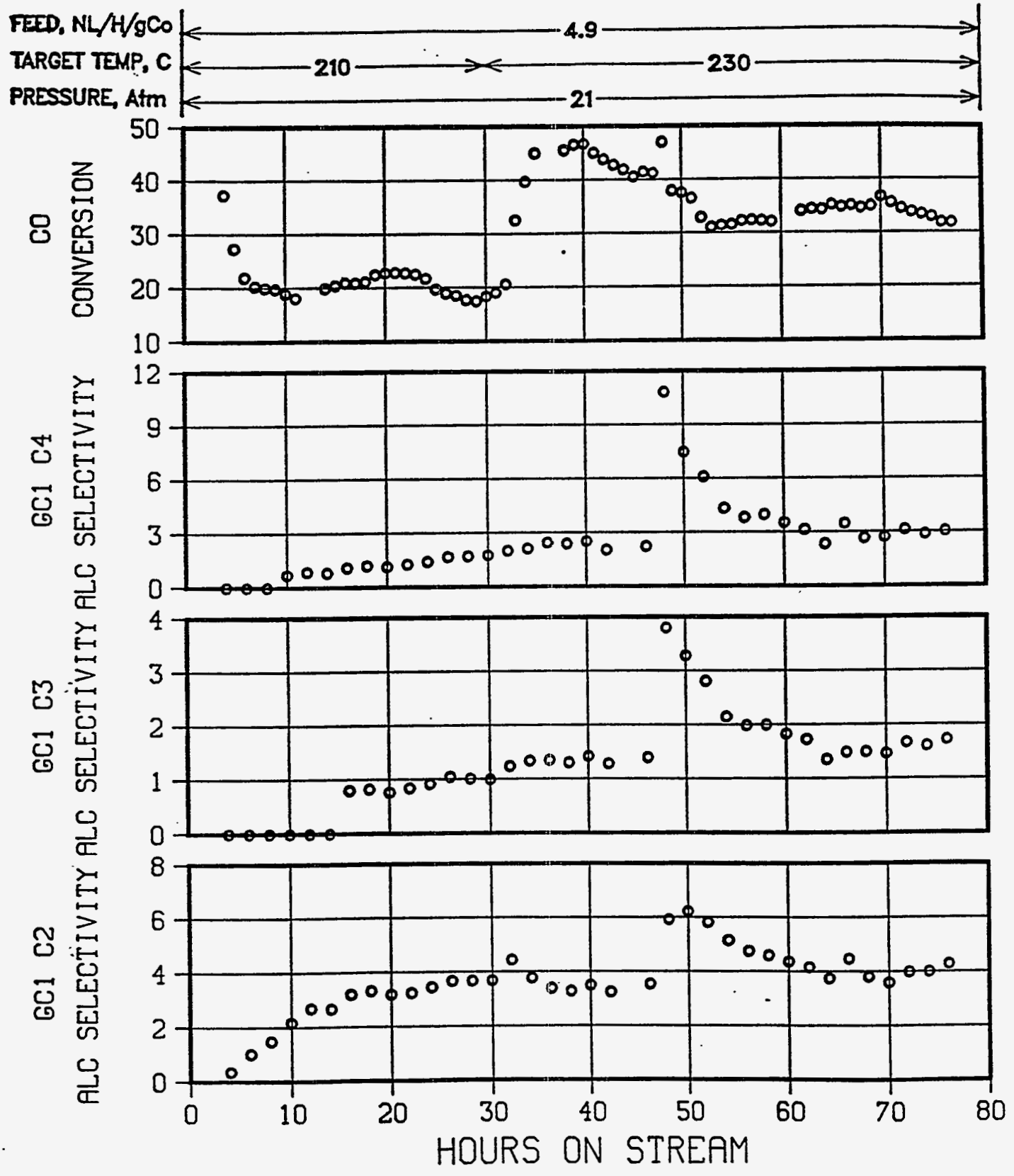

FIGURE 51

PLT 700A RUN 73 Co,Ru on 50/50 Al_2O_3/TiO_2

6531-134 w/7.45% Co via aq. impreg 2:1 H_2:CO in feed

13g Active in 160g SiO_2 sand

FEED, NL/H g Co	4.9	2.4	4.9
TARGET TEMP,C	211	231	
PRESSURE, psig	287		

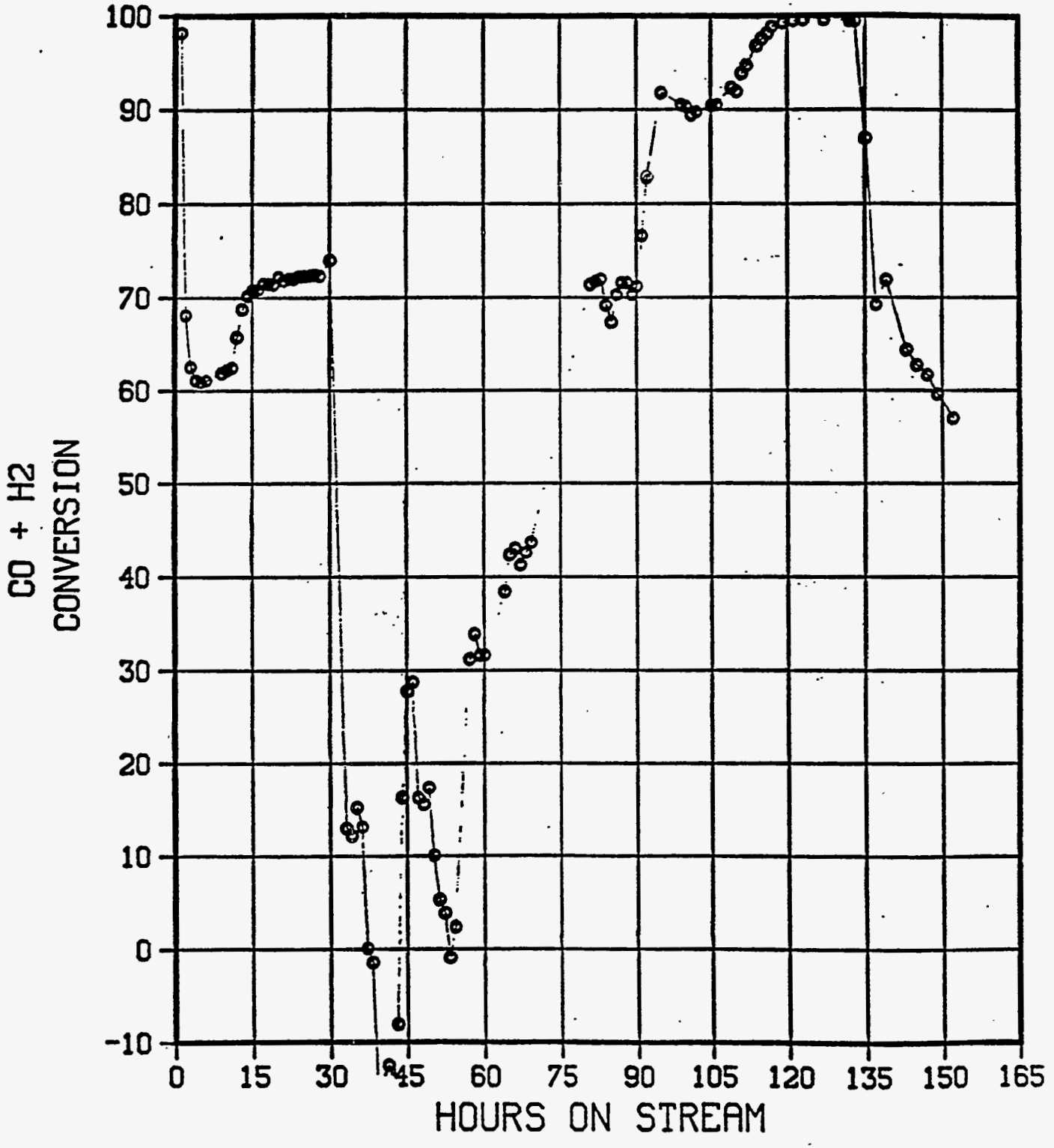

FIGURE 52

PLT 700A RUN 73 Co,Ru on 50/50 Al_2O_3/TiO_2

6531-134 w/7.45% Co via aq. Impreg 2:1 H_2:CO in feed

13g Active in 160g SiO_2 sand

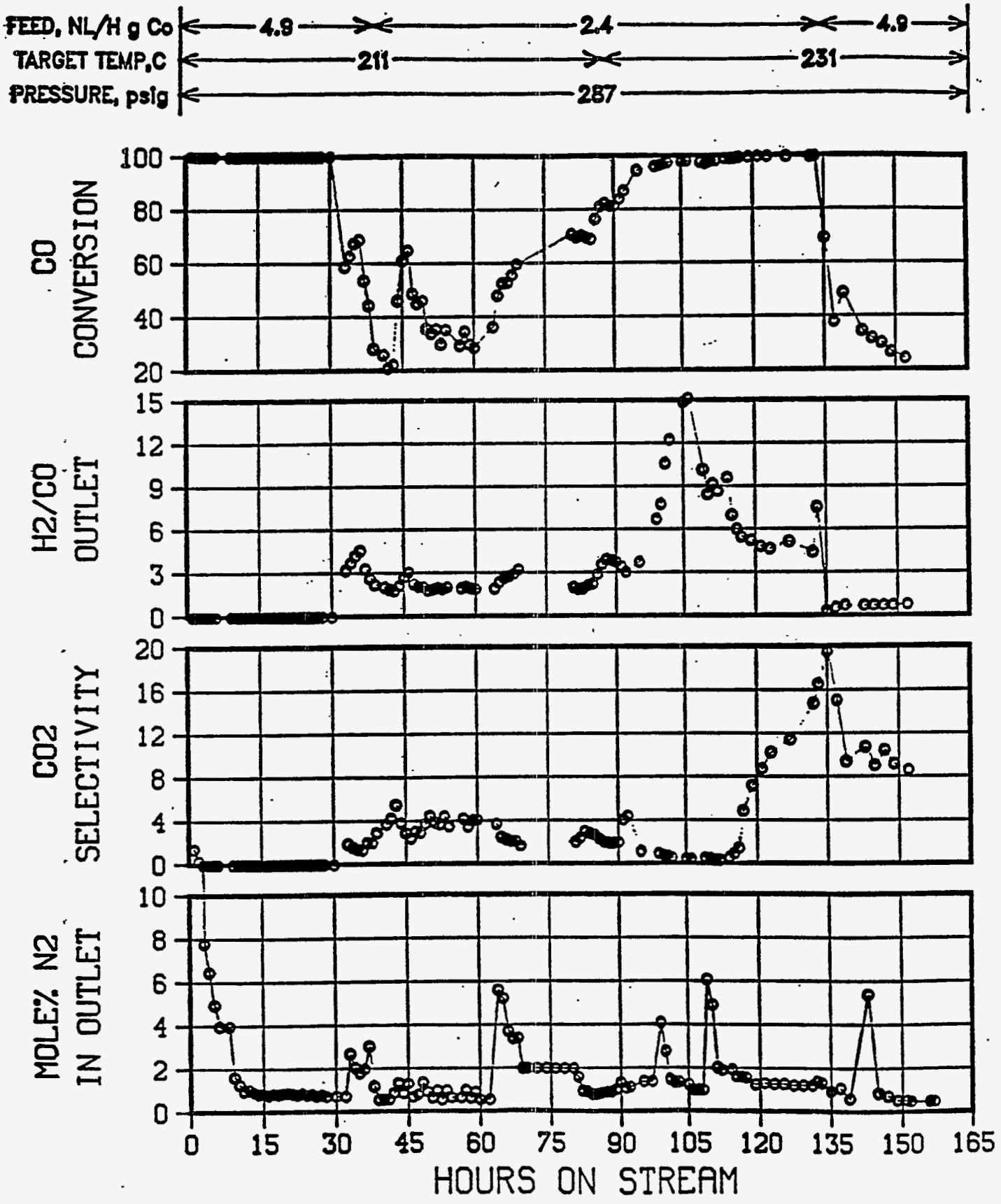

FIGURE 53

PLT 700A RUN 73 Co,Ru on 50/50 Al_2O_3/TiO_2

6531-134 w/7.45% Co via aq. impreg 2:1 H_2:CO in feed

13g Active in 160g SiO_2 sand

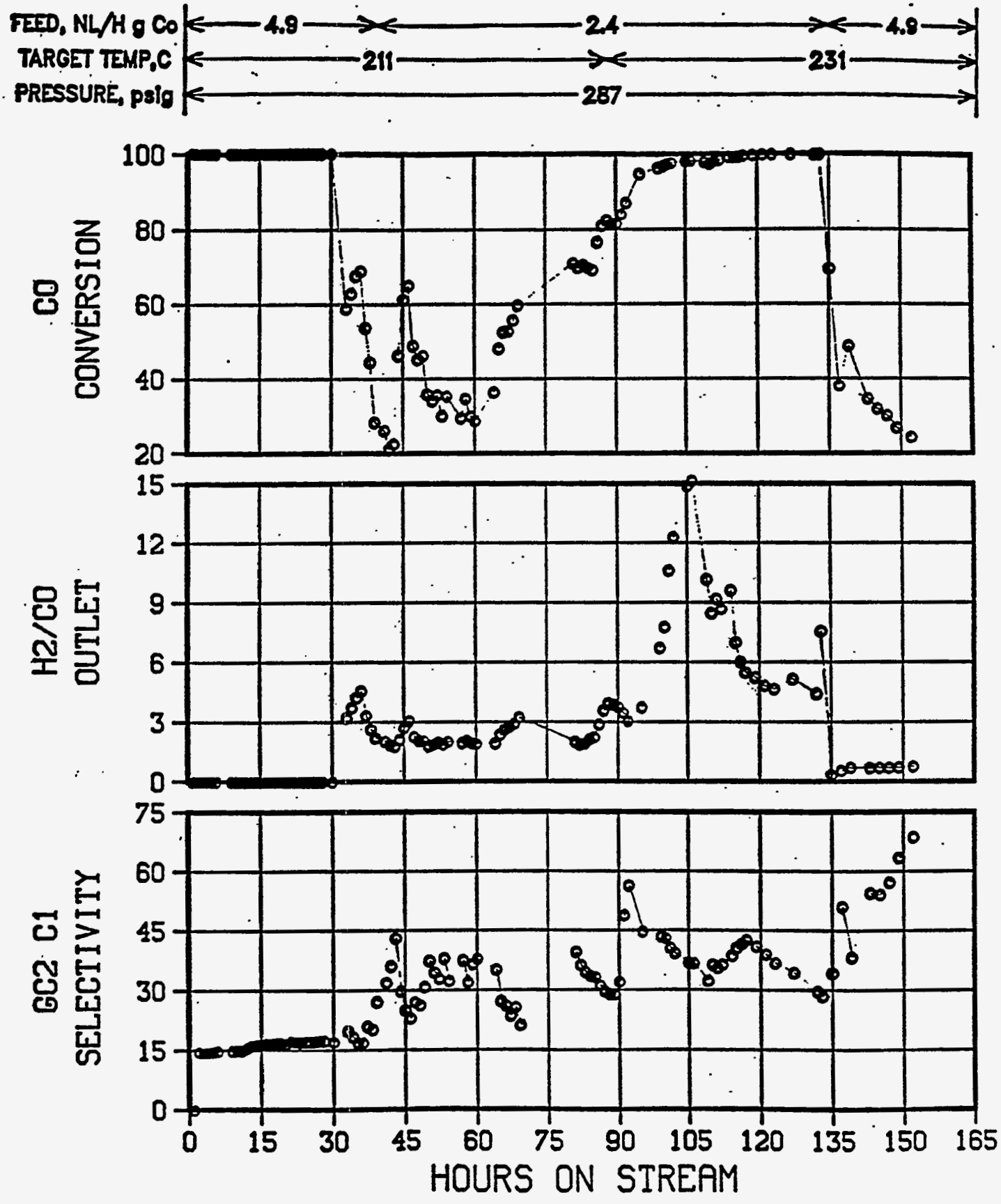

FIGURE 54

PLT 700A RUN 73 Co,Ru on 50/50 Al_2O_3/TiO_2

6531–134 w/7.45% Co via aq. impreg 2:1 H_2:CO in feed

13g Active in 160g SiO_2 sand

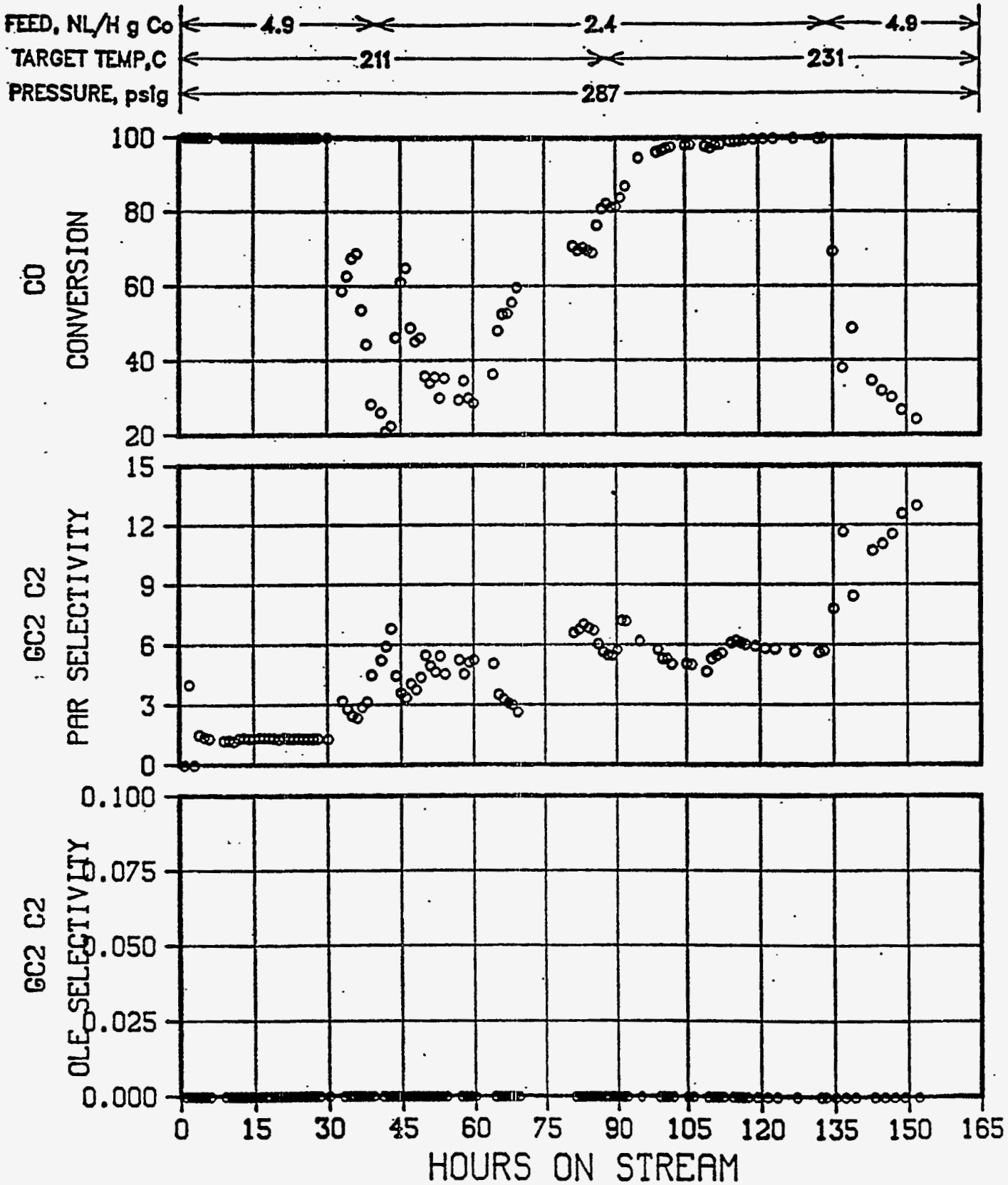

FIGURE 55

PLT 700A RUN 73 Co,Ru on 50/50 Al_2O_3/TiO_2

6531-134 w/7.45% Co via aq. impreg 2:1 H_2:CO in feed

13g Active in 160g SiO_2 sand

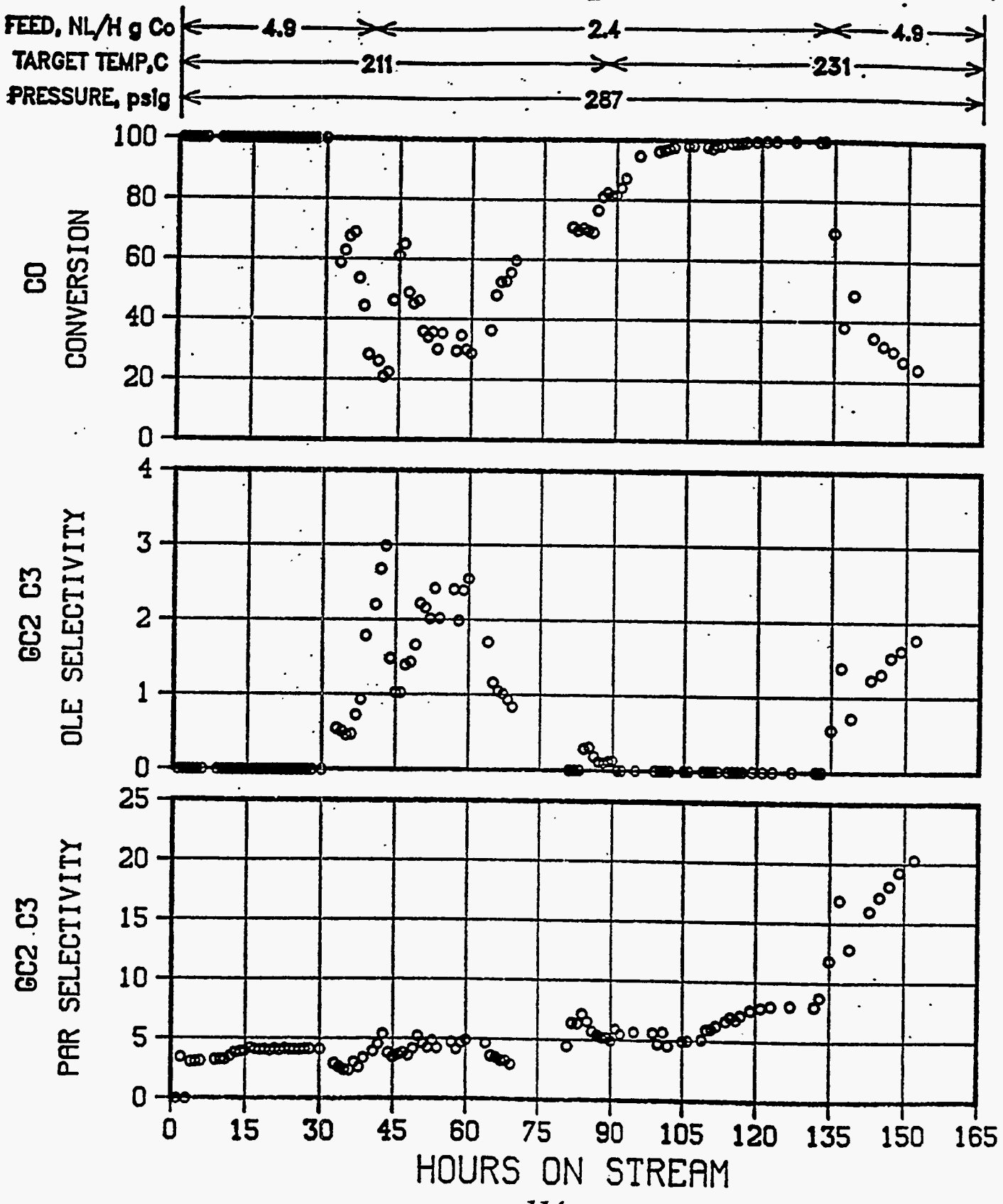

FIGURE 56

PLT 700A RUN 73 Co,Ru on 50/50 Al_2O_3/TiO_2

6531–134 w/7.45% Co via aq. Impreg 2:1 H_2:CO in feed

13g Active in 160g SiO_2 sand

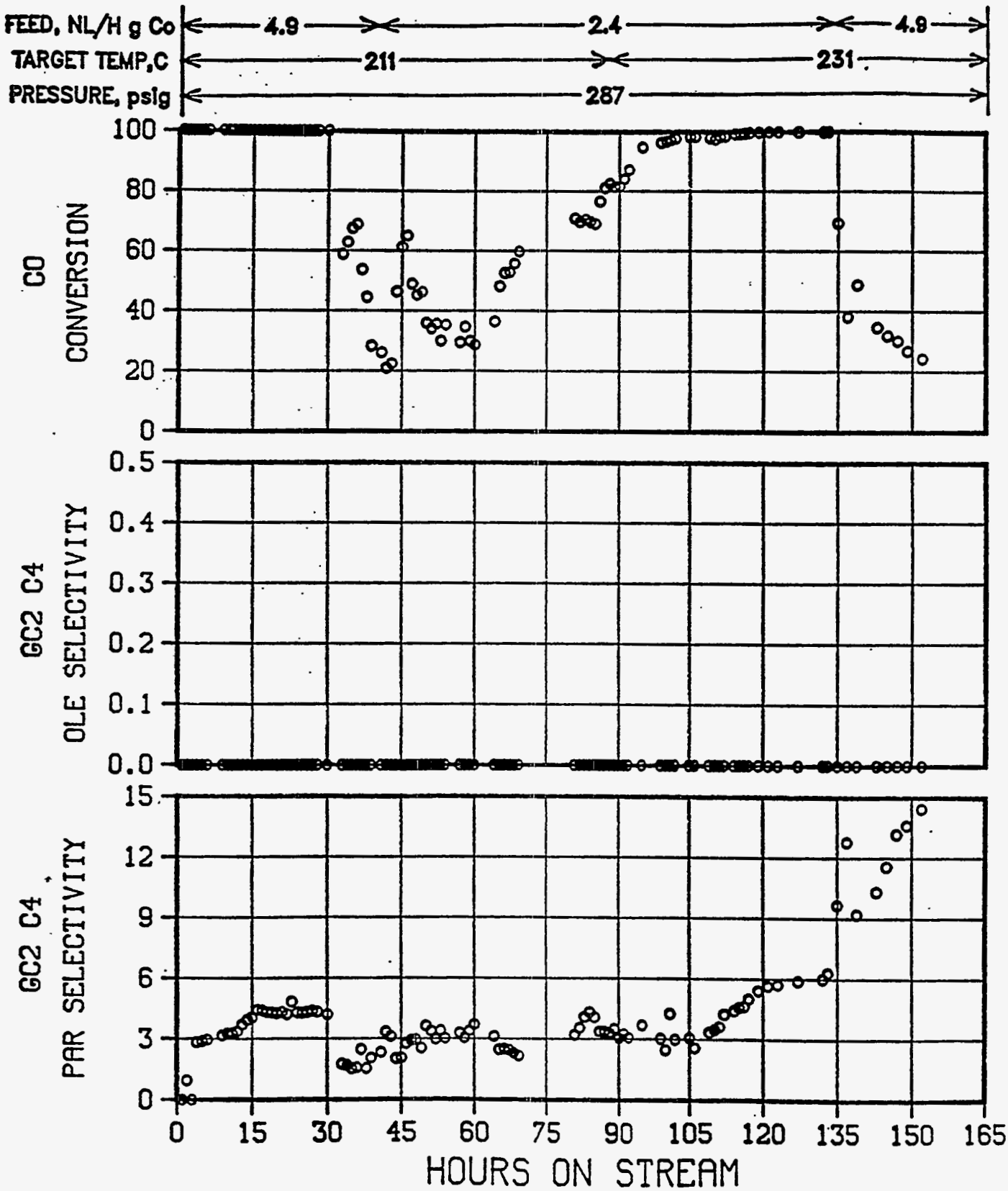

FIGURE 57

PLT 700A RUN 73 Co,Ru on 50/50 Al_2O_3/TiO_2

6531-134 w/7.45% Co via aq. impreg 2:1 H_2:CO in feed

13g Active in 160g SiO_2 sand

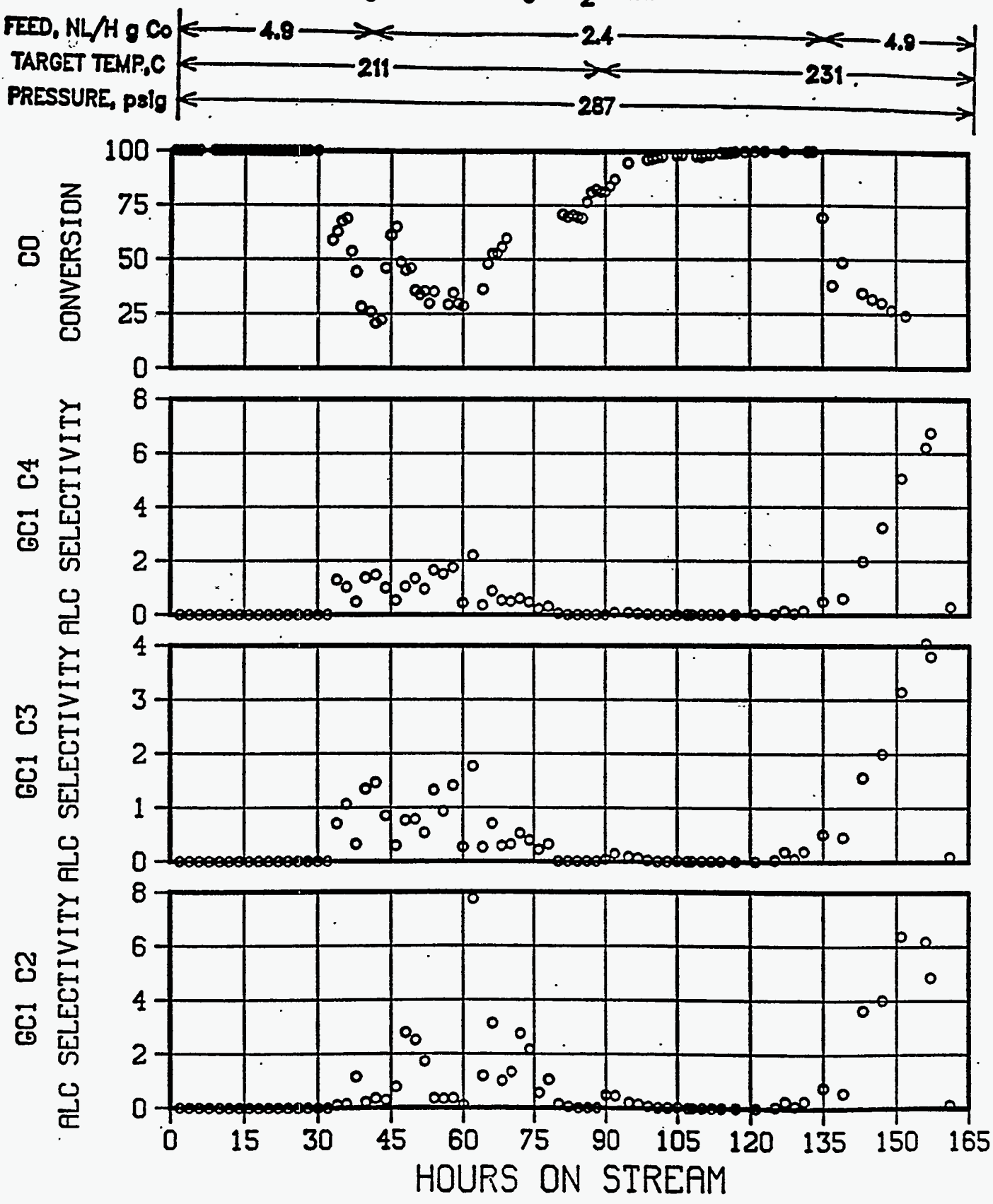

FIGURE 58

Particle Analysis

12524-27

Particle #	Weight % Si	Weight % Mn	Weight % Co	Weight % Zr
1	68.33	4.30	24.78	2.59
2	73.21	3.56	21.43	1.81
3	76.71	3.30	17.41	2.51
4	77.68	3.09	16.37	2.86
5	77.09	3.44	16.87	2.60
6	74.35	3.51	19.69	2.45
7	74.10	3.73	20.00	2.17
8	72.41	3.60	20.14	3.86
9	69.38	4.77	23.79	2.06
10	79.47	2.91	16.49	1.13
11	72.49	4.49	21.66	1.36
Average	79.11 ± 3.45	3.70 ± 0.58	19.88 ± 2.90	2.31 ± 0.75

FIGURE 59

Crystallite Atomic % Composition and Ratio as a Function of Size

6531-86

Crystallite Size (nm)	Atomic % Mn	Atomic % Co	Atomic % Zr	Atomic % Ru	Atomic Ratios Mn/Co	Atomic Ratios Zr/Co	Atomic Ratios Ru/Co
20	0.91	99.09	0	0	0.01	0	0
15	1.49	98.32	0.04	0.14	0.02	0.0004	0.001
20	0.66	99.28	0	0.07	0.01	0	0.001
20	11.08	87.52	0.71	0.69	0.13	0.01	0.01
6	8.57	91.43	0	0	0.09	0	0
6	1.05	98.40	0.21	0.33	0.01	0.002	0.003
8	2.14	96.57	0.49	0.81	0.02	0.01	0.01
10	2.55	94.98	1.00	1.47	0.03	0.01	0.02
8	2.09	94.42	2.53	0.96	0.02	0.03	0.01
15	6.50	84.11	5.37	4.01	0.08	0.06	0.05
10	0.99	98.83	0.18	0	0.01	0.002	0
8	0.67	98.94	0.02	0.36	0.01	0.0002	0.004
10	0.75	99.21	0	0.04	0.01	0	0.0004

FIGURE 60

Co-Ru Atomic Composition and Ratio as a Function of Crystallite Size

Ru/Co on MgO (6531-120)

Crystallite Size (nm)	Atomic % Co	Atomic % Ru	Ru/Co Atomic Ratio
15	93.74	6.26	0.067
10	96.00	4.00	0.042
15	93.78	6.22	0.066
10	92.78	7.22	0.078
25	91.37	8.63	0.094
20	97.13	2.87	0.030
30	96.83	3.17	0.033
30	95.24	4.76	0.050
20	98.53	1.47	0.015
20	92.00	8.00	0.087

FIGURE 61

Crystallite Atomic % Composition
and Ratio as a Function of Size

6531-112

Crystallite Size (nm)	Atomic % Co	Atomic % Ru	Atomic Ratio Ru/Co
4	98.53	1.47	0.01
6	100.00	0.00	0.00
4	100.00	0.00	0.00
4	100.00	0.00	0.00
4	100.00	0.00	0.00
4	100.00	0.00	0.00
6	98.67	1.33	0.01
4	100.00	0.00	0.01
4	96.22	3.78	0.04
6	96.46	3.54	0.04
4	100.00	0.00	0.00
6	95.51	4.49	0.05
4	94.7	5.30	0.06
3	99.55	0.45	0.004
	93.58	6.42	0.07

FIGURE 62

6531-160

Crystallite Size (nm)	Weight %		Atomic %		Atomic Ratio
	Co	Ru	Co	Ru	Ru/Co
4	89.54	10.46	93.63	6.37	0.068
4	60.64	39.36	72.54	27.46	0.38
4	10.49	89.51	16.74	83.26	4.97
4	59.85	40.15	71.89	28.11	0.39
4	37.24	62.76	50.47	49.56	0.98
6	54.19	45.81	66.99	33.01	0.49
10	85.94	14.06	91.29	8.71	0.095
10	73.67	26.33	82.76	17.24	0.21
50	94.07	5.93	96.46	3.54	0.037
30	92.56	7.44	95.53	4.47	0.047
30	93.28	6.72	95.97	4.03	0.042
100	95.71	4.29	97.45	2.55	0.026
20	94.02	5.98	96.42	3.58	0.037
8	95.59	4.41	97.38	2.62	0.027
20	92.34	7.66	95.39	4.61	0.048
20	94.77	5.23	96.88	3.12	0.032
15	95.98	4.02	97.62	2.38	0.024
15	97.57	2.43	98.57	1.43	0.014
10	96.81	3.19	98.12	1.88	0.019
15	93.36	6.64	96.02	3.98	0.041
15	97.57	2.43	98.57	1.43	0.015

FIGURE 63

Particle Analysis

6531-104

Particle #	Weight % Al	Weight % Ti	Weight % Co	Weight % Ru
1	42.18	50.21	6.33	1.28
2	44.51	48.49	5.43	1.57
3	43.94	57.23	3.83	0.00
4	43.15	53.77	3.03	0.05
5	43.15	53.27	3.58	0.00
6	41.83	54.52	3.52	0.13
7	44.02	52.51	3.47	0.00
8	48.33	47.6	4.03	0.04
9	47.53	49.18	3.26	0.03
10	47.36	48.76	3.82	0.06
11	47.04	48.98	3.91	0.07
Average	44.82 ± 2.32	50.86 ± 2.44	4.02 ± 0.99	0.29 ± 0.56

FIGURE 64

6531-134

Particle #	Weight %			
	Al	Ti	Co	Ru
1	44.80	40.41	13.21	1.58
2	54.86	36.10	7.68	1.36
3	48.60	43.96	6.12	1.32
4	52.29	37.75	8.64	1.32
5	41.66	44.02	12.58	1.74
6	64.20	25.59	9.18	1.03
7	55.54	37.08	6.09	1.29
8	46.30	40.97	11.25	1.48
9	59.36	30.11	8.59	1.94
10	41.14	39.19	18.44	1.22
11	51.83	34.56	12.55	1.07
12	46.29	36.72	15.06	1.92
13	47.01	38.74	12.93	1.32
14	46.67	40.36	11.72	1.25
15	45.21	37.03	15.89	1.86
Average	49.72 ± 6.54	37.51 ± 4.82	11.33 ± 3.60	1.45 ± 0.30

FIGURE 65
STANDARD CATALYST PREPARATION

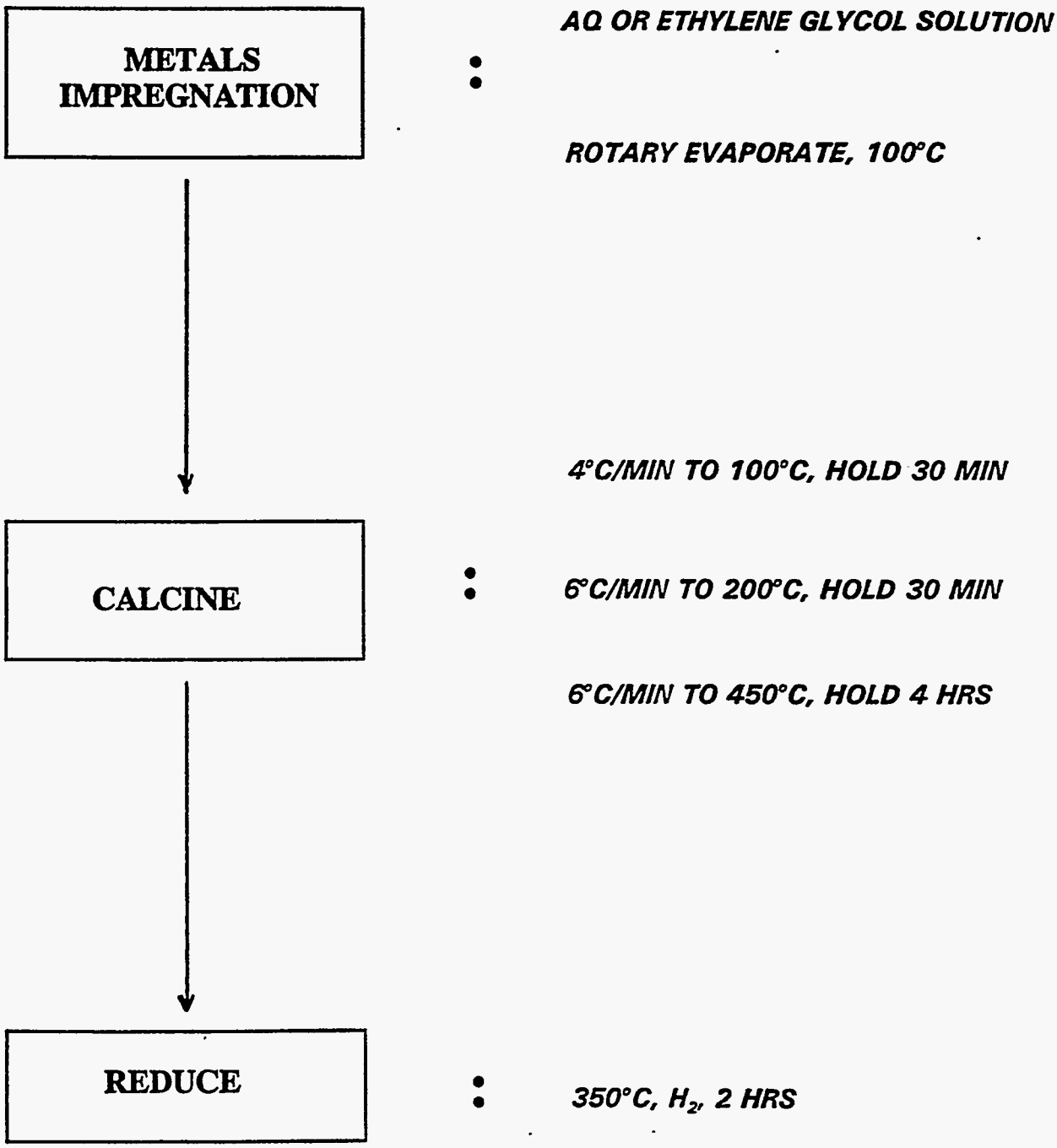

PROPERTIES OF SUPPORTED METAL OXIDES ON STEAMED Y ZEOLITE (CATALYST PRECURSORS PRIOR TO REDUCTION)

ATOMIC ABSORBTION SPECTROSCOPY		
CATALYST SOURCE RUN NO	SUPPORT	AAS, WT %
TARRYTOWN 65[1]	STEAMED, ACID-WASHED Y ZEOL	Co, 8.3; Mn, 1.3; Zr, 1.0
DES PLAINES 81[1]	STEAMED Y ZEOLITE[2]	Co, 8.1; Mn, O.36; Zr, 1.0
DES PLAINES 82[1]	STEAMED Y ZEOLITE[2]	Co, 7.3; Mn, 0.64; Zr, 0.99
DES PLAINES 78[1]	STEAMED Y ZEOLITE[2]	Co, 7.3; Ru, 1.2; Mn, 0.6; Zr, 1.0
DES PLAINES 80[1]	STEAMED Y ZEOLITE[2]	Co, 7.5

1. AQUEOUS IMPREGNATION
2. SA = 591 m^2/g; PV = 51 cc/G

FIGURE 66

PERFORMANCE OF CATALYSTS ON STEAMED Y ZEOLITE HYDROCARBON PRODUCTS

THREE-CONDITION SCREENING TEST SUMMARY			
RUN NO	% CO CONVERSION/HYDROCARBON SELECS; C_1: C_2: $C_2^=$: C_3: $C_3^=$		
	CONDITION 1	2	3
65	58/7: 0.6: 0.00: 1.7: 2		
81	35/18: 3.2: 0.00: 4.0: 3.0	78/17: 2.8: 0.2: 3.5: 2.2	82/18: 3.0: 0.15: 3.7: 2.3
82	40/17: 3.8: 0.00: 6.0: 4.0	75/18: 3.3: 0.2: 5.0: 2.1	85/17: 3.0: 0.15: 5.0: 1.5
78	35/24: 5: 2: 4.8: 1.5	65/30: 2.2: 0.00: 4.9: 1.6	80/27: 2.2: 0.00: 5: 1.3
80	41/18: 1.8: 0.00: 2.8: 1.9	77/18: 1.8: 0.00: 2.9: 1.2	86/17: 2.2: 0.00: 3.0: 1.1

FIGURE 67

PERFORMANCE OF CATALYSTS ON STEAMED Y ZEOLITE ALCOHOL PRODUCTS

THREE-CONDITION SCREENING TEST SUMMARY			
RUN NO	% CO CONV/ALCOHOL SELECS; C_2: C_3: C_4 CONDITION		
	1	2	3
65	58/0.5: 0.2: 0.2		
81	35/0.00: 0.00: 0.00	70:0.2: 0.05: 0.02	82/0.1: 0.02: 0.02
82	40/0.4: 0.1: 0.00	75/0.2: 0.05: 0.03	85/0.10: 0.03: 0.02
78	35/0.4: 0.00: 0.00	65/0.3: 0.06: 0.04	80/0.2: 0.06: 0.06
80	41/0.1: 0.00: 0.00	77/0.1: 0.03: 0.01	86/0.1: 0.02: 0.01

FIGURE 68

CATALYST PRECURSORS: SUPPORTED OXIDES ON STEAMED/ACID-WASHED Y ZEOLITES

SUPPORT PROPERTIES			CATALYST NO./ RUN NO.	CATALYST METALS, AAS WT%		
TRTMNTS	SA[1]/PV[2]	Al[3]		Co	Mn	Zr
STMD	591/0.51	5.24	6531-176/80 6531-167/81 6531-166/82	7.5 8.1 7.3	 0.4 0.6	 1.0 1.0
STMD/ HNO_3[4]	562/0.49	4.83	6531-178/83 6531-180/84	7.7 8.5	 1.7	 1.1
STMD/ HNO_3[5]	586/0.51	3.86	6531-182/85	9.4		
STMD/ HNO_3[6]	596/0.54	2.94	6531-188/86 6531-186/87	9.1 8.9		

1. m^2/g
2. cc/g
3. wt %
4. WASH 36 HOURS WITH 2M HNO_3.
5. WASH 36 HOURS WITH 3M HNO_3.
6. WASH 72 HOURS WITH 3M HNO_3.

FIGURE 69

FIGURE 70

ACTIVITY AND HYDROCARBON SELECTIVITY OF CATALYSTS

Run No.	*Test Conditions*	*CO Conversion, %*	*Hydrocarbon Selectivity, %*				
			C_1	C_2	$C_2^=$	C_3	$C_3^=$
65	*1*	*58*	*7*	*0.6*	*0*	*1.7*	*2.0*
80	*1*	*41*	*18*	*1.8*	*0*	*2.8*	*1.9*
	2	*77*	*18*	*1.8*	*0*	*2.9*	*1.2*
	3	*86*	*17*	*2.2*	*0*	*3.0*	*1.1*
83	*1*	*43*	*18*	*2.5*	*0*	*3.2*	*2.4*
	2	*70*	*20*	*2.5*	*0*	*3.2*	*2.0*
	3	*81*	*20*	*2.5*	*0.1*	*3.2*	*1.7*
81	*1*	*35*	*18*	*3.2*	*0*	*4.0*	*3.0*
	2	*78*	*17*	*2.8*	*0.2*	*3.5*	*2.2*
	3	*82*	*18*	*3.0*	*0.2*	*3.7*	*2.3*
82	*1*	*40*	*17*	*3.8*	*0*	*6.0*	*4.0*
	2	*75*	*18*	*3.3*	*0.2*	*5.0*	*2.1*
	3	*85*	*17*	*3.0*	*0.2*	*5.0*	*1.5*
84	*1*	*32*	*18*	*4.1*	*0*	*5.1*	*4.1*
	2	*72*	*16*	*3.6*	*0.2*	*4.2*	*3.0*
	3	*85*	*17*	*3.3*	*0.2*	*3.8*	*2.7*

FIGURE 70 CONT.

ACTIVITY AND HYDROCARBON SELECTIVITY OF CATALYSTS

Run No.	Test Conditions	CO Conversion, %	Hydrocarbon Selectivity, %				
			C_1	C_2	$C_2^=$	C_3	$C_3^=$
65	1	58	7	0.6	0	1.7	2.0
85	1	51	15	1.6	0	2.1	2.0
	2	83	14	1.6	0	2.1	1.5
	3	95	13	1.7	0	2.4	1.3
86	1	40	15	3.2	0	4.2	5.0
	2	82	15	3.0	0	4.0	3.0
	3	85	16	3.0	0	3.1	3.0
87	1	82	10	1.1	0.1	1.3	2.0
	2	90	13	1.3	0	2.0	1.0
	3	95	12	1.4	0	2.0	1.1

FIGURE 71

ACTIVITY AND ALCOHOL SELECTIVITY OF CATALYSTS

Run No.	*Test Conditions*	*CO Conversion, %*	*Alcohol Selectivity, %*		
			C_2	C_3	C_4
65	*1*	*58*	*0.5*	*0.6*	*2.0*
80	*1*	*41*	*0.1*	*0*	*0*
	2	*77*	*0.1*	*0.03*	*0.01*
	3	*86*	*0.1*	*0.02*	*0.01*
83	*1*	*43*	*0.3*	*0*	*0*
	2	*70*	*0.2*	*0.03*	*0.01*
	3	*81*	*0.2*	*0.03*	*0.01*
81	*1*	*35*	*0*	*0*	*0*
	2	*70*	*0.2*	*0.05*	*0.02*
	3	*82*	*0.1*	*0.02*	*0.02*
82	*1*	*40*	*0.4*	*0.1*	*0*
	2	*75*	*0.2*	*0.05*	*0.03*
	3	*85*	*0.1*	*0.03*	*0.02*
84	*1*	*32*	*0.4*	*0.1*	*0.08*
	2	*72*	*0.3*	*0.1*	*0.05*
	3	*85*	*0.2*	*0.08*	*0.03*

FIGURE 71 CONT.

ACTIVITY AND ALCOHOL SELECTIVITY OF CATALYSTS

Run No.	*Test Conditions*	*CO Conversion, %*	*Alcohol Selectivity, %*		
			C_2	C_3	C_4
65	*1*	*58*	*0.5*	*0.6*	*2.0*
85	*1*	*51*	*0.3*	*0.2*	*0.1*
	2	*83*	*0.1*	*0.05*	*0.05*
	3	*95*	*0.1*	*0.05*	*0.05*
86	*1*	*40*	*0.5*	*0.2*	*0.15*
	2	*82*	*0.4*	*0.2*	*0.1*
	3	*85*	*0.2*	*0.1*	*0.05*
87	*1*	*82*	*0.2*	*0.05*	*0.03*
	2	*90*	*0.4*	*0.1*	*0.03*
	3	*95*	*0.2*	*0.03*	*0*

STEAMED VS STEAMED + ACID-WASHED Y
COMPARISON OF POROSITY
ADSORPTION OF NITROGEN

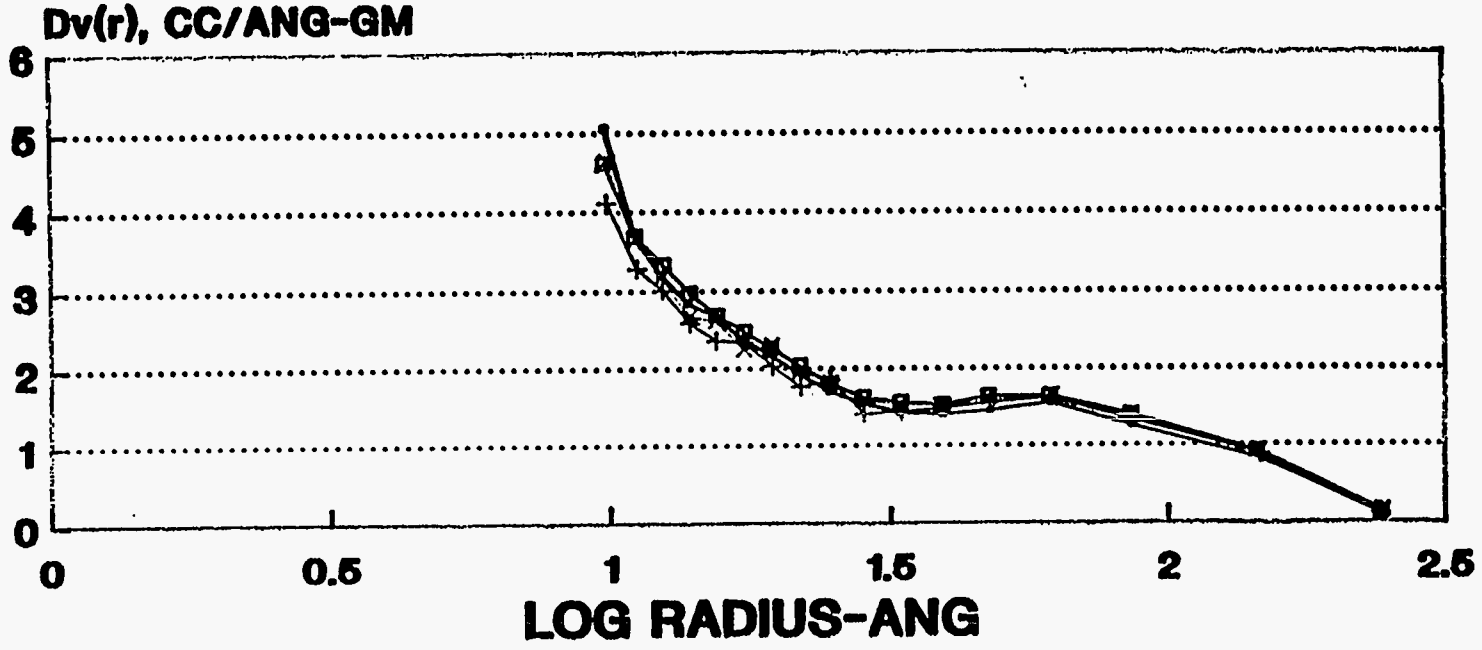

(1) 36 HR WASH
(2) 72 HR WASH

FIGURE 72

FIGURE 73

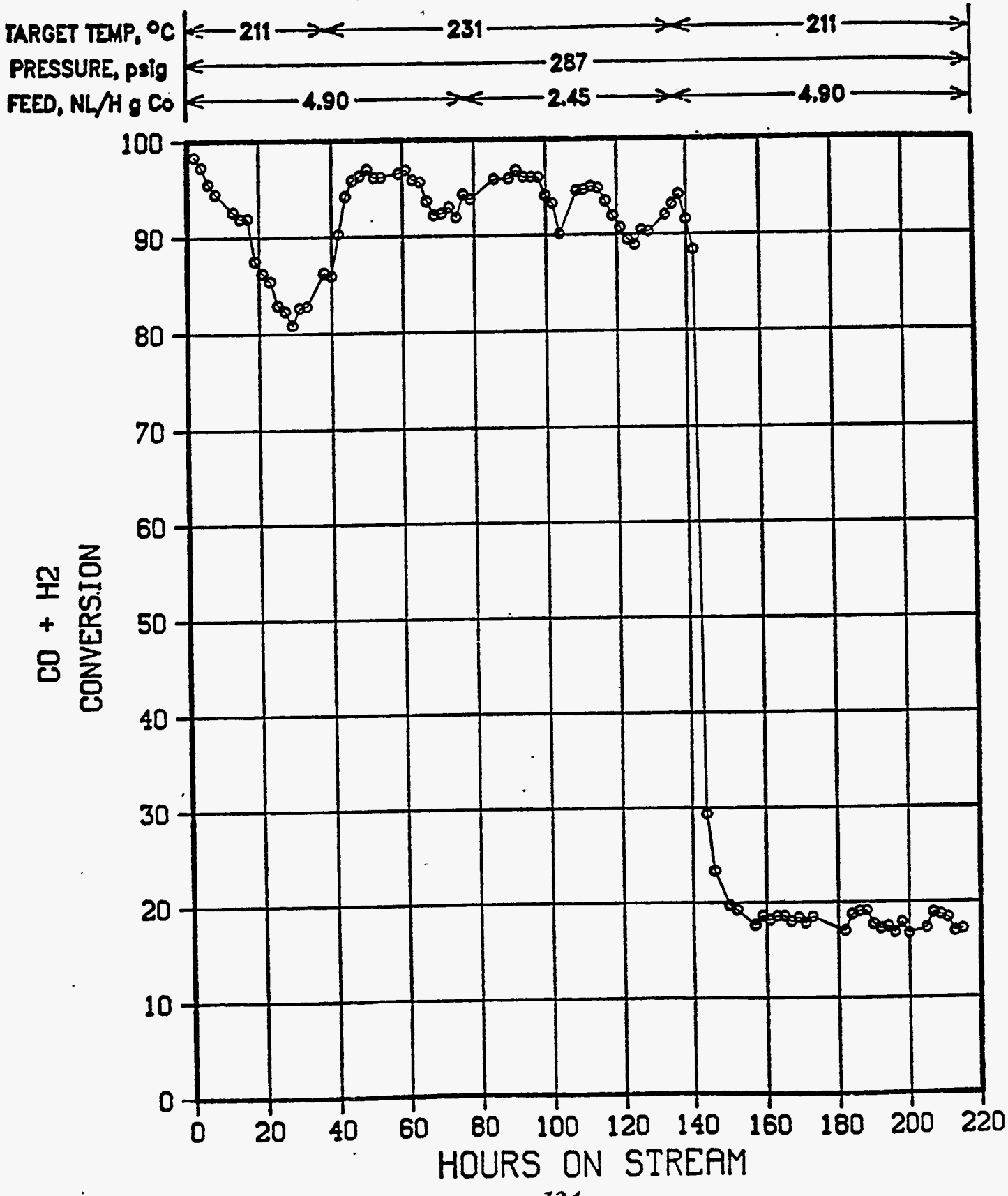
PLT 700A RUN 87 Co on steamed, 72hr acid washed Y-Zeolite
6531-186 w/8.91% Co via aq. impreg 2:1 H_2:CO in feed
13g active in 160g quartz sand
TARGET TEMP, °C
211
231
211
PRESSURE, psig
287
FEED, NL/H g Co
4.90
2.45
4.90
CO + H2 CONVERSION
100
90
80
70
60
50
40
30
20
10
0
0
20
40
60
80
100
120
140
160
180
200
220
HOURS ON STREAM

FIGURE 74

PLT 700A RUN 87 Co on steamed, 72hr acid washed Y-Zeolite

6531-186 w/8.91% Co via aq. impreg 2:1 H_2:CO in feed

13g active in 160g quartz sand

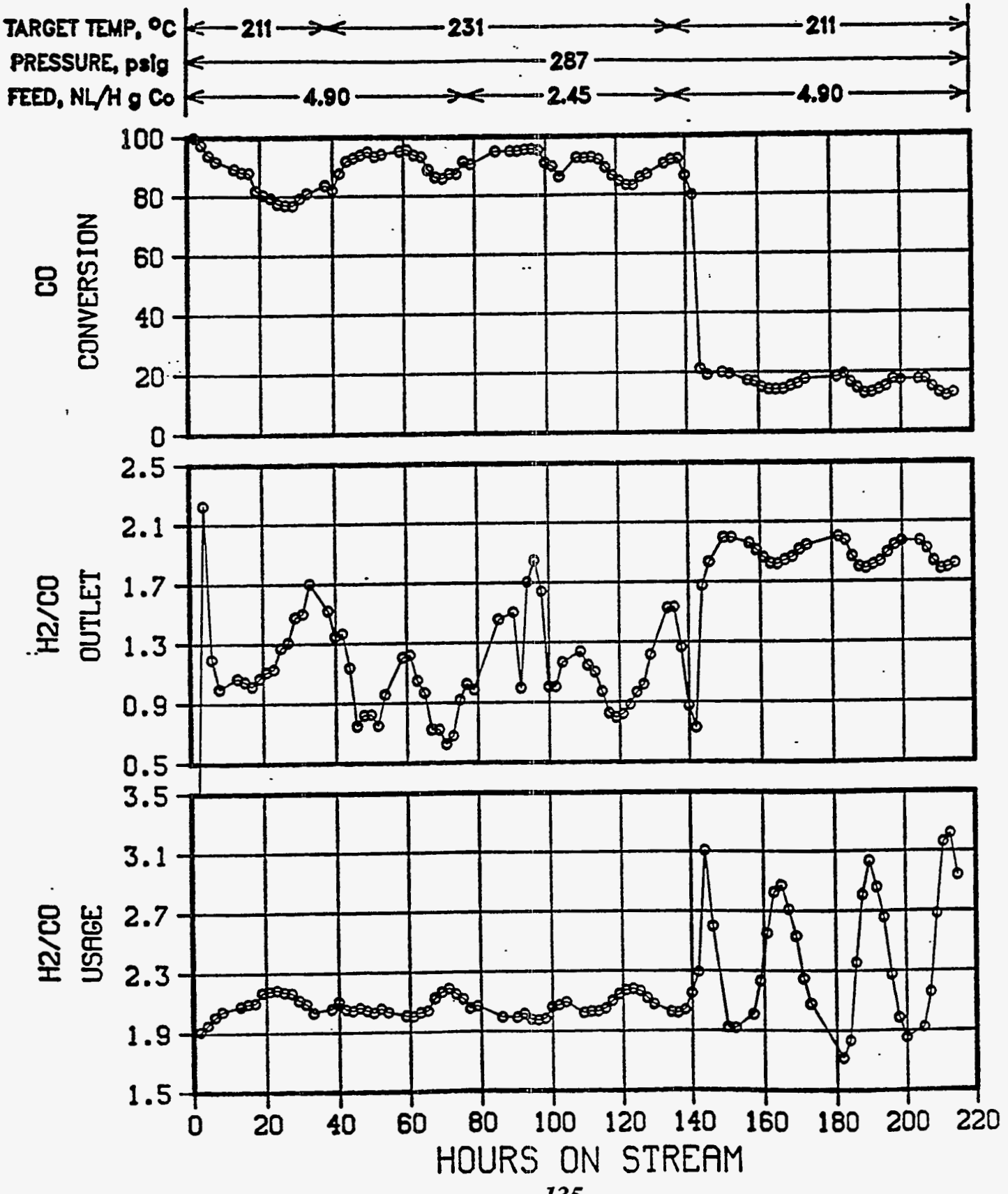

FIGURE 75

PLT 700A RUN 87 Co on steamed, 72hr acid washed Y-Zeolite

6531-186 w/8.91% Co via aq. Impreg 2:1 H_2:CO in feed

13g active in 160g quartz sand

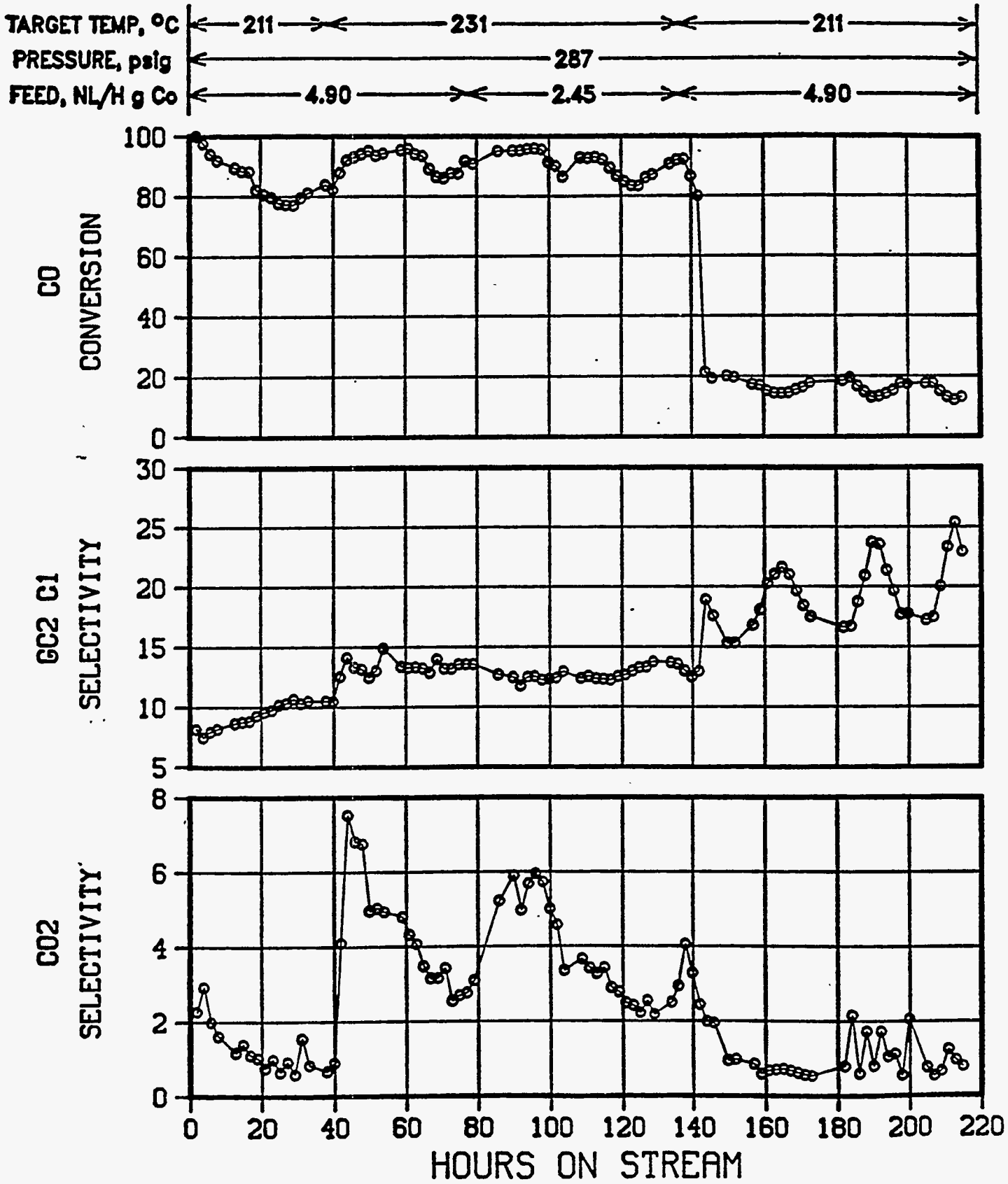

FIGURE 76

PLT 700A RUN 87 Co on steamed, 72hr acid washed Y-Zeolite

6531-186 w/8.91% Co via aq. Impreg 2:1 H_2:CO in feed

13g active in 160g quartz sand

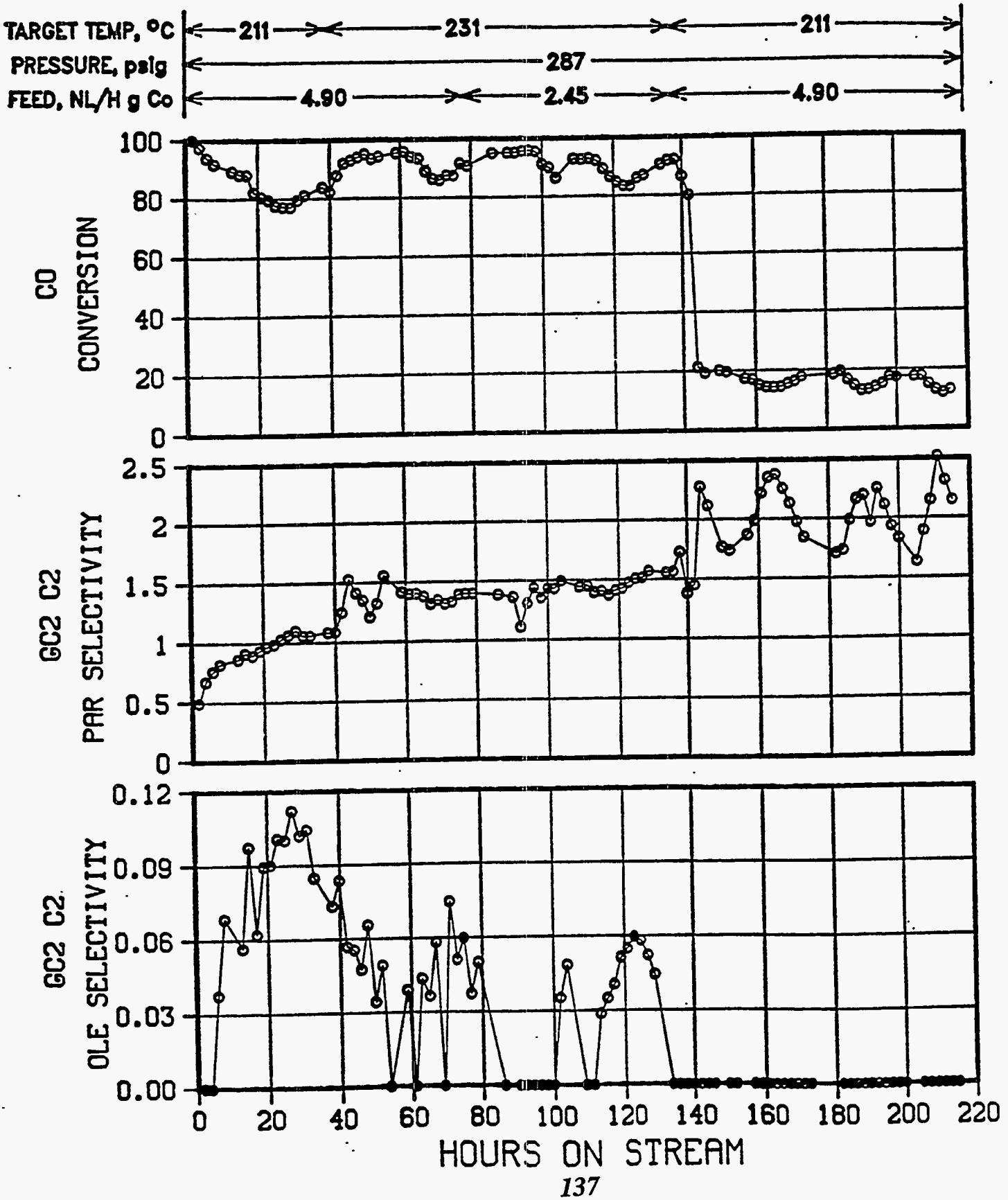

FIGURE 77

PLT 700A RUN 87 · Co on steamed, 72hr acid washed Y–Zeolite

6531–186 w/8.91% Co via aq. impreg 2:1 H_2:CO in feed

13g active in 160g quartz sand

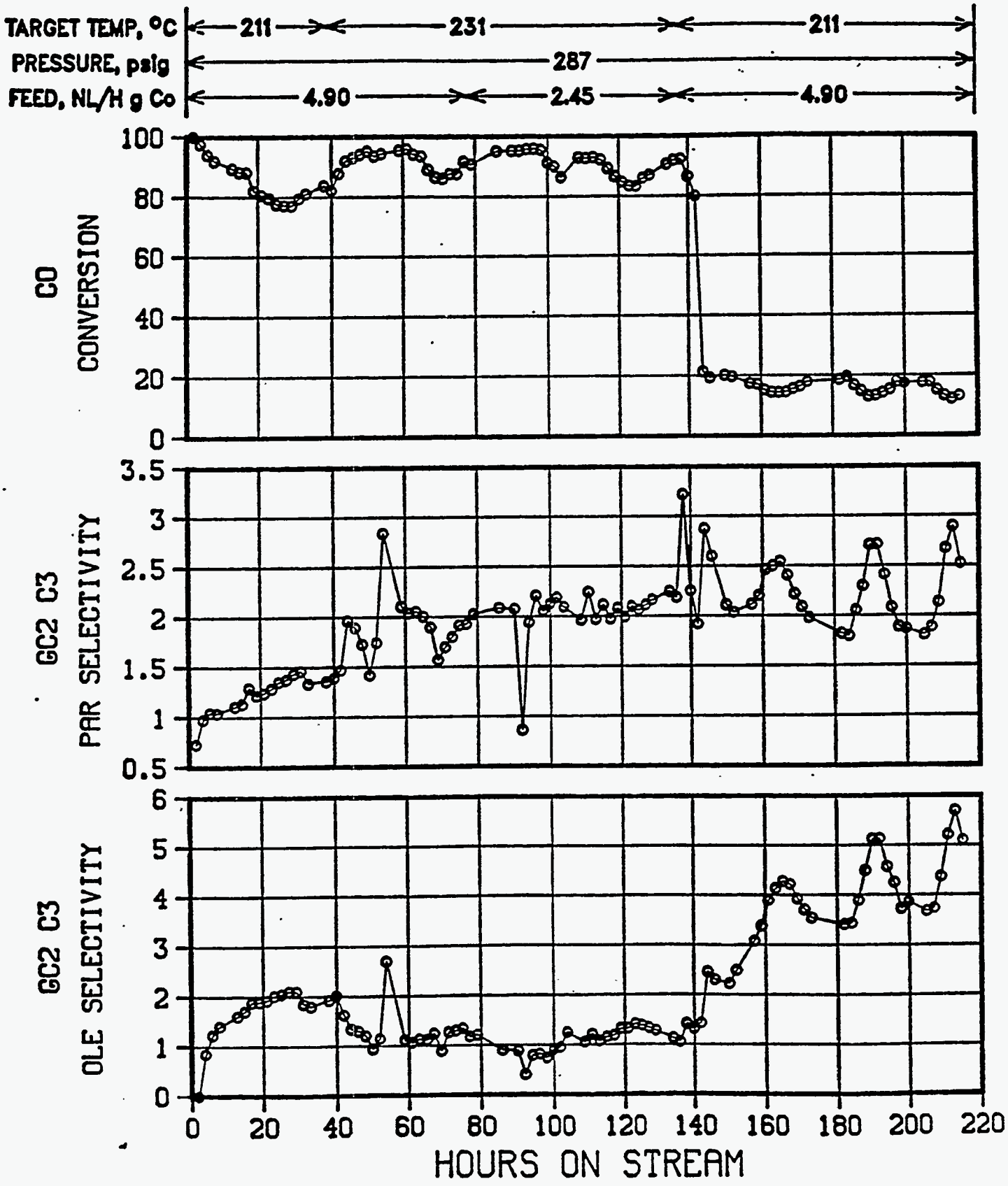

FIGURE 78

PLT 700A RUN 87 Co on steamed, 72hr acid washed Y-Zeolite

6531-186 w/8.91% Co via aq. impreg 2:1 H_2:CO in feed

13g active in 160g quartz sand

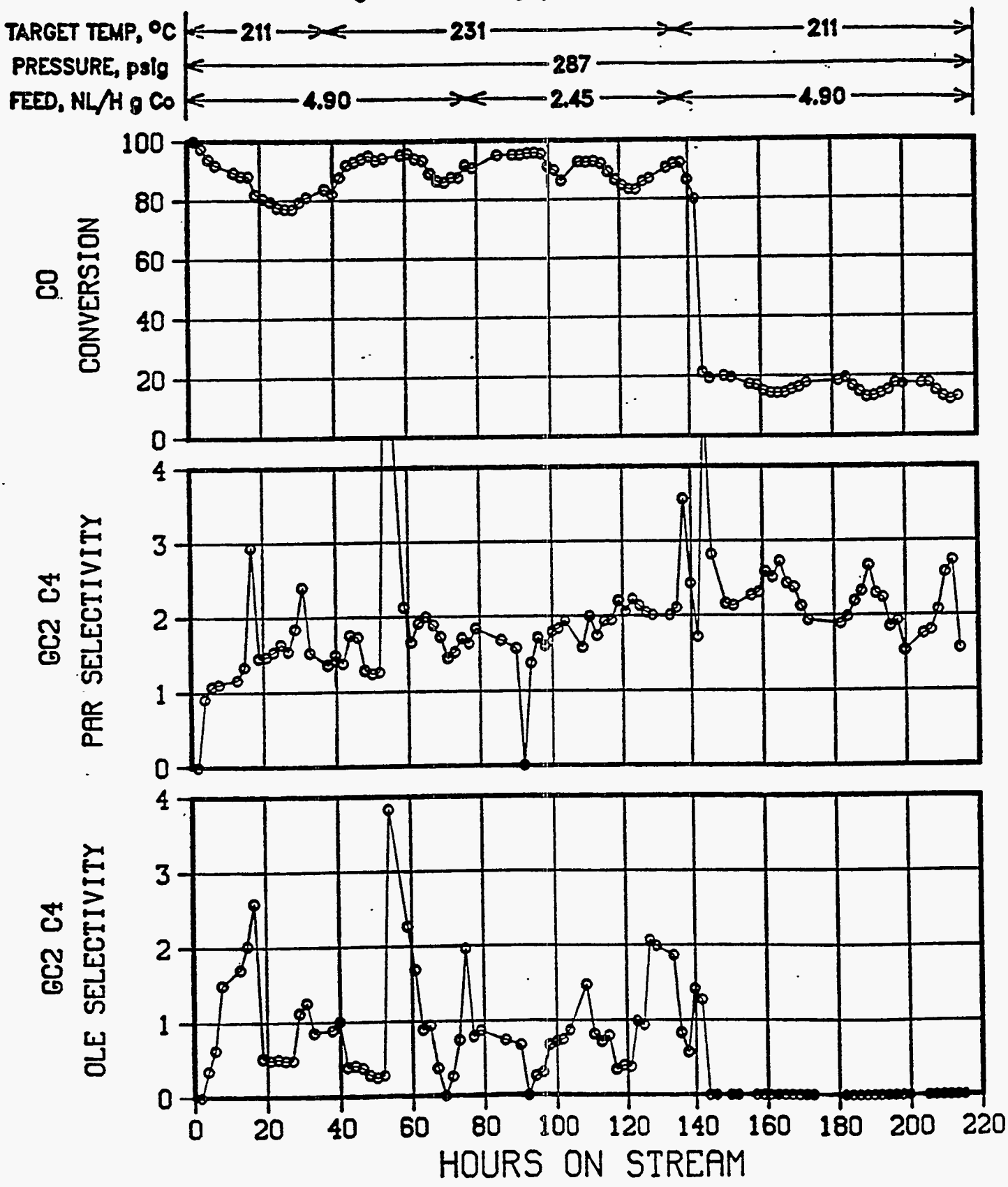

CATALYST PRECURSORS: SUPPORTED OXIDES ON STEAMED/ACID-WASHED Y ZEOLITES

SUPPORT PROPERTIES			CATALYST NO./ RUN NO.	CATALYST METALS, AAS WT%		
TRTMNTS	SA[1]/PV[2]	Al[3]		Co	Mn	Zr
STMD	591/0.51	5.24	6531-176/80	7.5		
	591/0.51	5.24	6531-167/81	8.1	0.4	1.0
	591/0.51	5.24	6531-166/82	7.3	0.6	1.0
STMD/ HNO_3[4]	562/0.49	4.83	6531-178/83	7.7		
	562/0.49	4.83	6531-180/84	8.5	1.7	1.1
STMD/ HNO_3[5]	586/0.51	3.86	6531-182/85	9.4		
STMD/ HNO_3[6]	596/0.54	2.94	6531-188/86	9.1		
	596/0.54	2.94	6531-186/87	8.9		
	574/0.51	4.01	6827-79/95[7]	9.4	1.9	0.47

1. m^2/g
2. cc/g
3. wt %
4. WASH 36 HOURS WITH 2M HNO_3.
5. WASH 36 HOURS WITH 3M HNO_3.
6. WASH 72 HOURS WITH 3M HNO_3.
7. THIS CATALYST ALSO CONTAINED 0.43 wt% RHENIUM.

FIGURE 79

FIGURE 80

PLT 700A RUN 95 Co,Mn,Zr,Re ON HCl Washed Y

6827–79 w/9.4% Co via eth–glycol pore fill

13g unreduced active in 160g quartz sand

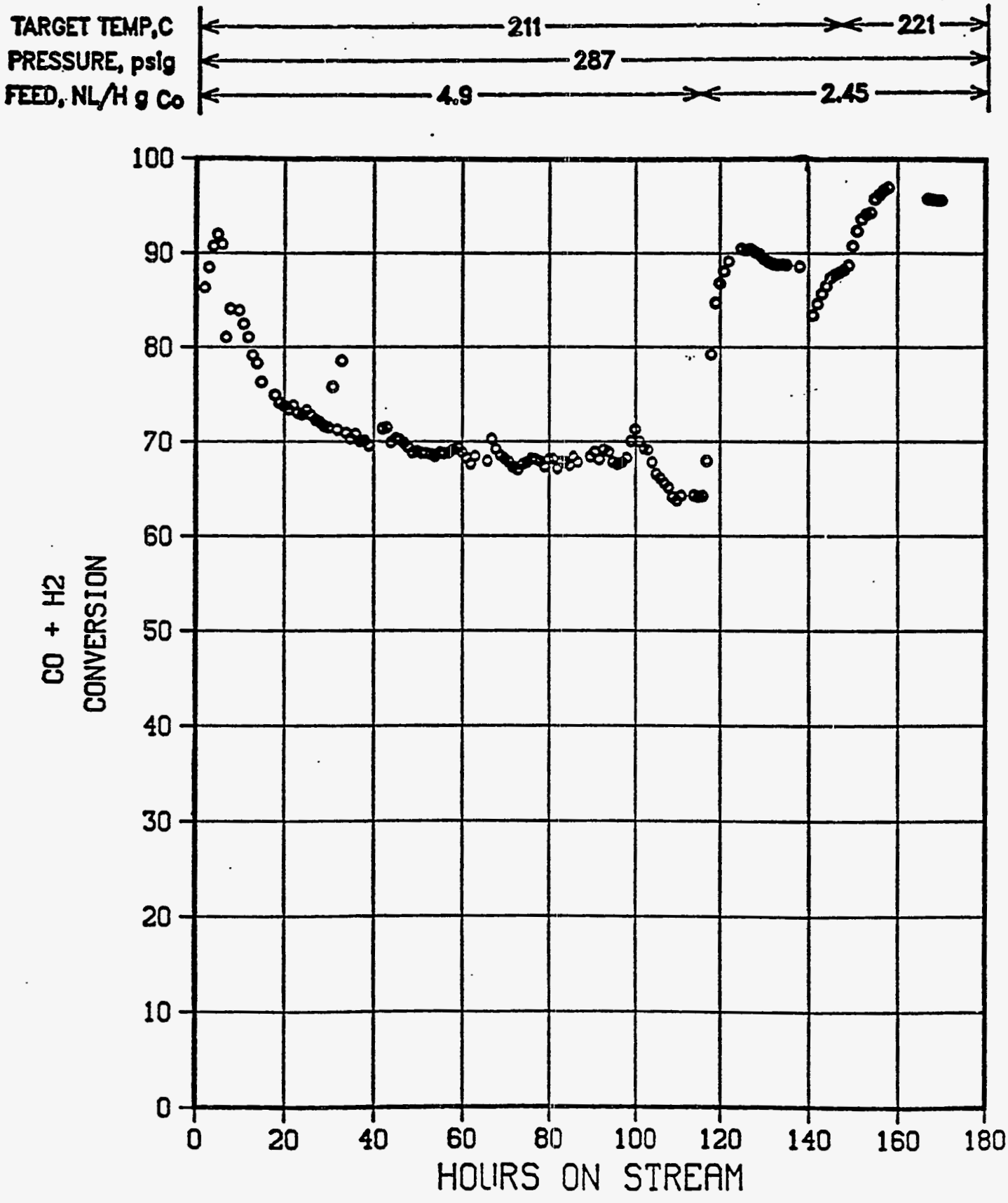

FIGURE 81

PLT 700A RUN 95 Co,Mn,Zr,Re ON HCl Washed Y

6827–79 w/9.4% Co via eth–glycol pore fill

13g unreduced active in 160g quartz sand

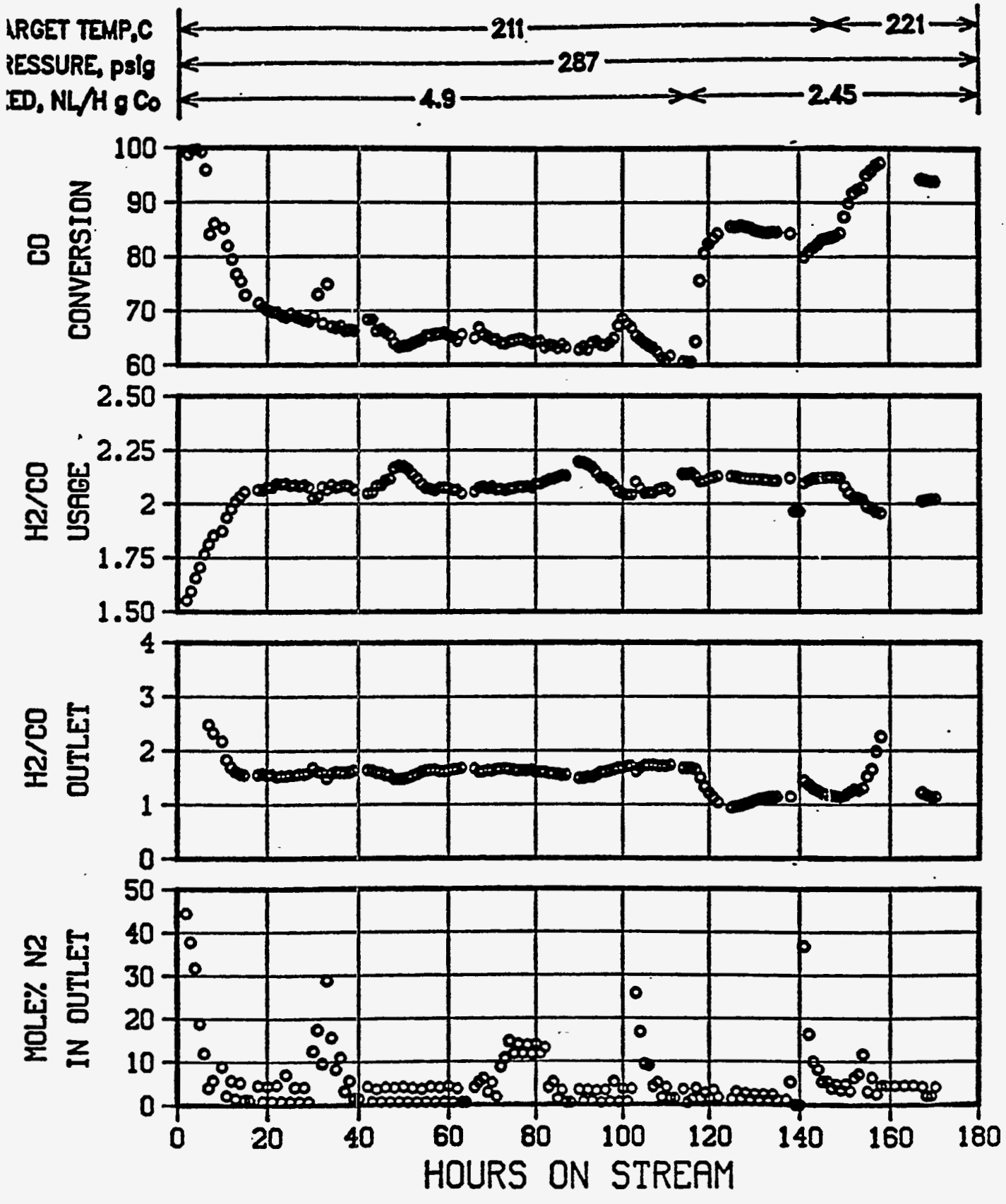

FIGURE 82

PLT 700A RUN 95 Co,Mn,Zr,Re ON HCl Washed Y
6827–79 w/9.4% Co via eth–glycol pore fill
13g unreduced active in 160g quartz sand

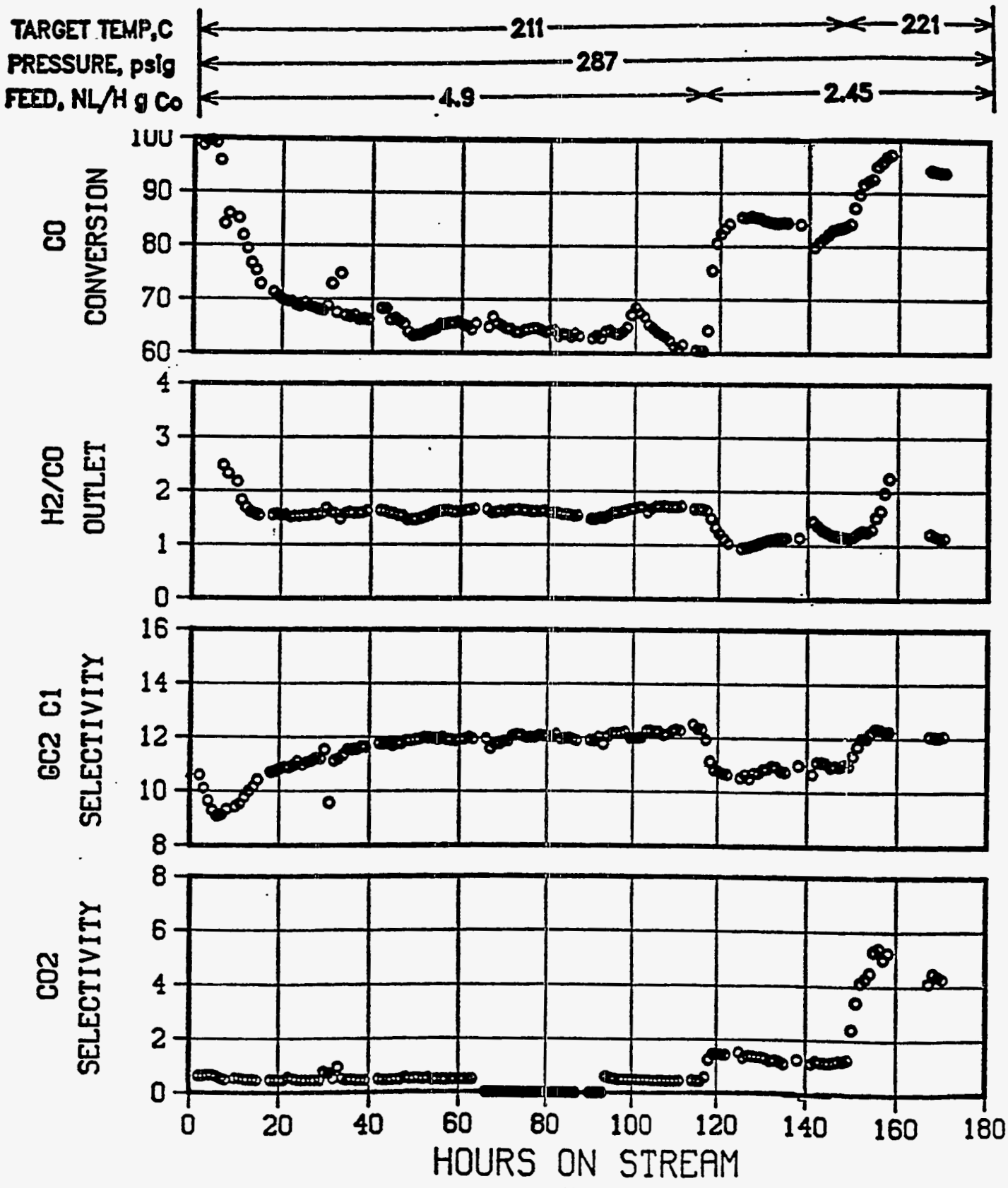

FIGURE 83

PLT 700A RUN 95 Co,Mn,Zr,Re ON HCl Washed Y

6827–79 w/9.4% Co via eth–glycol pore fill

13g unreduced active in 160g quartz sand

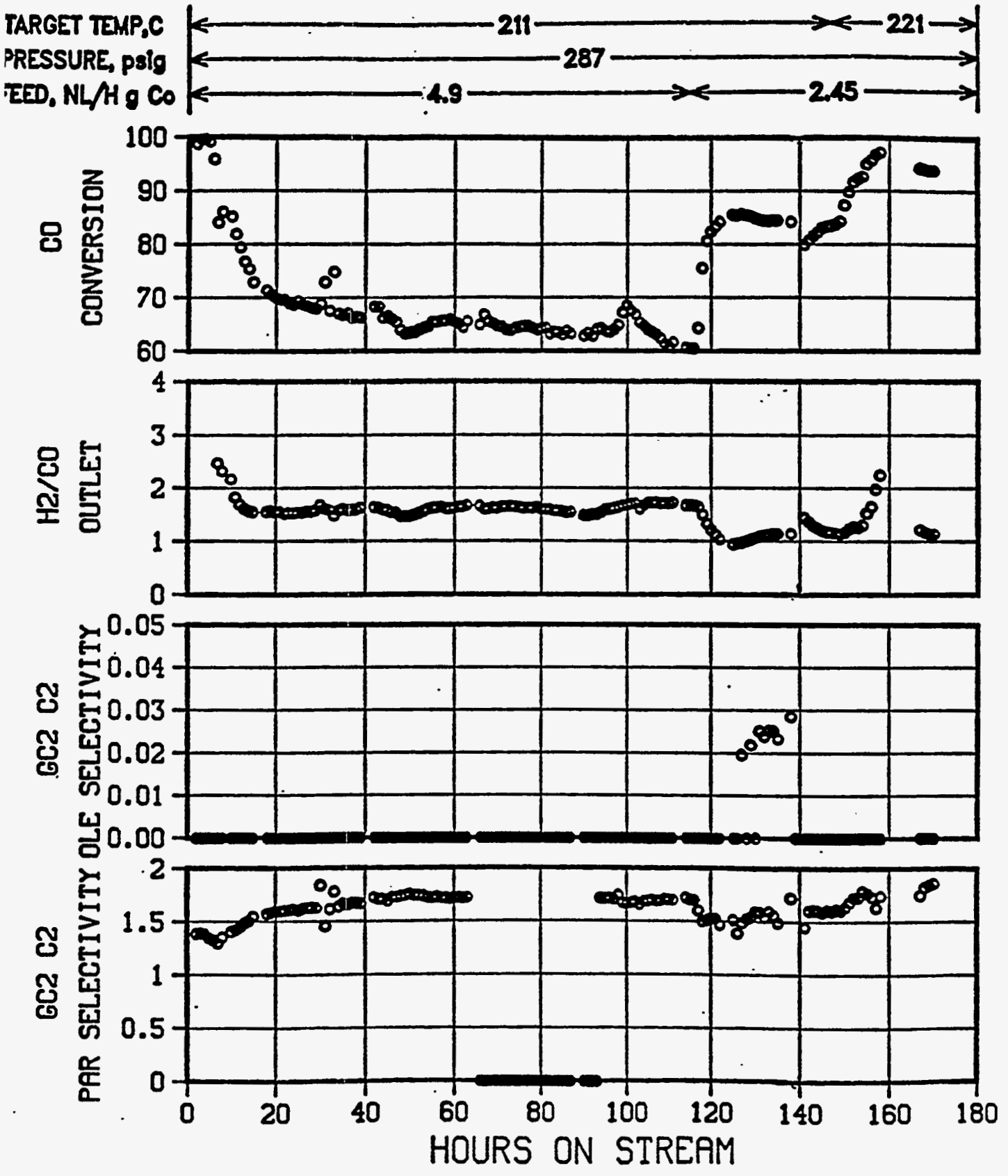

FIGURE 84

PLT 700A RUN 95 Co,Mn,Zr,Re ON HCl Washed Y

6827-79 w/9.4% Co via eth-glycol pore fill

13g unreduced active in 160g quartz sand

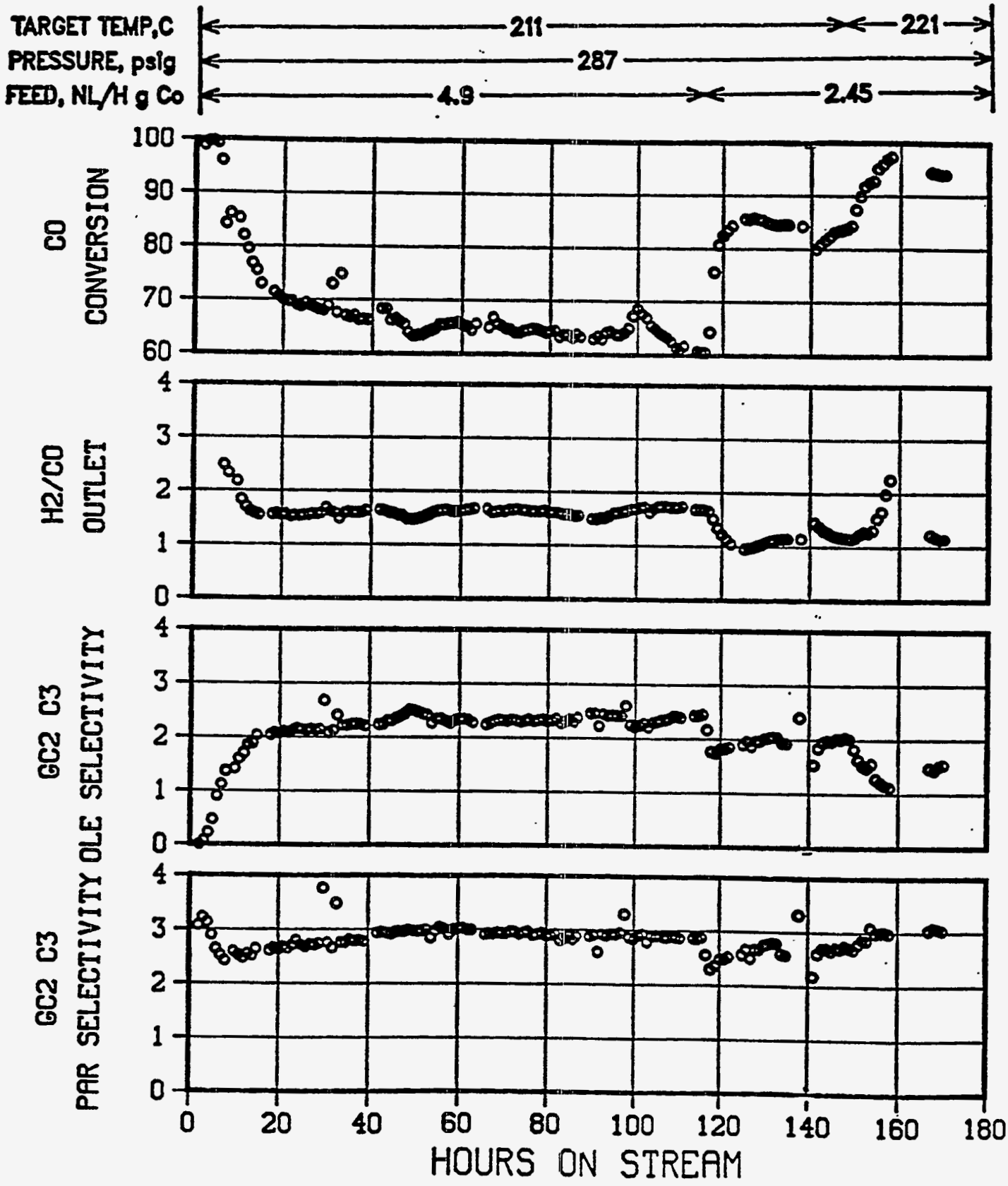

FIGURE 85

PLT 700A RUN 95 Co,Mn,Zr,Re ON HCl Washed Y

6827–79 w/9.4% Co via eth–glycol pore fill

13g unreduced active in 160g quartz sand

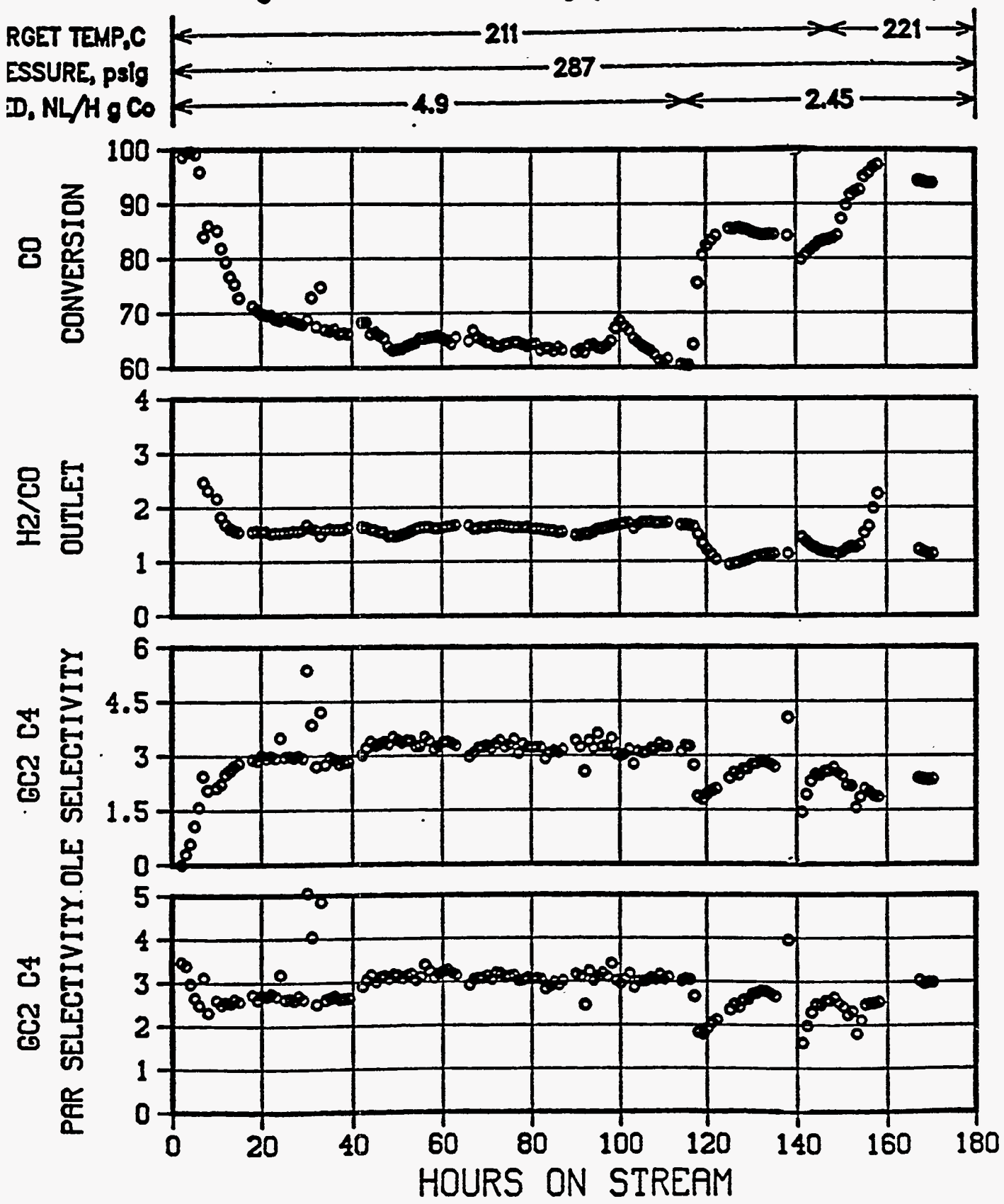

CATALYST PRECURSORS: SUPPORTED OXIDES ON STEAMED/ACID-WASHED Y ZEOLITES

SUPPORT PROPERTIES				CATALYST NO./ RUN NO.	CATALYST METALS, AAS WT%			
TRTMNTS	X-RAY[1]	SA[2]/PV[3]	Al[4]		Co	Mn	Zr	Ru
STMD	86.3 ± 0.3	591/0.51	5.24	6531-176/80	7.5			
		591/0.51	5.24	6531-167/81	8.1	0.4	1.0	
		591/0.51	5.24	6531-166/82	7.3	0.6	1.0	
STMD/ HNO_3[5]		596/0.54	2.94	6531-188/86	9.1			
		596/0.54	2.94	6531-186/87	8.9			
	86.6 ± 0.3	574/0.51	4.01	6827-79/95[6]	9.4	1.9	0.47	
STMD/ HCl[7]	84.2 ± 0.3	582/0.56	0.46	6827-81/97	17.6	2.0	1.6	1.0
	84.5 ± 0.3	574/0.54	0.48	6827-95/101	27.4	1.1	1.6	0.3
		561/0.54	0.37	6827-123/110	26.8	2.3	1.0	0.4
	84.5 ± 0.3	574/0.54	0.48	6827-99/102, 104	18.5	2.2	2.0	1.3

1. ABSOLUTE INTENSITY VS. LZ 210 (UNSTEAMED Y ZEOLITE) WHICH = 99.7 ± 1.7.
2. m^2/g
3. cc/g
4. wt %
5. WASH 72 HOURS WITH 3M HNO_3.
6. THIS CATALYST ALSO CONTAINED 0.43 wt% RHENIUM.
7. WASH 3 HOURS WITH 4M HCl.

FIGURE 86

FIGURE 87

PLT 700A RUN 97 Co,Mn,Zr,Ru on HCl washed Y

6827–81 w/17.6 % Co via eth–glycol pore fill

13g unreduced active in 160g quartz sand

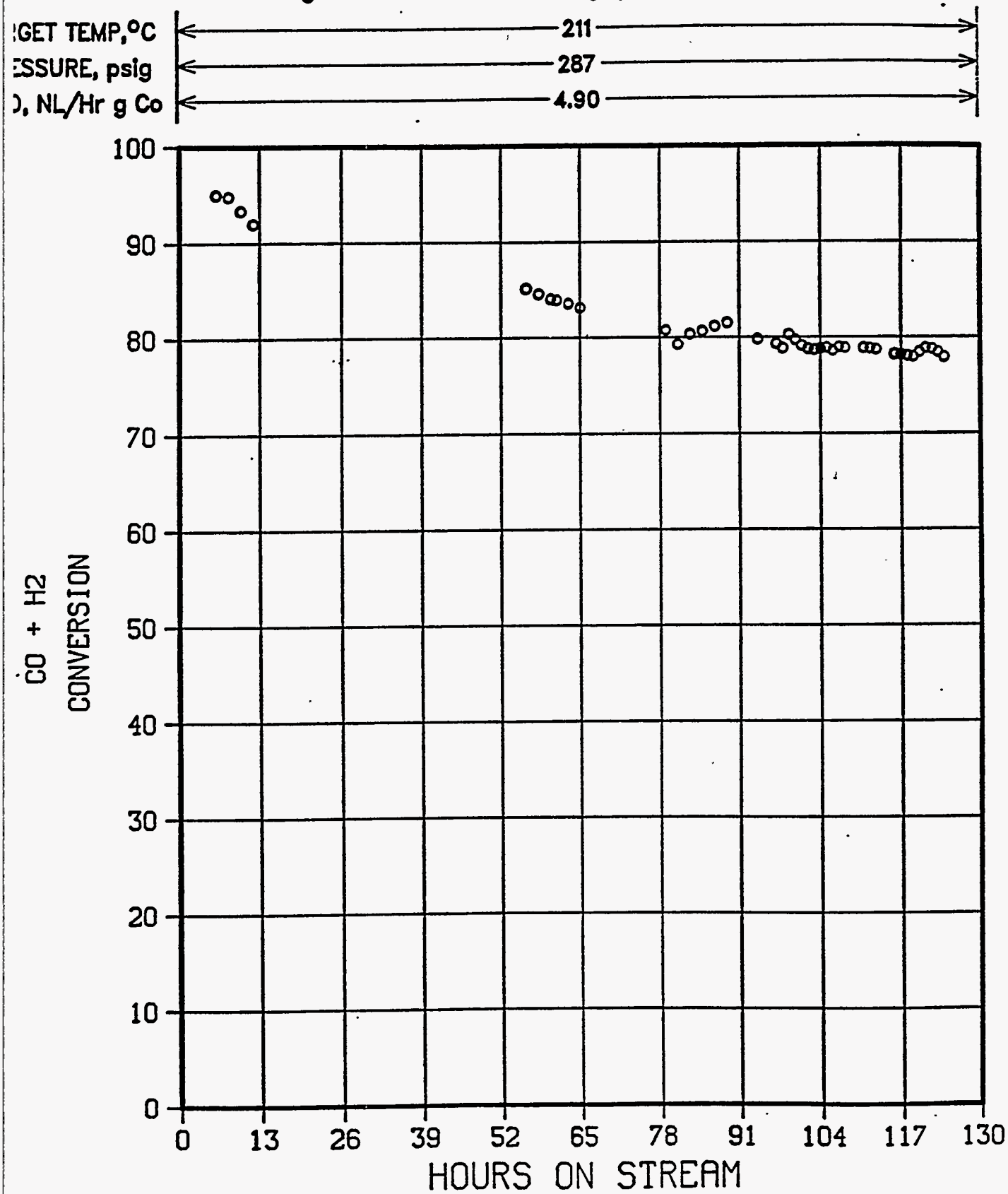

FIGURE 88

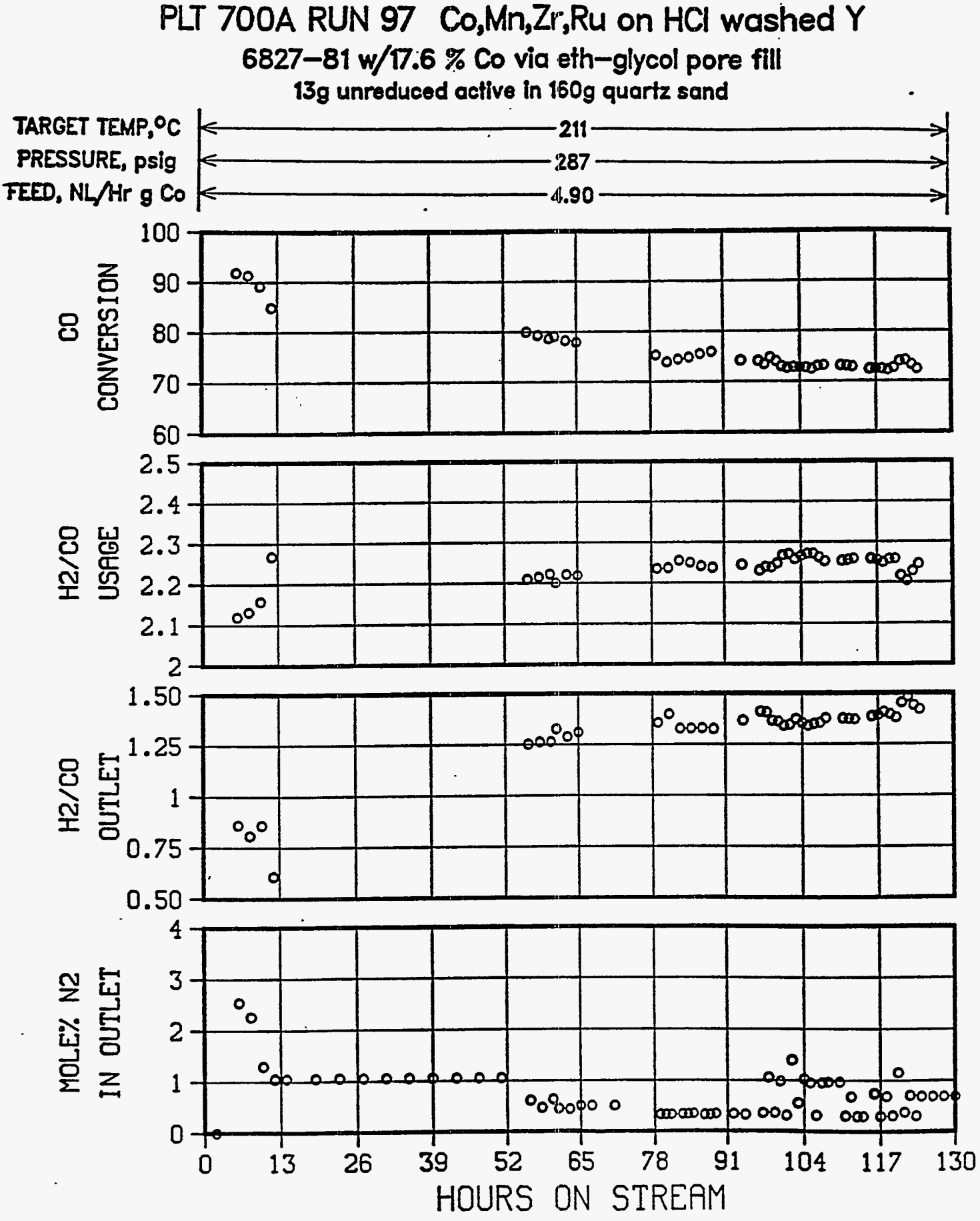
PLT 700A RUN 97 Co,Mn,Zr,Ru on HCl washed Y
6827–81 w/17.6 % Co via eth–glycol pore fill
13g unreduced active in 160g quartz sand
TARGET TEMP,°C
211
PRESSURE, psig
287
FEED, NL/Hr g Co
4.90
CO CONVERSION
100
90
80
70
60
H2/CO USAGE
2.5
2.4
2.3
2.2
2.1
2
H2/CO OUTLET
1.50
1.25
1
0.75
0.50
MOLE% N2 IN OUTLET
4
3
2
1
0
0
13
26
39
52
65
78
91
104
117
130
HOURS ON STREAM

FIGURE 89

PLT 700A RUN 97 Co,Mn,Zr,Ru on HCl washed Y

6827–81 w/17.6 % Co via eth–glycol pore fill

13g unreduced active in 160g quartz sand

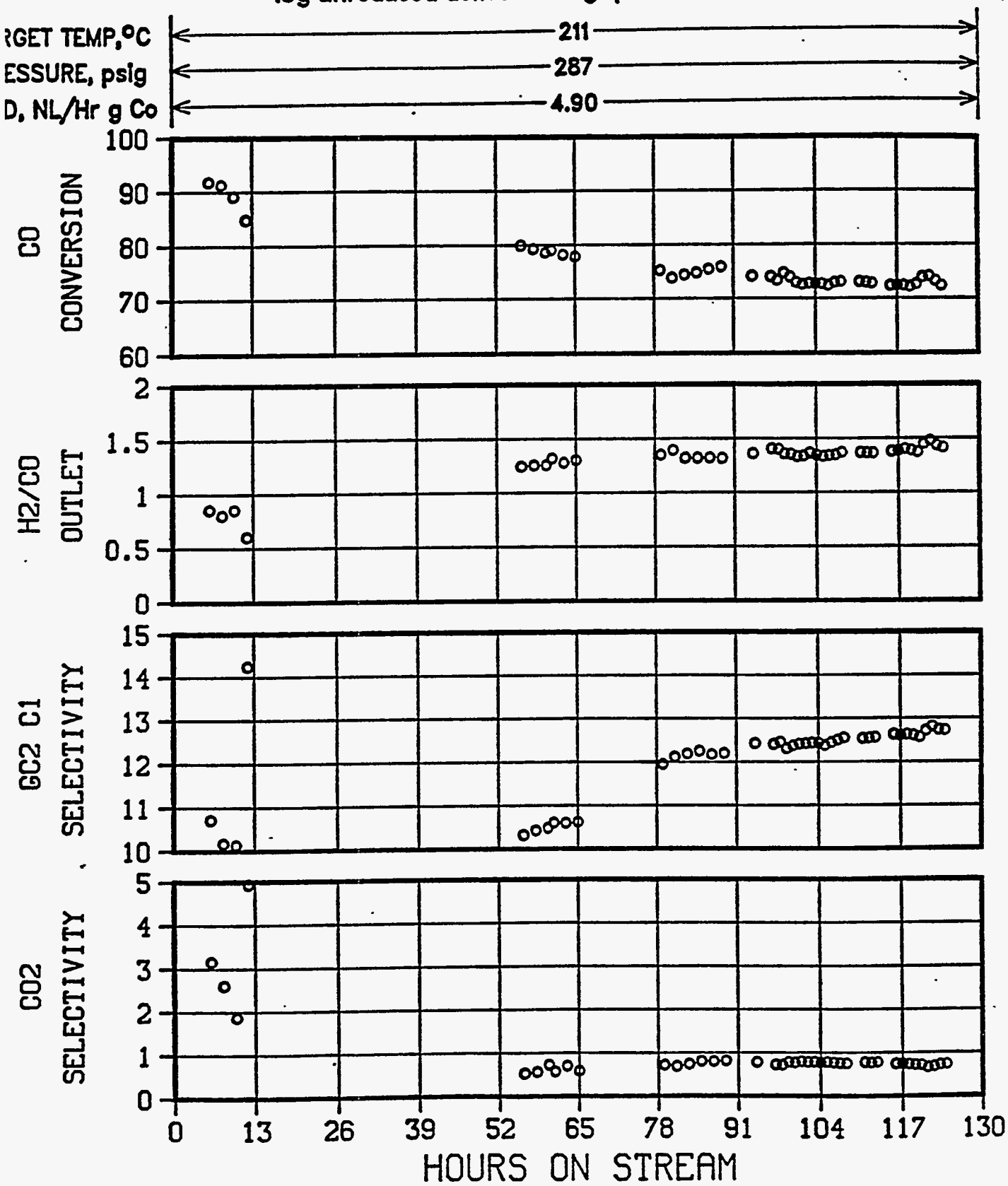

FIGURE 90

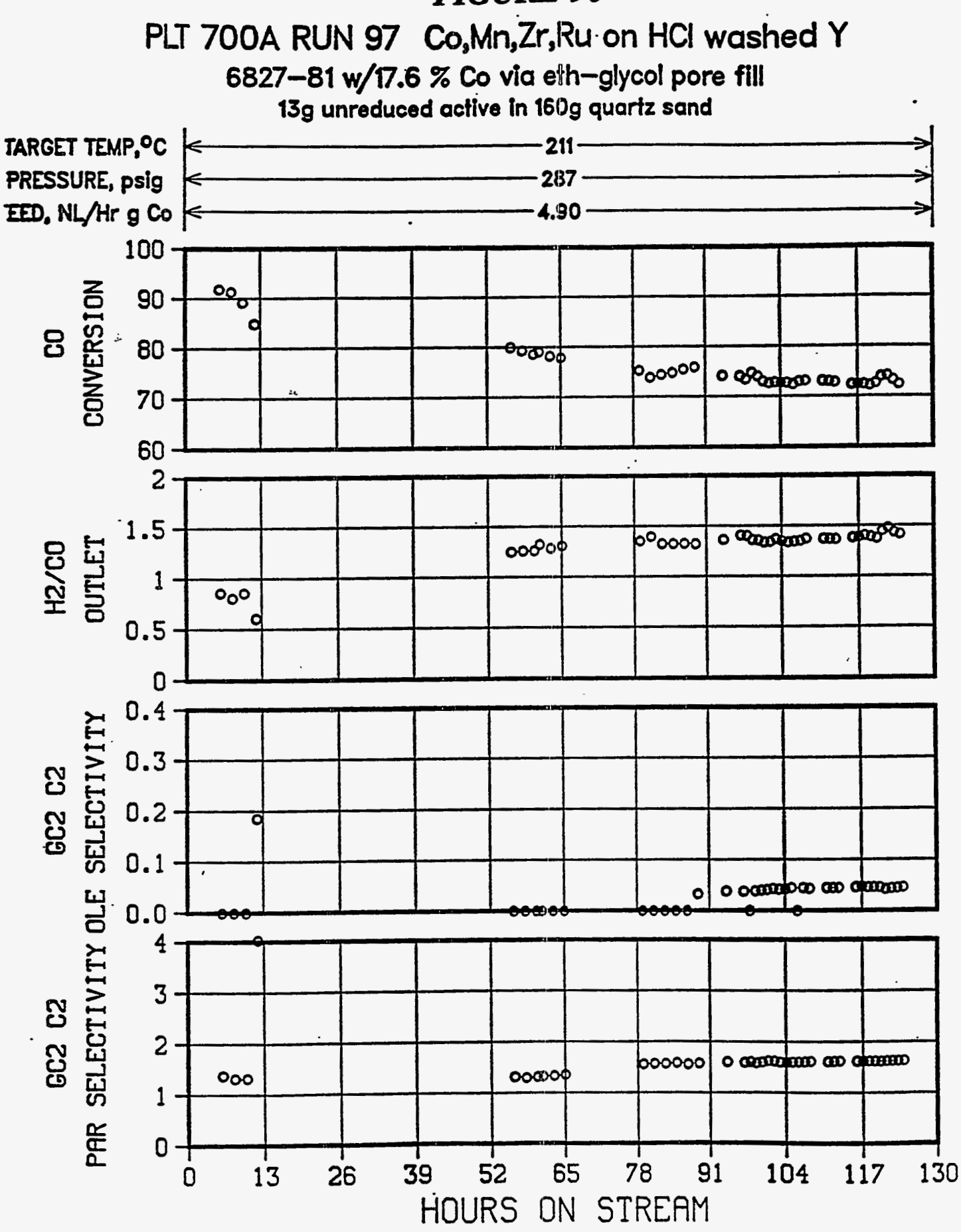
PLT 700A RUN 97 Co,Mn,Zr,Ru on HCl washed Y
6827–81 w/17.6 % Co via eth–glycol pore fill
13g unreduced active in 160g quartz sand
TARGET TEMP,°C
PRESSURE, psig
EED, NL/Hr g Co
211
287
4.90
CO CONVERSION
H2/CO OUTLET
GC2 C2 PAR SELECTIVITY OLE SELECTIVITY
GC2 C2
HOURS ON STREAM

FIGURE 91

PLT 700A RUN 97 Co,Mn,Zr,Ru on HCl washed Y

6827–81 w/17.6 % Co via eth–glycol pore fill

13g unreduced active in 160g quartz sand

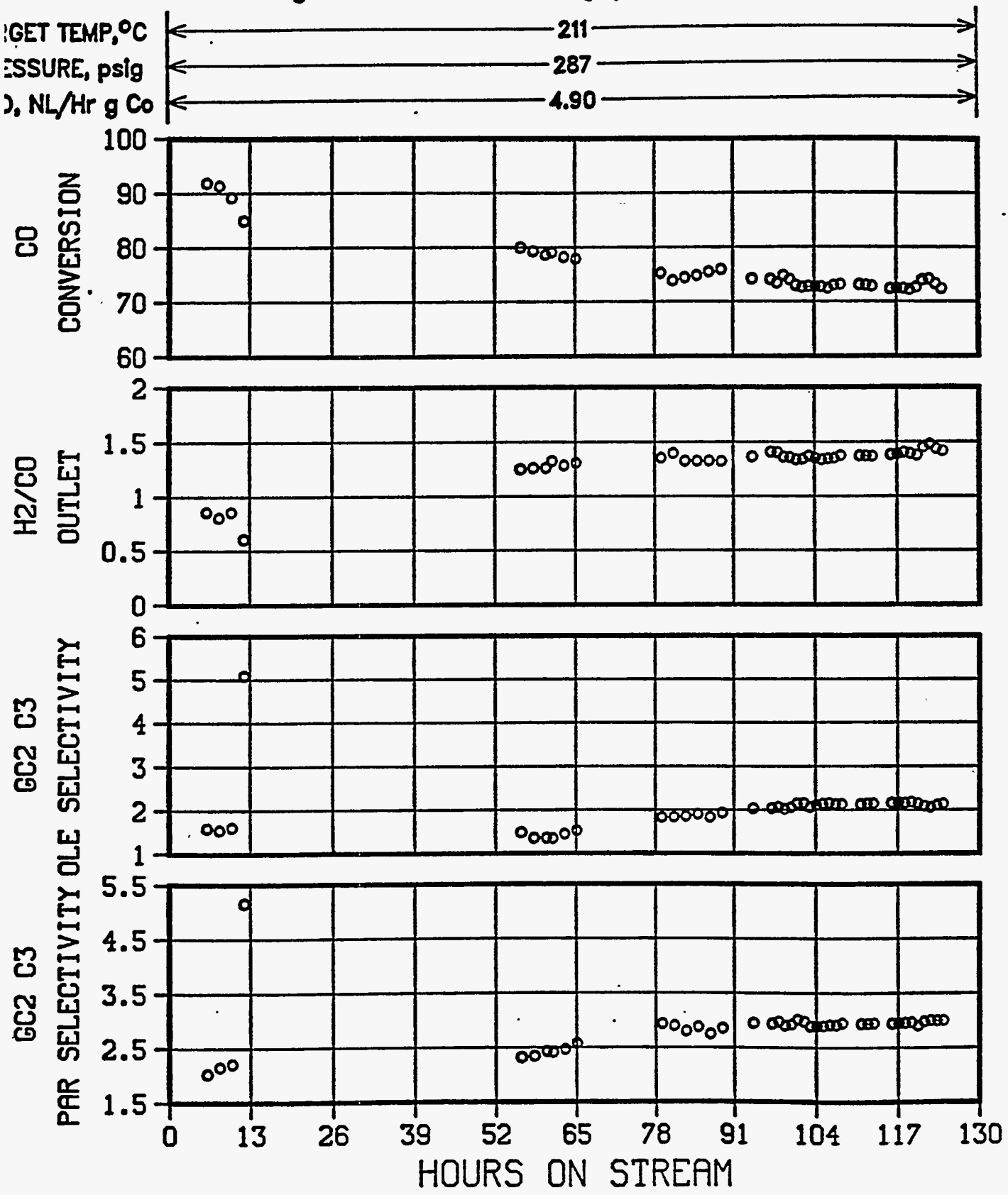

FIGURE 92

PLT 700A RUN 97 Co,Mn,Zr,Ru on HCl washed Y

6827–81 w/17.6 % Co via eth–glycol pore fill

13g unreduced active in 160g quartz sand

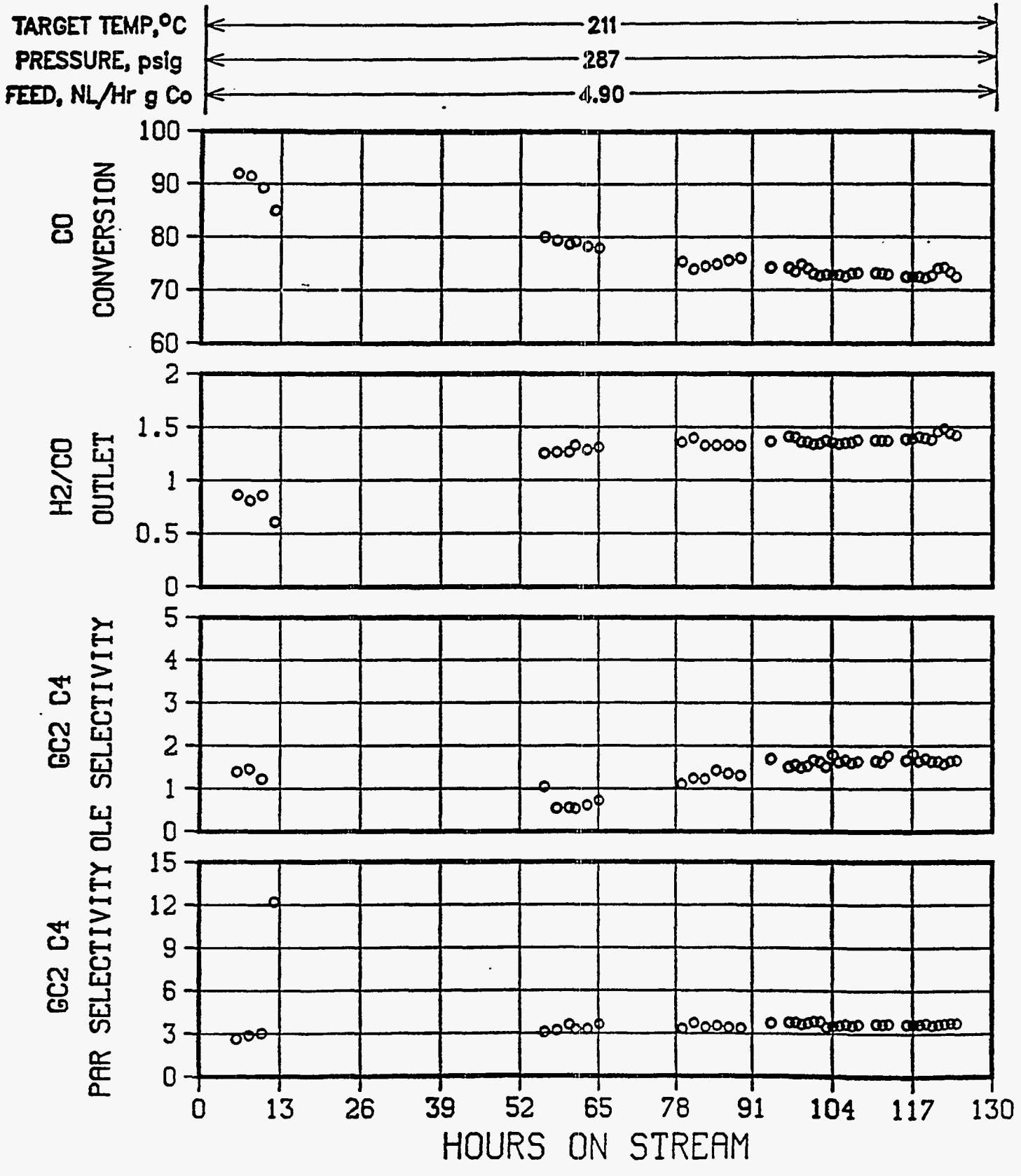

FIGURE 93

PLT 700A RUN 97 Co,Mn,Zr,Ru on HCl washed Y

6827–81 w/17.6 % Co via eth–glycol pore fill

13g unreduced active in 160g quartz sand

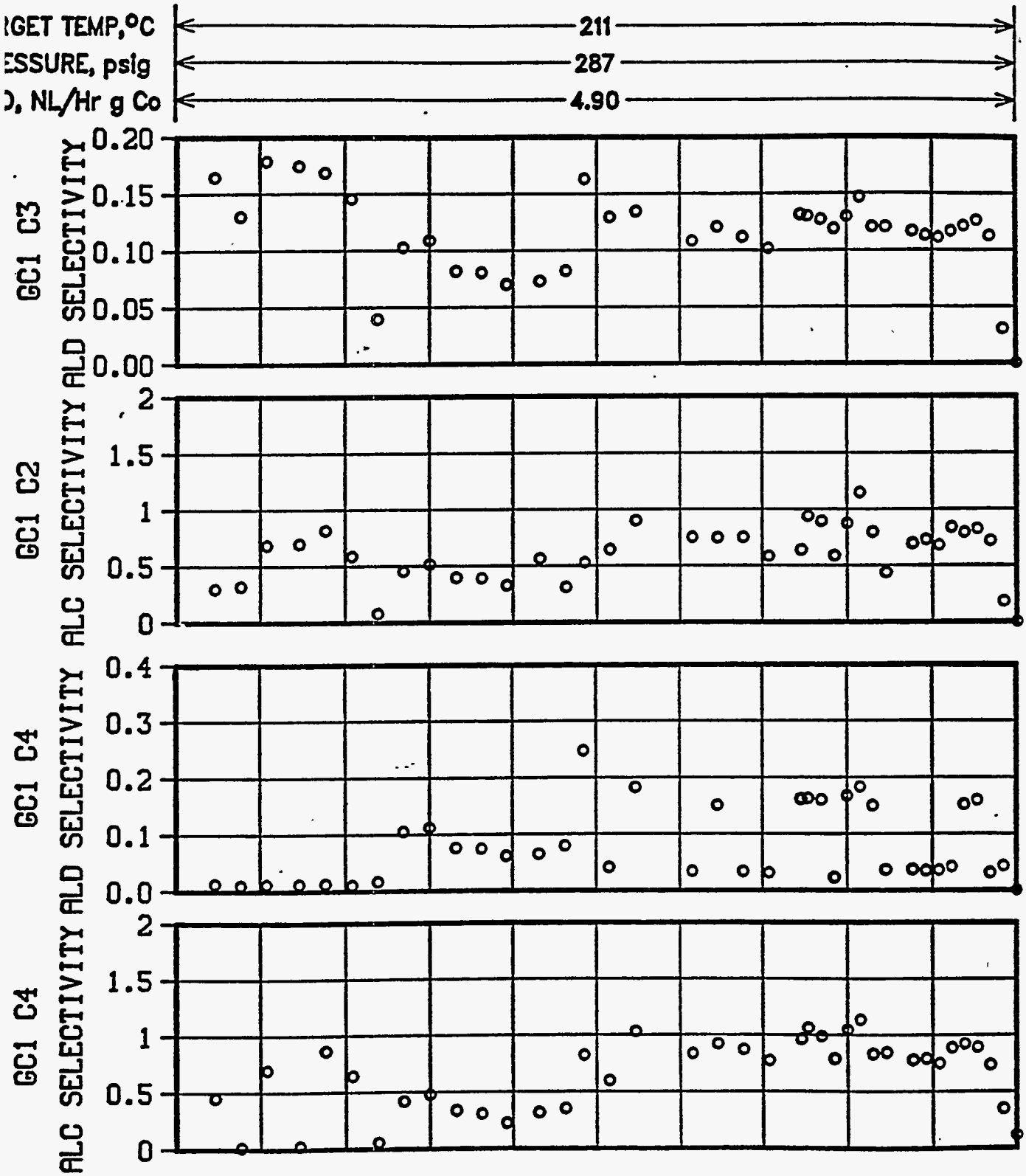

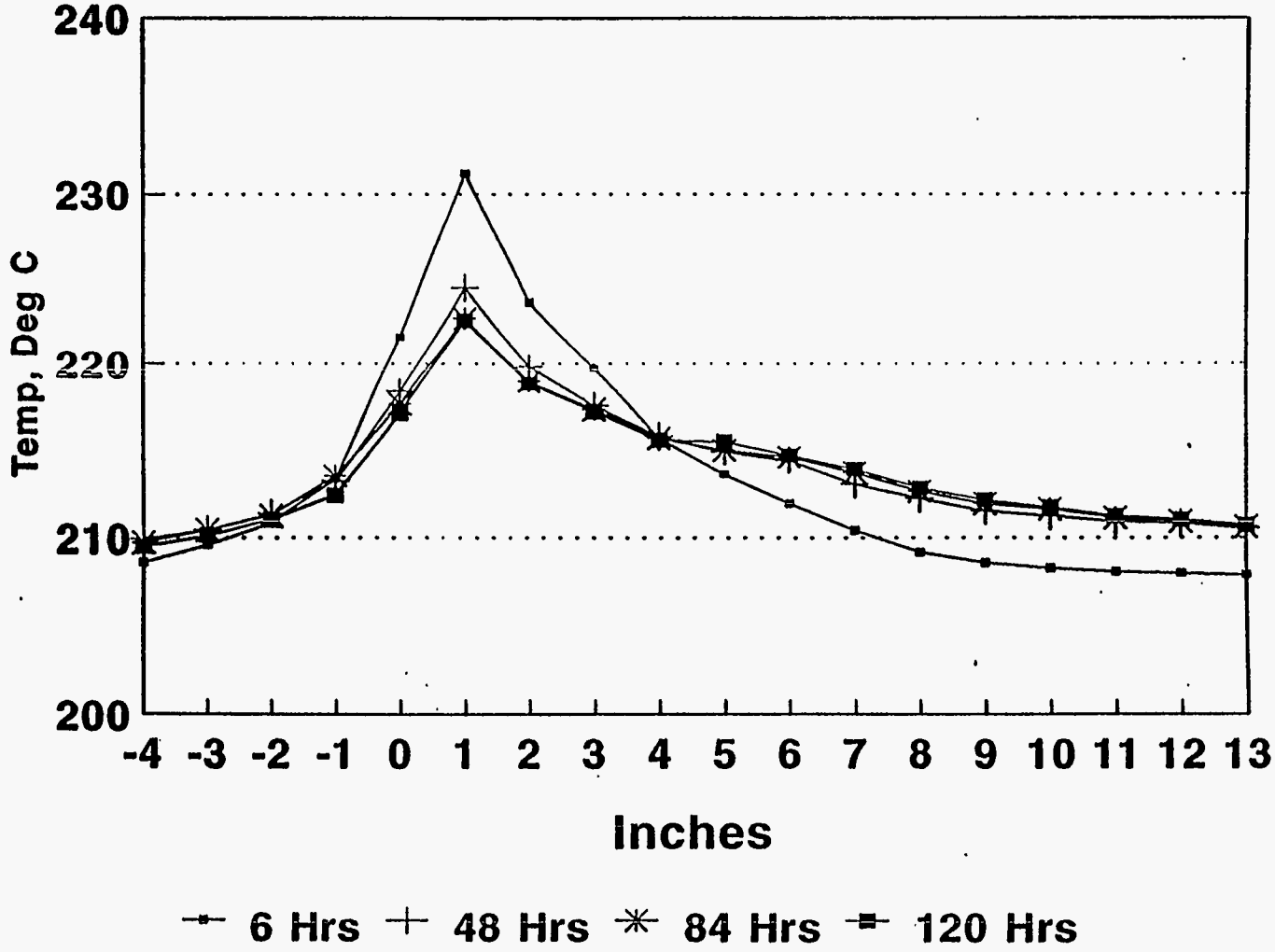
Temp Profiles RUN 97
240
230
220
210
200
Temp, Deg C
-4 -3 -2 -1 0 1 2 3 4 5 6 7 8 9 10 11 12 13
Inches
6 Hrs
48 Hrs
84 Hrs
120 Hrs

FIGURE 94

DESCRIPTIONS OF UNBOUND AND BOUND COBALT CATALYSTS

SUPPORT	**STEAMED, HCl-WASHED[1] Y ZEOLITE**	
SA, m^2/g	582	
PV, cc/g	0.46	
XRD, % Abs Int	84.2 ± 0.3[2]	
CATALYSTS	**UNBOUND**	**BOUND**
BINDER/WT%	NONE	LUDOX/25
METALS, AAS WT%		
Co	17.6	12.7
Mn	2.0	1.5
Zr	1.6	1.4
Ru	1.0	0.7

1. BEFORE ACID WASH: 591 m^2/g, 0.5 cc/g, XRD = 86.3 ± 0.3
2. ABSOLUTE COMPARED TO LZ-210 = 100

FIGURE 95

FIGURE 96

PLANT 700 RUN 99 Co,Mn,Zr,Ru on HCl washed Y

6827–83 w/12.7 % Co via eth–glycol pore fill

18g unreduced active in 160g quartz sand

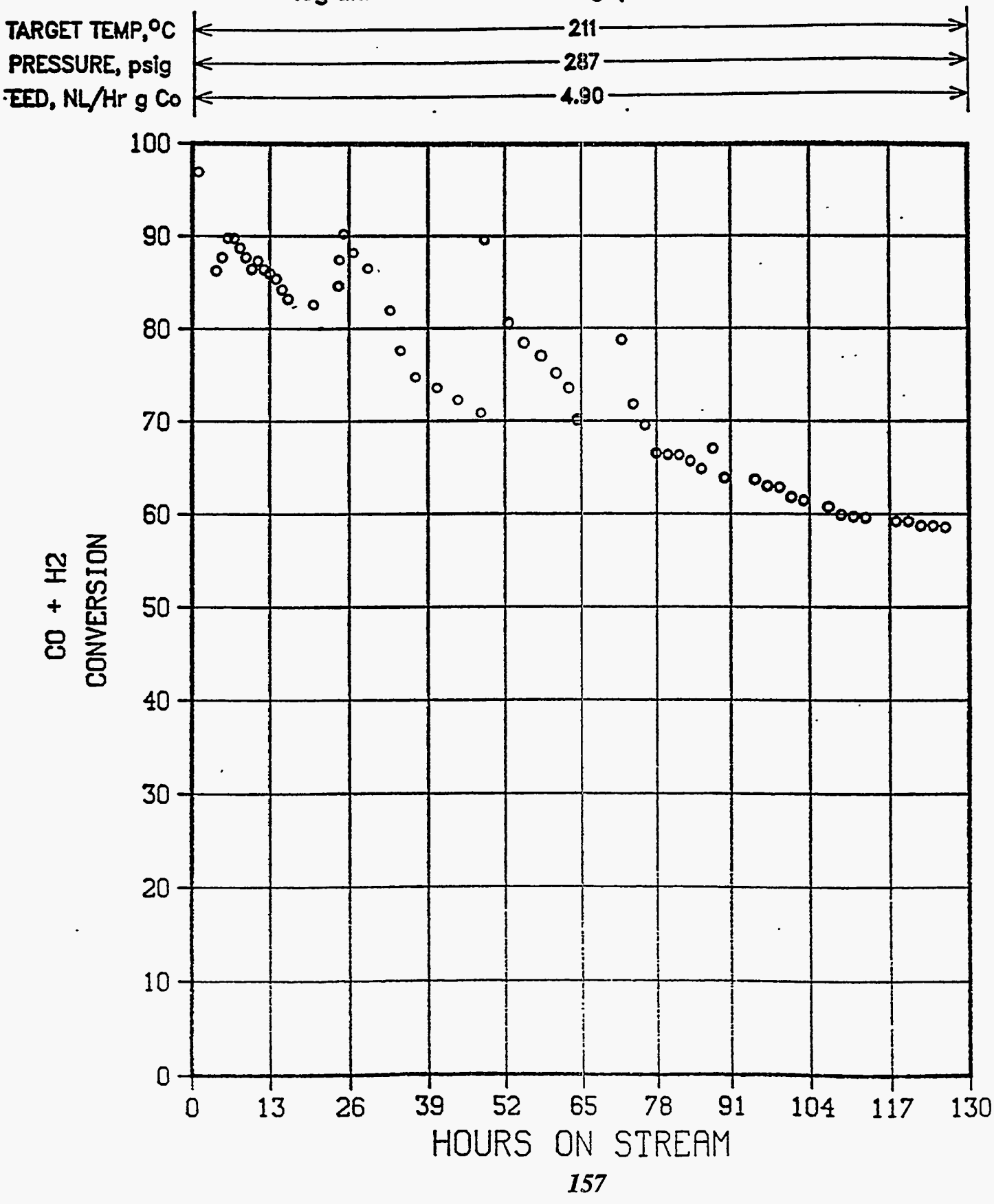

FIGURE 97

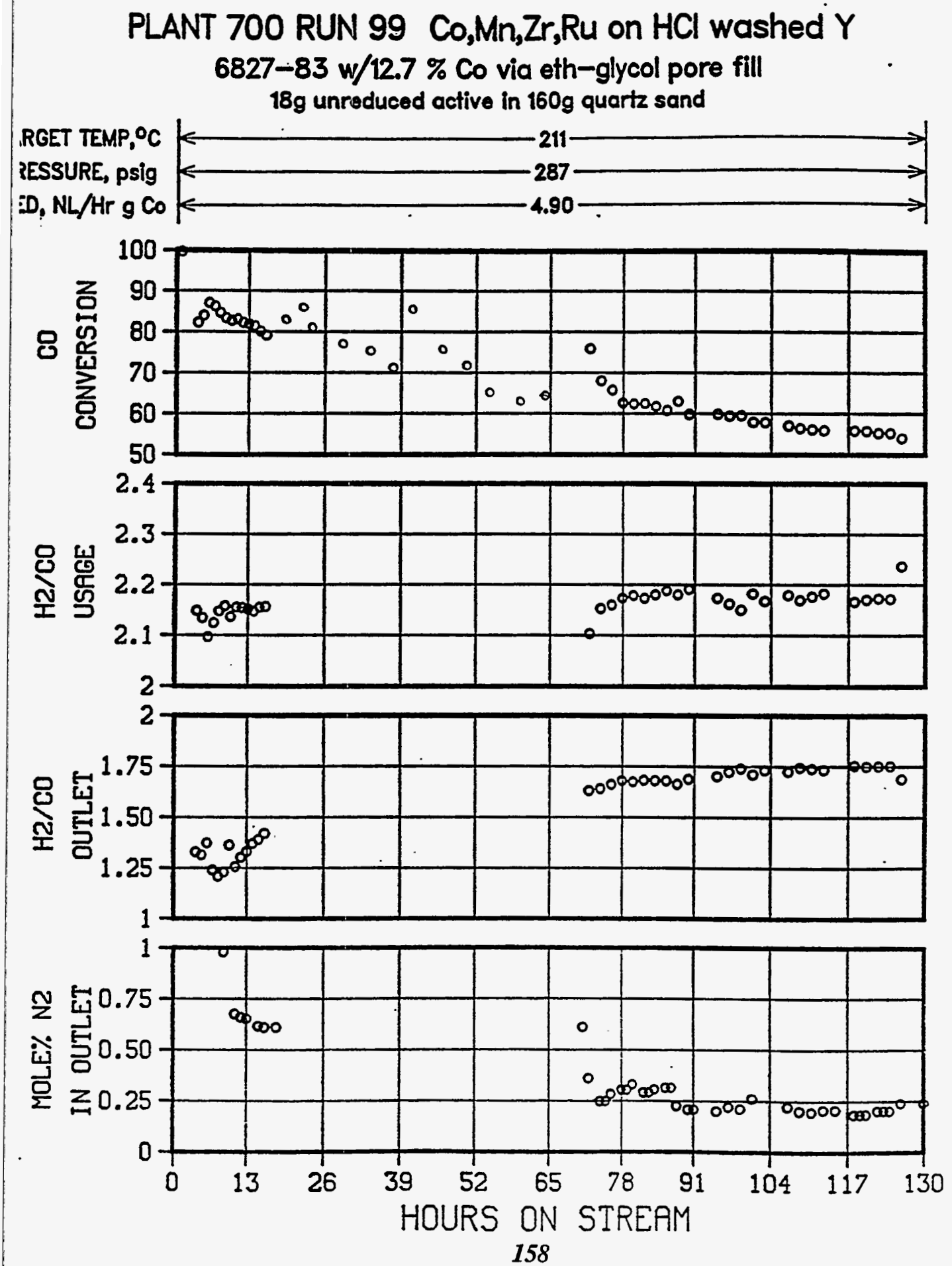
PLANT 700 RUN 99 Co,Mn,Zr,Ru on HCl washed Y
6827-83 w/12.7 % Co via eth-glycol pore fill
18g unreduced active in 160g quartz sand
RGET TEMP,°C 211
RESSURE, psig 287
ED, NL/Hr g Co 4.90
CO CONVERSION
100
90
80
70
60
50
H2/CO USAGE
2.4
2.3
2.2
2.1
2
H2/CO OUTLET
2
1.75
1.50
1.25
1
MOLE% N2 IN OUTLET
1
0.75
0.50
0.25
0
0
13
26
39
52
65
78
91
104
117
130
HOURS ON STREAM

FIGURE 98

PLANT 700 RUN 99 Co,Mn,Zr,Ru on HCl washed Y

6827–83 w/12.7 % Co via eth–glycol pore fill

18g unreduced active in 160g quartz sand

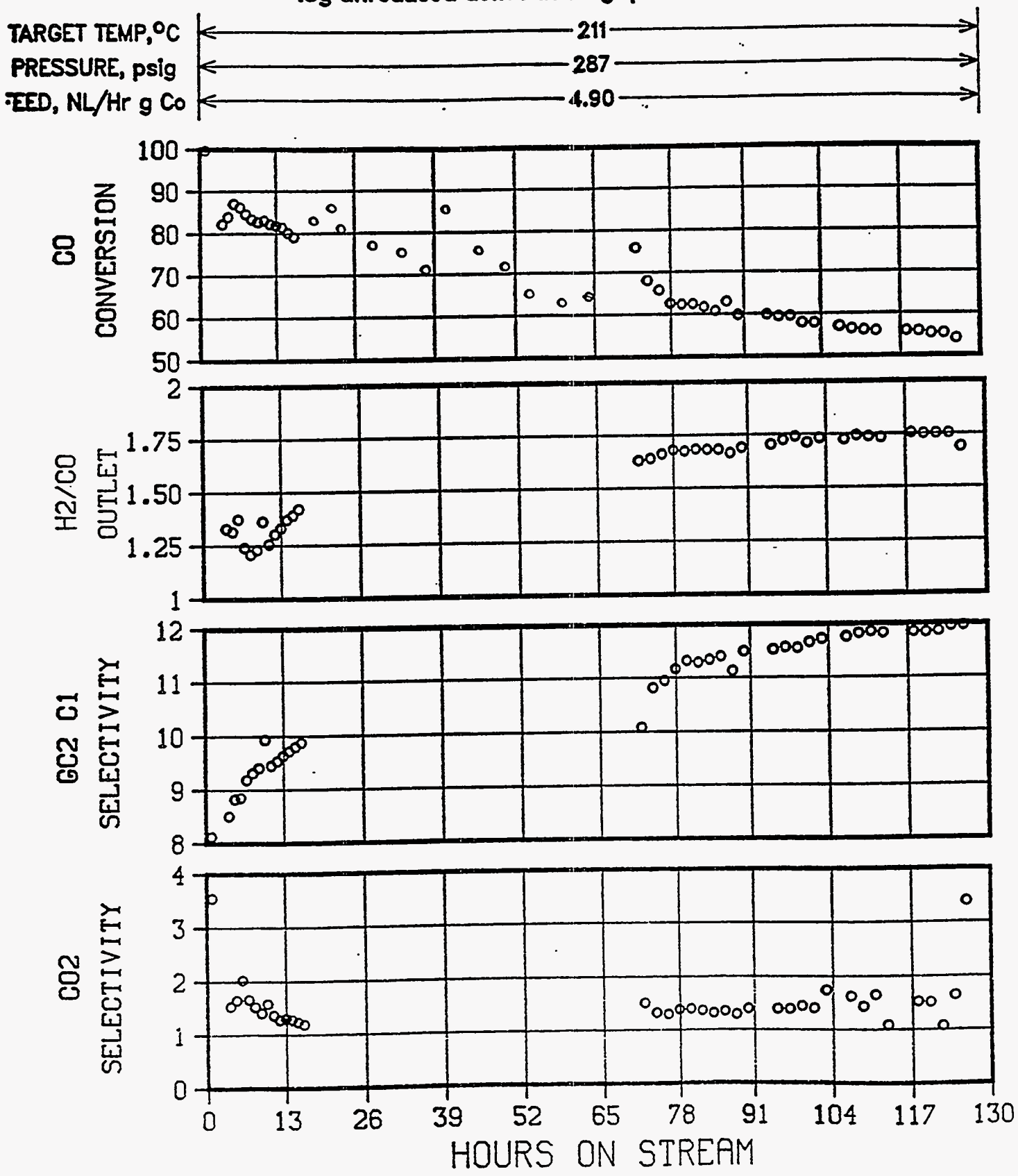

FIGURE 99

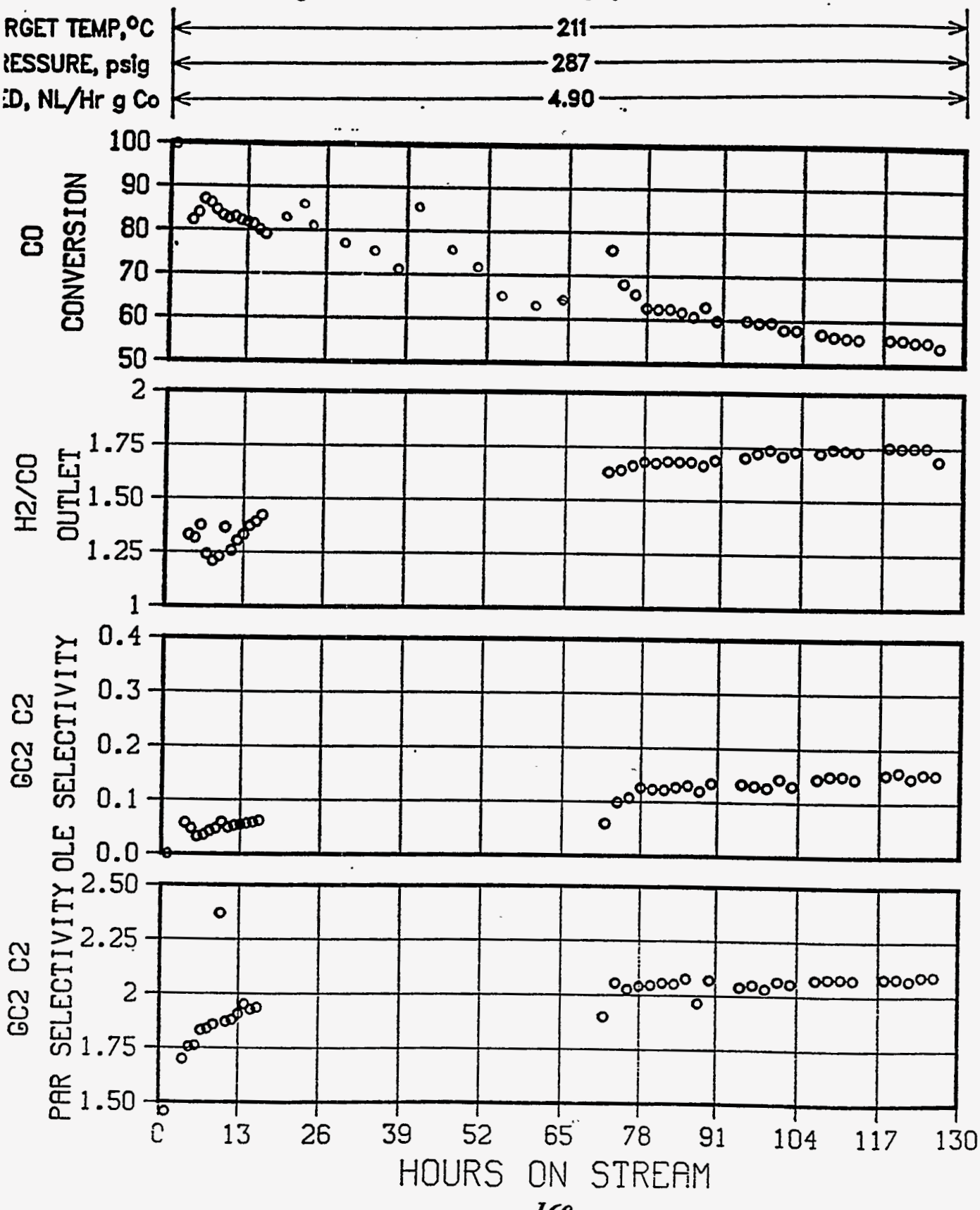
PLANT 700 RUN 99 Co,Mn,Zr,Ru on HCl washed Y
6827-83 w/12.7 % Co via eth-glycol pore fill
18g unreduced active in 160g quartz sand
RGET TEMP,°C
ESSURE, psig
D, NL/Hr g Co
211
287
4.90
CO CONVERSION
100
90
80
70
60
50
H2/CO OUTLET
2
1.75
1.50
1.25
1
GC2 C2 OLE SELECTIVITY
0.4
0.3
0.2
0.1
0.0
GC2 C2 PAR SELECTIVITY
2.50
2.25
2
1.75
1.50
0
13
26
39
52
65
78
91
104
117
130
HOURS ON STREAM

FIGURE 100

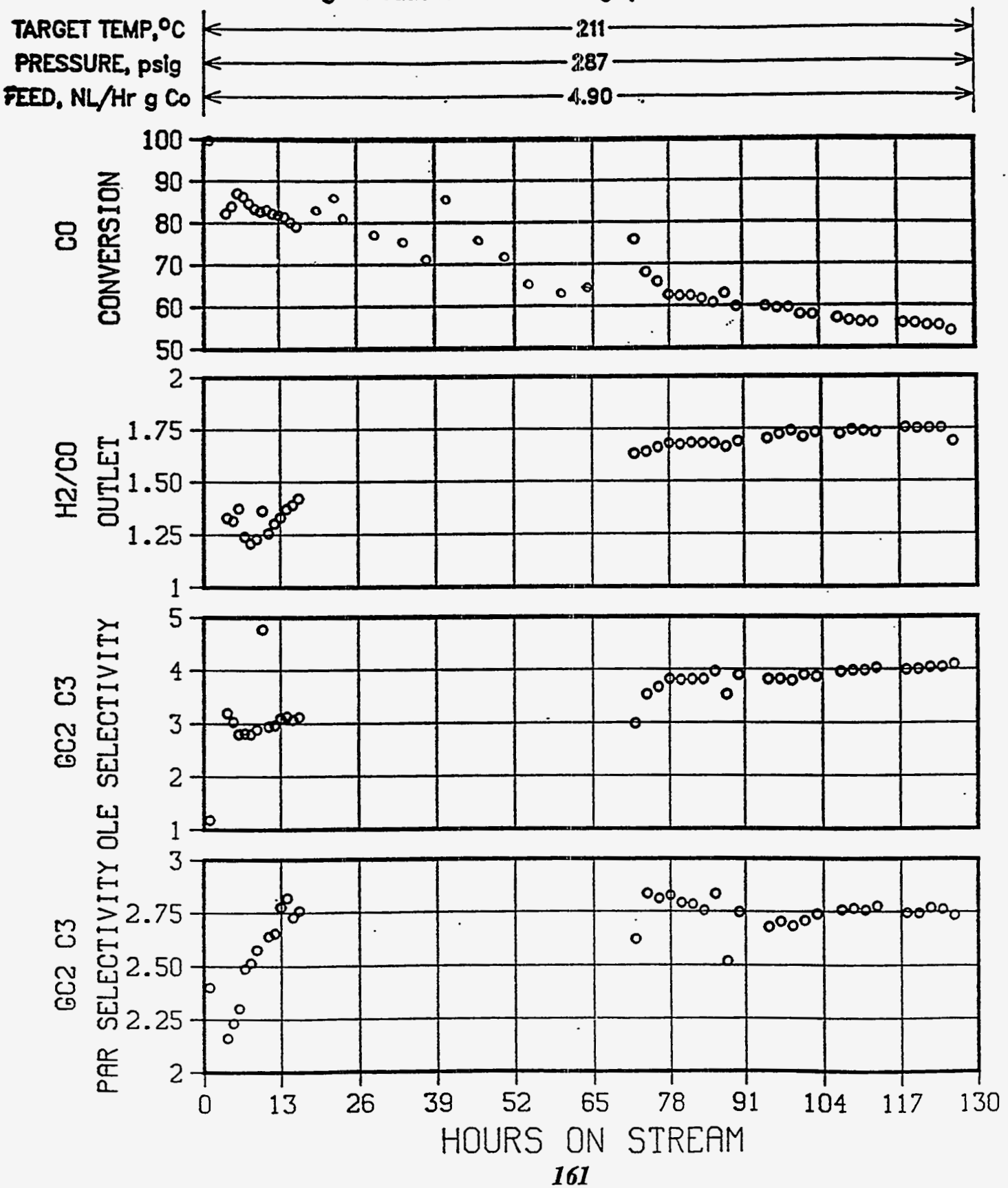
PLANT 700 RUN 99 Co,Mn,Zr,Ru on HCl washed Y
6827-83 w/12.7 % Co via eth-glycol pore fill
18g unreduced active in 160g quartz sand
TARGET TEMP,°C 211
PRESSURE, psig 287
FEED, NL/Hr g Co 4.90
CO CONVERSION
100
90
80
70
60
50
H2/CO OUTLET
2
1.75
1.50
1.25
1
GC2 C3 PAR SELECTIVITY OLE SELECTIVITY
5
4
3
2
1
GC2 C3
3
2.75
2.50
2.25
2
0
13
26
39
52
65
78
91
104
117
130
HOURS ON STREAM

FIGURE 101

PLANT 700 RUN 99 Co,Mn,Zr,Ru on HCl washed Y

6827–83 w/12.7 % Co via eth–glycol pore fill

18g unreduced active in 160g quartz sand

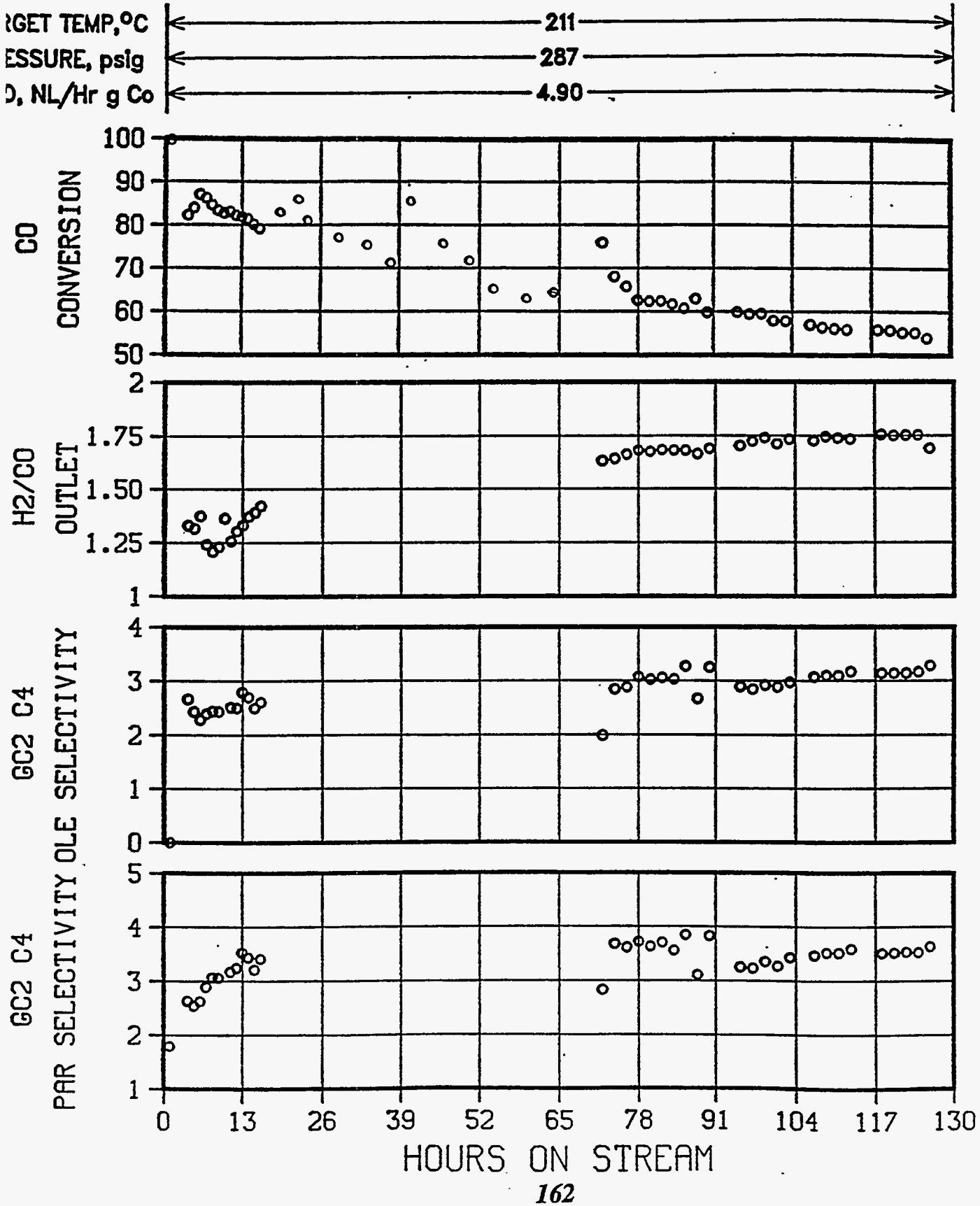

FIGURE 102

PLANT 700 RUN 99 Co,Mn,Zr,Ru on HCl washed Y

6827–83 w/12.7 % Co via eth–glycol pore fill

18g unreduced active in 160g quartz sand

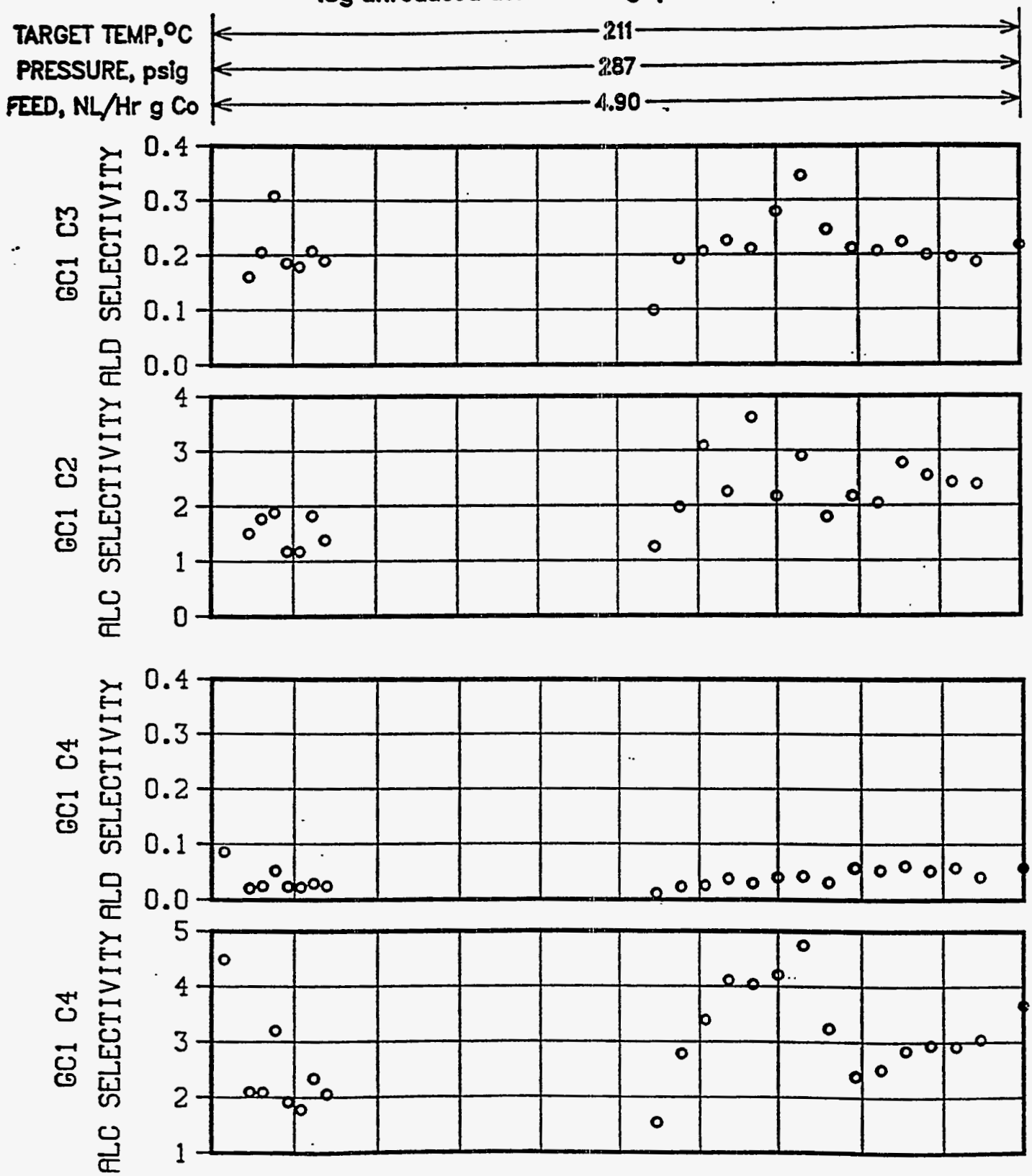

PERFORMANCE OF UNBOUND AND BOUND CATALYSTS

PLT/RUN NO.	700/97	700/99	701/61
REACTOR	TUBE		SLURRY AUTO.
LOADING CATALYST/g DILUENT/g	UNBOUND/13 QUARTZ SAND/ 160	BOUND/18 QUARTZ SAND/ 160	BOUND/18 C_{30} OIL/ 290
CATALYST PRETREATMENT	350°C/H_2/2 HRS		
FEED H_2:CO	2.1		
TEST CONDITIONS FEED RATE (NL/HR·G Co) TEMP, °C PRESS, PSIG	4.9 211(INLET) 287	4.9 211(INLET) 287	4.9 221 287
PERFORMANCE SUMMARY[1]			
CONVERSION, % CO H_2	72 80	55 60	58 60
SELECTIVITY, MOL% C_1 C_2 $C_1^=$ CO_2	13 1.8 0.1 0.8	12 2.1 0.1 1.5	10 1.9 0.1 2.0

1. AT 130 HOURS ON STREAM

FIGURE 103

FIGURE 104

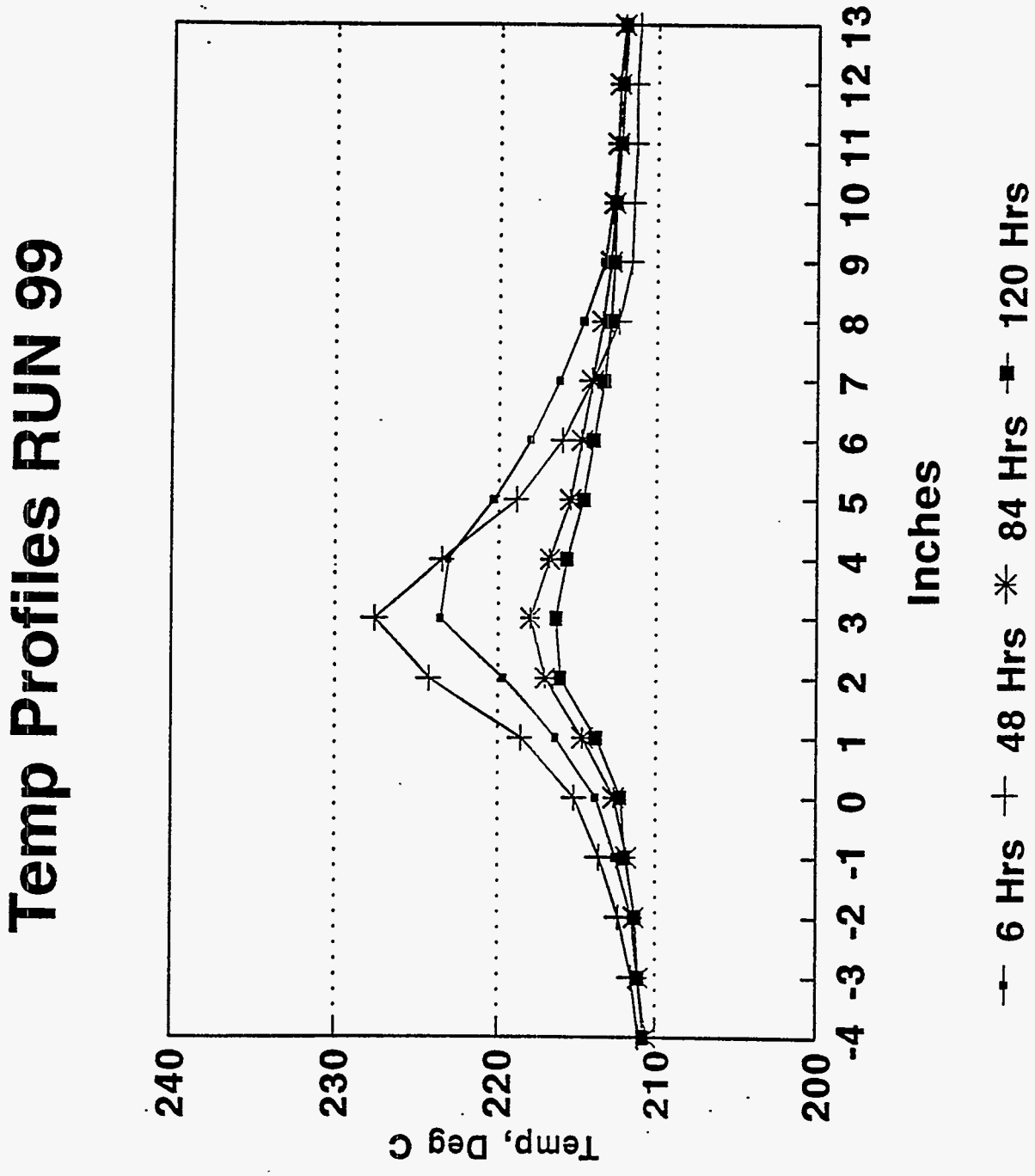
Temp Profiles RUN 99
Temp, Deg C
240
230
220
210
200
-4 -3 -2 -1 0 1 2 3 4 5 6 7 8 9 10 11 12 13
Inches
6 Hrs
48 Hrs
84 Hrs
120 Hrs

FIGURE 105

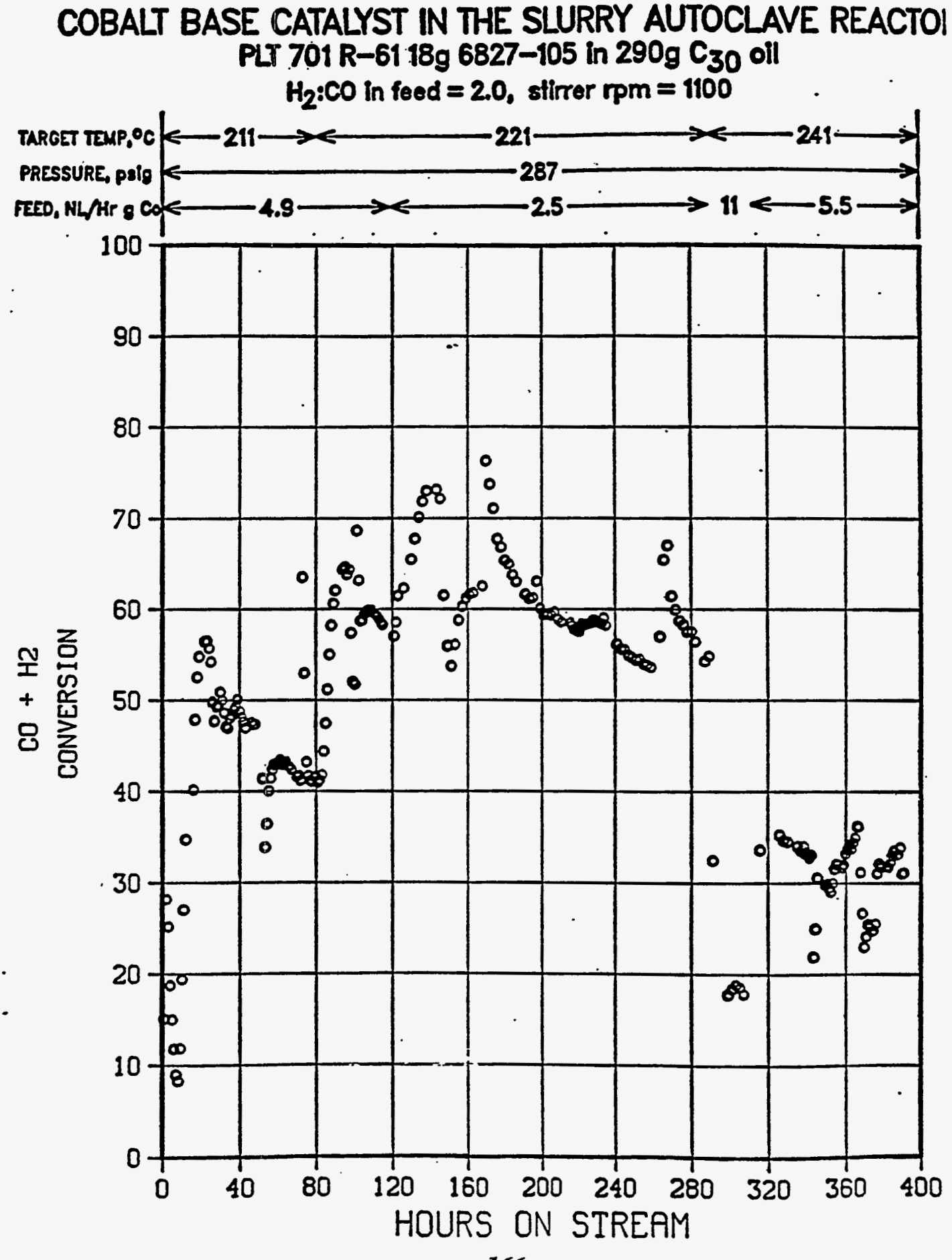
COBALT BASE CATALYST IN THE SLURRY AUTOCLAVE REACTOI
PLT 701 R-61 18g 6827-105 in 290g C30 oil
H2:CO in feed = 2.0, stirrer rpm = 1100
TARGET TEMP,°C
211
221
241
PRESSURE, psig
287
FEED, NL/Hr g Co
4.9
2.5
11
5.5
CO + H2 CONVERSION
100
90
80
70
60
50
40
30
20
10
0
0
40
80
120
160
200
240
280
320
360
400
HOURS ON STREAM

FIGURE 106

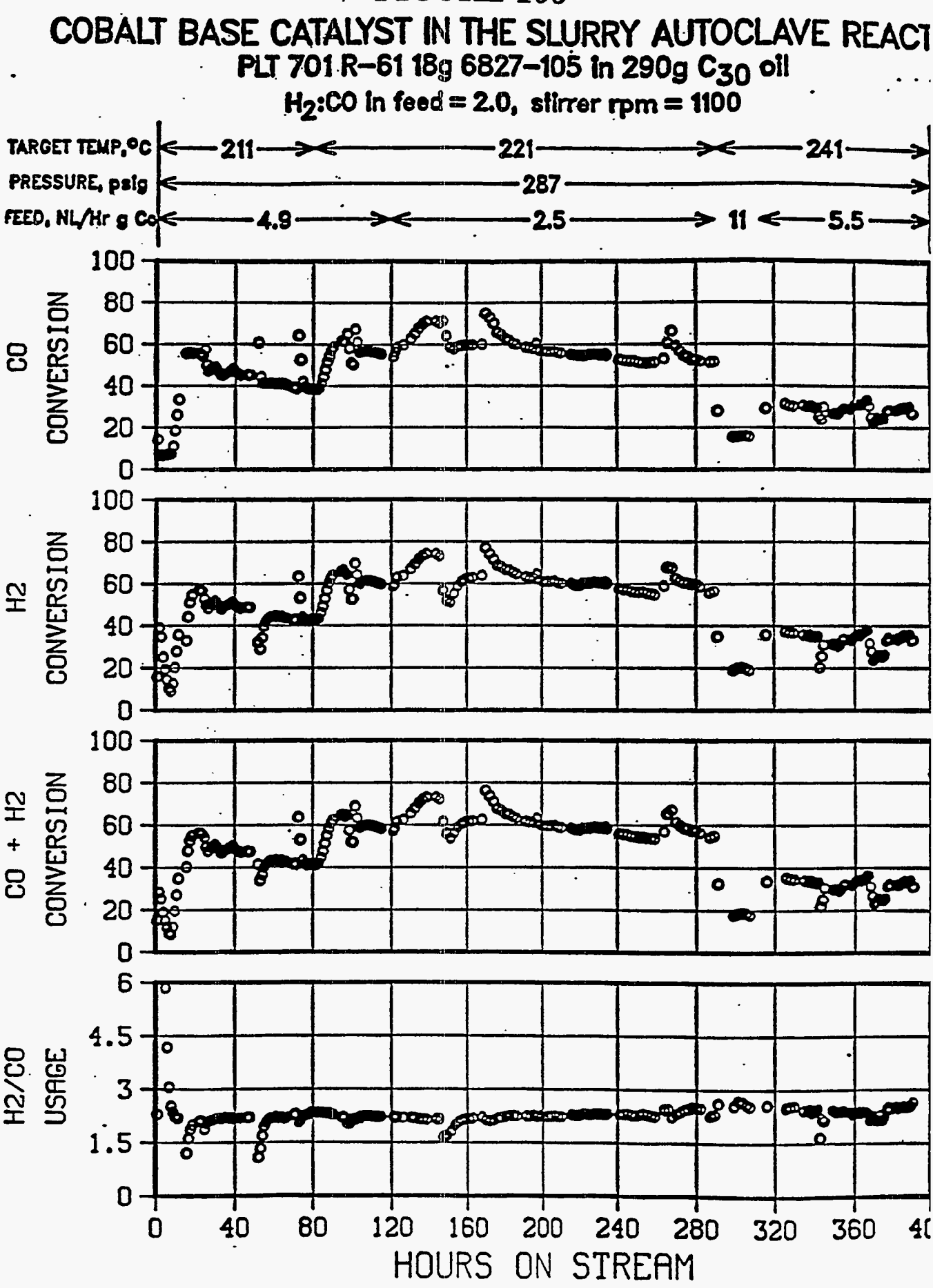
COBALT BASE CATALYST IN THE SLURRY AUTOCLAVE REACT
PLT 701 R-61 18g 6827-105 in 290g C30 oil
H2:CO in feed = 2.0, stirrer rpm = 1100
TARGET TEMP,°C
211
221
241
PRESSURE, psig
287
FEED, NL/Hr g Co
4.9
2.5
11
5.5
CO CONVERSION
H2 CONVERSION
CO + H2 CONVERSION
H2/CO USAGE
0
20
40
60
80
100
1.5
3
4.5
6
0
40
80
120
160
200
240
280
320
360
HOURS ON STREAM

FIGURE 107

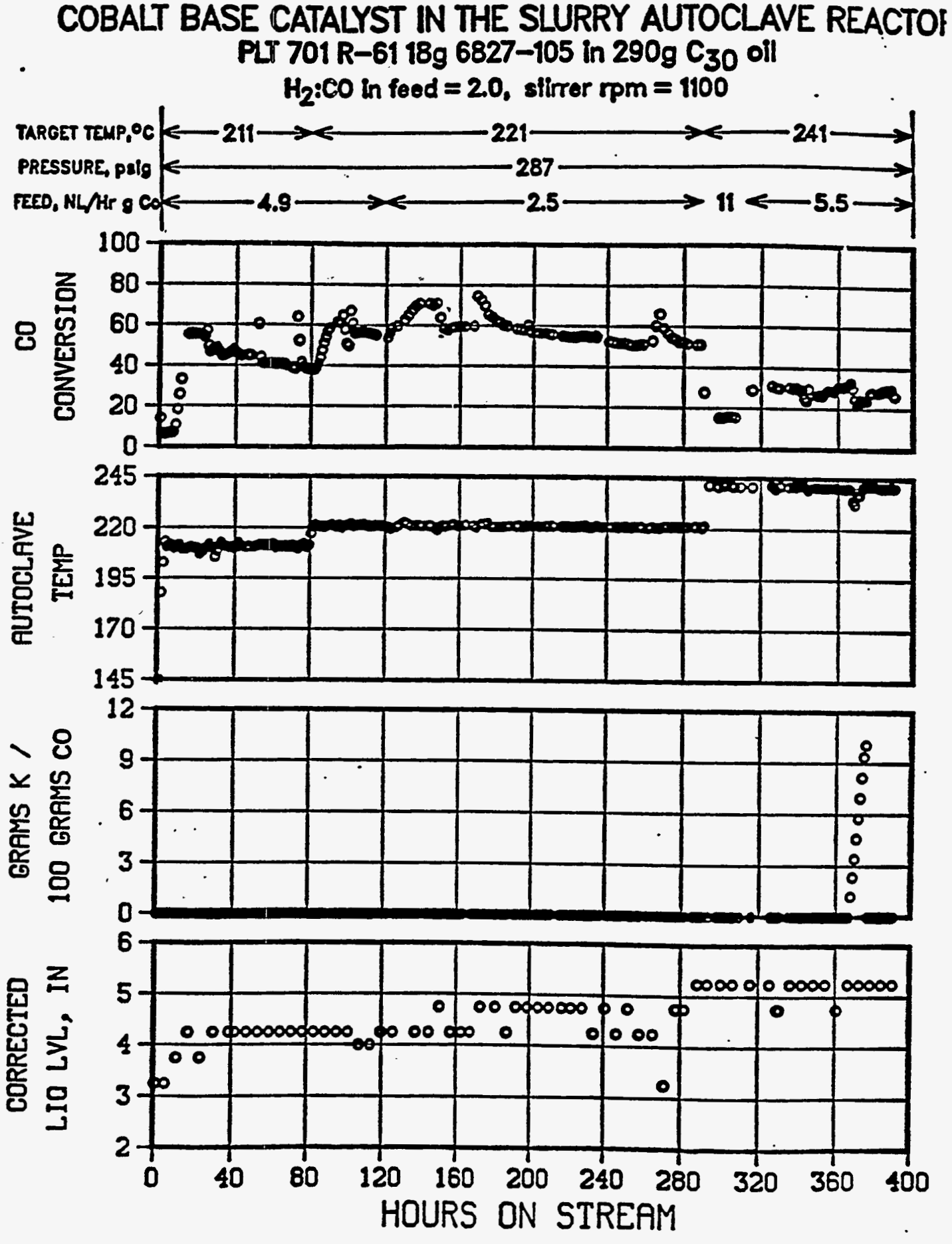
COBALT BASE CATALYST IN THE SLURRY AUTOCLAVE REACTOR
PLT 701 R-61 18g 6827-105 in 290g C_{30} oil
H_2:CO in feed = 2.0, stirrer rpm = 1100
TARGET TEMP,°C
211
221
241
PRESSURE, psig
287
FEED, NL/Hr g Co
4.9
2.5
11
5.5
CO CONVERSION
AUTOCLAVE TEMP
GRAMS K / 100 GRAMS CO
CORRECTED LIQ LVL, IN
HOURS ON STREAM

FIGURE 108

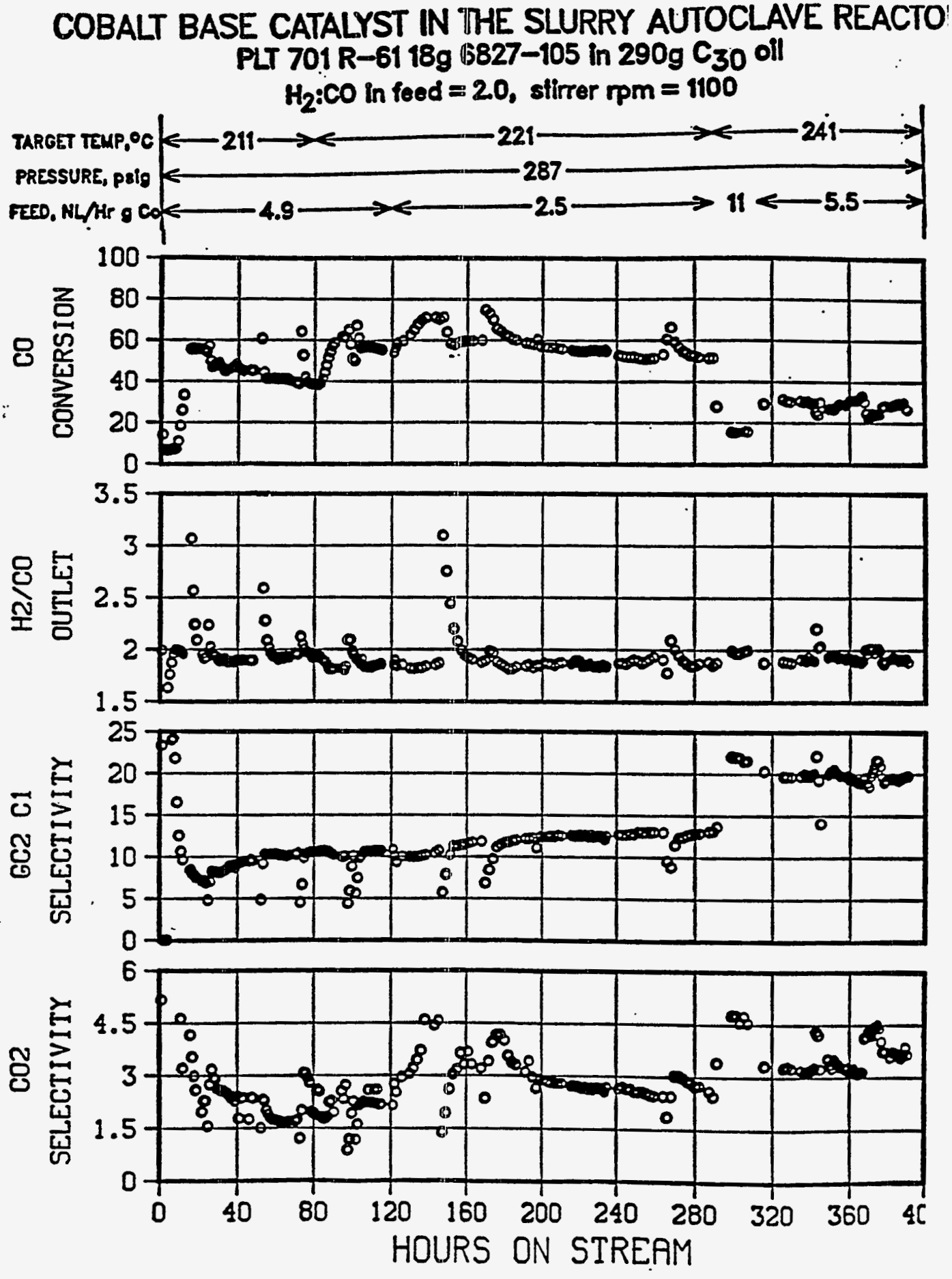
COBALT BASE CATALYST IN THE SLURRY AUTOCLAVE REACTO
PLT 701 R-61 18g 6827-105 in 290g C30 oil
H2:CO in feed = 2.0, stirrer rpm = 1100
TARGET TEMP,°C
211
221
241
PRESSURE, psig
287
FEED, NL/Hr g Co
4.9
2.5
11
5.5
CO CONVERSION
H2/CO OUTLET
GC2 C1 SELECTIVITY
CO2 SELECTIVITY
HOURS ON STREAM

FIGURE 109

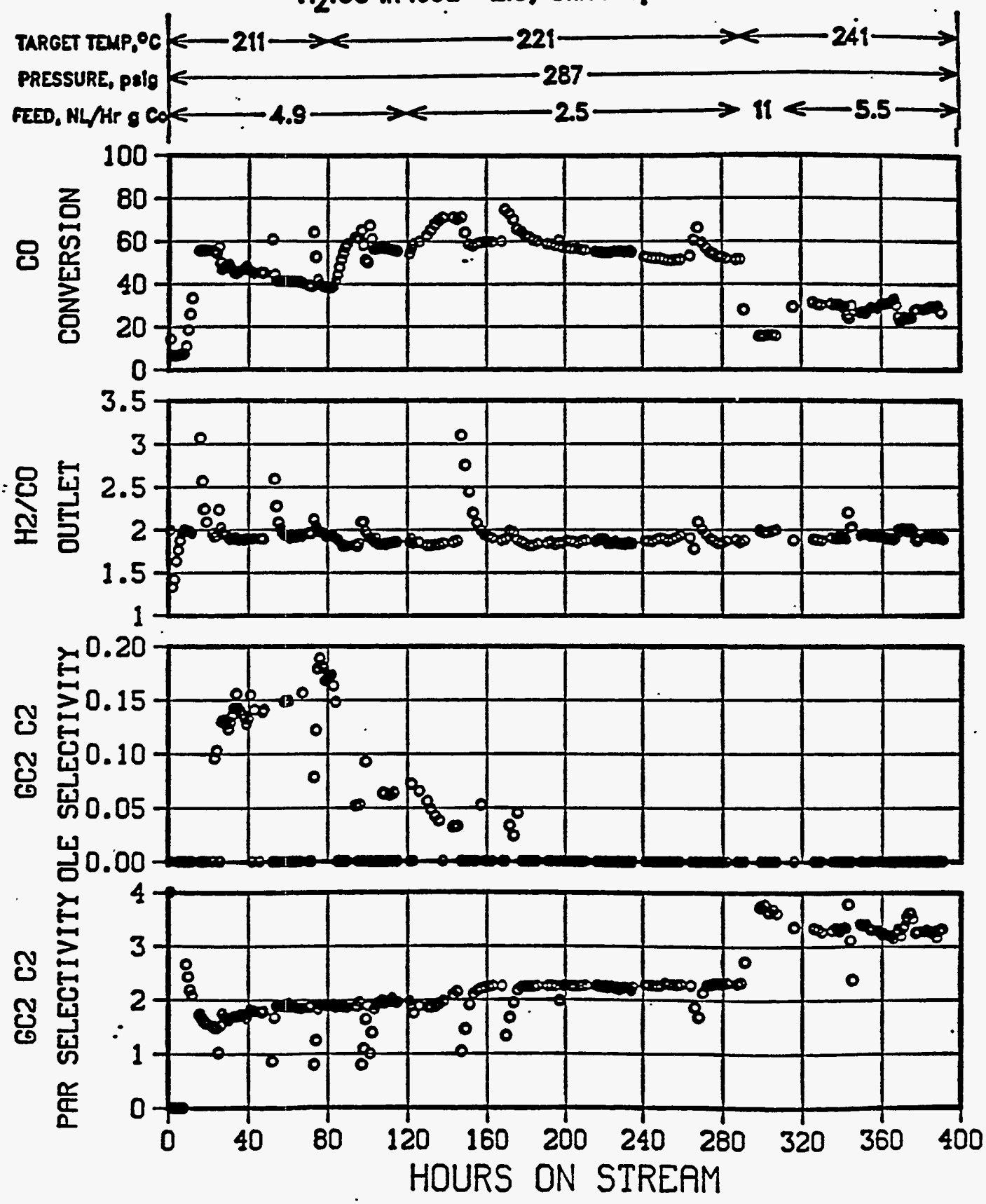
COBALT BASE CATALYST IN THE SLURRY AUTOCLAVE REACTOR
PLT 701 R-61 18g 6827-105 in 290g C_{30} oil
H_2:CO in feed = 2.0, stirrer rpm = 1100
TARGET TEMP,°C
211
221
241
PRESSURE, psig
287
FEED, NL/Hr g Co
4.9
2.5
11
5.5
CO CONVERSION
H2/CO OUTLET
GC2 C2 PAR SELECTIVITY OLE SELECTIVITY
HOURS ON STREAM

FIGURE 110

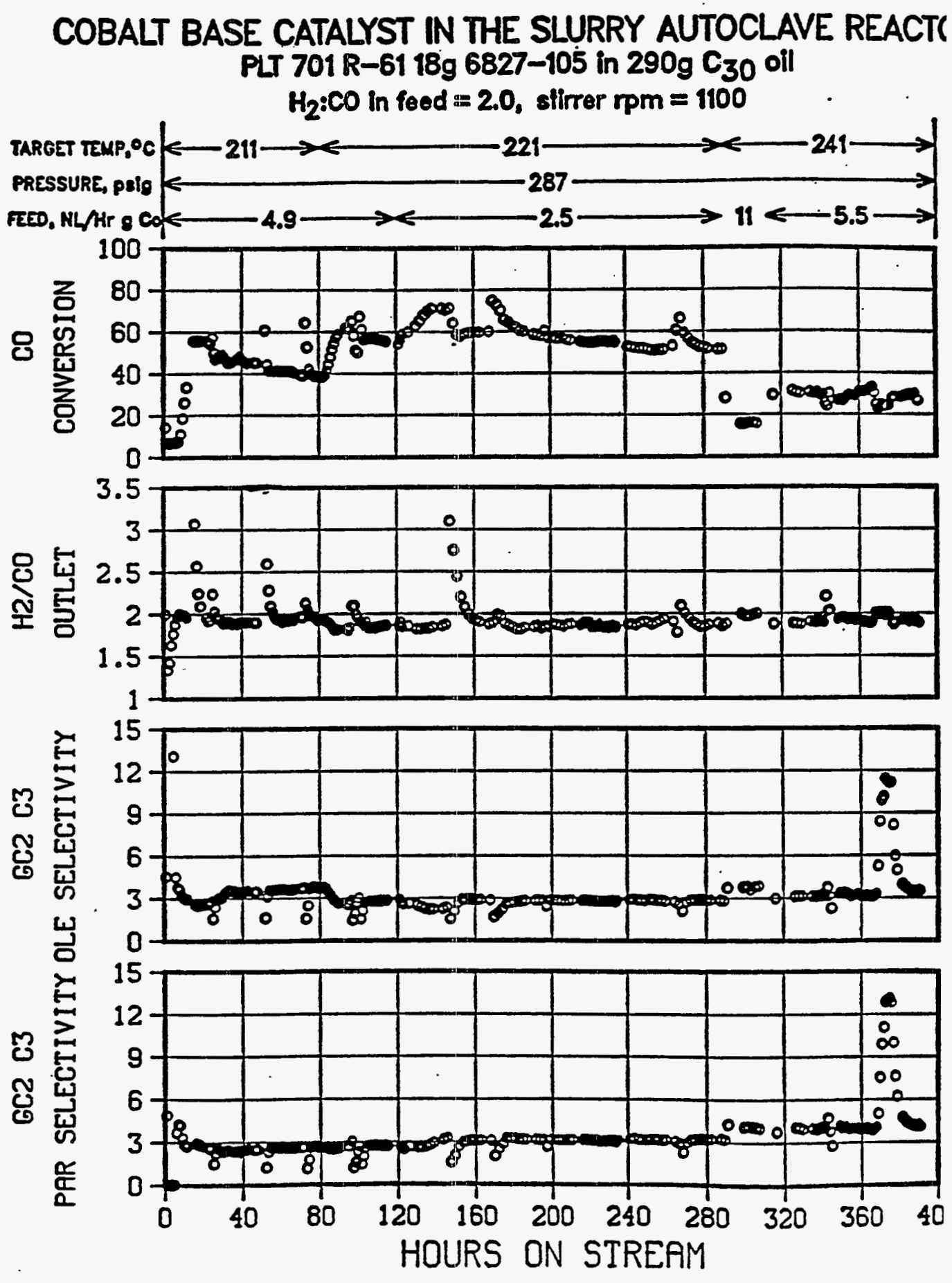
COBALT BASE CATALYST IN THE SLURRY AUTOCLAVE REACTO
PLT 701 R-61 18g 6827-105 in 290g C30 oil
H2:CO in feed = 2.0, stirrer rpm = 1100
TARGET TEMP,°C
211
221
241
PRESSURE, psig
287
FEED, NL/Hr g Co
4.9
2.5
11
5.5
CO CONVERSION
H2/CO OUTLET
GC2 C3 PAR SELECTIVITY OLE SELECTIVITY
HOURS ON STREAM

FIGURE 111

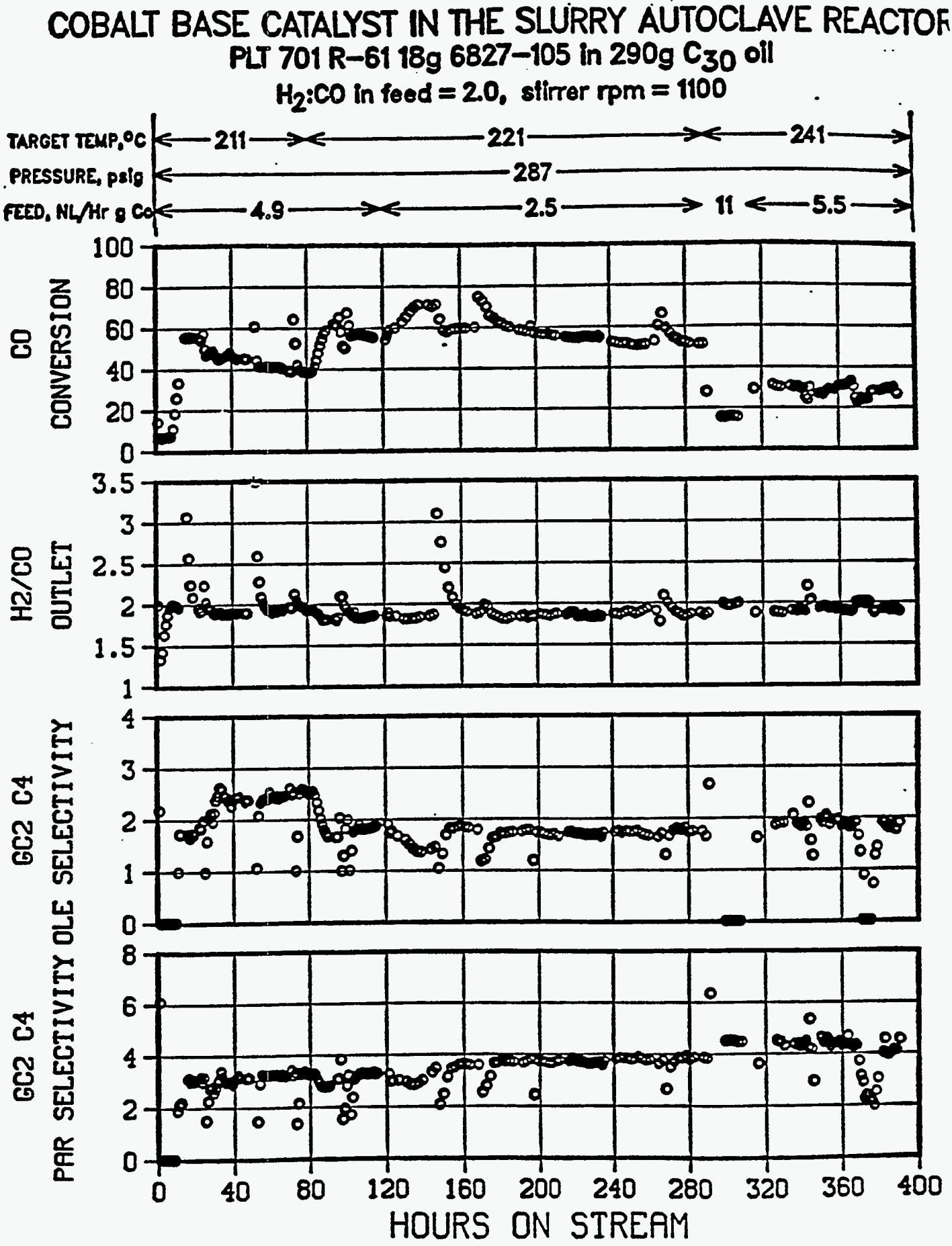
COBALT BASE CATALYST IN THE SLURRY AUTOCLAVE REACTOR
PLT 701 R-61 18g 6827-105 in 290g C30 oil
H2:CO in feed = 2.0, stirrer rpm = 1100
TARGET TEMP,°C
211
221
241
PRESSURE, psig
287
FEED, NL/Hr g Co
4.9
2.5
11
5.5
CO CONVERSION
H2/CO OUTLET
GC2 C4 PAR SELECTIVITY OLE SELECTIVITY
HOURS ON STREAM

FIGURE 112

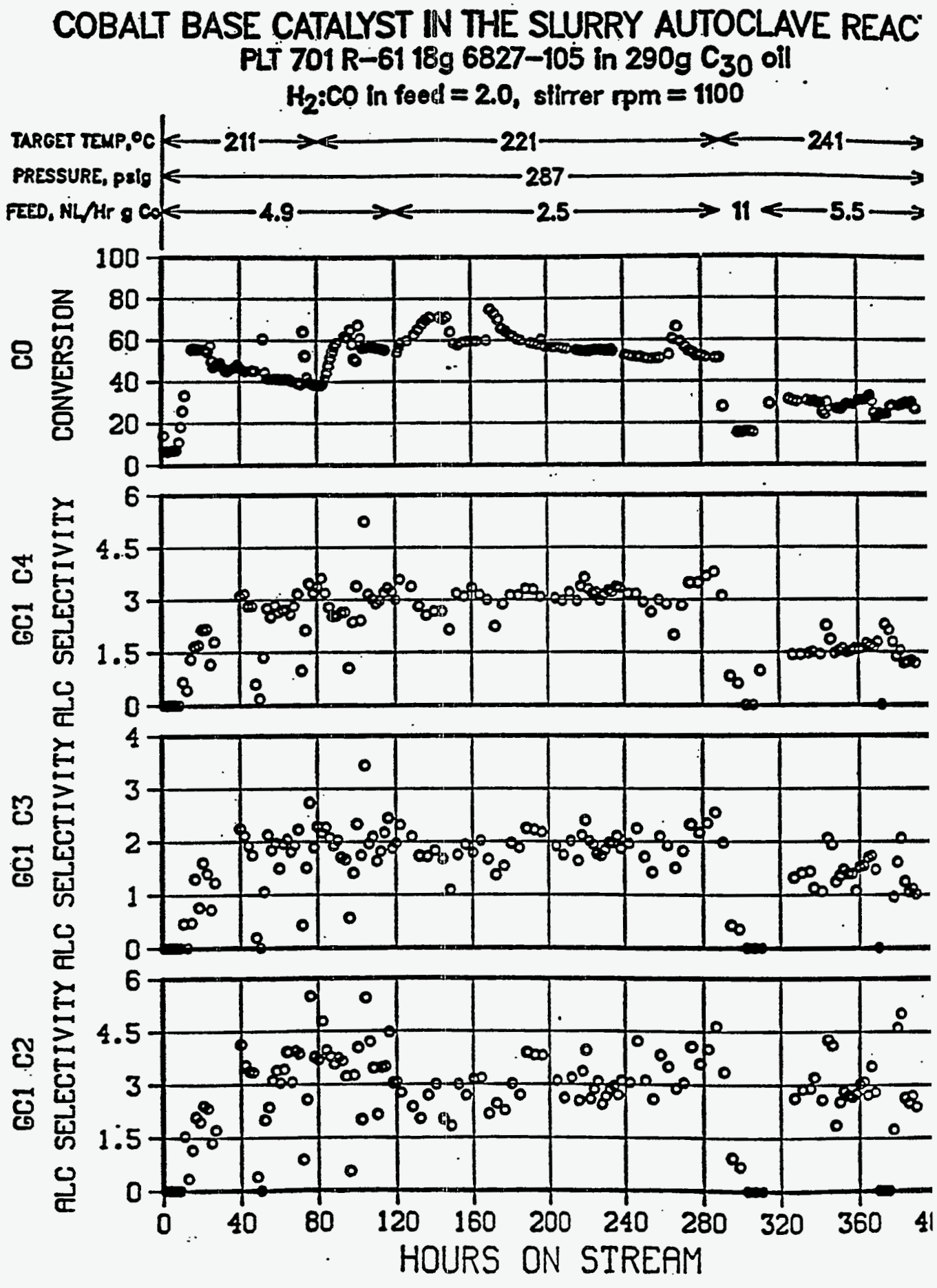
COBALT BASE CATALYST IN THE SLURRY AUTOCLAVE REAC
PLT 701 R-61 18g 6827-105 in 290g C30 oil
H2:CO in feed = 2.0, stirrer rpm = 1100
TARGET TEMP,°C
211
221
241
PRESSURE, psig
287
FEED, NL/Hr g Co
4.9
2.5
11
5.5
CO CONVERSION
GC1 C4 ALC SELECTIVITY
GC1 C3 ALC SELECTIVITY
GC1 C2 ALC SELECTIVITY
HOURS ON STREAM

EFFECT OF REDUCTION CONDITIONS ON CATALYST PERFORMANCE
SUMMARY OF SCREENING IN FIXED-BED PLANT

RUN NO.	104	97	102
LOADING			
CATALYST, G		13	
DILUENT, G		160	
CATALYST PRETREAT.	325°/H_2/2 HRS	350°/H_2/2 HRS	375°/H_2/2 HRS
TEST CONDITIONS			
FEED H_2/CO		2.1	
FEED RATE (NL/HR·G Co)		4.9	
TEMP, °C		211(INLET)	
PRESSURE, PSIG		287	
PERFORMANCE SUMMARY[1]			
CONVERSION, %			
CO + H_2	72	78	49
CO	67	72	47
SELECTIVITY, MOLE %			
C_1	11.8	13	13
C_2	1.9	1.8	2.0
$C_2^=$	0.1	0.1	0.2
C_3	3.1	3.0	3.5
$C_3^=$	2.0	2.1	2.7
CO_2	1.8	0.8	1.0

1. AT 100 HOURS ON STREAM

FIGURE 113

Figure 1 - Composition of Crystallites for 6827-99

Location	
A	9.3 at % Mn, 88.3 at % Co, 2.4 at % Ru
B	15.4 at % Mn, 78.8 at % Co, 5.8 at % Zr
C	15.6 at % Mn, 80.1 at % Co, 4.3 at % Zr

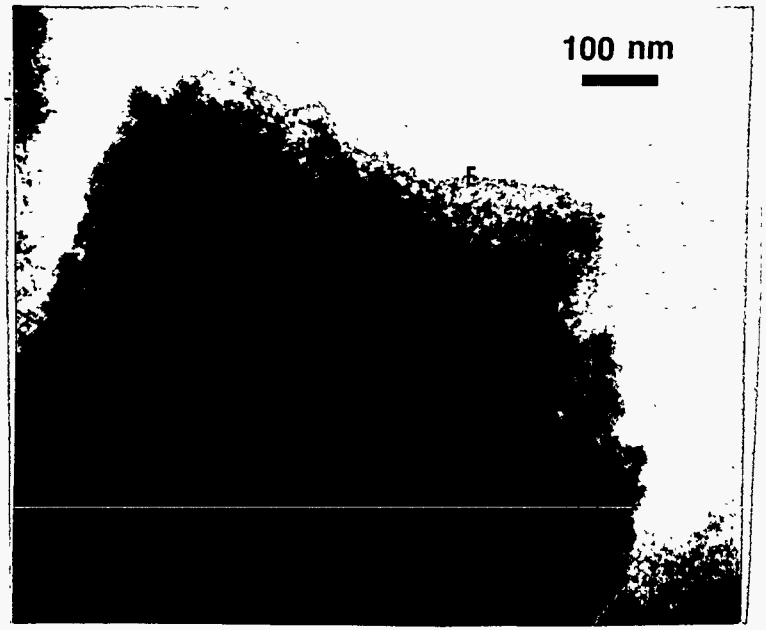

Figure 2 - Composition of Crystallites for 6827-99

Location	
D	8.1 at % Mn, 88..9 at % Co, 3.0 at % Ru
E	12.6 at % Mn, 87.4 at % Co
F	7.2 at % Mn, 90.3 at % Co, 2.5 at % Ru
G	12.0 at % Mn, 83.4 at % Co, 3.6 at % Ru

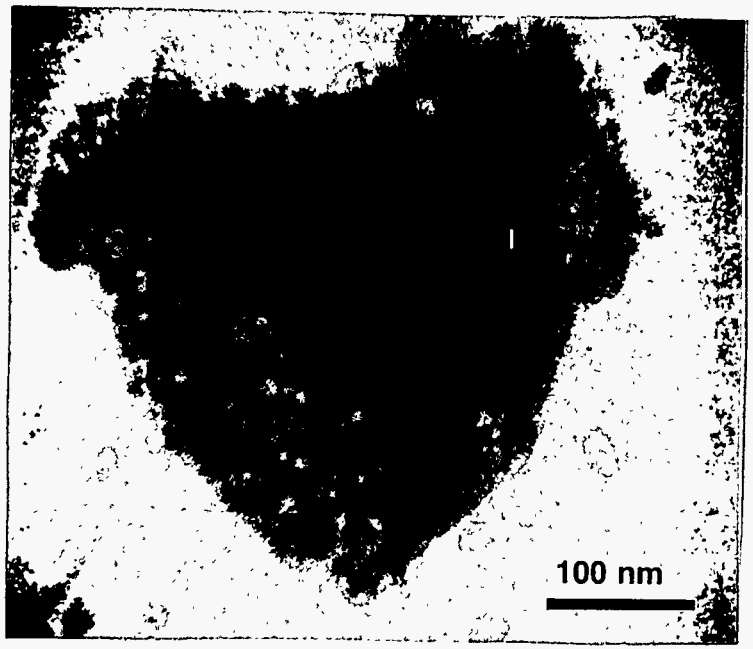

Figure 3 - Composition of Crystallites for 6827-99

Location	
H	10.9 at % Mn, 89.1 at % Co
I	17.0 at % Mn, 87.0 at % Co
J	14.3 at % Mn, 66.9 at % Co, 16.5 at % Zr, 2.3 at %Ru
K	15.4 at % Mn, 78.8 at % Co, 5.8 at % Zr

175

FIGURE 114

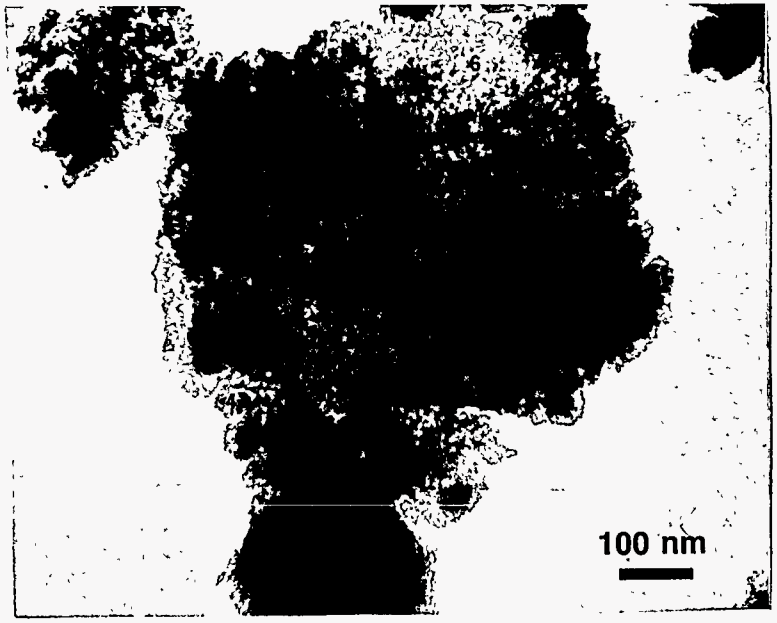

Figure 4 - Composition of Crystallites for 6827-123

Location	
1	2.8 at % Mn, 97.3 at % Co
2	4.7 at % Mn, 95.3 at % Co
3	8.4 at % Mn, 90.7 at % Co, 0.7 at % Ru
4	6.3 at % Mn, 93.1 at % Co, 0.6 at % Ru
5	4.2 at % Mn 95.8 at % Co
6	10.0 at % Mn, 87.9 at % Co, 2.1 at % Zr

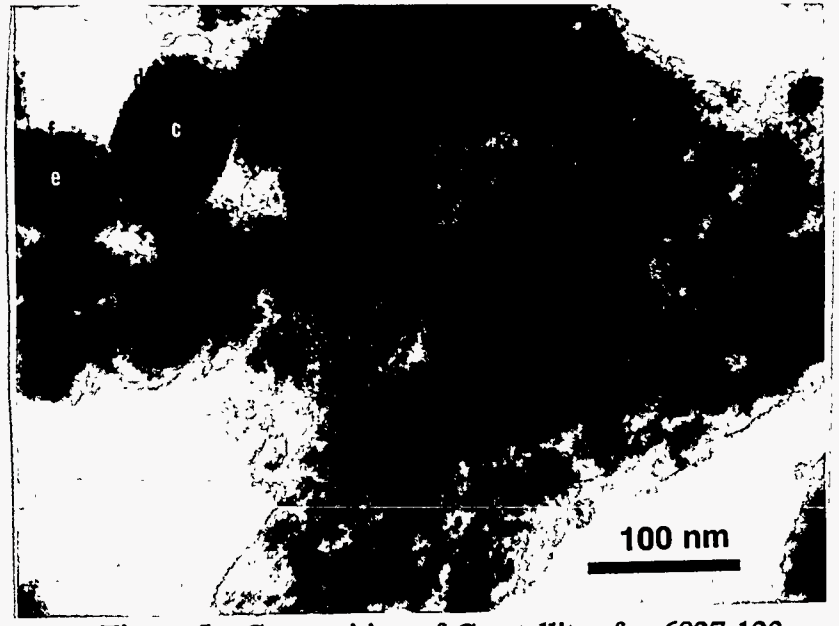

Figure 5 - Composition of Crystallites for 6827-123

Location	
a	3.1 at % Mn, 96.9 at % Co
b	8.5 at % Mn. 90.6 at % Co, 0.9 at % Ru
c	2.0 at % mn, 98.0 at % Co
d	3.9 at % Mn, 96.1 at % Co
e	2.9 at % Mn, 97.1 at % Co
f	.31 at % Mn, 96.9 at % Co
g	8.7 at % Mn, 89.5 at % Co, 1.8 at % Zr

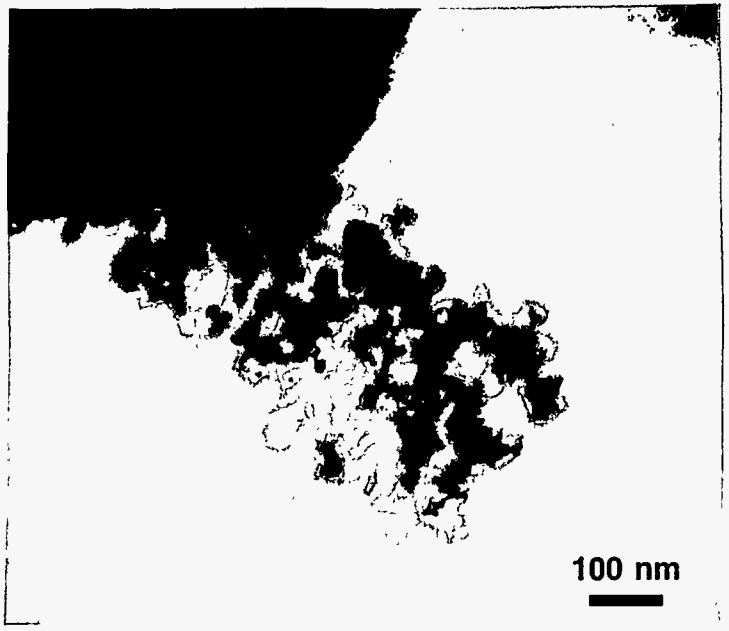

Figure 6 - Raney-Type Morphology for 6827-123

176

FIGURE 115

FIGURE 116

COMPOSITION OF CRYSTALLITES FOR 6827-99
(atomic percent)

Size Range (nm)	Mn	Co	Zr	Ru
≥ 30	11.4 ± 4.4	85.5 ± 4.0	1.4 ± 2.4	2.5 ± 1.8
3-30	12.8 ± 5.9	78.6 ± 8.9	8.1 ± 5.3	1.3 ± 2.3
<3	14.5 ± 4.7	71.6 ± 4.1	11.8 ± 5.3	2.1 ± 2.9

COMPOSITION OF CRYSTALLITES FOR 6827-123
(atomic percent)

Size Range (nm)	Mn	Co	Zr	Ru
≥ 30	4.2 ± 2.0	95.4 ± 2.2	0.04 ± 0.14	0.4 ± 0.4
3-30	6.4 ± 1.9	92.9 ± 2.2	0.4 ± 0.4	0.4 ± 0.5
<3	8.6 ± 1.3	89.4 ± 1.3	1.9 ± 0.4	0.1 ± 0.2

FIGURE 117

PLANT 700 RUN 101 Co,Mn,Zr,Ru ON HCL Washed Y

6827–95 w/27.4 % Co via eth–glycol pore fill

18g unreduced active in 160g quartz sand

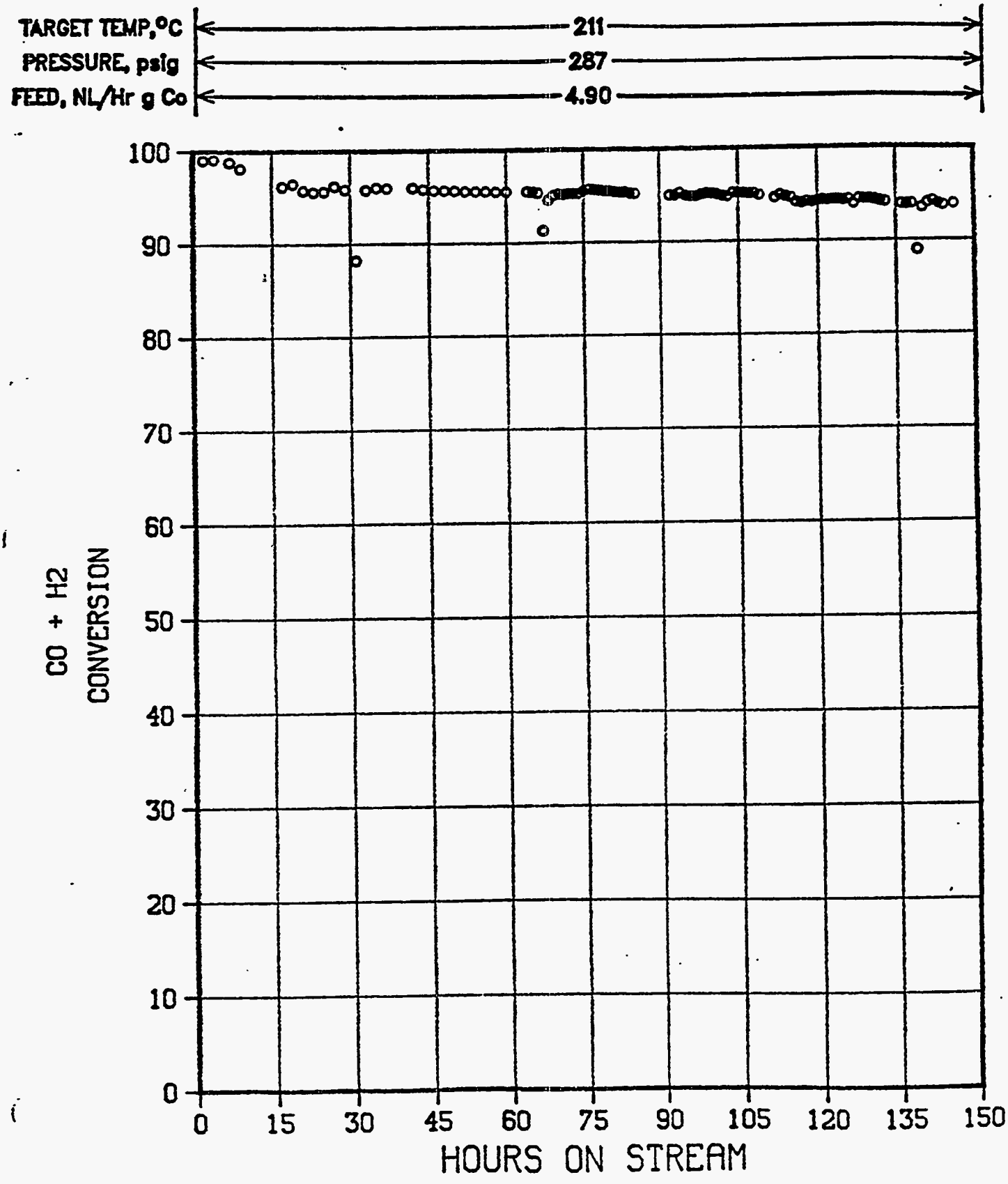

FIGURE 118

PLANT 700 RUN 101 Co,Mn,Zr,Ru ON HCL Washed Y

6827–95 w/27.4 % Co via eth–glycol pore fill

18g unreduced active in 160g quartz sand

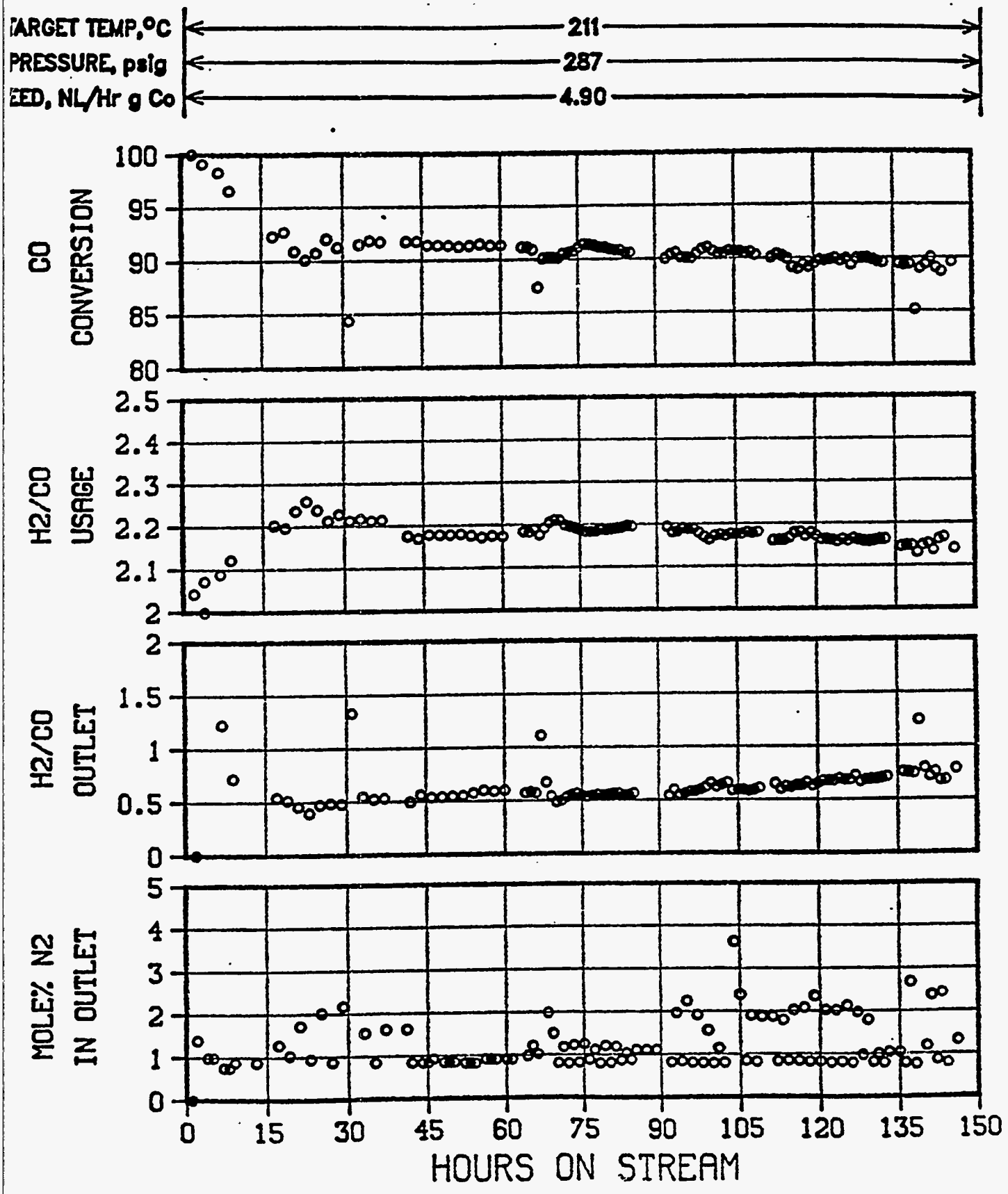

FIGURE 119

PLANT 700 RUN 101 Co,Mn,Zr,Ru ON HCL Washed Y

6827–95 w/27.4 % Co via eth–glycol pore fill
18g unreduced active in 160g quartz sand

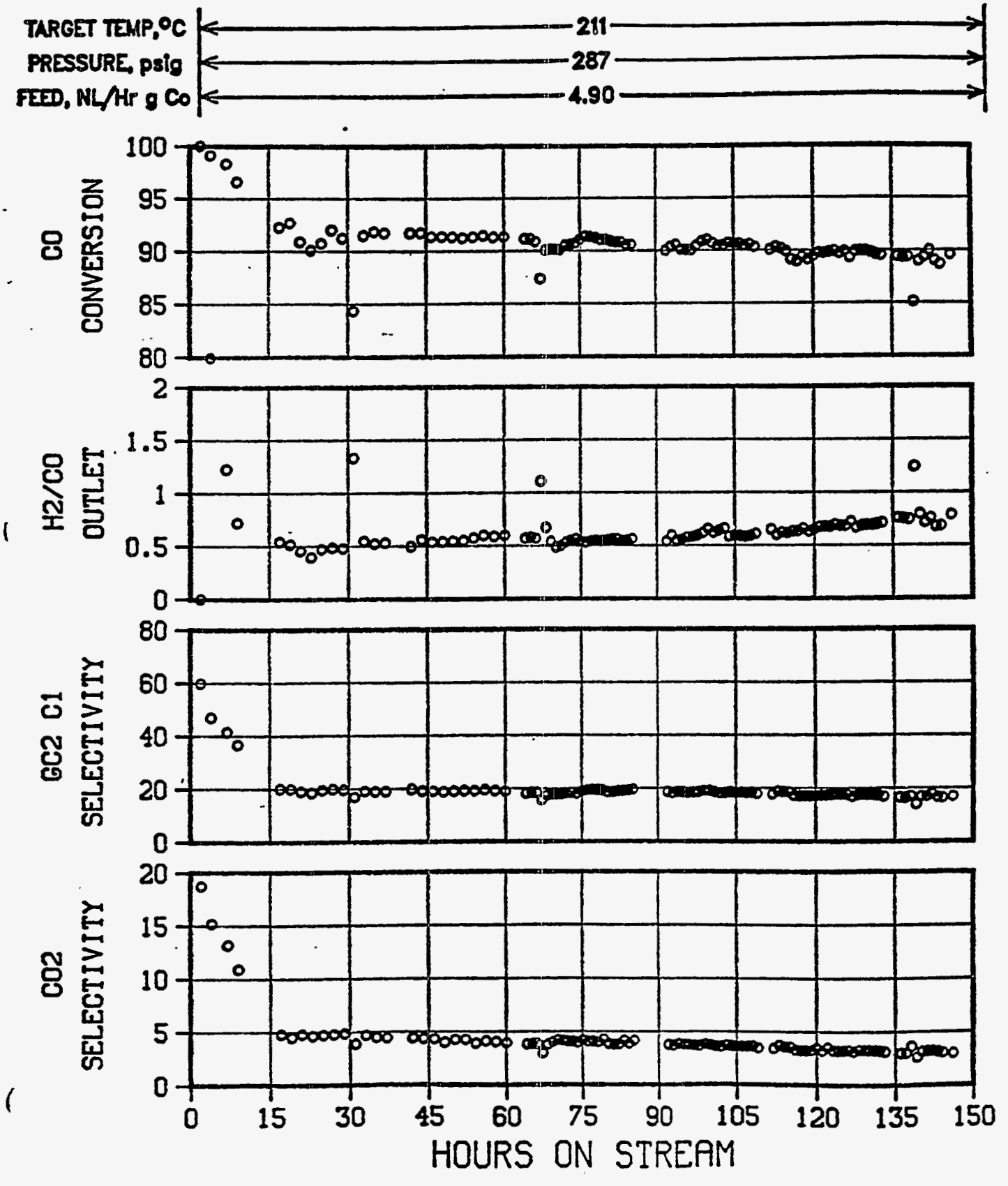

FIGURE 120

PLANT 700 RUN 101 Co,Mn,Zr,Ru ON HCL Washed Y

6827–95 w/27.4 % Co via eth–glycol pore fill
18g unreduced active in 160g quartz sand

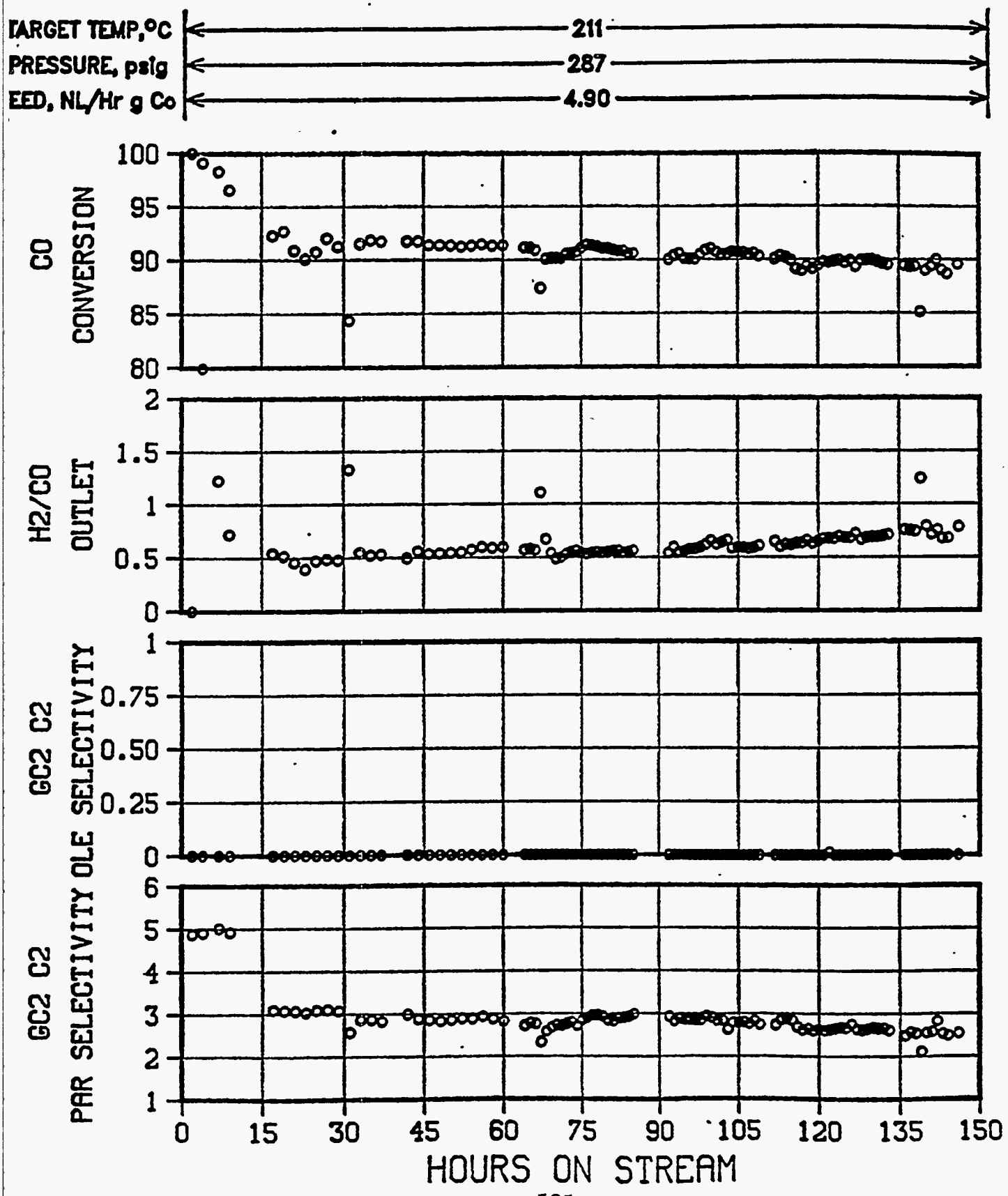

FIGURE 121

PLANT 700 RUN 101 Co,Mn,Zr,Ru ON HCL Washed Y

6827–95 w/27.4 % Co via eth–glycol pore fill

18g unreduced active in 160g quartz sand

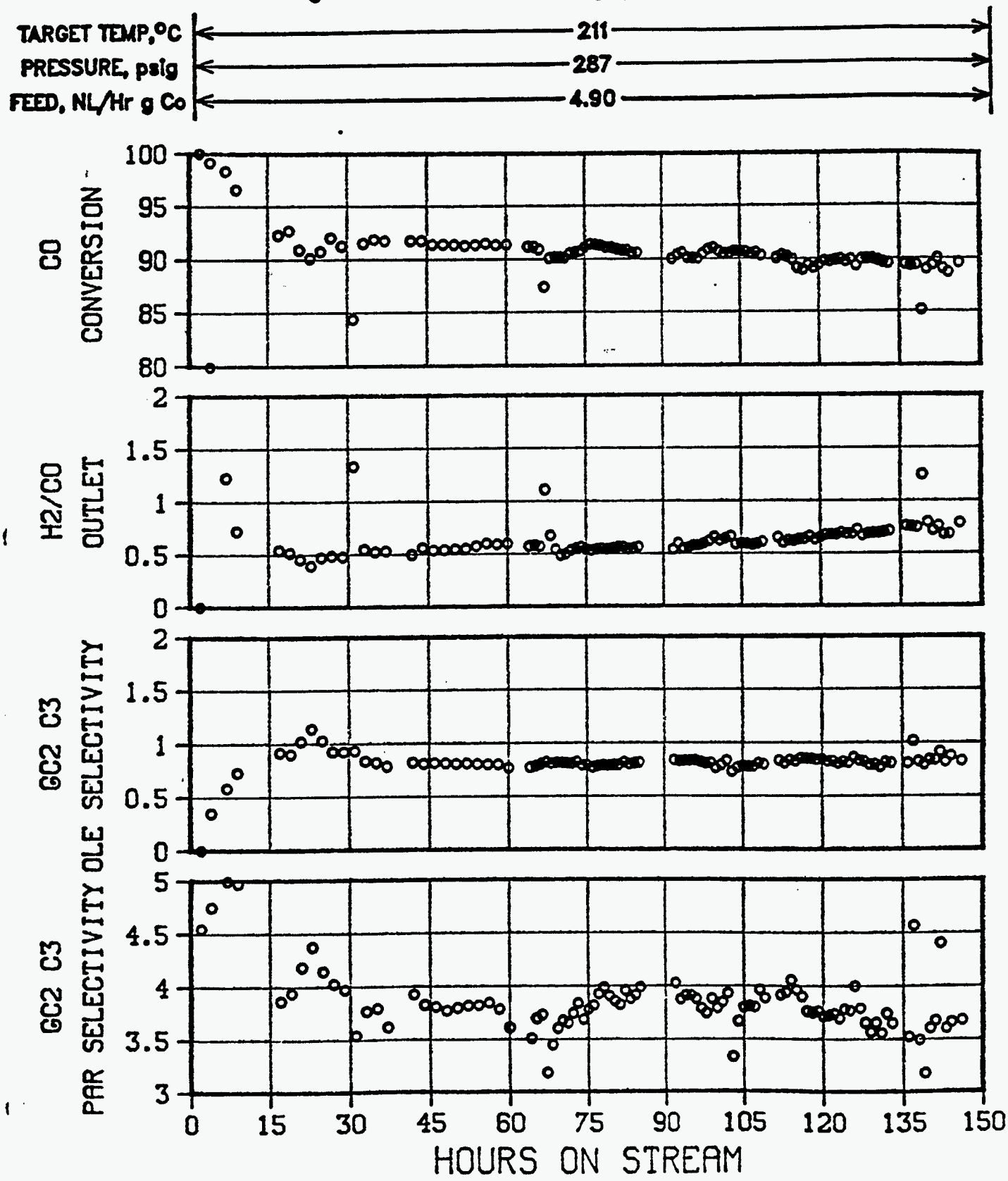

FIGURE 122

PLANT 700 RUN 101 Co,Mn,Zr,Ru ON HCL Washed Y

6827-95 w/27.4 % Co via eth-glycol pore fill

18g unreduced active in 160g quartz sand

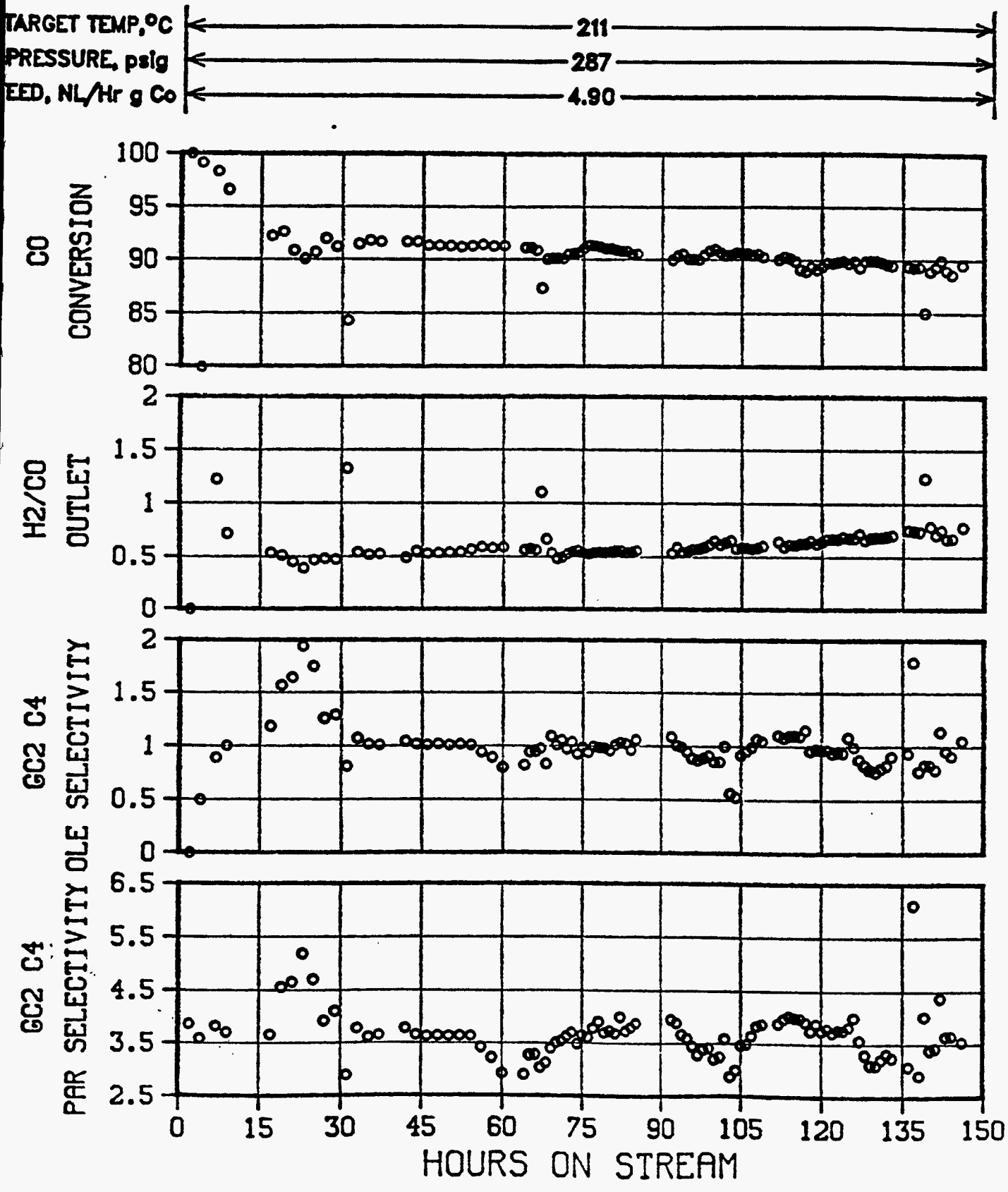

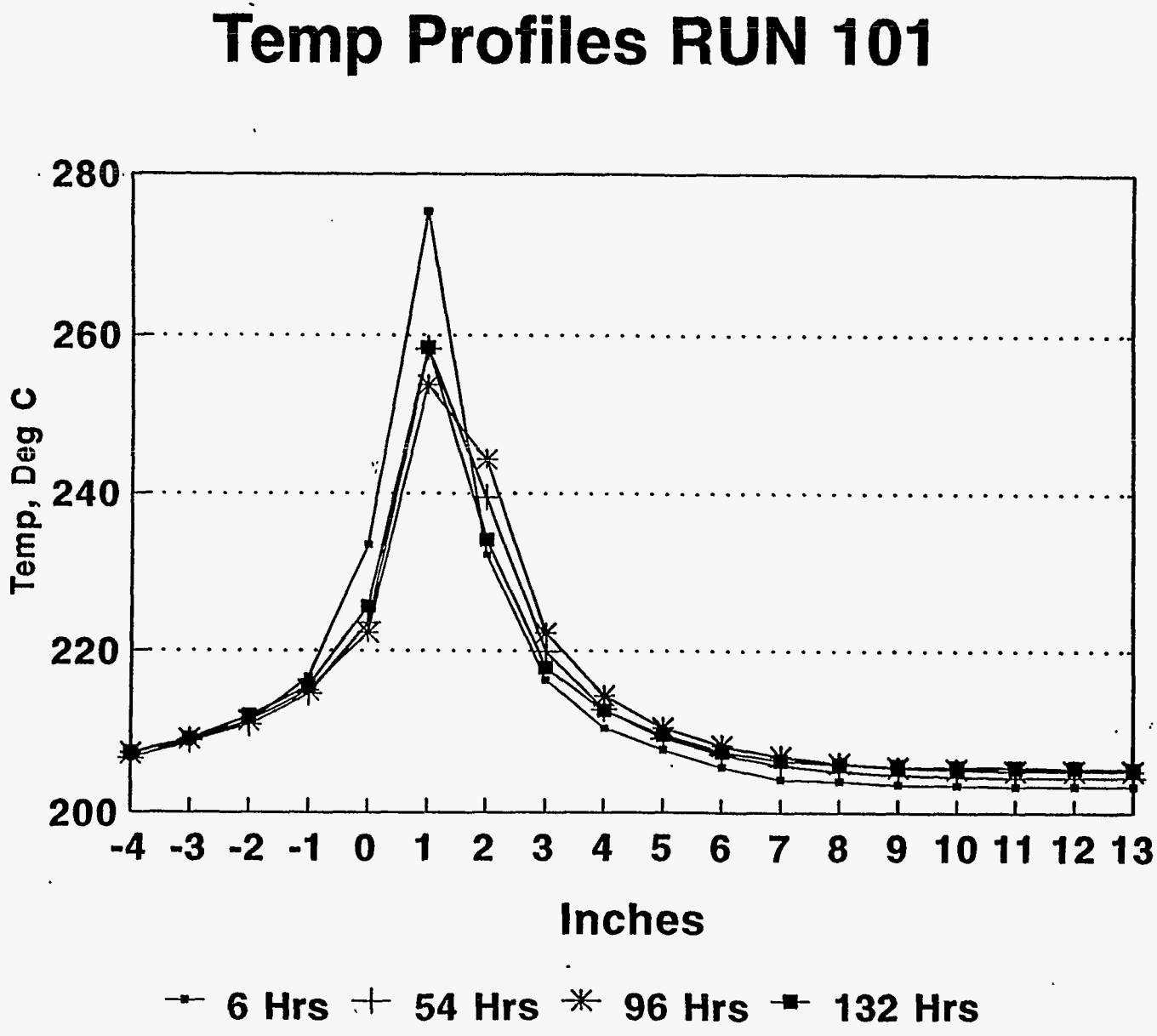
Temp Profiles RUN 101
Temp, Deg C
280
260
240
220
200
-4 -3 -2 -1 0 1 2 3 4 5 6 7 8 9 10 11 12 13
Inches
6 Hrs
54 Hrs
96 Hrs
132 Hrs

FIGURE 123

FIGURE 124

PLT 700A RUN 110 Co,Mn,Zr,Ru on HCl Washed Y

6827–123 w/26.8 % Co via eth–glycol pore fill

6.5 unreduced active in 166.5g quartz sand

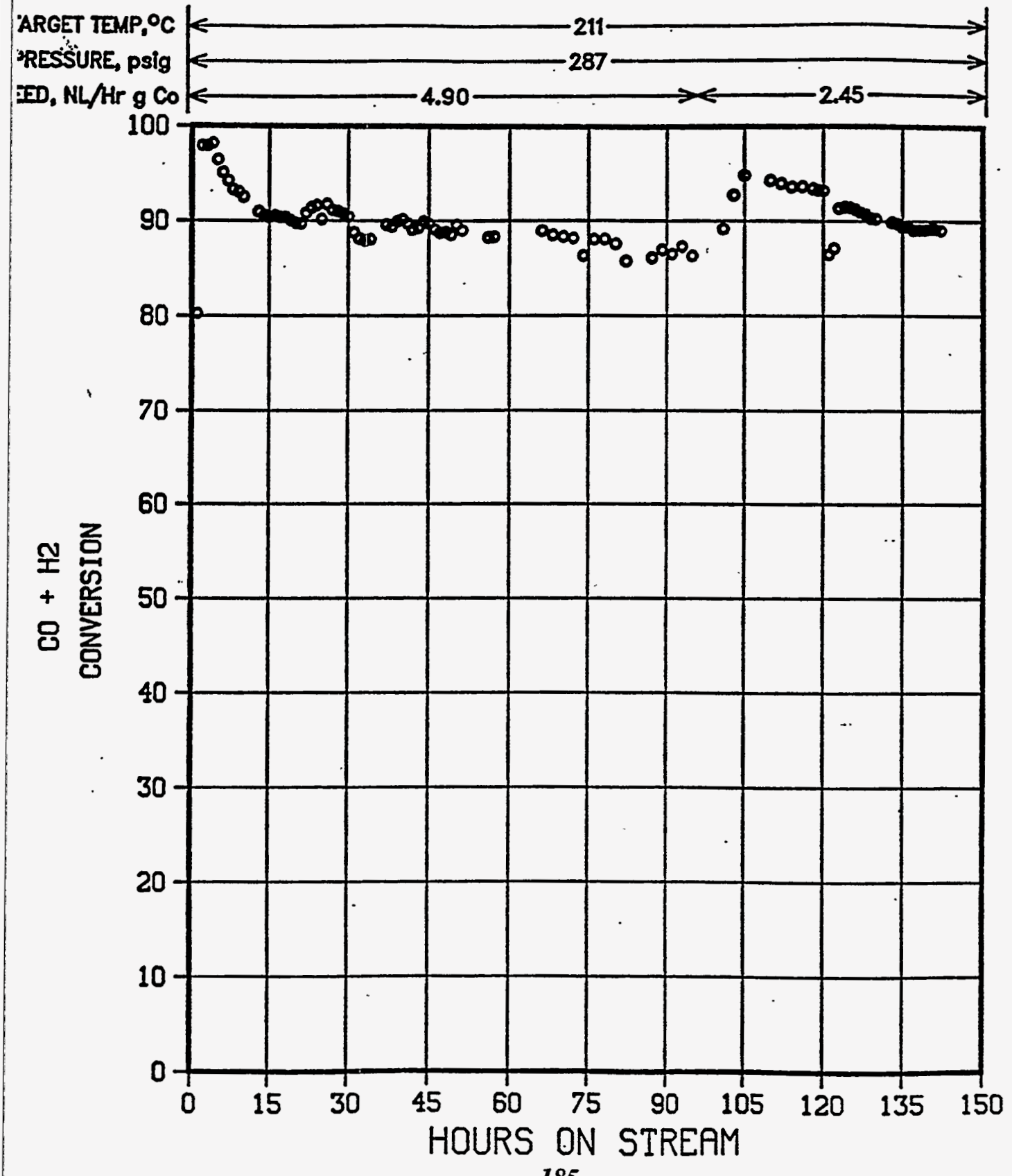

FIGURE 125

PLT 700A RUN 110 Co,Mn,Zr,Ru on HCl Washed Y

6827–123 w/26.8 % Co via eth–glycol pore fill

6.5 unreduced active in 166.5g quartz sand

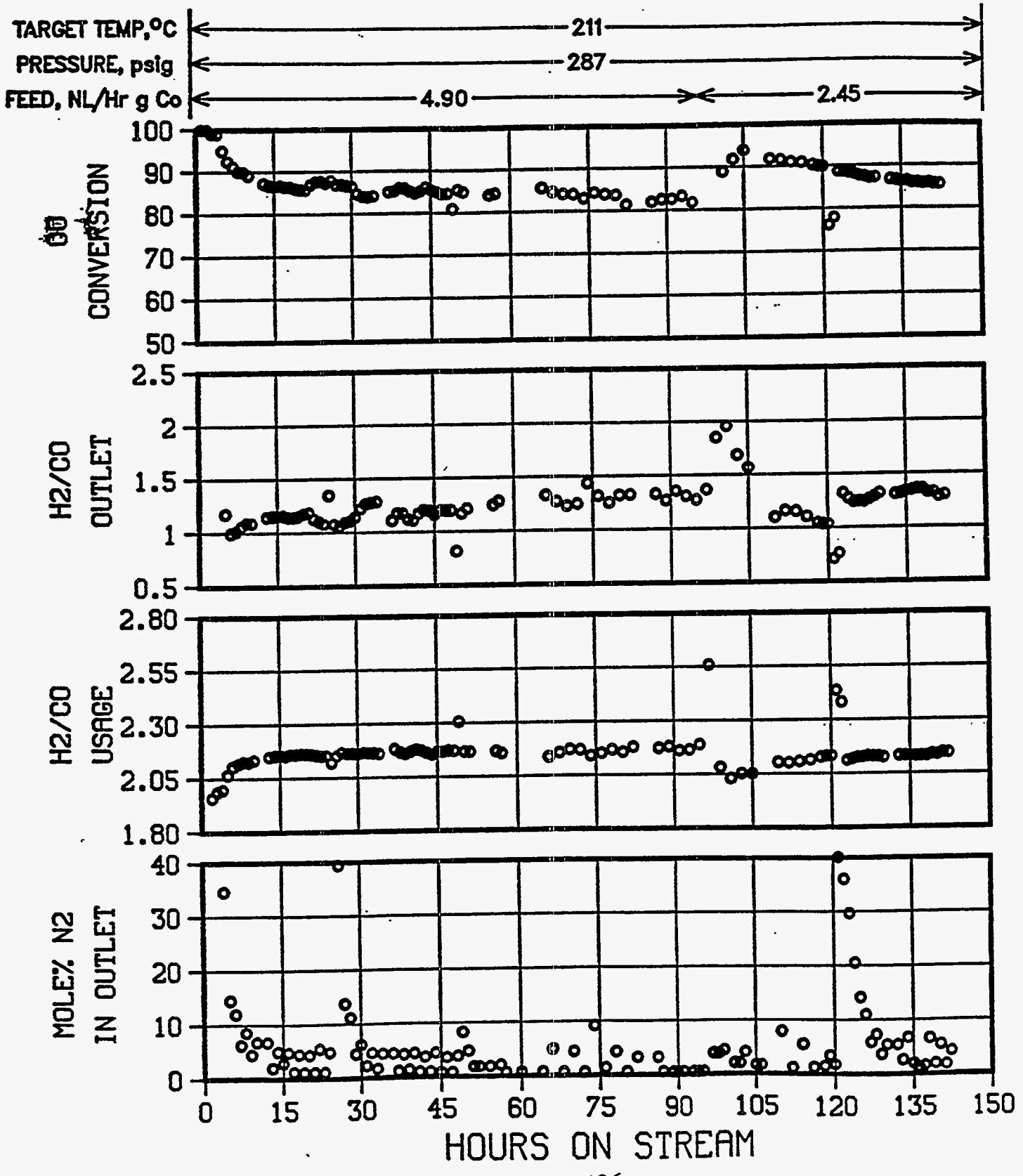

FIGURE 126

PLT 700A RUN 110 Co,Mn,Zr,Ru on HCl Washed Y

6827-123 w/26.8 % Co via eth-glycol pore fill

6.5 unreduced active in 166.5g quartz sand

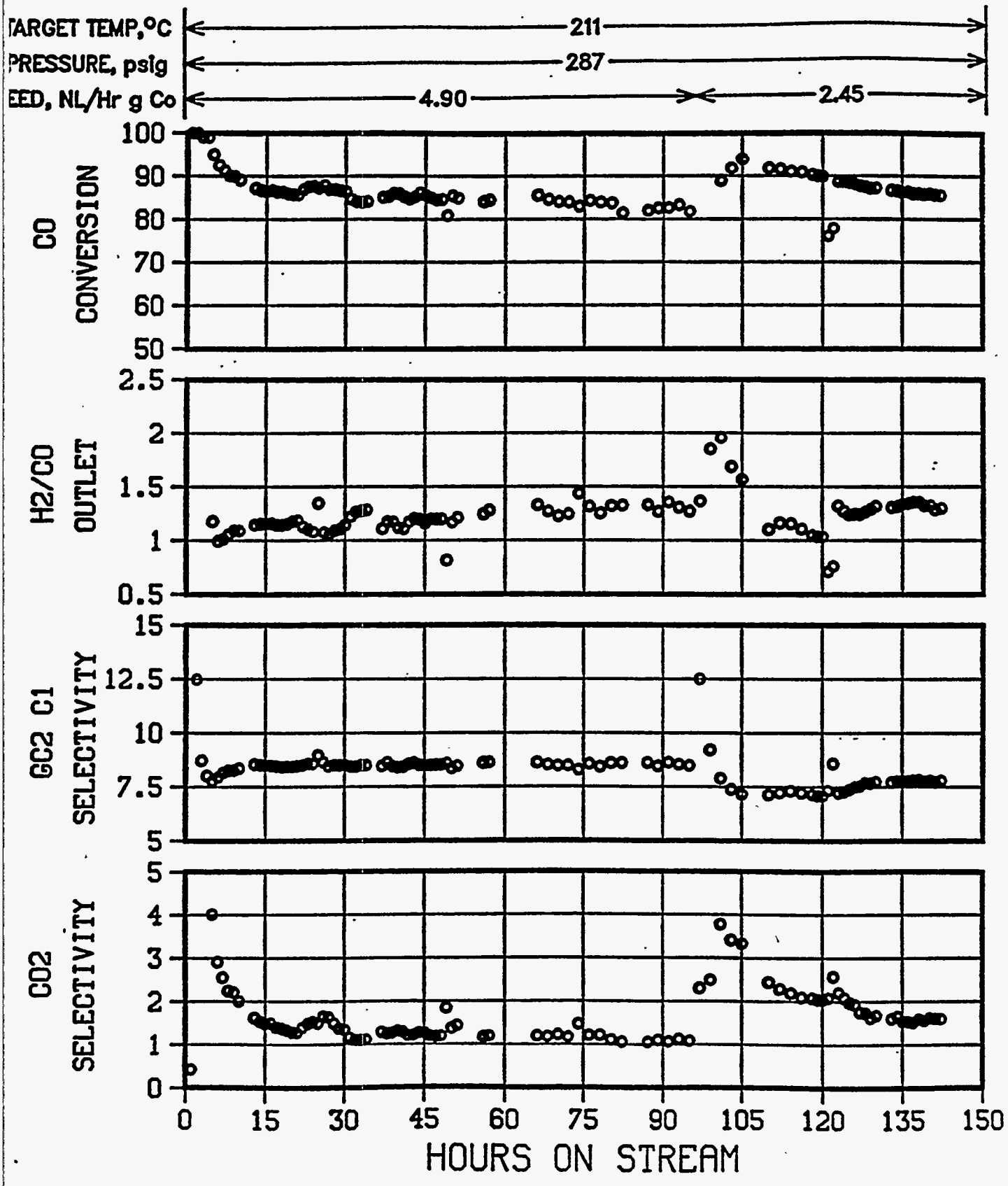

FIGURE 127

PLT 700A RUN 110 Co,Mn,Zr,Ru on HCl Washed Y

6827–123 w/26.8 % Co via eth–glycol pore fill

6.5 unreduced active in 166.5g quartz sand

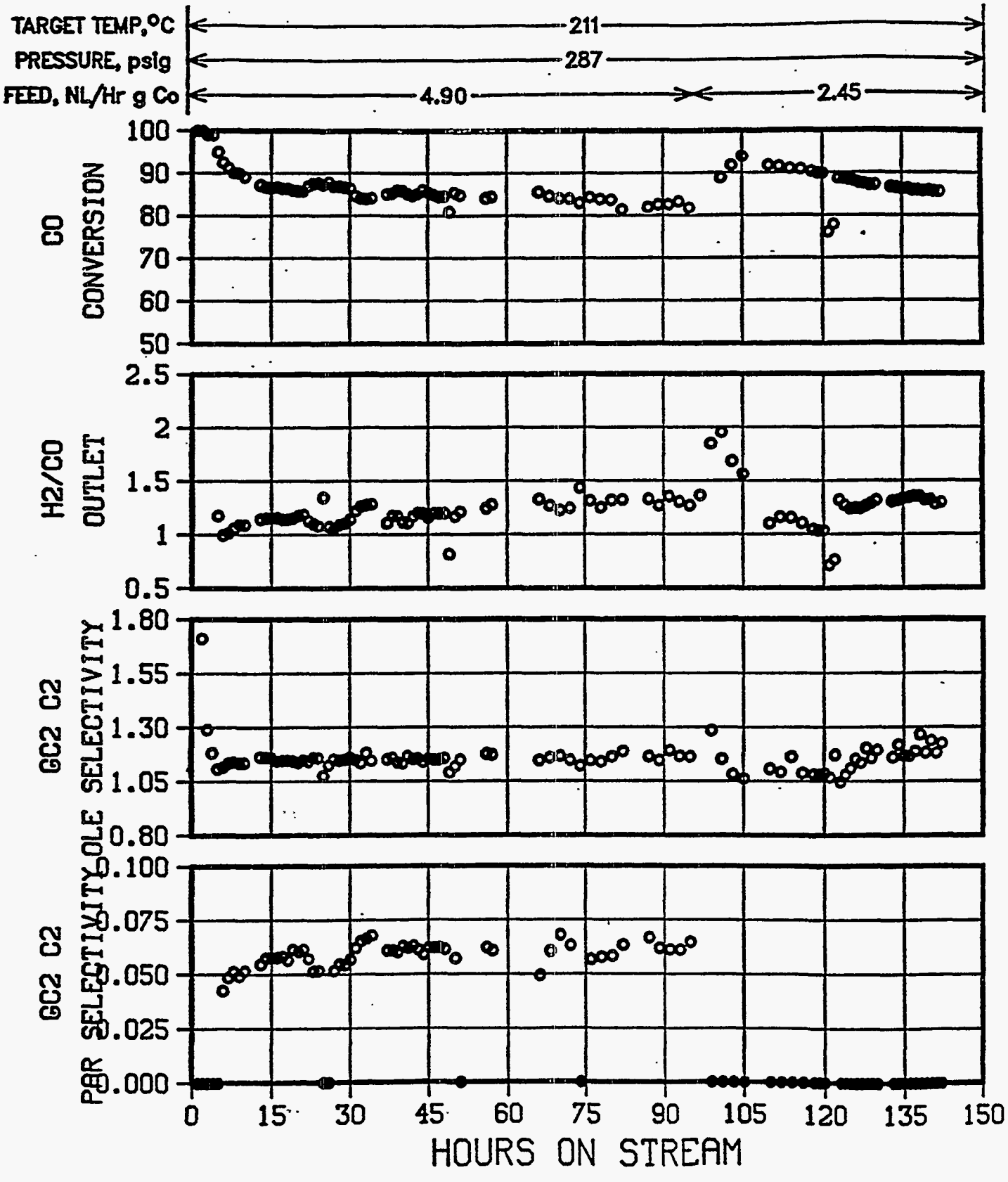

FIGURE 128

PLT 700A RUN 110 Co,Mn,Zr,Ru on HCl Washed Y

6827–123 w/26.8 % Co via eth–glycol pore fill

6.5 unreduced active in 166.5g quartz sand

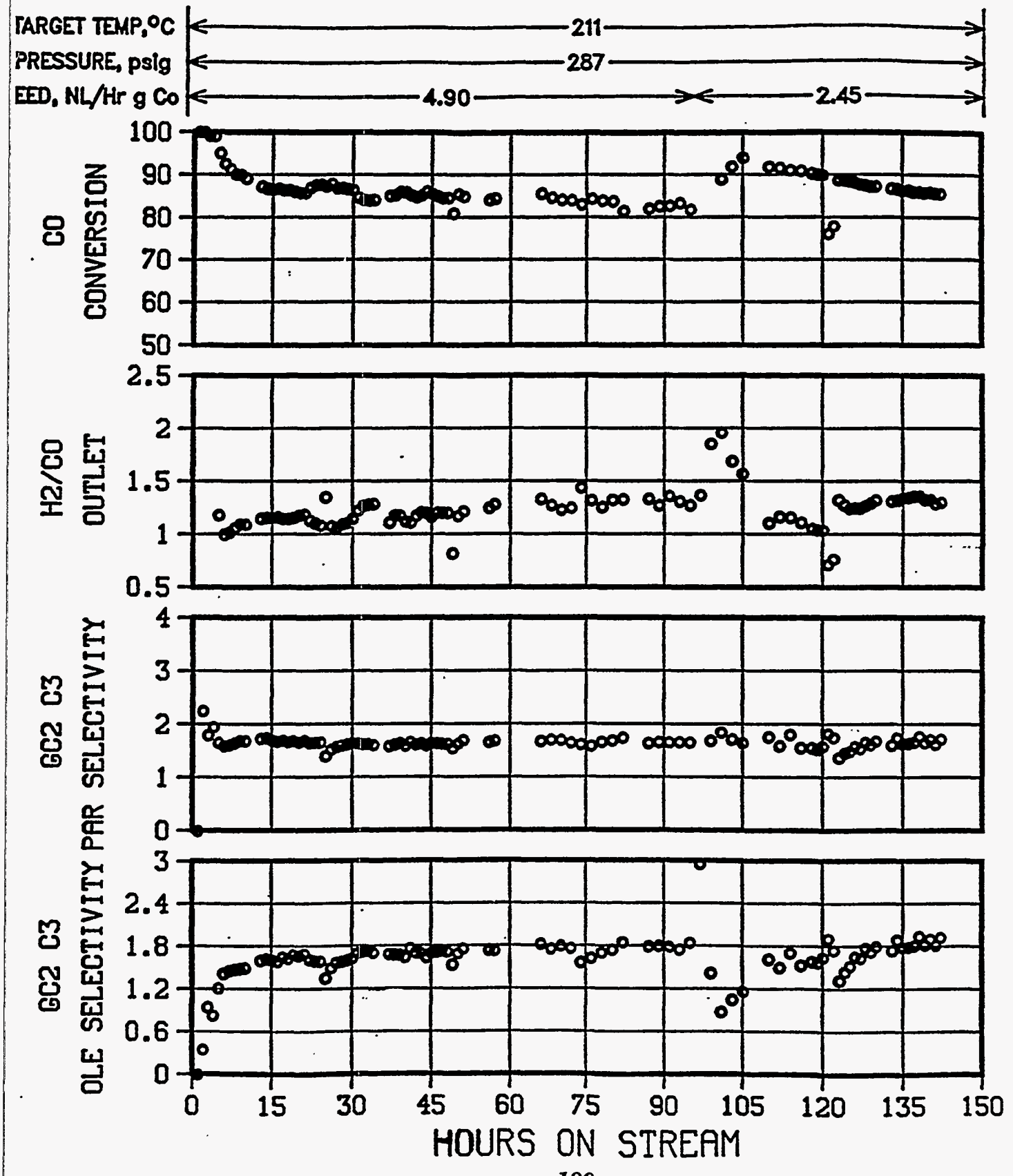

FIGURE 129

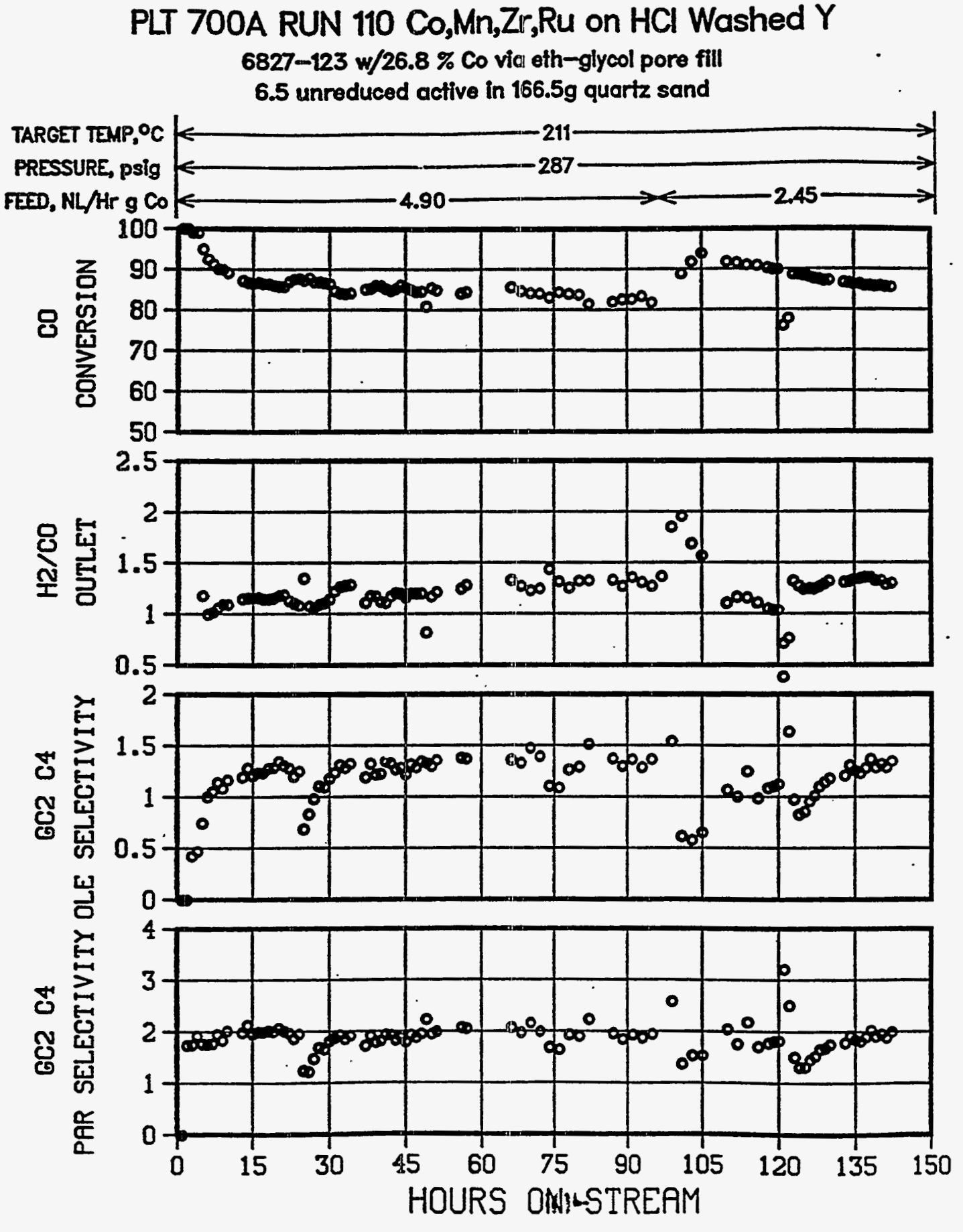
PLT 700A RUN 110 Co,Mn,Zr,Ru on HCl Washed Y
6827-123 w/26.8 % Co via eth-glycol pore fill
6.5 unreduced active in 166.5g quartz sand
TARGET TEMP,°C
211
PRESSURE, psig
287
FEED, NL/Hr g Co
4.90
2.45
CO CONVERSION
100
90
80
70
60
50
H2/CO OUTLET
2.5
2
1.5
1
0.5
GC2 C4 OLE SELECTIVITY
2
1.5
1
0.5
0
GC2 C4 PAR SELECTIVITY
4
3
2
1
0
0
15
30
45
60
75
90
105
120
135
150
HOURS ON-STREAM

FIGURE 130

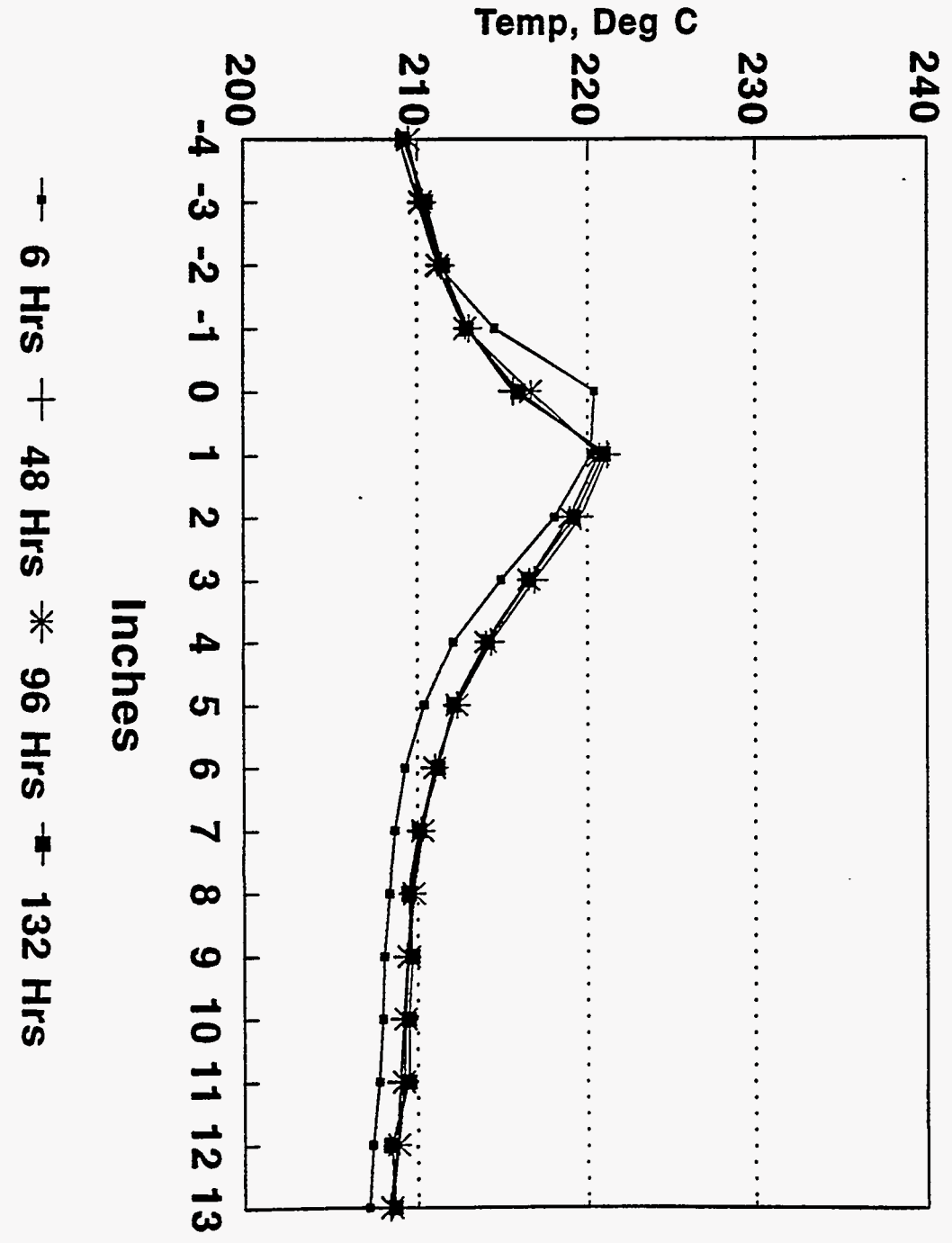
Temp Profiles RUN 110
Temp, Deg C
200
210
220
230
240
-4 -3 -2 -1 0 1 2 3 4 5 6 7 8 9 10 11 12 13
Inches
6 Hrs
48 Hrs
96 Hrs
132 Hrs

FIGURE 131

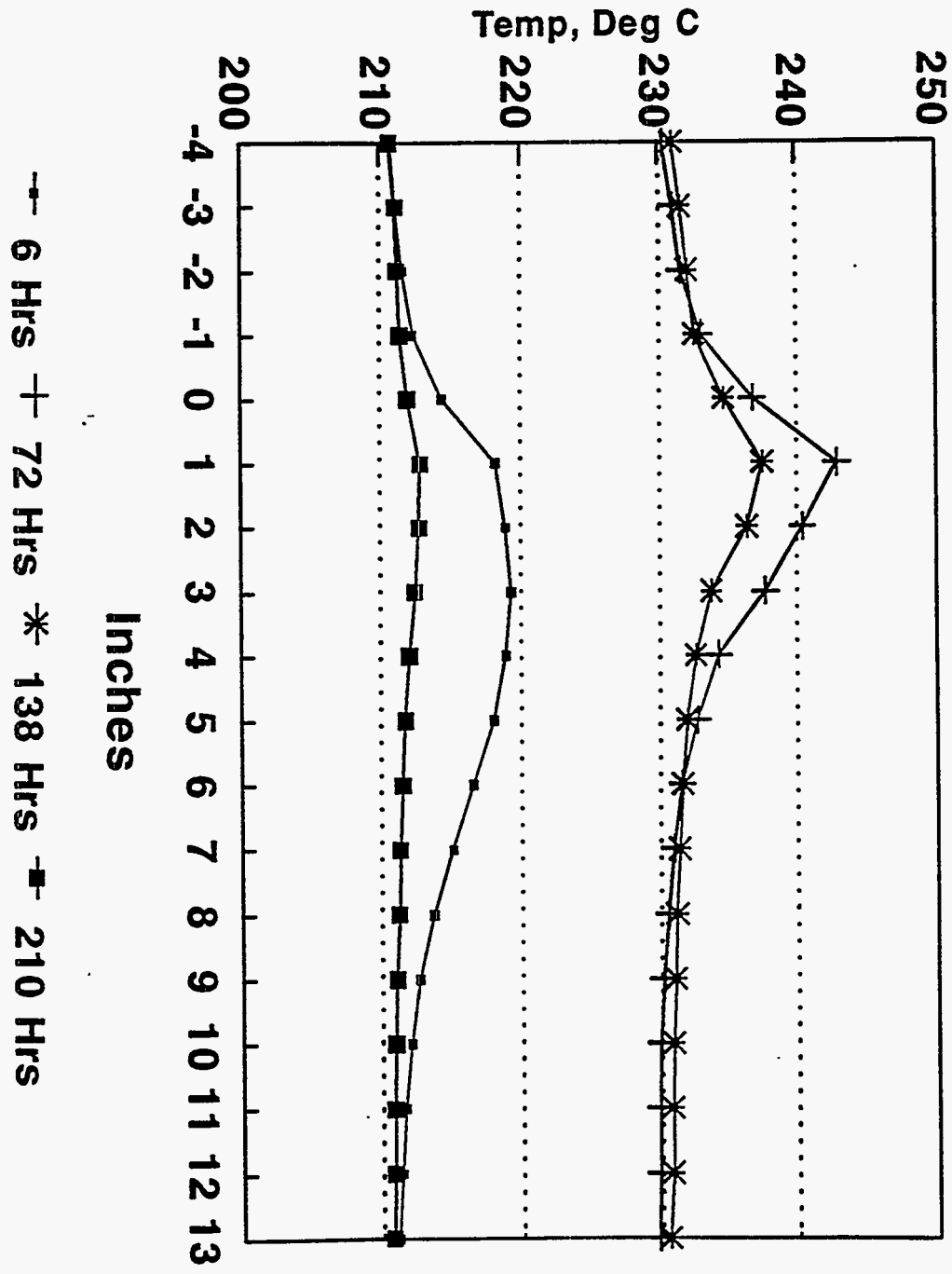
Temp Profiles RUN 97
Temp, Deg C
200
210
220
230
240
250
-4 -3 -2 -1 0 1 2 3 4 5 6 7 8 9 10 11 12 13
Inches
6 Hrs
72 Hrs
138 Hrs
210 Hrs

COMPARISON OF HIGH AND VERY HIGH COBALT LEVEL CATALYSTS
SUMMARY OF SCREENING IN FIXED-BED PLANT

RUN NO.	97	101	110
LOADING			
CATALYST, G	13 (17.6% Co)	13 (27.4% Co)	6.5 (26.8% Co)
DILUENT, G	160	160	166.5
CATALYST PRETREAT.	350° C/H_2/2 HRS		
TEST CONDITIONS			
FEED H_2/CO	2.1		
FEED RATE (NL/HR·G Co)	4.9		
TEMP, °C	211(INLET)		
PRESSURE, PSIG	287		
PERFORMANCE SUMMARY[1]			
CONVERSION, %			
CO + H_2	78	95	86
CO	72	90	82
SELECTIVITY, MOLE %			
C_1	13	20	8.6
C_2	1.8	2.6	1.2
$C_2^=$	0.1	0.0	0.0
C_3	3.0	3.7	1.8
$C_3^=$	2.1	0.8	1.8
CO_2	0.8	3.0	1.0

1. AT 100 HOURS ON STREAM

FIGURE 132

CATALYST PRECURSORS: SUPPORTED OXIDES ON STEAMED/ACID-WASHED Y ZEOLITES

SUPPORT PROPERTIES				CATALYST NO./ RUN NO.	CATALYST METALS, AAS WT%			
TRTMNTS	X-RAY[1]	SA[2]/PV[3]	Al[4]		Co	Mn	Zr	Ru
STMD/ HCl[5]	84.2 ± 0.3[6]	582/0.56[7]	0.46	6827-81/97	17.6	2.0	1.6	1.0
	84.5 ± 0.3[6]	574/0.54[7]	0.48	6827-95/101	27.4	1.1	1.6	0.3
		561/0.54[7]	0.37	6827-123/110	26.8	2.3	1.0	0.4
		588/0.55[8]	0.59	6827-160/122	28.5	1.7	1.3	0.5
		588/0.55[8]	0.59	6827-161/123	28.7	1.8	1.1	

1. ABSOLUTE INTENSITY VS. LZ 210 (UNSTEAMED Y ZEOLITE) WHICH = 99.7 ± 1.7.
2. m^2/g
3. cc/g
4. wt %
5. WASH 3 HOURS WITH 4M HCl.
6. BEFORE ACID WASH: 591 m^2/g, 0.5 cc/g.
7. BEFORE ACID WASH: 86.3 ± 0.3.
8. FROM WASH OF THE SECOND OF TWO COMMERCIAL STEAMED Y-ZEOLITES USED IN THIS WORK.

FIGURE 133

FIGURE 134

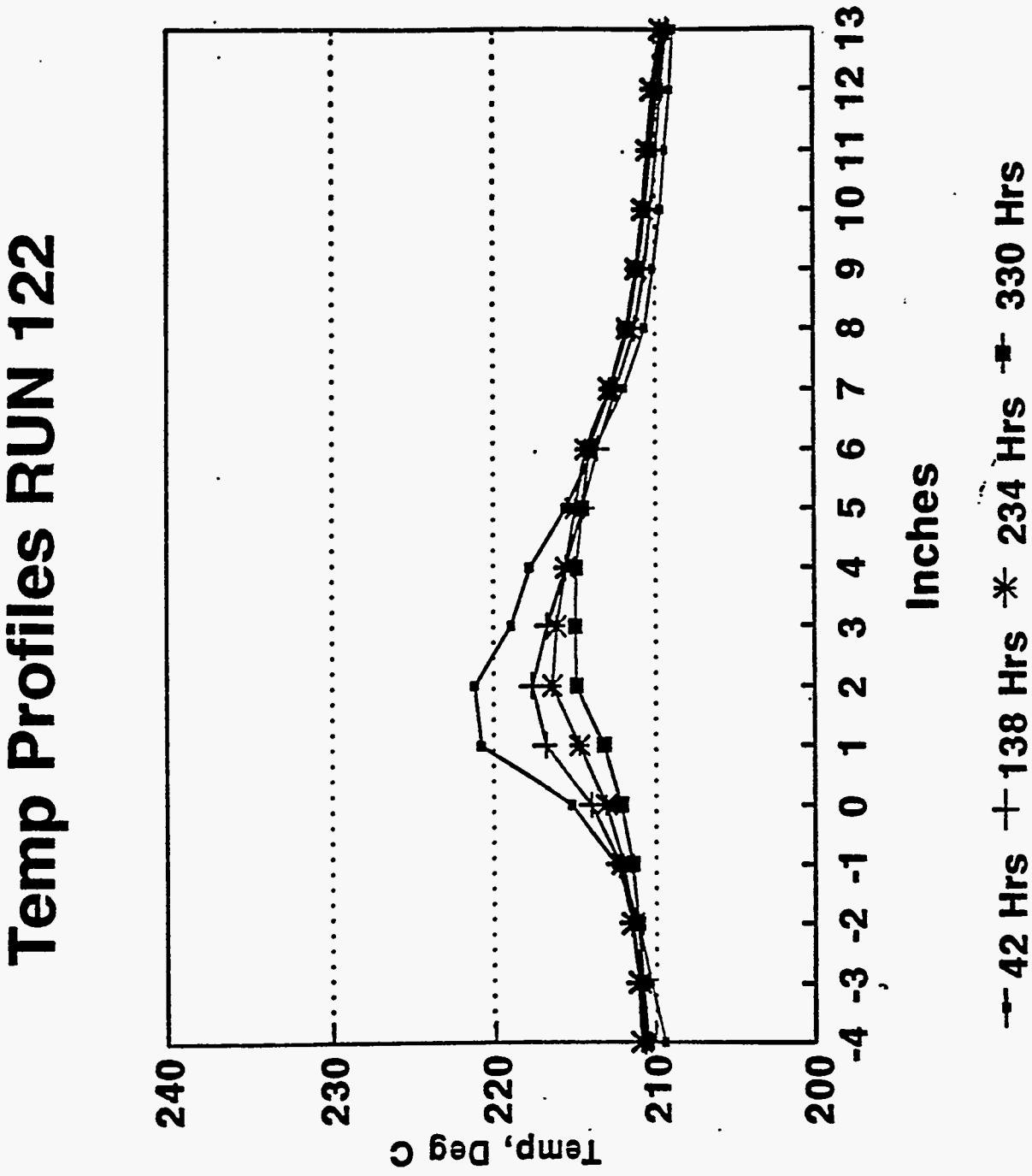
Temp Profiles RUN 122
Temp, Deg C
240
230
220
210
200
-4 -3 -2 -1 0 1 2 3 4 5 6 7 8 9 10 11 12 13
Inches
42 Hrs
138 Hrs
234 Hrs
330 Hrs

FIGURE 135

PLT 700 RUN 122 Co;Mn,Zr,Ru On steamed, acid washed Y-ZLT

6827-160w/28.5 % Co via eth-glycol pore fill

6.5g active in 166.5g quartz sand 5/31--->6/14/93

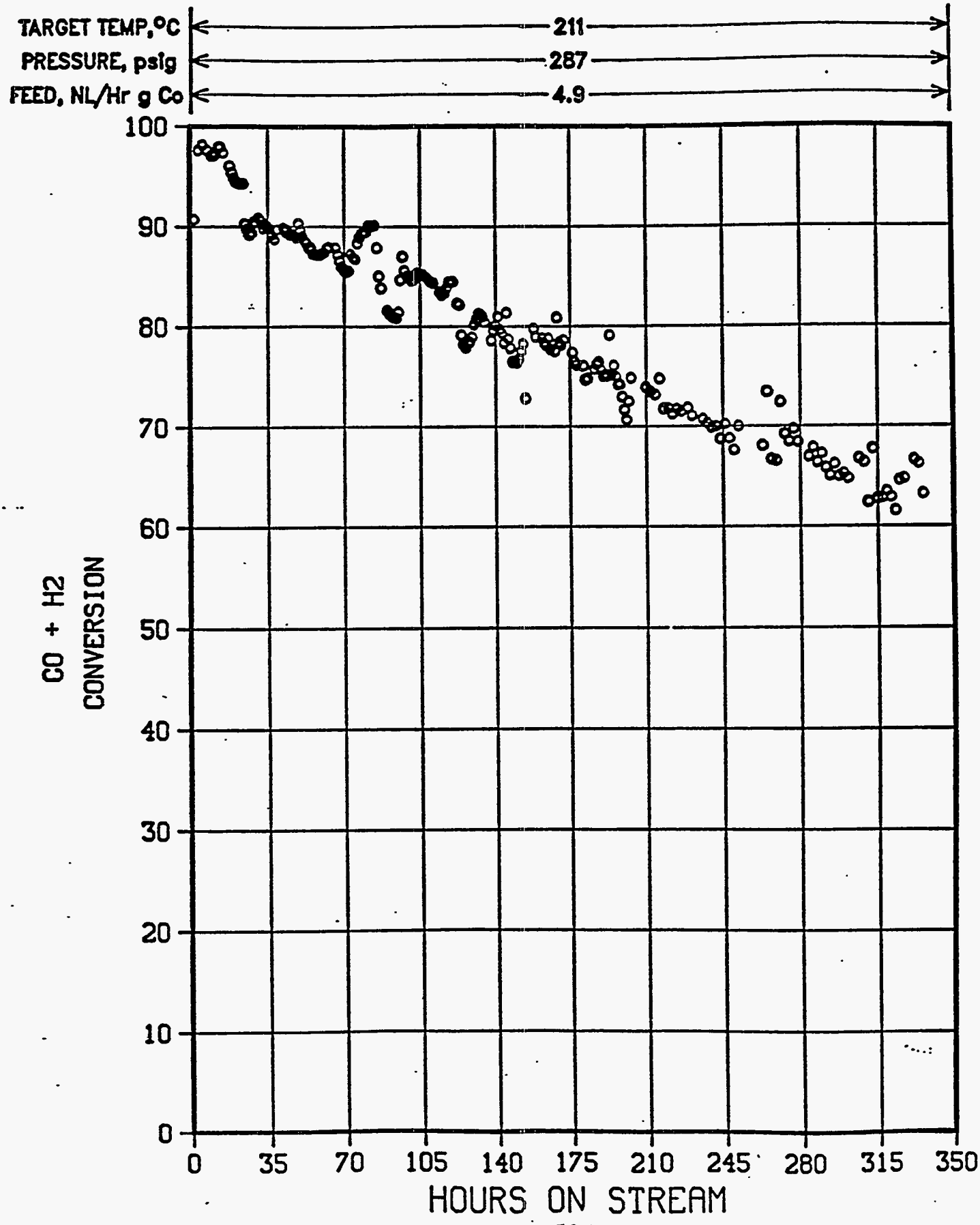

FIGURE 136

T 700 RUN 122 Co,Mn,Zr,Ru On steamed, acid washed Y–ZLT

6827–160w/28.5.% Co via eth–glycol pore fill

6.5g active in 166.5g quartz sand 5/31---->6/14/93

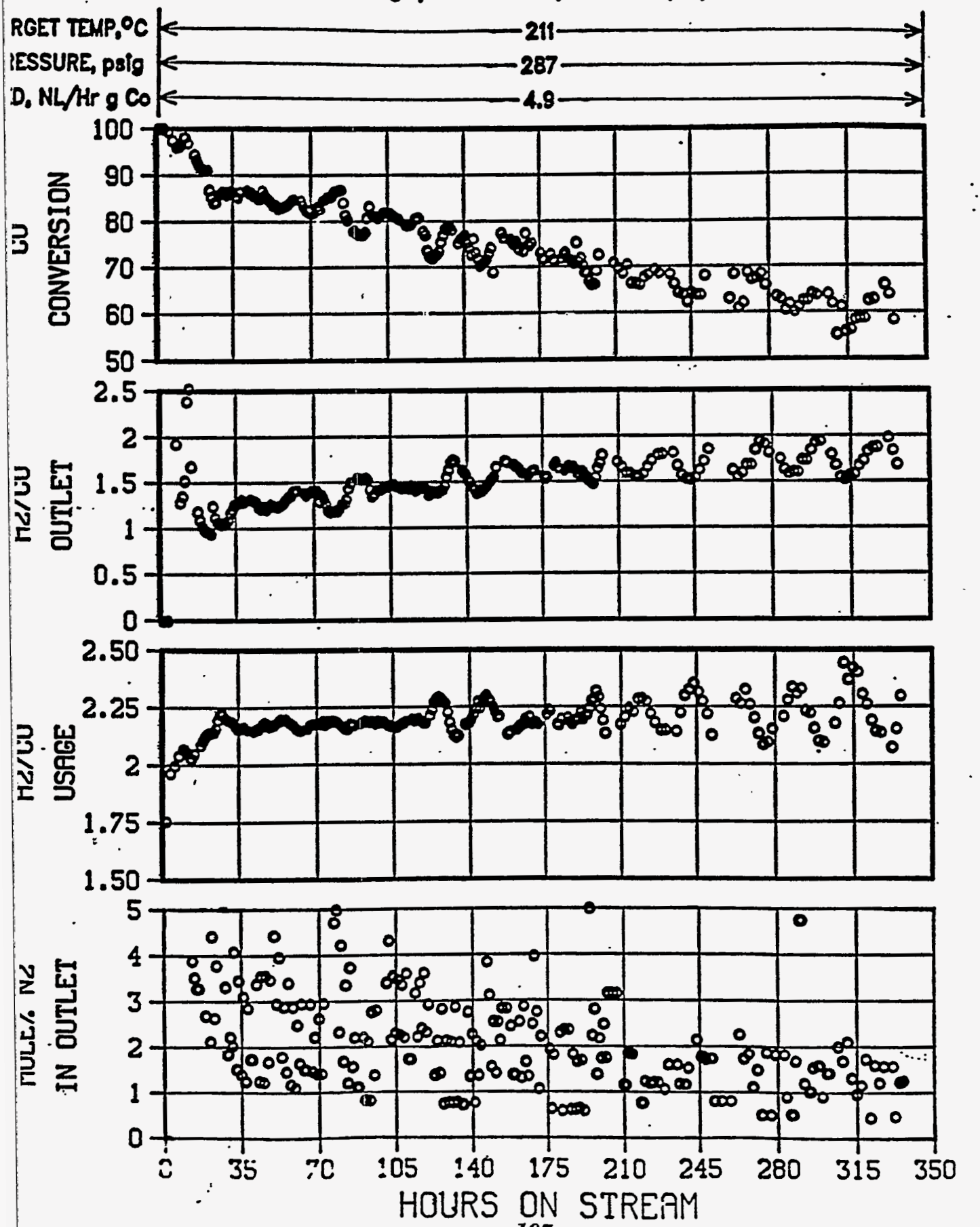

FIGURE 137

PLT 700 RUN 122 Co,Mn,Zr,Ru On steamed, acid washed Y-ZLT

6827-160 w/28.5 % Co via eth-glycol pore fill

6.5g active in 166.5g quartz sand 5/31--->6/14/93

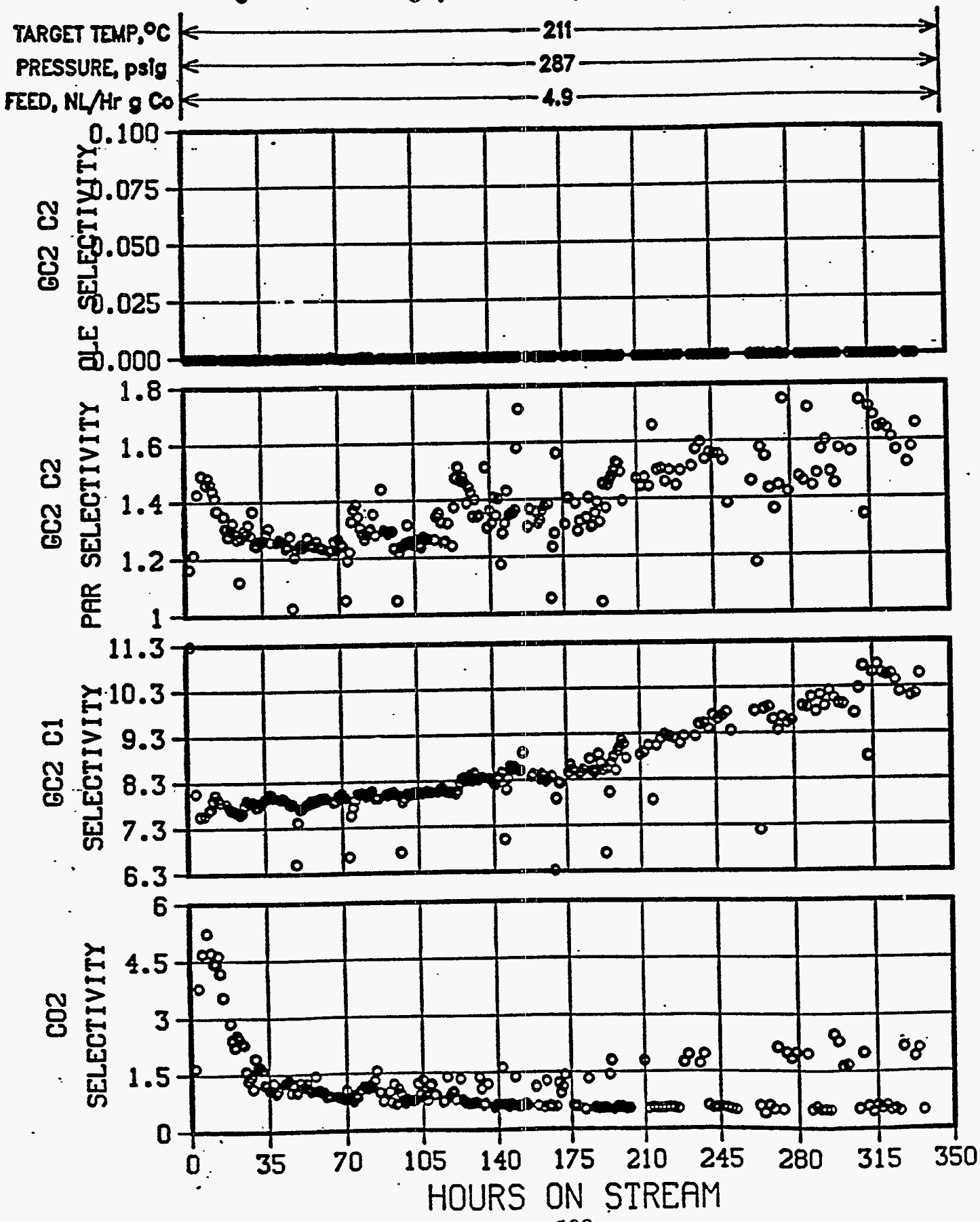

FIGURE 138

LT 700 RUN 122 Co,Mn,Zr,Ru On steamed, acid washed Y–ZLT

6827–160w/28.5 % Co via eth–glycol pore fill

6.5g active in 166.5g quartz sand 5/31--->6/14/93

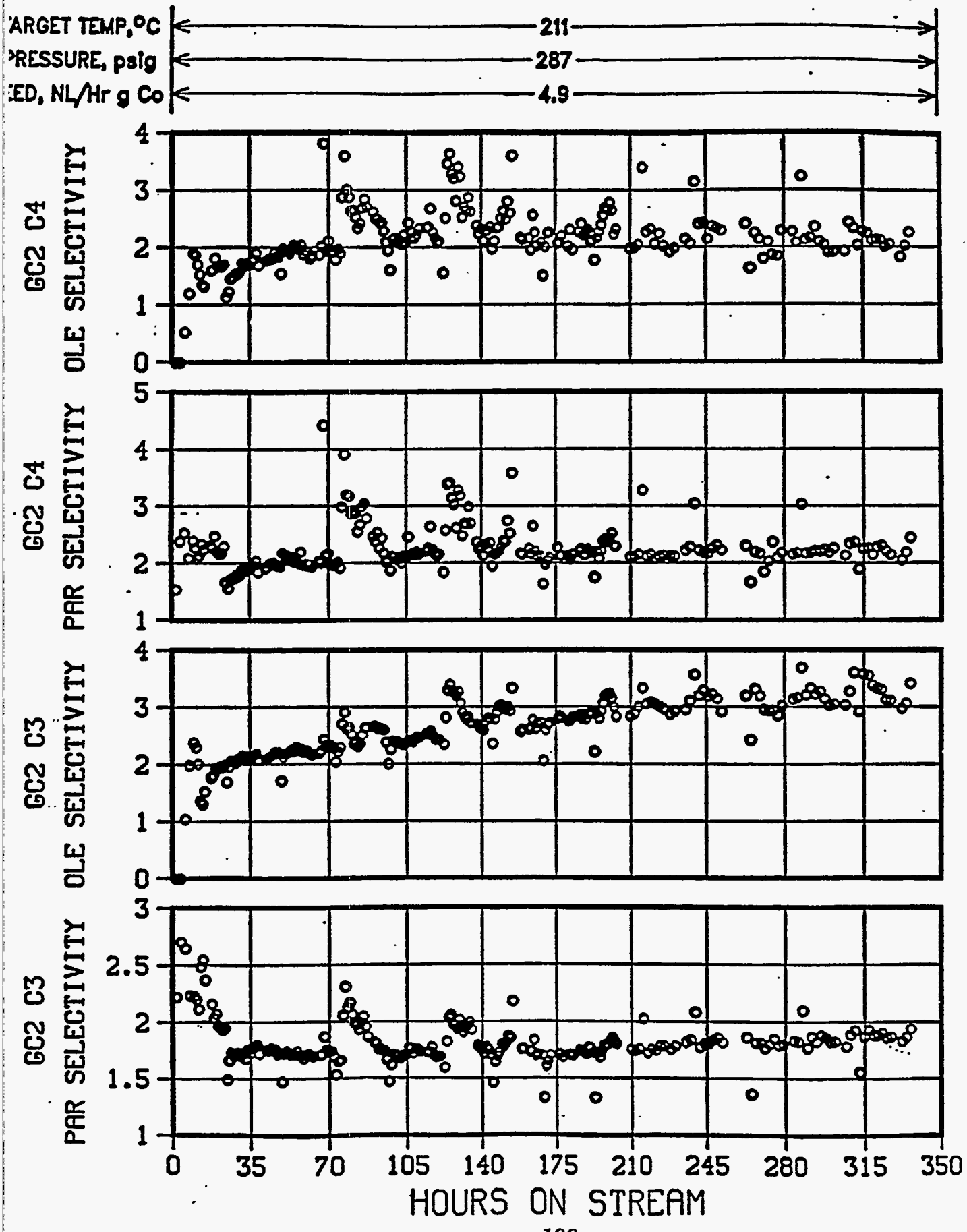

FIGURE 139

PLT 700 RUN 122 Co,Mn,Zr,Ru On steamed, acid washed Y-ZLT

6827-160w/28.5 % Co via eth-glycol pore fill

6.5g active in 166.5g quartz sand 5/31--->6/14/93

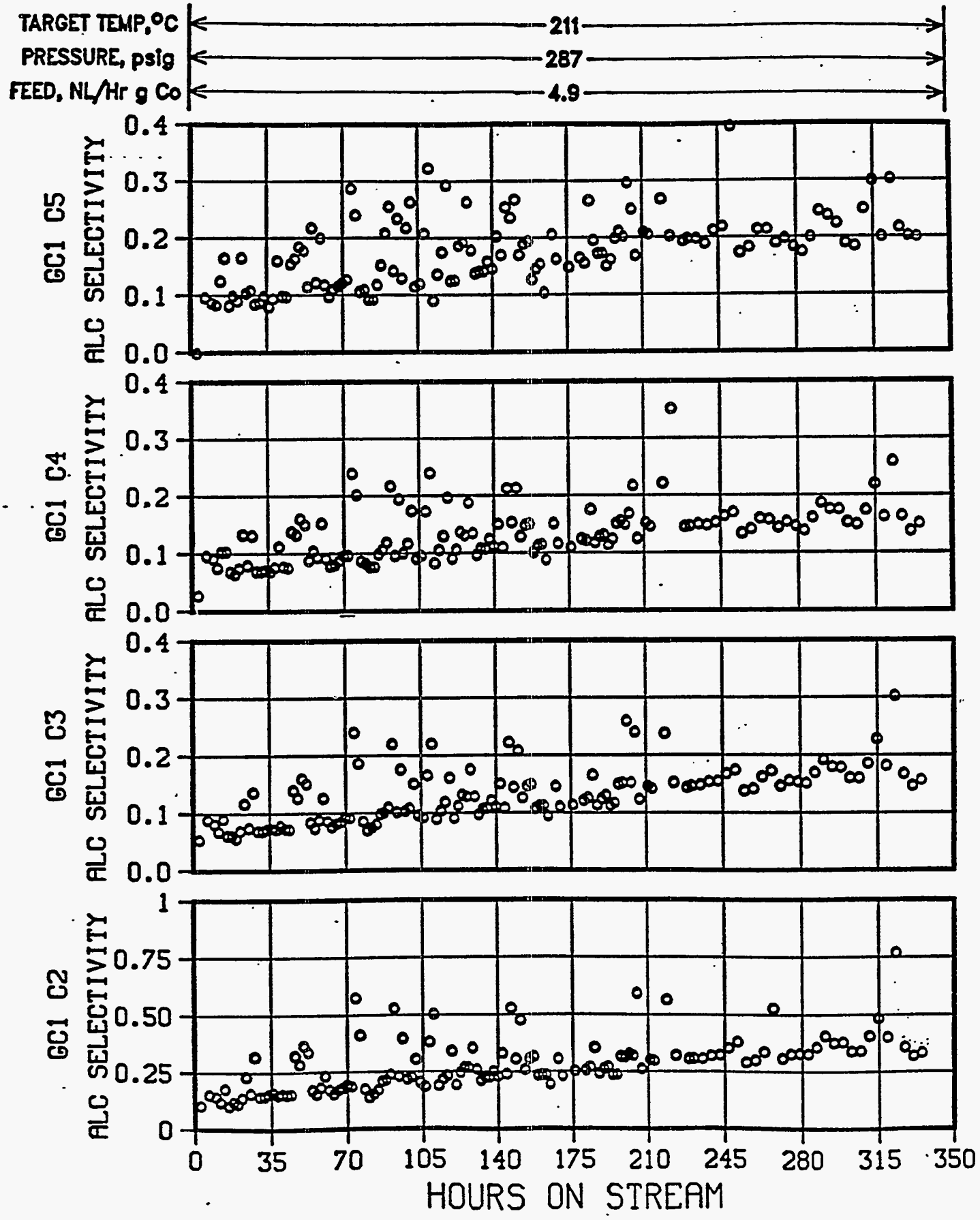

FIGURE 140

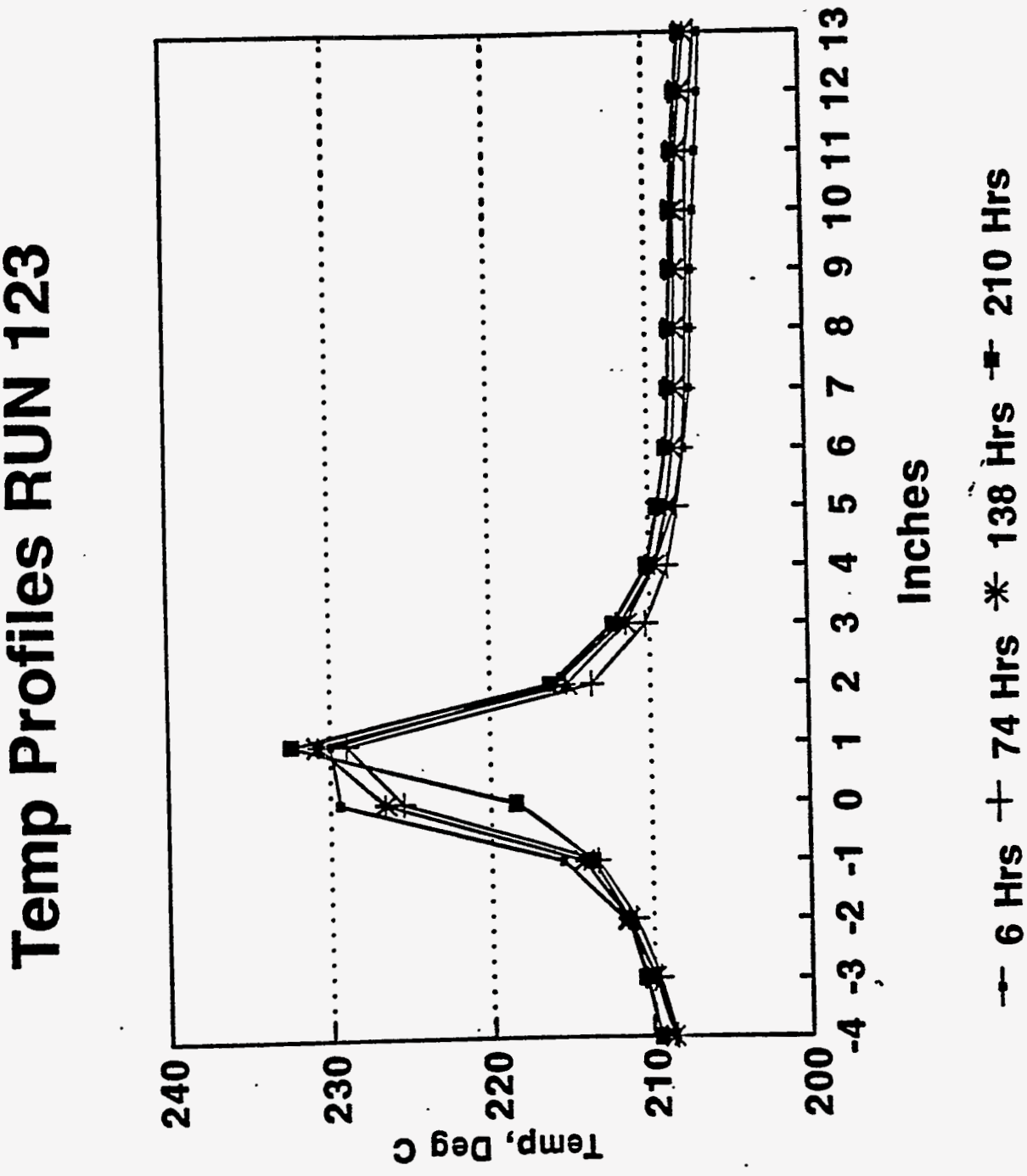
Temp Profiles RUN 123
Temp, Deg C
240
230
220
210
200
-4 -3 -2 -1 0 1 2 3 4 5 6 7 8 9 10 11 12 13
Inches
6 Hrs
74 Hrs
138 Hrs
210 Hrs

COMPARISON OF HIGH COBALT CATALYSTS WITH AND WITHOUT RUTHENIUM
SUMMARY OF SCREENING IN FIXED-BED PLANT

RUN NO.	110	123
LOADING CATALYST, G DILUENT, G	6.5 (26.8% Co/0.4% Ru) 166.5	6.5 (28.7% Co) 166.5
CATALYST PRETREAT.	350° C/H_2/2 HRS	
TEST CONDITIONS FEED H_2/CO FEED RATE (NL/HR·G Co) TEMP, °C PRESSURE, PSIG	2.1 4.9 211(INLET) 287	
PERFORMANCE SUMMARY[1]		
CONVERSION, % CO + H_2 CO	86 82	90 85
SELECTIVITY, MOLE % C_1 C_2 C_2^- C_3 C_3^- CO_2	8.6 1.2 0.0 1.8 1.8 1.0	10.5 1.5 0.0 2.1 1.0 2.5

1. AT 100 HOURS ON STREAM

FIGURE 141

FIGURE 142

PLT 700 RUN 123 Co,Mn,Zr On steamed, acid washed Y–ZLT.

6827–161 w/28.7 % Co via eth–glycol pore fill

6.5g active in 166.5g quartz sand 6/20--->6/29/93

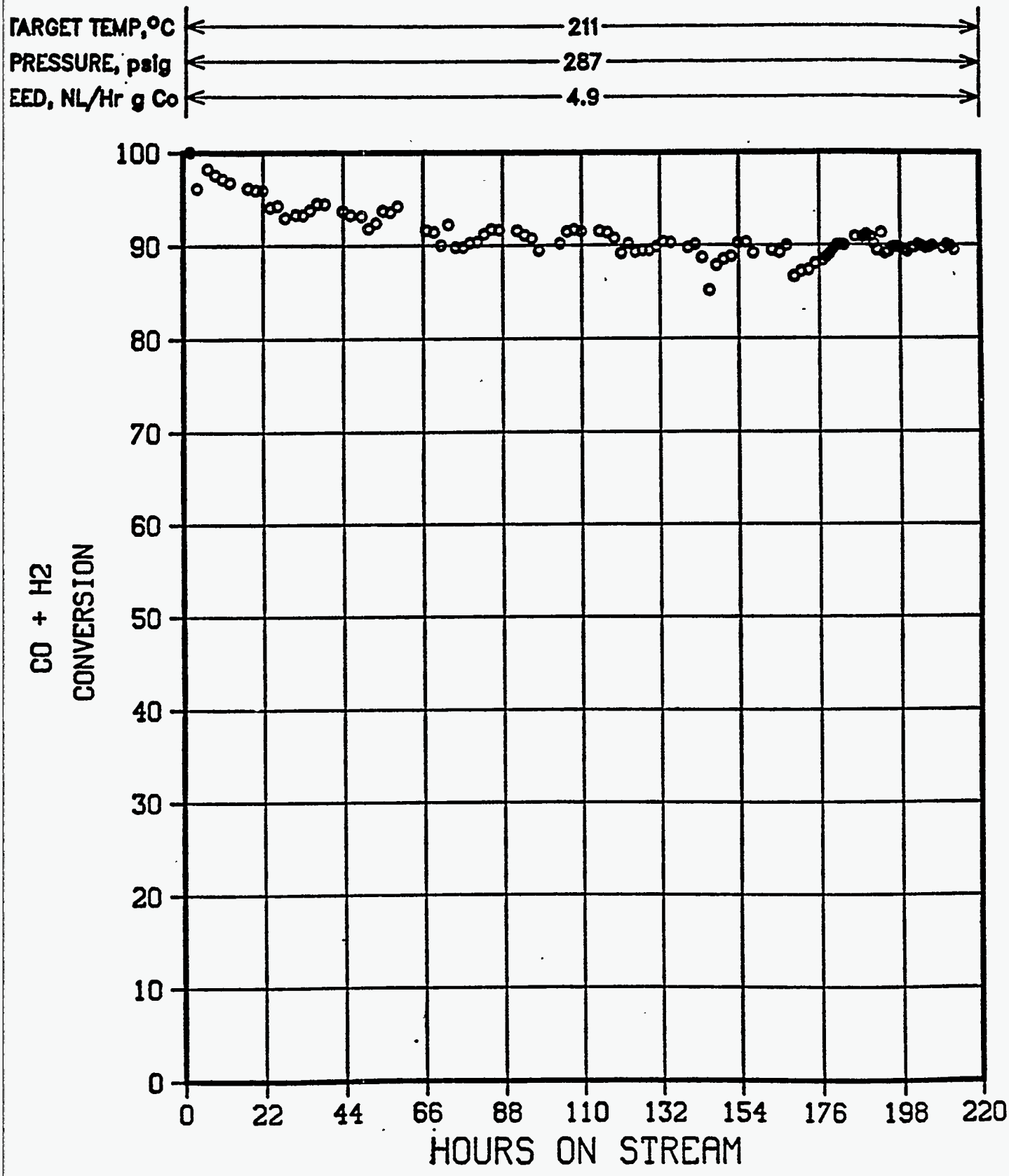

FIGURE 143

PLT 700 RUN 123 Co,Mn,Zr On steamed, acid washed Y-ZLT.

6827-161 w/28.7 % Co via eth-glycol pore fill

6.5g active in 166.5g quartz sand 6/20---->6/29/93

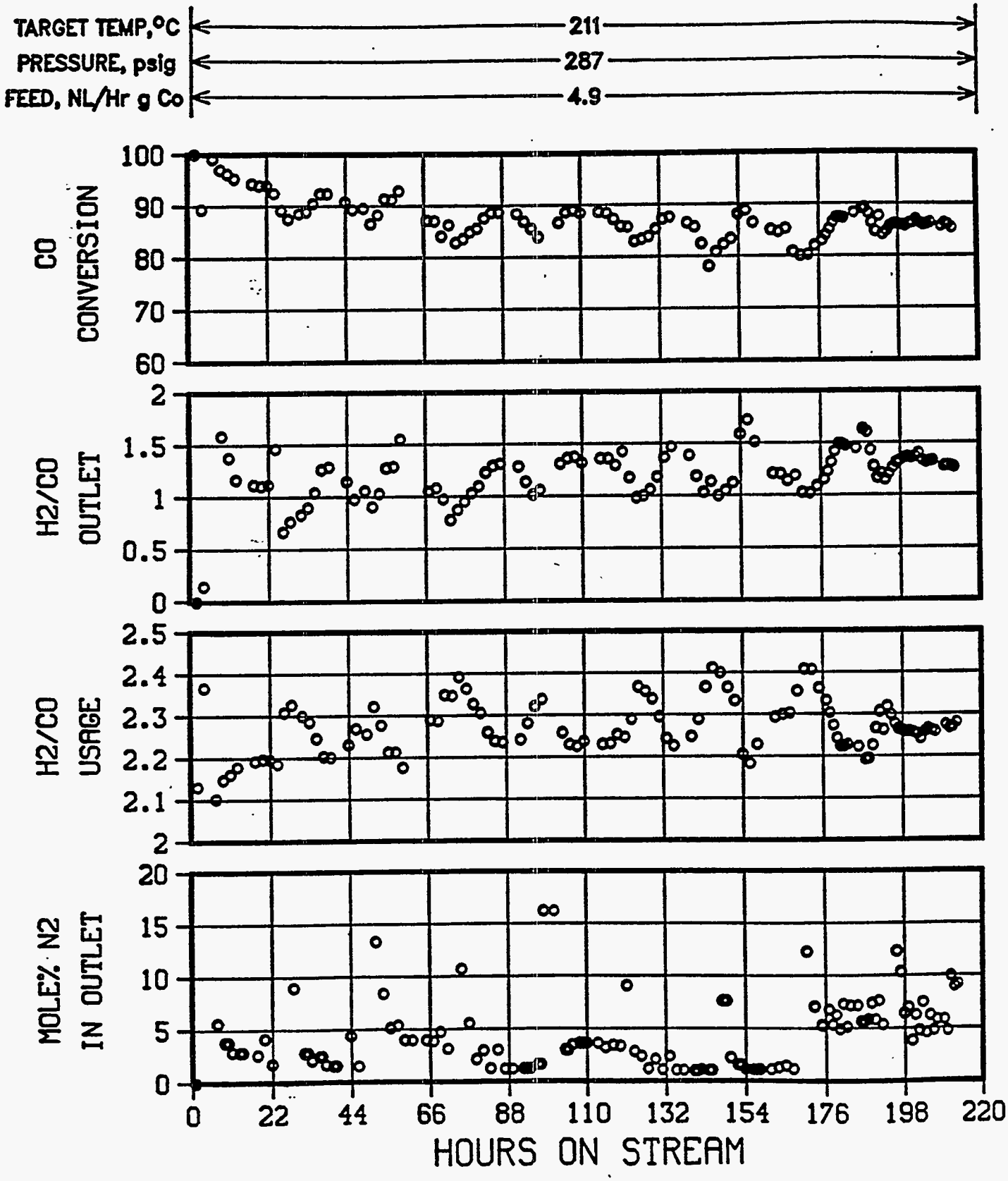

FIGURE 144

PLT 700 RUN 123 Co,Mn,Zr On steamed, acid washed Y-ZLT.

6827-161 w/28.7 % Co via eth-glycol pore fill

6.5g active in 166.5g quartz sand 6/20--->6/29/93

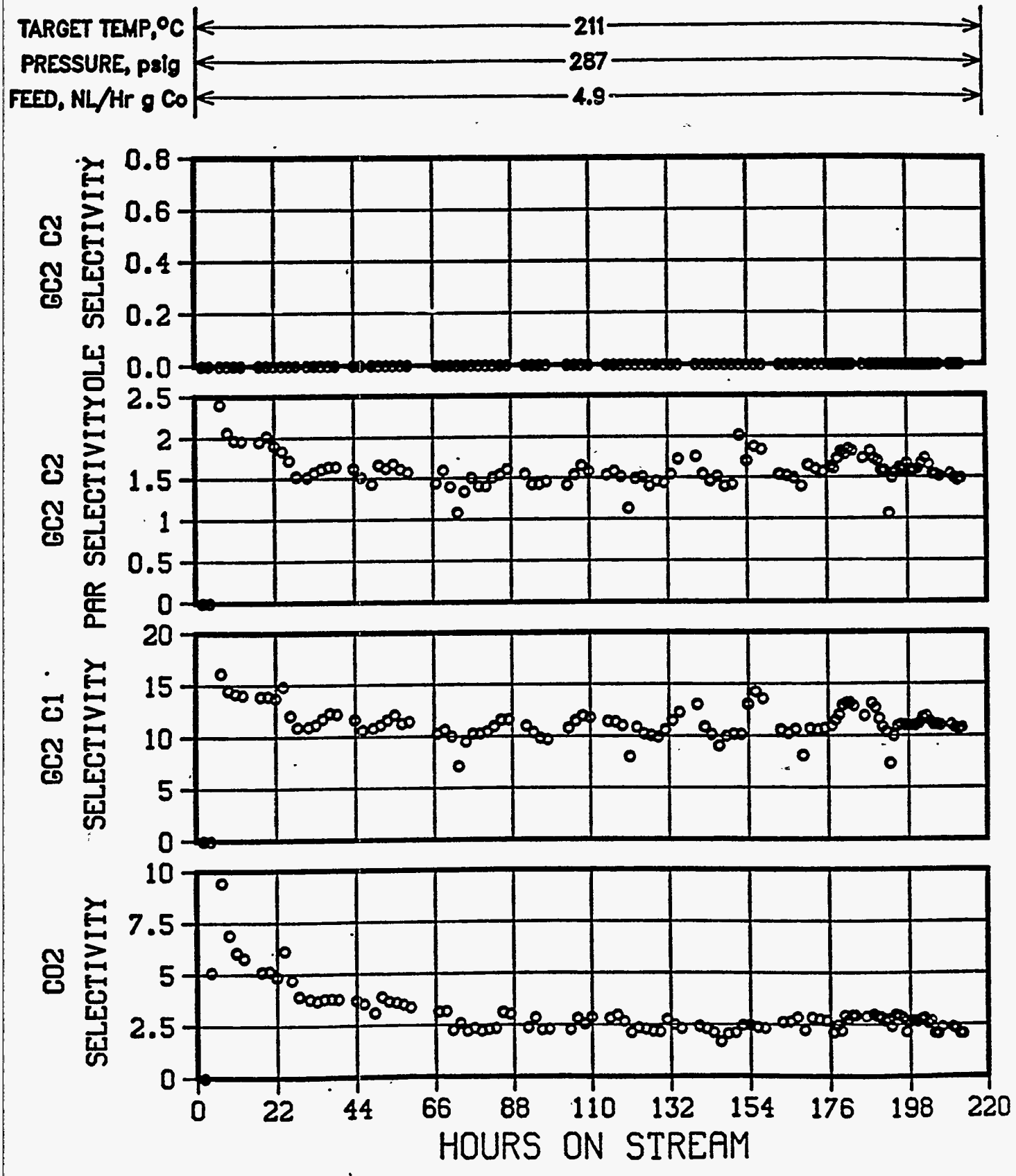

FIGURE 145

PLT 700 RUN 123 Co,Mn,Zr On steamed, acid washed Y–ZLT.

6827–161 w/28.7 % Co via eth–glycol pore fill

6.5g active in 166.5g quartz sand 6/20–––>6/29/93

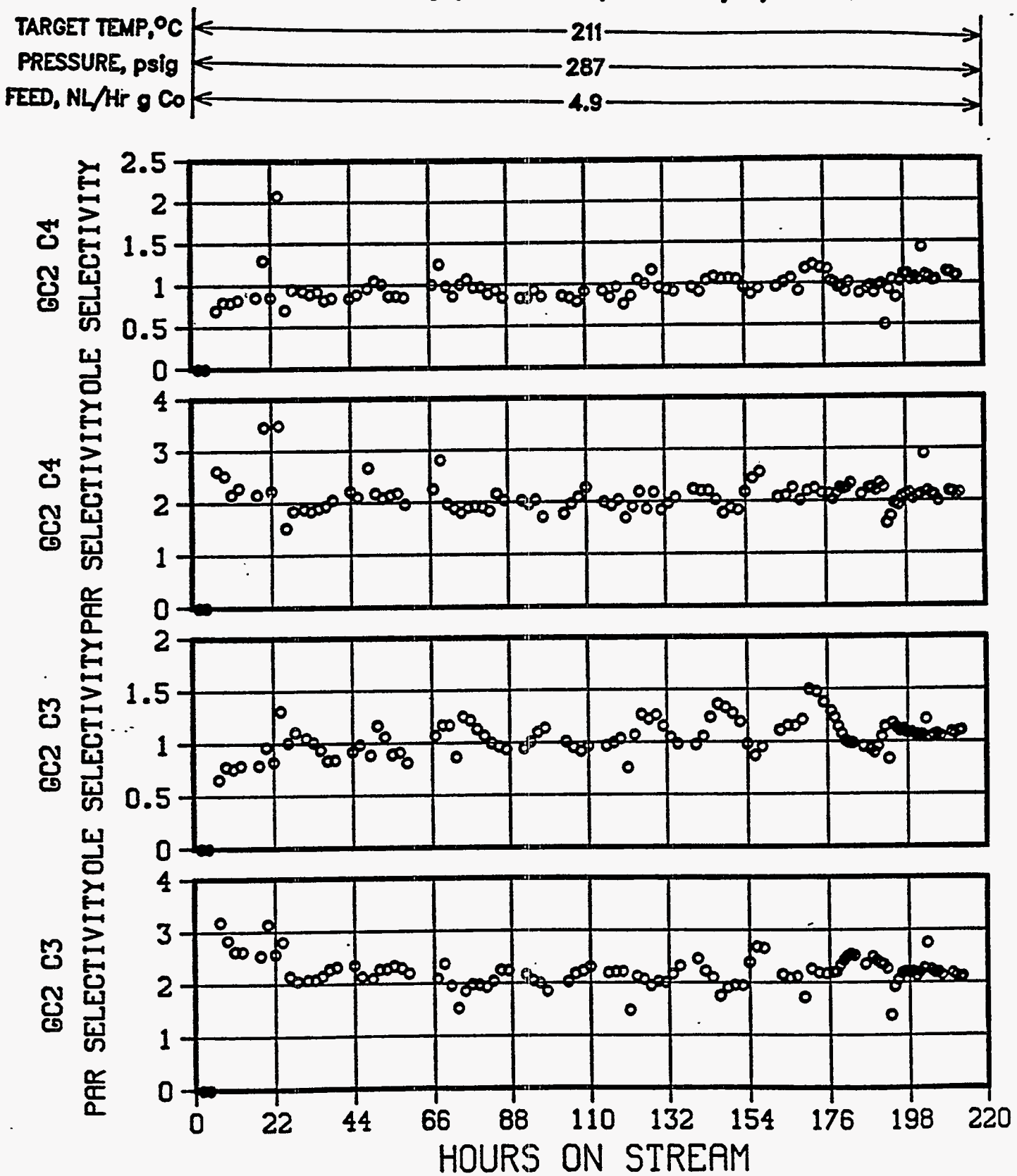

FIGURE 146

COBALT BASE CATALYST IN THE SLURRY AUTOCLAVE REACTOR

PLT 701 R-73 66.5g 6827-178 in 290g C_{30} oil

H_2:CO in feed = 2.0, stirrer rpm = 1100

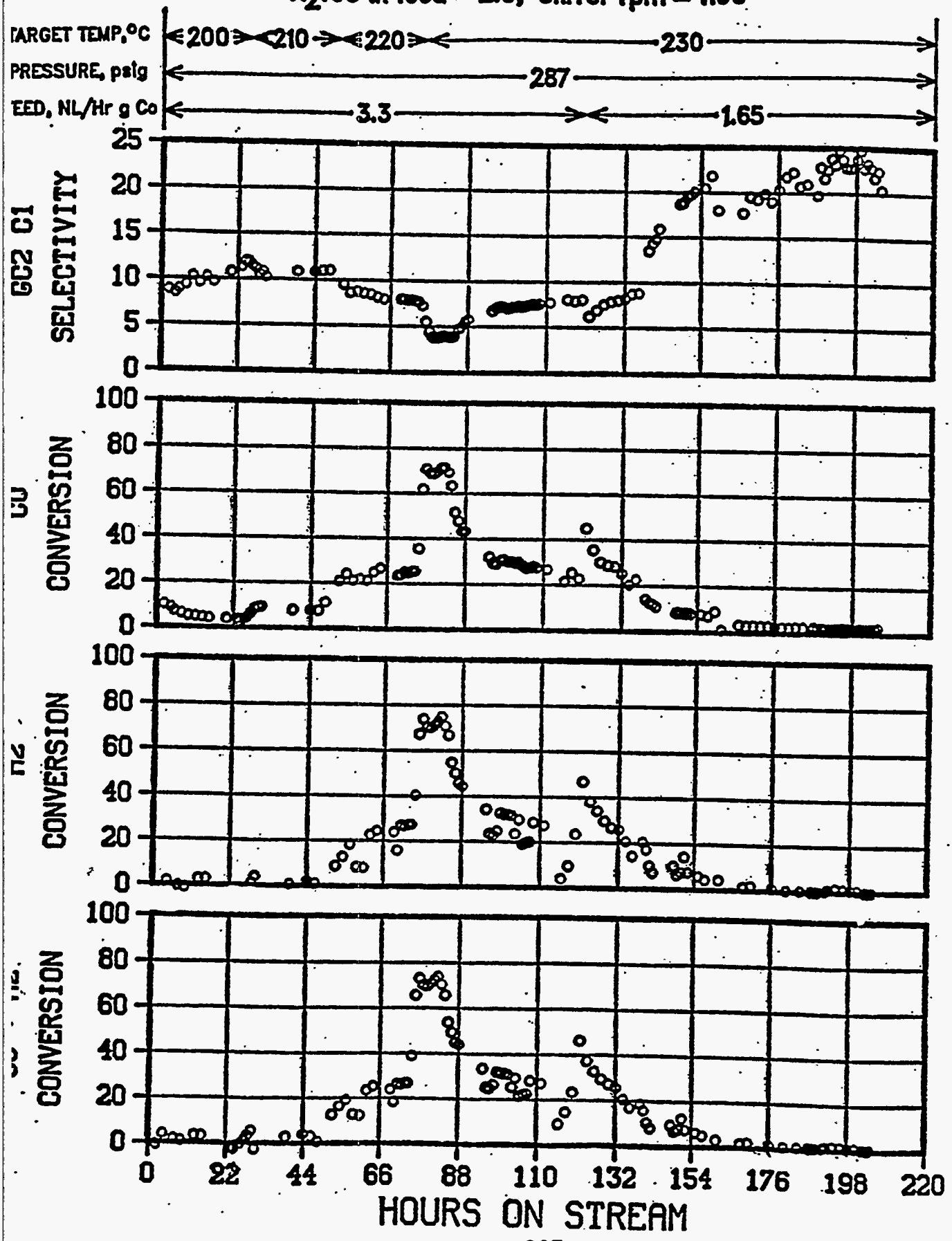

FIGURE 147

COBALT BASE CATALYST IN THE SLURRY AUTOCLAVE REACTOR

PLT 701 R-73 66.5g 6827-178 in 290g C_{30} oil

H_2:CO in feed = 2.0, stirrer rpm = 1100

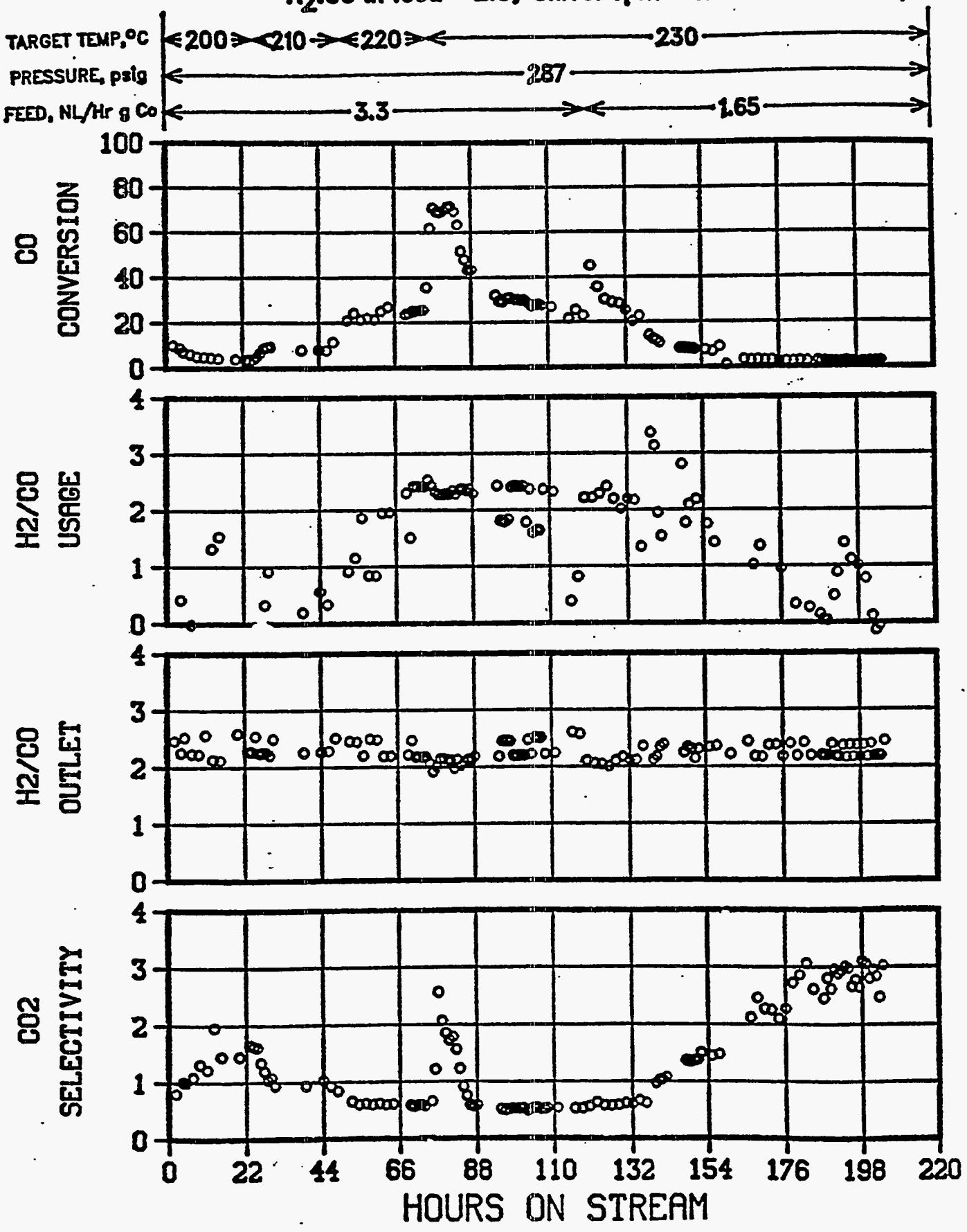

FIGURE 148

COBALT BASE CATALYST IN THE SLURRY AUTOCLAVE REACTOR

PLT 701 R-73 66.5g 6827-178 in 290g C_{30} oil

H_2:CO in feed = 2.0, stirrer rpm = 1100

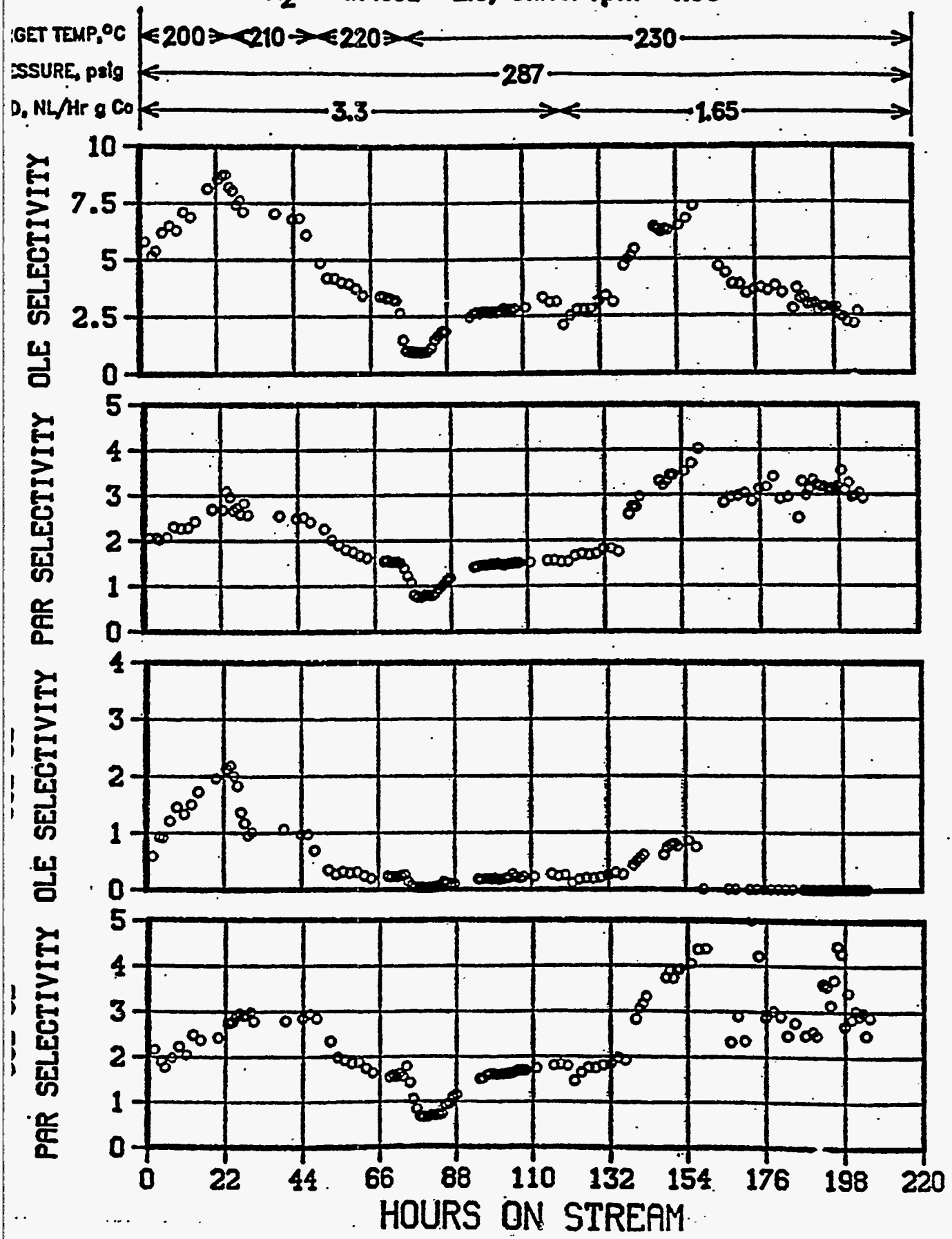

FIGURE 149

COBALT BASE CATALYST IN THE SLURRY AUTOCLAVE REACTOR

PLT 701 R-73 66.5g 6827-178 in 290g C_{30} oil

H_2:CO in feed = 2.0, stirrer rpm = 1100

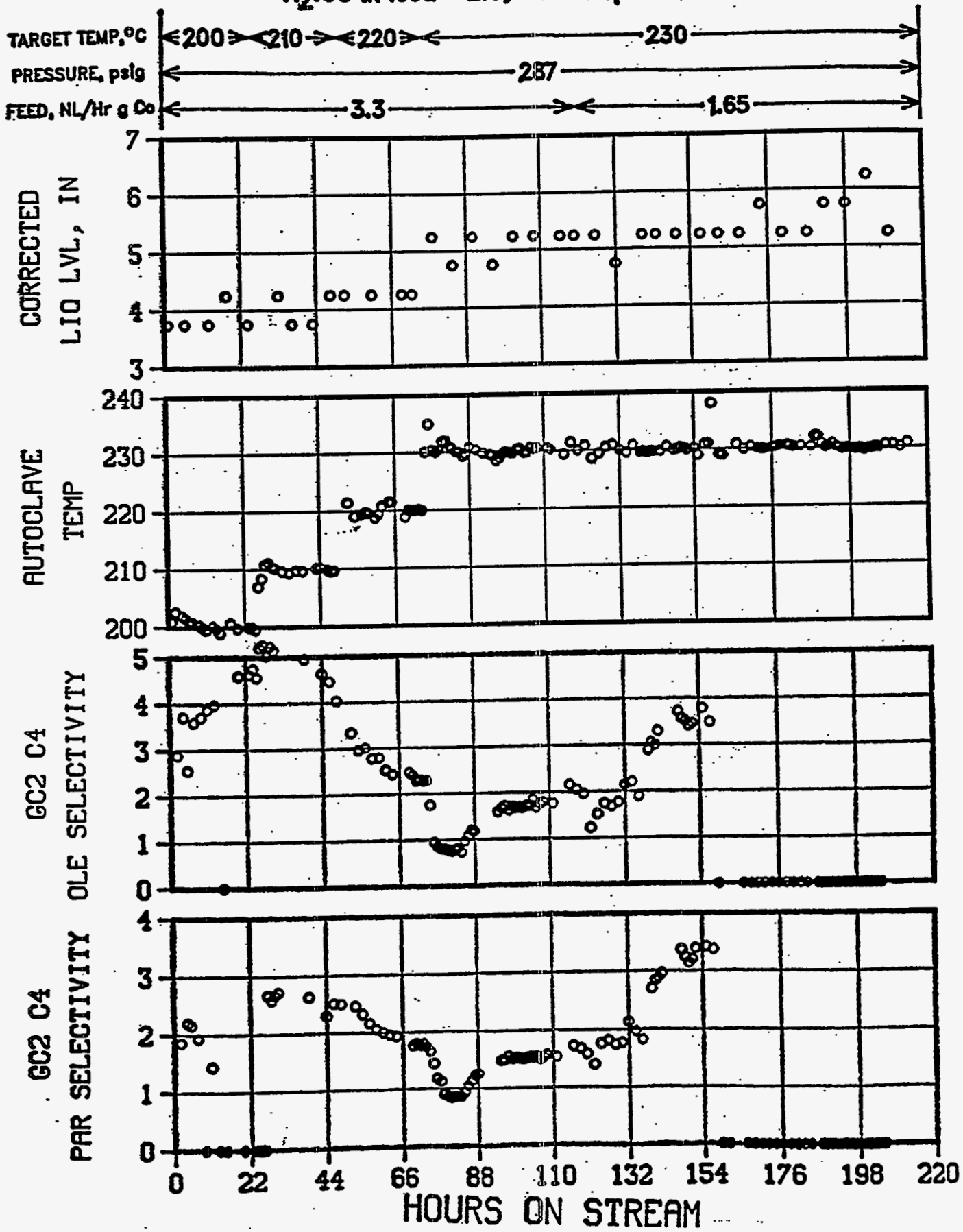

FIGURE 150

COBALT BASE CATALYST IN THE SLURRY AUTOCLAVE REACTOR

PLT 701 R-73 66.5g 6827-178 in 290g C_{30} oil

H_2:CO in feed = 2.0, stirrer rpm = 1100

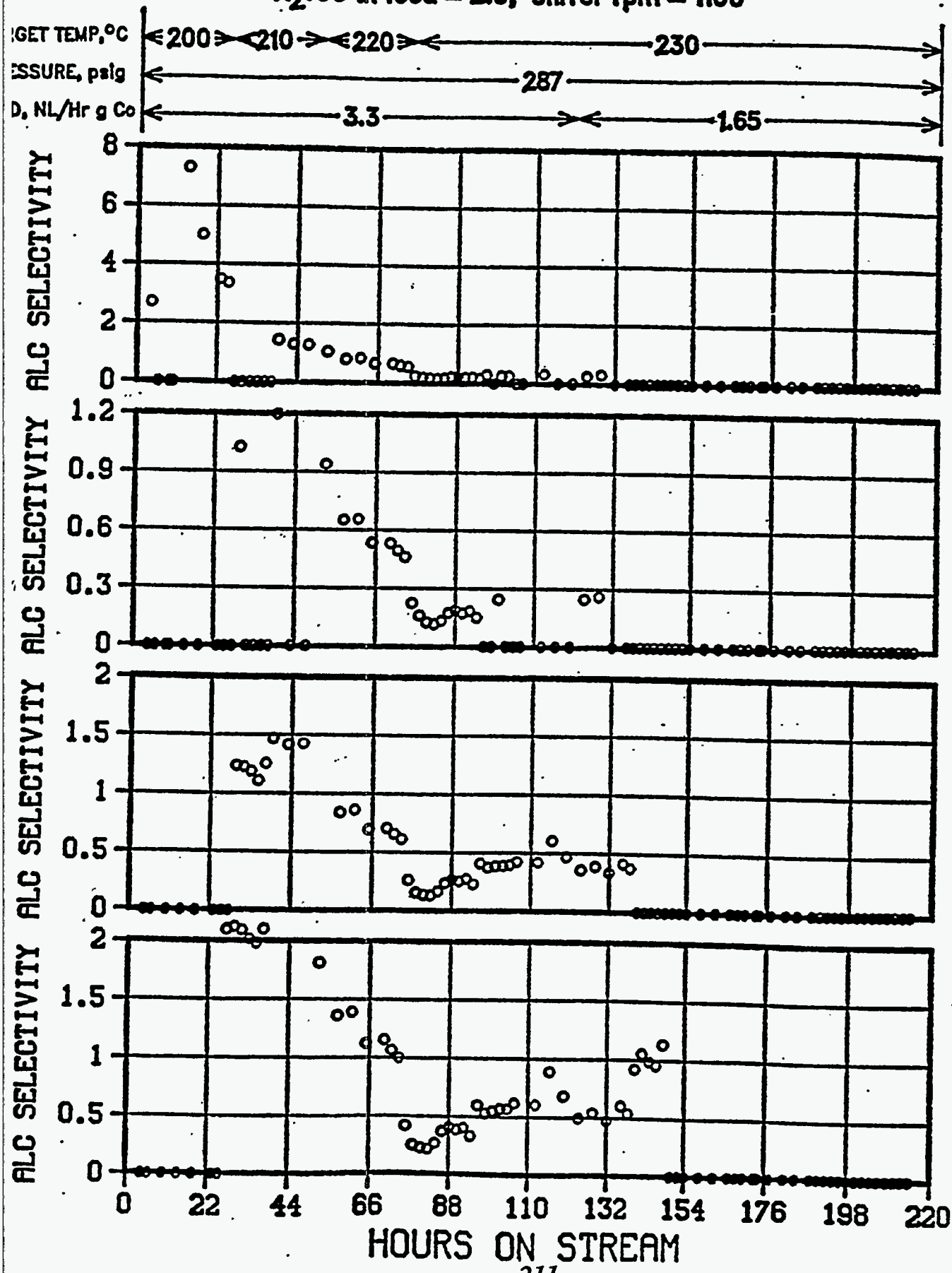

FIGURE 151

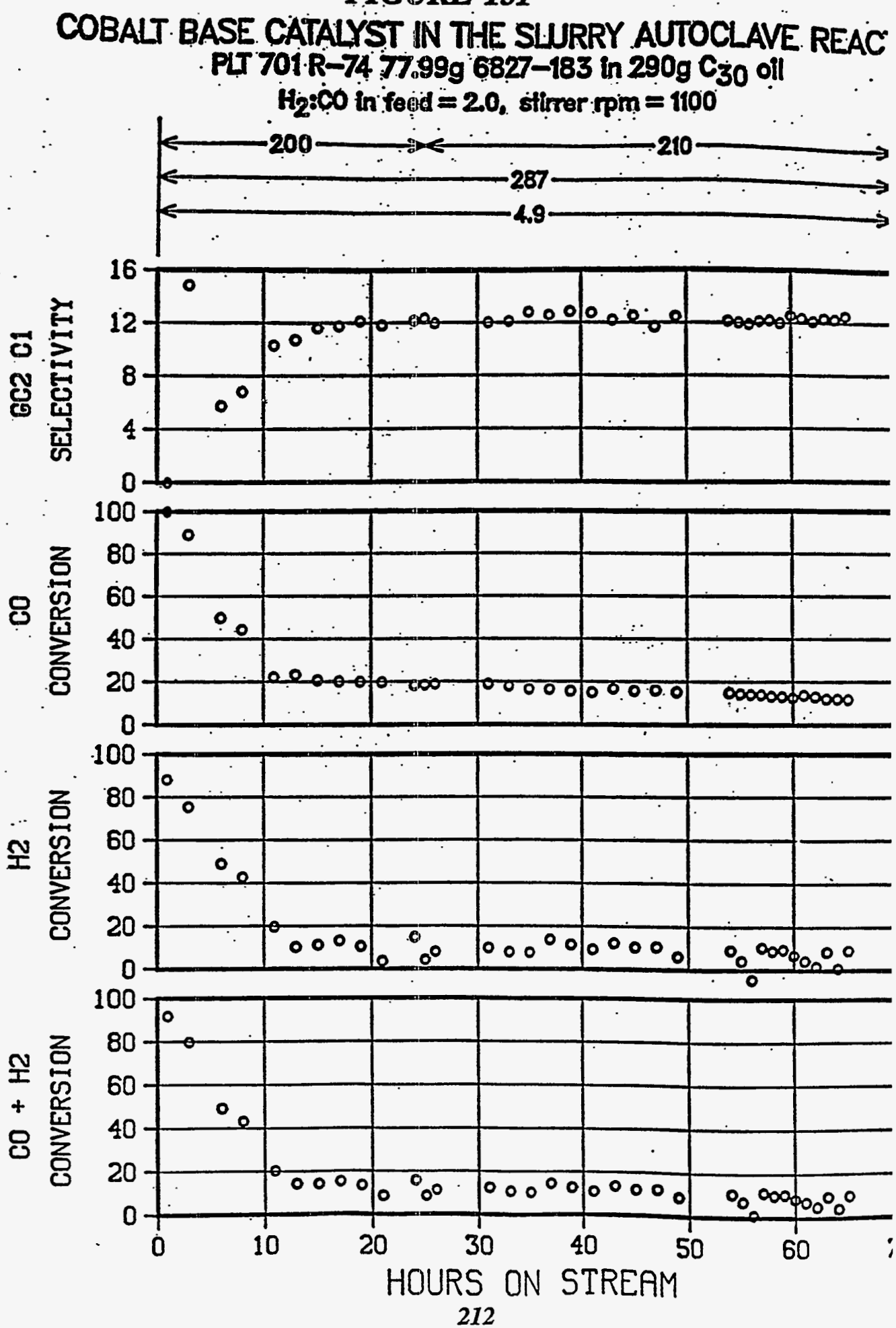
COBALT BASE CATALYST IN THE SLURRY AUTOCLAVE REAC
PLT 701 R-74 77.99g 6827-183 in 290g C30 oil
H2:CO in feed = 2.0, stirrer rpm = 1100
200
210
287
4.9
GC2 C1 SELECTIVITY
CO CONVERSION
H2 CONVERSION
CO + H2 CONVERSION
HOURS ON STREAM

FIGURE 152

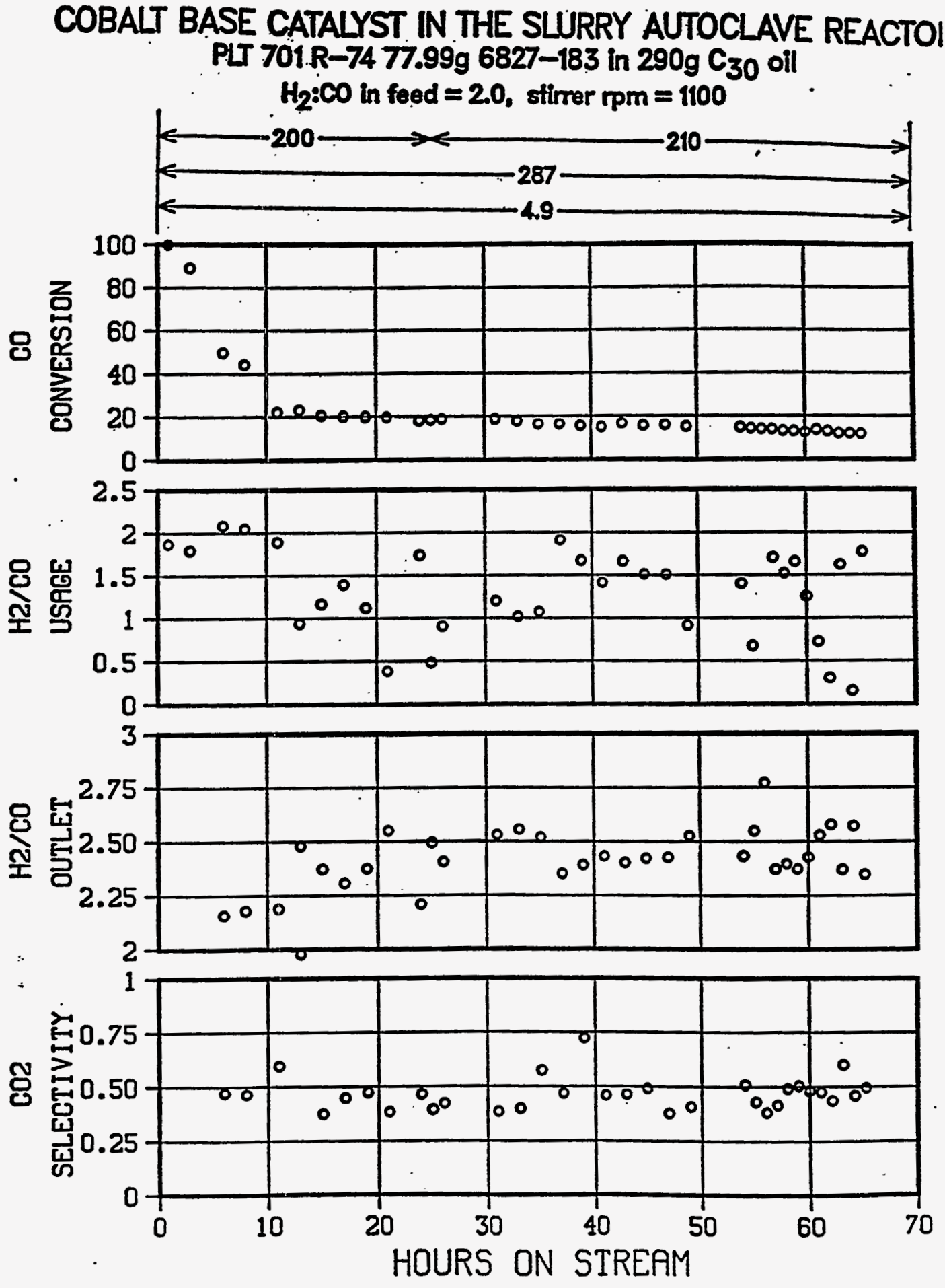
COBALT BASE CATALYST IN THE SLURRY AUTOCLAVE REACTOI
PLT 701 R–74 77.99g 6827–183 in 290g C_{30} oil
H_2:CO in feed = 2.0, stirrer rpm = 1100
200
210
287
4.9
CO CONVERSION
100
80
60
40
20
0
H2/CO USAGE
2.5
2
1.5
1
0.5
0
H2/CO OUTLET
3
2.75
2.50
2.25
2
CO2 SELECTIVITY
1
0.75
0.50
0.25
0
0
10
20
30
40
50
60
70
HOURS ON STREAM

FIGURE 153

COBALT BASE CATALYST IN THE SLURRY AUTOCLAVE REACTOR

PLT 701 R-74 77.99g 6827-183 in 290g C_{30} oil

H_2:CO in feed = 2.0, stirrer rpm = 1100

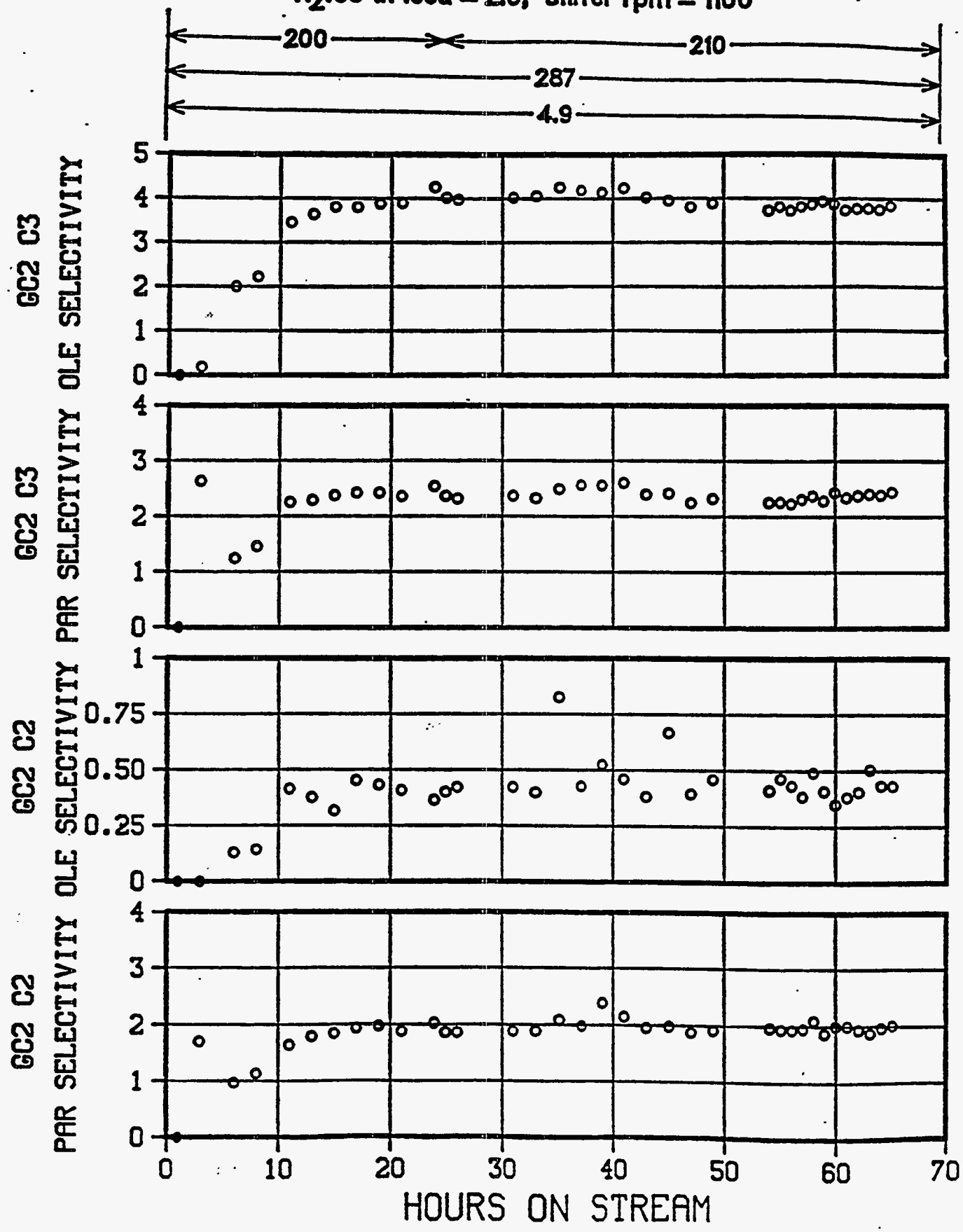

FIGURE 154

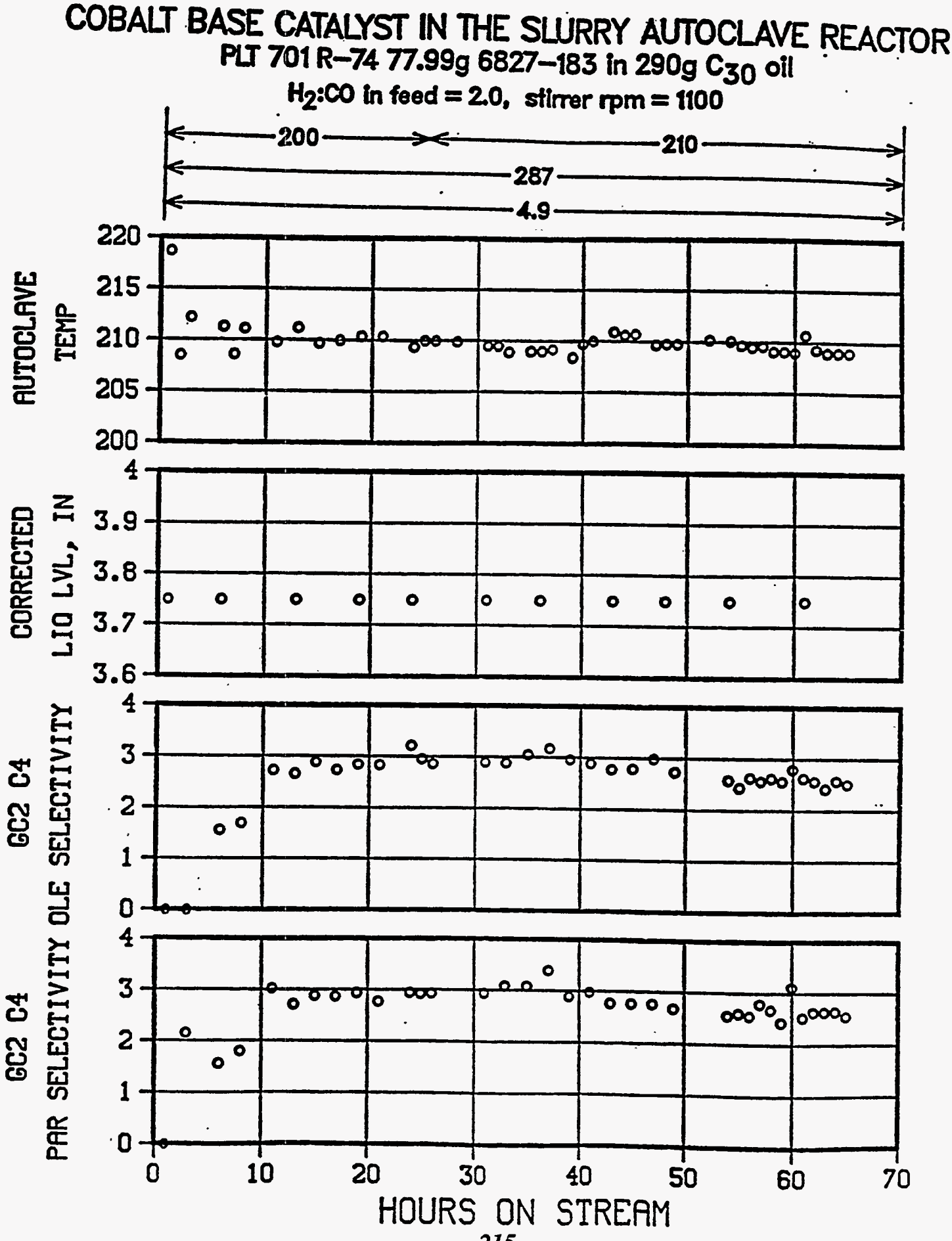
COBALT BASE CATALYST IN THE SLURRY AUTOCLAVE REACTOR
PLT 701 R-74 77.99g 6827-183 in 290g C_{30} oil
H_2:CO in feed = 2.0, stirrer rpm = 1100
200
210
287
4.9
AUTOCLAVE TEMP
220
215
210
205
200
CORRECTED LIQ LVL, IN
4
3.9
3.8
3.7
3.6
GC2 C4 PAR SELECTIVITY OLE
4
3
2
1
0
GC2 C4 PAR SELECTIVITY OLE
4
3
2
1
0
0
10
20
30
40
50
60
70
HOURS ON STREAM

FIGURE 155

COBALT BASE CATALYST IN THE SLURRY AUTOCLAVE REACTOR

PLT 701 R-74 77.99g 6827-183 in 290g C_{30} oil

H_2:CO in feed = 2.0, stirrer rpm = 1100

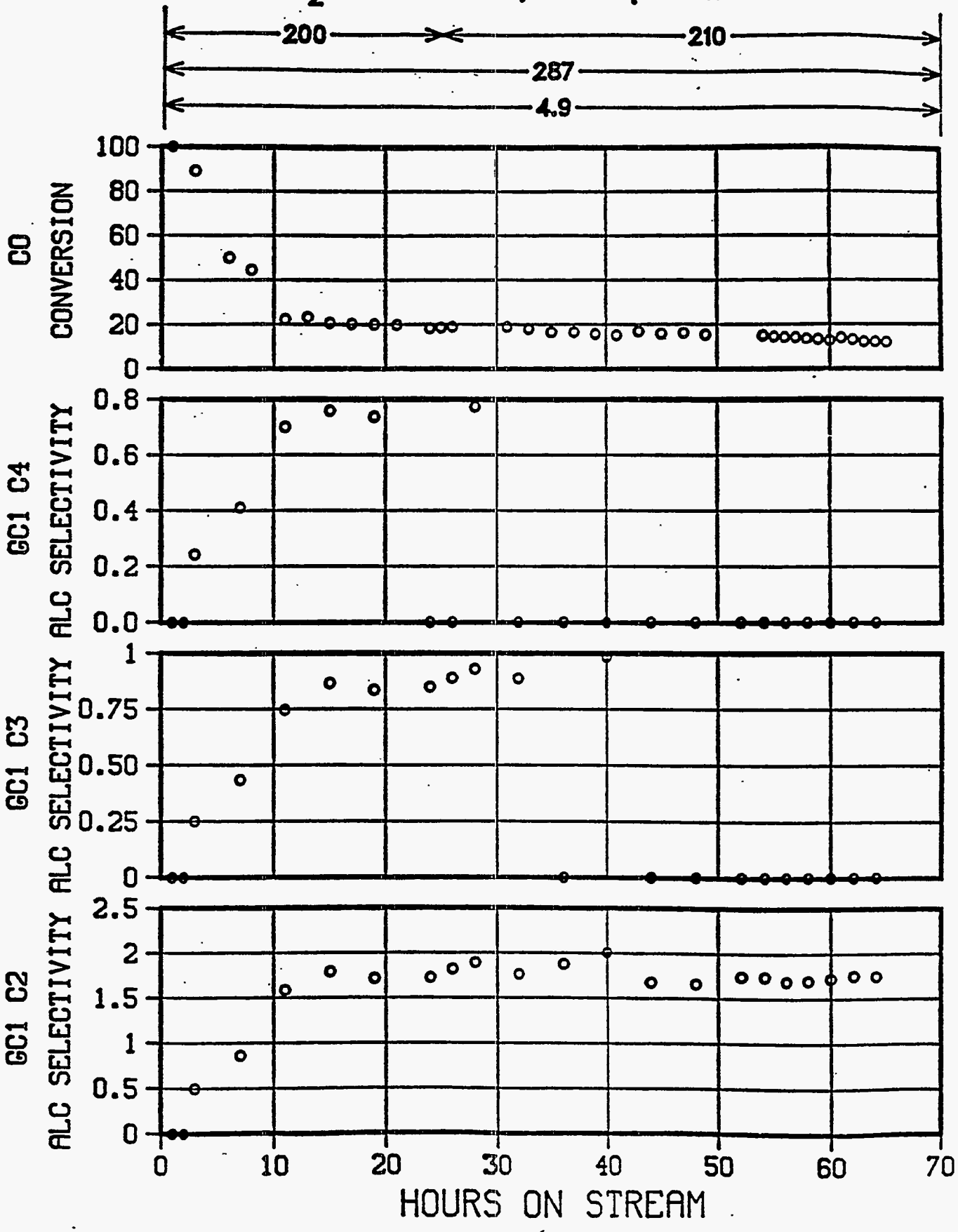

FIGURE 156

STEM

Reduced Ru-Free Catalyst

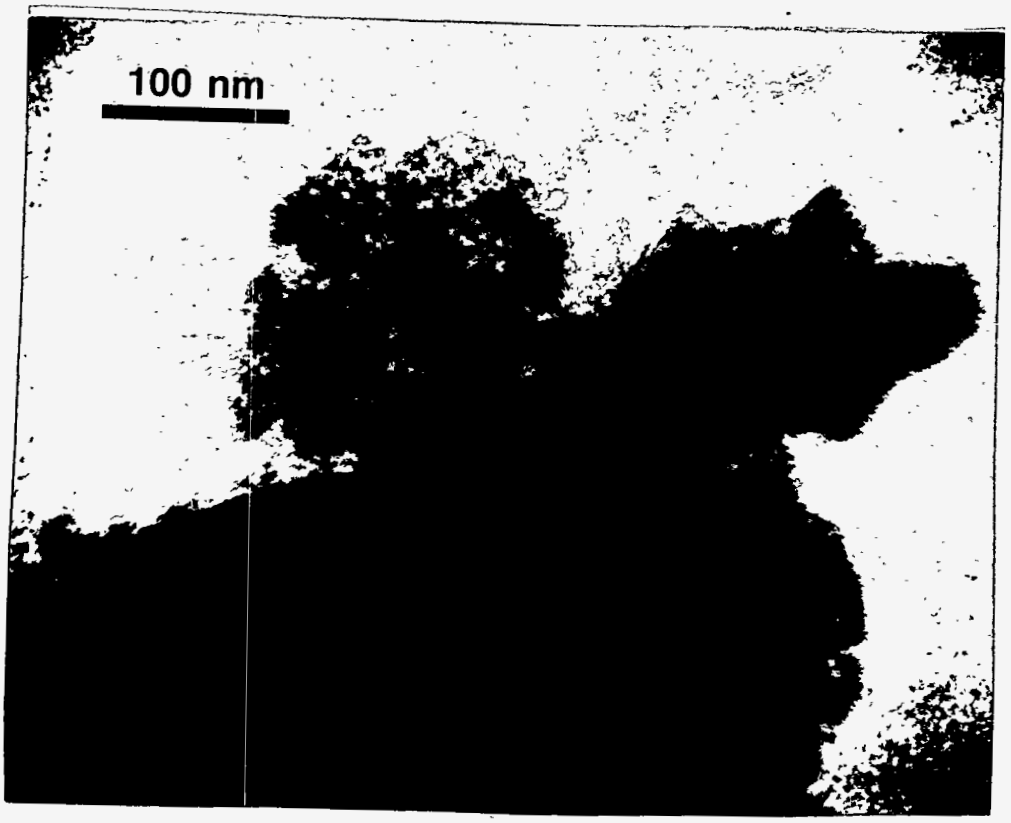

FIGURE 157
STEM

Reduced Ru-Free Catalyst

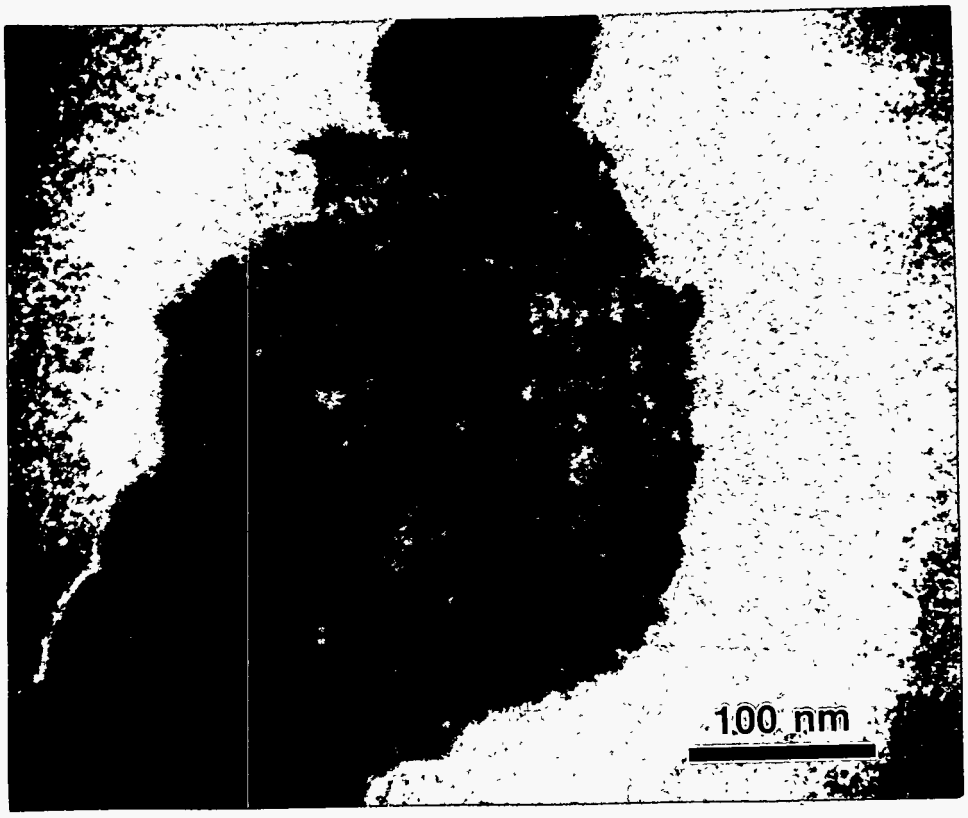

FIGURE 158

ZIRCONIUM CONTENT AS A FUNCTION OF CRYSTALLITE SIZE REDUCED FORM OF THE CATALYST

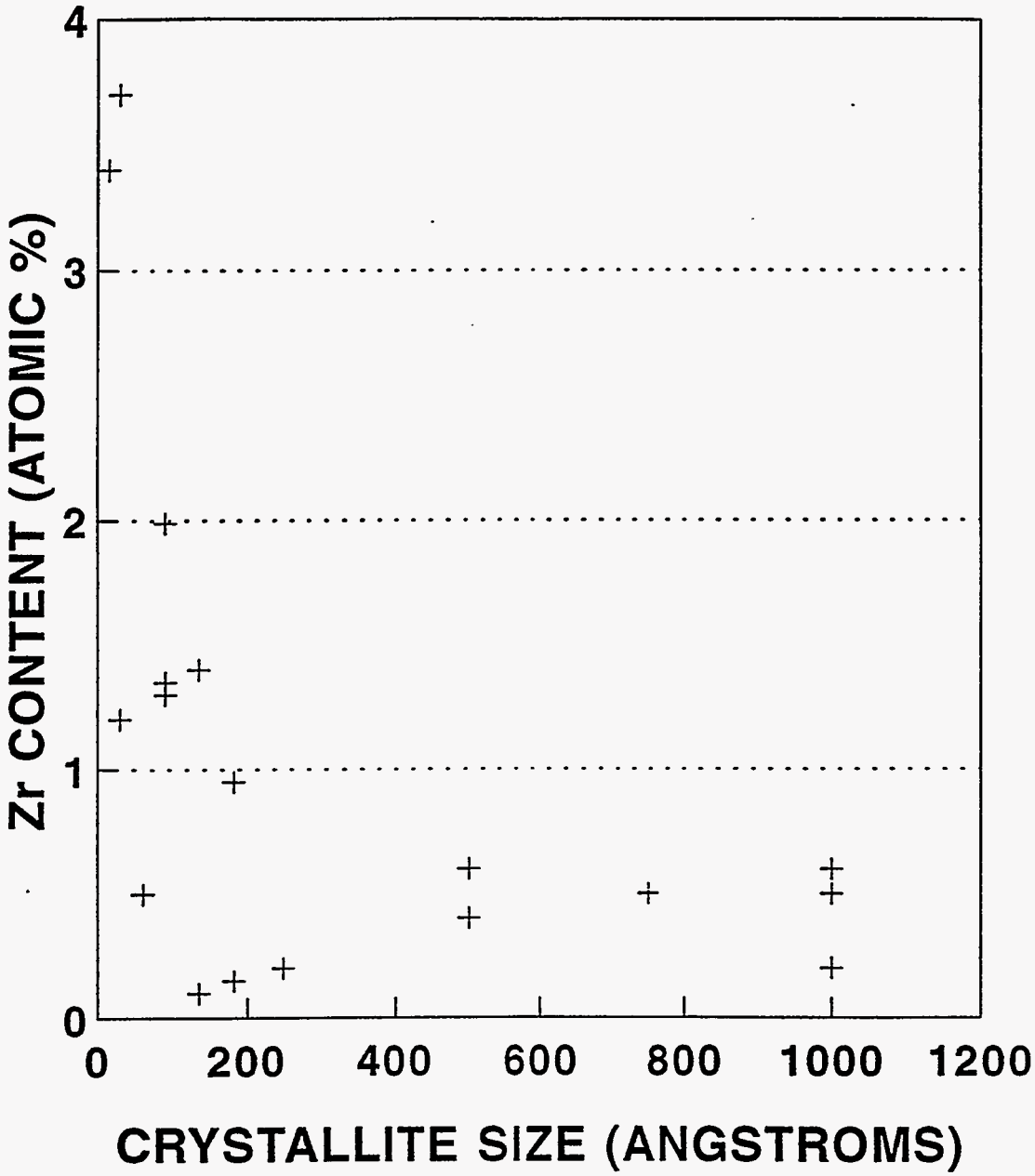

+ Ru-FREE

Mn IN ALL CRYSTALLITES AT ABOUT SAME LEVEL

APPENDIX

CONVERSION AND SELECTIVITY CALCULATIONS

CALCULATIONS USE ON LINE GAS ANALYSES

C = CONCENTRATION IN MOLE %

CONVERSIONS

$$\text{CONVERSION (CO)} = \frac{\left(\frac{C_{CO}}{C_{Ar}}\right)_{Feed} - \left(\frac{C_{CO}}{C_{Ar}}\right)_{Prod}}{\left(\frac{C_{CO}}{C_{Ar}}\right)_{Feed}}$$

$$\text{CONVERSION } (H_2) = \frac{\left(\frac{C_{H_2}}{C_{Ar}}\right)_{Feed} - \left(\frac{C_{H_2}}{C_{Ar}}\right)_{Prod}}{\left(\frac{C_{H_2}}{C_{Ar}}\right)_{Feed}}$$

$$\text{CONVERSION } (CO + H_2) = \frac{\left(\frac{C_{CO} + C_{H_2}}{C_{Ar}}\right)_{Feed} - \left(\frac{C_{CO} + C_{H_2}}{C_{Ar}}\right)_{Prod}}{\left(\frac{C_{CO} + C_{H_2}}{C_{Ar}}\right)_{Feed}}$$

SELECTIVITIES

$$S_a = \frac{\left(\frac{C_A}{C_{Ar}}\right)_{Prod}}{\left(\frac{C_{Co}}{C_{Ar}}\right)_{Feed} - \left(\frac{C_{Co}}{C_{Ar}}\right)_{Prod}}$$

The equation above yields carbon-based selectivities. Before being used the selectivities were corrected for carbon dioxide formation in all cases except for that of carbon dioxide itself. Since carbon dioxide selectivities were usually about 50%, the corrected selectivities were about twice as high as they would have been if the carbon going to carbon dioxide had been taken into account in their calculation.

CALCULATION OF CONTACT TIME

$\bar{V}$ is Volume of liquid in Autoclave

W is weight in grams of iron

material balance:

$$F_o - F = \bar{r} \cdot W \cdot \bar{V}$$

$$F_o - F_o(1-x) = \bar{r} \cdot W \cdot \bar{V}$$

$$F_o x = \bar{r} \cdot W \cdot \bar{V}$$

$$\bar{r} = \frac{F_o x}{W \bar{V}} = \frac{x}{\left(\frac{W\bar{V}}{F_o}\right)}$$

$\frac{W\bar{V}}{F_o}$ = CONTACT TIME (SPACE TIME)